UNIVERSITÀ
DEGLI STUDI
DI PADOVA

DEPARTMENT OF GENERAL PSYCHOLOGY

PhD Course in Psychological Sciences

XXXII Series

SELECTION FOR ACTION IN *DROSOPHILA MELANOGASTER*

COORDINATOR: Prof. Giovanni Galfano

SUPERVISOR: Ch.mo Prof. Umberto Castiello

CO-SUPERVISOR: Prof. Aram Megighian

PhD STUDENT: Giovanni Frighetto

25th September 2019

Giovanni Frighetto

Selection for action in Drosophila

This dissertation was submitted to University of Padova in fulfilment of the requirements for the PhD Course in Psychological Sciences.

C O N T A C T

✉ giovanni.frighetto@phd.unipd.it

Supervisor

Ch.mo Prof. Umberto Castiello

Co-supervisor

Prof. Aram Megighian

Date of submission

25th September 2019

Date of oral defence

SYNOPSIS

The present work focuses on the mechanisms of selection for the control of action in *Drosophila melanogaster* (*D. melanogaster*), also known as fruit fly: the gnat which inhabits our houses nearby the bowl of fruit placed on the kitchen table. The use of an invertebrate for studying this process is justified by the pivotal role this 'model organism' is playing for the comprehension of the neural substrates underlying behaviour at all levels, from molecules to circuits (Bellen et al., 2010). *D. melanogaster* has a rich repertoire of innate and learned behaviours and a quite simple brain, composed by roughly 100,000 neurons, which can be studied by means of sophisticated techniques. Therefore, it offers the possibility to study complex behaviour in a brain structure simpler than that of higher organisms. As a consequence the neurobiological underpinning of its behaviour can be understood in an easier manner. The comparisons of its behaviour with similar behaviours shown by different and evolutively distant animals can provide important insights about their relationship with different or conserved underlying neural circuits.

This thesis was conceptualized to sketch out whether selection for action processes underlying the behaviour of mammals might be shared with lower organisms such as *D. melanogaster*. Selection for action entails a close interaction between visual and motor systems allowing to select a specific stimulus in the environment to which act upon. This process allows to filter out irrelevant information for action.

The introductory chapter (Chapter 1) of this thesis will provide the theoretical and the methodological framework within which the experimental work is nested. The first two sections will provide an overview of the research concerned with the mechanisms of selection for the control of action and the underlying visuomotor processes. One section will introduce how this topic has been studied in humans, while the other section will introduce how this topic has been studied in non-human primates. This subdivision offers an evolutive perspective of the problem at stake here. Then, in the ensuing sections, the model system will be introduced. Specifically, there will be a section dedicated to the functional

neuroanatomy of *D. melanogaster*, with a focus on the visual system, the motor system and other relevant neural structures. Another section is devoted to the tools used for studying the cognitive neuroscience of *D. melanogaster*.

In Chapter 2, that is the experimental component of this thesis, I will show the work I conducted during my PhD.

In first section I will describe the first experiment aimed at investigating whether flies have an action-based attention. Are flies able to inhibit via attentional mechanisms the response to an upcoming stimulus in order to successfully end an ongoing action? In particular, I observed whether flies are prone to interference effects caused by the upcoming appearance of a competitive stimulus (i.e., a distractor). I expected this inhibitory mechanism to be played out on spatial trajectories. In this study, flies were engaged in a walking task aimed at reaching a visual target (i.e., a bright stripe) while an abrupt identical distractor was laterally presented.

In the second section an experiment aimed at extending the finding of the first experiment will be outlined. In particular, this second experiment will consider the angular distance between target and distractor. The aim of this study was to test the hypothesis that the shorter the distance between target and distractor the greater is the level of inhibition.

Then, in the third section I shall present an experiment targeting the hypothetical neural circuit underlying the behavioural effects observed in the previous experiments. Based on the increasing evidence for an intriguing homology between a specific neuropil of flies (Central Complex; CX) and the mammals' neural structure involved in action selection, the idea was to test flies with a lesioned CX during the behavioural task used in the previous experiments. To do this, I used a technique based on the GAL4-UAS binary system in order to downregulate specific dopamine receptors in a very selected neural circuit, the so-called E-PG neurons, by means of RNA interference (RNAi) method. Moreover, I adopted an optogenetic technique for *in vivo* neural manipulation. I employed flies bearing light-sensitive ion channels in the same selected neural circuit of CX to briefly activate such neurons during the task. This neural circuit forms a donut-shape structure which it has been proposed to be an integrative

circuit between visual and motor systems and to perform an attention-like function. The underlying idea was to perturb, by activating the entire neuronal population, the vector space representation regarding the position of an internal goal which this circuit seems to maintain.

In the fourth section I will include a series of experiments aimed at characterizing the considered neural circuit from a neurochemical perspective. The hypothesis was that the dopaminergic system, involved in the action selection process of mammals, could also modulate the neurophysiological response within the CX of flies. Specifically, I recorded *in vivo* the neural response to dopamine application in CX of flies by using a bioluminescence technique based on a genetically encoded calcium indicator.

A general discussion, contextualizing the results obtained in the studies here presented will follow (Chapter 3).

All in all, this work represents an attempt to tackle the mechanisms of selection for the control of action in flies. The interference paradigm I developed establishes a powerful platform to further explore the problem of selection for action in flies which might be useful for clarifying similar processes in higher organisms.

CONTENTS

LIST OF FIGURES

1 INTRODUCTION

The most intriguing feature of an organism equipped with a brain is, with no doubts, the ability to interact with the surrounding environment for detecting the relevant information to release an adequate behavioural response. To do this first it is necessary to obtain a faithful description of the context by means of the sensory systems and then select and prepare an appropriate response to be implemented by the motor system (Marr, 1982). For example, while humans have refined motor responses for interacting with objects, "lower" animals have refined motor responses for foraging, to avoid predator attacks or to confront a conspecific for mating (Collett & Collett, 2002; Hardcastle & Krapp, 2016; Card, 2012). According to this evidence, the information flow would proceed from an internal representation of the external environment to the action selection and the specification of the parameters needed for muscular contraction necessary for required kinematic output.

1.1 MECHANISMS OF SELECTION FOR THE CONTROL OF ACTION

Survival often requires deciding what to do in a particular situation. For instance, to select an appropriate action within a complex natural environment might be a difficult process. In the majority of "higher" animals, such as mammals, action selection is mainly based on the integration of the visual and the motor systems. In this respect a process termed 'selective attention' plays a crucial role to this endeavour (James, 1890). Selective attention allows for a specific stimulus to be selected among many others in order to act appropriately upon it. For example, let us consider a situation in which we are sitting in a pub with friends in front of

cold glasses of beer and we need to select our glass for drinking. The first stage of such selection process is figure-ground segmentation, where, in a largely automatic manner, the glasses are discriminated from their background. After this segmentation, the visual scene remains very complex due to the presence of many glasses. Hence, a second stage of feature selection is needed. It is at this second stage that attentional mechanisms are thought to operate. In a hundred of milliseconds, by enhancing the processing of some glasses and suppressing the information from others, we are able to select our glass of beer.

As pointed out by Marr (1982), attentional processes can be best understood within the specific environment where organism evolve, and consequently within the core of resultant behavioural requirement. With this in mind the next sections will provide an overview of the mechanisms of selection for the control of action in an evolutive perspective from the vertebrate to the invertebrate organisms. The aim is to shed light on a common cognitive mechanism employed by different organisms to select actions which may share the same neural circuit core design. Although it has been demonstrated that the selection for action process is multisensory in nature, here I shall limit the dissertation to the visual modality.

1.1.1 Humans

Visual perception can flow automatically into actions, such that the latter can be evoked with little or no conscious intention to act. In this respect, Gibson coined the term “affordances” to define object possibilities for action (Gibson, 1979). This concept melts the automatic binding between the perception of an object and the potential actions it elicits in the perceiver. In this view, perception and action are two processes strictly linked. Such an idea is extremely close to what stated by Sperry, according to which perception is basically an implicit preparation to respond (Sperry, 1952). Thus, perceiving an object elicits inevitably a motor response for acting upon it (Cisek, 2007). Consider the example of a person in choosing a piece of fruit from a bowl, many fruits are visible and within the reaching space, but only the one that the person would like to pick up governs

the particular pattern and direction of movement. How our motor system would react in such situations? In principle all fruits would trigger a variety of motor programs resulting in a behavioural chaos (Castiello, 1999). Contrariwise, this chaos is avoided by the striking selectivity shown by humans' behaviour, witnessed by the ability to inhibit the many actions evoked by visual inputs. In this regard, attentional mechanisms have been proposed to operate with the purpose of preserving the perception for action system from overload.

Although there is now abundant evidence in support of a predominant role for attention in shaping behaviour by influencing motor output, the mechanisms through which attention exerts its effect remain a controversial issue (Castiello, 1996; Chieffi et al., 1993; Colman et al., 2017; Jackson et al., 1995; Johansson et al., 2001; Kritikos et al., 2000; Mon-Williams et al., 2001; Saling et al., 1998; Tipper et al., 1997; Tresilian, 1998; Welsh & Elliott, 2004). This process has been defined as "selection-for-action" (Allport, 1987). According to this process, in order to minimize action-interference effects information about irrelevant stimuli is effectively inhibited from a motor perspective.

To shed light on this issue, ecological experimental paradigms employing three-dimensional (3D) stimuli rather than those using two-dimensional (2D) stimuli presented on computer screens or tachistoscopes for studying selective visual attention (Posner, 1980), have been deviced. In these studies the problem of stimulus selection for the control of overt actions has been addressed (Castiello, 1999; Tipper et al., 1998). They have highlighted the mechanisms upon which the selection-for-action would be based proposing models and their neurophysiological possible underpinnings. A common behavioural effect guides the conclusions of these studies. To wit, during an action aimed at a target object, some information from irrelevant non-target objects attracts our attention and they influences the motor outputs related to the main action (i.e., which one directed towards the target). This phenomenon has been defined as "interference effect".

In particular two major models have been proposed. For one, Castiello (1999) has proposed a model in which spatial attention mediates the selection getting access to the attributes of objects which are relevant for action. For another,

Tipper and collaborators (1998) have put forward a model where an action-based inhibitory mechanism selects the target from competing distractors through a representation of the peripersonal space. Looking at the role played by selective attention during a dual-task entailing 3D objects in an ecological context, Castiello (1996) has suggested that attention needs to access object representation, which in turn provides information for the coding of volumetric boundaries necessary for positioning the fingers appropriately on the object. Specifically, in this study Castiello (1996) investigated the interference effects in a series of reaching-to-grasp tasks, where a fruit as the target was presented with passive neighbouring distractors (i.e., other fruits) that would require an alternative reach-to-grasp movement. In these experiments, participants were seated in front of a working surface with their right hand placed on it in the midsagittal plane. A soon as the target fruit (i.e., apple, mandarin, cherry, or banana), was highlighted by a spotlight, the participants were required to reach, grasp the fruit and bring it to the starting position. Together with the target fruit a distractor fruit was presented. The participants were never requested to act upon the distractor. In such circumstances the distractor did not elicit any changes at the level of the kinematic of movement directed towards the target. However, when the reaching-to-grasp task was associated to another counting-times task interference did emerge. In particular, participants, during grasping were required to maintain gaze fixation on the target, to count the number of times that a laterally placed distractor was highlighted and then report this count at the end of the trial. This eye movements constraint allows investigating of the covert spatial attention, which differ from overt spatial attention which is accompanied by eye movements (Posner, 1980). In such circumstances an interference effect on movement parameterization was found. If the central target to reach and grasp was a cherry, the amplitude of peak grip aperture was greater than when the distractor fruit was an apple or a banana. Conversely, if the target was an apple, the amplitude of peak grip aperture was smaller when the lateral fruit was a cherry rather than a mandarin. Furthermore, this effect was greater when the counting-times began prior to movement onset, but it was still persistent when the counting began at later stages of the movement. Put simply,

these results indicate that the process of anchoring covert attention to another stimulus in such an active manner (i.e., counting-times task) affects the kinematic patterning of the primary motor task (i.e., reaching-to-grasp task). No kinematic interference effects were evident when the location and identity of target were known in advance, regardless of the distractor location. Additionally, the interference effects shown in this dual-task paradigm were not due to the counting-times task per se. Therefore, the frame of reference upon which attention functions might be related to volumetric object representation as well as to the behavioural goal of the task.

To further understand the role of covert and overt visuo-spatial attention in a similar task, Bonfiglioli and Castiello (1998) performed four experiments in which the influence of distractor objects on the temporal evolution of the reach-to-grasp movement towards a target object (i.e., an apple) was examined. In the first experiment, the distractor was another apple, which moved laterally behind the target and occasionally changed direction towards the target, thus becoming the to-be-grasped object. In the second and third experiments, the distractor was a stationary piece of fruit (i.e., a raspberry), which sometimes became the to-be-grasped object because of a change in beam of light. The fourth experiment was a combination of the first two experiments. In all cases, selective interference effects on the transport and manipulation components were observed only when attention to the distractor was covert rather than overt. It is proposed that covert visuo-spatial attention selects information about distracting but potentially important stimuli, such that a registration of significance is accomplished without the need to process all available information. Put simply, interference effects emerge when the distractor receives more attention. Such a conclusion, finds support in patients with spatial neglect. In these patients, who have an attentional bias towards the ipsilesional side, the interference effects for distractors located on that side become more evident during reaching movement (Chieffi et al., 1993).

In a more recent study, to test whether paying attention to an upcoming target object could induce kinematic changes during a grasping action, a sequential motor task has been employed (LeBlanc & Westwood, 2016). An unintentional

motor plan could arise in a movement sequence when an object is attended to. Participants had to reach and grasp a target followed by either a perceptual judgment or motor task associated with a second object. Specifically, once they grasped the target object, they had to verbally report the size of the second object or reach out and grasp it. The formal hypothesis was that, because a sequential action task is processed as a whole (Henry & Rogers, 1960; Hesse & Deubel, 2010), peak grip aperture during the primary grasping action would be scaled towards the size of the second object. These intriguing results have shown that the expected interference effects were only produced when participants attended to the size of second object for a verbal estimation, but not when planning an action to the second object.

The other mechanism proposed for guiding the selection for action process, it is based on an internal representation whereby the action is defined by the direction and distance between the origin of the hand and the target (Howard & Tipper, 1997; Tipper et al., 1992; Tipper et al., 1997). Reaching movements are planned within a hand-centres frame of reference rather than a head- or shoulder-centred frame of reference (Soechting & Flanders, 1989). Support for this claim comes from tasks in which the location of the target and the distractor is not known in advance, and for these reasons it can be assumed that attention is distributed across the scene. These effects are evident on the spatial path of the hand as it reaches for a target. The most significant result of these studies is that the reach path veers towards or away from the objects or locations whose representations should supposedly be inhibited by selective attention (Tipper et al., 1997). In brief, when the target was simultaneously presented with a nearby distractor, the reaching path was affected as the hand trajectory veered away from the distractor. On the contrary, when the target was simultaneously presented with a farther distractor, the hand trajectory veered towards the distractor. Instead, no deviations in hand trajectories were observed when no distractors were presented. In other words, when attention is allocated on the target object, inhibition acts on the representation of potential distractor (Tipper et al., 1998): both target and distractor evoke parallel actions, and competition between these simultaneous responses is resolved by inhibition mechanisms

(Tipper et al., 1997). Other studies based on reaction times and movement-time have shown that the reaction times are impaired less when the distractor is close to the reach path of the target than when off this path but close to the hand (Meegan & Tipper, 1998; Meegan & Tipper, 1999). In a similar experiment, it has been demonstrated that hand movements actually deviated towards and not away from distractor objects (Welsh et al., 1999). The authors suggested that this difference might exist because their distractor objects were not physical barriers to the movement, whereas in many previous studies the distractors were intended to be obstacles to movement. Thus, the deviation towards the distractor object may occur if actions to both objects are planned in parallel and parts of the distractor location "leak" into the movement plan for the target. In these experiments where similar objects were used as the target and the distractor, it is possible that effects were found only for the reaching component of the movement because from a functional and intrinsic point, they produced interference only at the level of the reaching component (Howard & Tipper, 1997; Tipper et al., 1992; Tipper et al., 1997; Welsh & Elliott, 2004; Welsh et al., 1999). An alternative view has been suggested by Tresilian (1998), according to which the changes in trajectory are not caused by selection mechanisms, but rather are a result of the distractor being a 3D obstacle that causes the hand to veer around it. Although this view is more parsimonious than the inhibitory mechanism proposed by Tipper and collaborators (Tipper et al., 1997), this theory is unable to explain many experimental observations that the model of Tipper may explain easily (Castiello, 1999). A clear demonstration of the reliability of the inhibitory mechanism of attention is present in a recent study testing whether selecting an object for perception prioritizes it for action (Sandoval Similä & McIntosh, 2015). In the first experiment, participants attended covertly to a flanker stimulus on one or the other side of a fixated target dot, prior to reaching for that target, which occasionally jumped, after reach onset, to the attended or non-attended side. Participants corrected their reaches for almost all target jumps. In the second experiment, participants were required to covertly monitor the flanker for a flicker during reaching. This concurrent perceptual task globally reduced correction behaviour for the target's jumps, indicating that perception and action

share a common attentional resource. Corrections were especially unlikely towards the attended flanker side. The authors assumed that for reaching to the central target, the participants must actively inhibit the primed flanker location in the relevant motor map, and this inhibition is revealed by a reduced likelihood of online correction if the target subsequently jumps to that location. As the perceptual attention primes an action towards the attended location, this primed action has to be inhibited in order to reach the target. The data thus imply that perceptual selection constrains online action guidance.

It can be advanced that the main difference between the two models here introduced might somehow be ascribable to the 3D properties of stimuli (Castiello, 1998; Castiello, 2001). In other words, when 3D stimuli to-be-grasped are employed in a task, the competition for selection is affected by the processing of graspable properties they shared. On the contrary, 2D shapes projected on the working surface are ungraspable and therefore the competition is resolved only at the reaching component driven by shape location.

All in all, effects like those described above have been interpreted within the context of an action-centred model of visuomotor processing, in which it is proposed that allocating attention to a distracting visual stimulus, whether in a voluntary or involuntary manner, can lead to the automatic planning of an action to that stimulus that competes with the primary action plan via spatial averaging or perhaps response inhibition (Welsh & Elliott, 2004).

1.1.2 Primates

The mechanisms of selection for the control of action have been studied also in non-human primates. In a naturalistic study conducted by Sartori and collaborators (2014), the grasping of objects was investigated in macaques monkeys in two condition. In the first condition, the to-be-grasped object was located to the left or to the right in respect of the monkey and no other objects were within the reaching space. In the second condition, the to-be-grasped object, either to the left or to the right side, was flanked by other objects located to the right of the monkey's outlook and within the reaching space. The results

showed that the amplitude of peak grip aperture correlated with the size of the object in the absence of any other potentially distracting objects in the vicinity. To wit, the amplitude of peak grip aperture was significantly smaller for the smaller objects than for the larger ones and vice versa. However, the most important finding was that, in the second condition, where the to-be-grasped object was not alone, but rather was nearby of other objects, the information from these flanking objects was not ignored, as the amplitude of peak grip aperture was affected by them. In sum, when the animal grasped a large target, flanked by an object eliciting a small grasp, the amplitude of peak grip aperture was smaller than it would have been if the target had been presented alone. The opposite was true, that is, when the animal grasped a small object, flanked by a large one, the amplitude of grip aperture was larger than in the situation with the target in insolation. Recently, in an analogous ecological context, the same research group has studied the macaques while they reached for an object in three different conditions (Bulgheroni et al., 2017). The target to-be-grasped could be presented with no other objects in the vicinity; with another close object but which did not represent an obstacle for reaching (i.e., not impeding movements or requiring changes in trajectory) or with a nearby object which represented a potential obstacle. Indeed, the data showed that the presence of nearby object representing an obstacle affected the wrist trajectory, as it demonstrated greater deviations from the path than in the condition with no other objects present within the reaching space. In particular, the maximum trajectory height, that is, the maximum height from the ground reached by the arm path, revealed that when the nearby object actually functioned as an obstacle, the arm pitched higher relative to the condition with the target situated alone. Interestingly, when a nearby object was present but represented no real impediment for reaching, maximum trajectory height was higher, as in the presence of a real obstacle. These findings demonstrated that the presence of a nearby object, whether it is actually an obstacle or not, renders the reaching trajectory towards the target wider and higher. The type of representation invoked by irrelevant objects contain information regarding the motoric plan that they elicit, and this information interferes with the action programmed for

the target object. Monkeys, like humans, are sensitive to the motoric features related to non-target objects, since they show the potential role as targets capable of triggering action (Castiello & Dadda, 2019).

The results presented here exactly mirror those obtained in the abovementioned studies of humans (Castiello, 1996; Castiello, 1999; Tipper et al., 1997; Tipper et al., 1998). Thus free-ranging macaques and humans appear to share a number of kinematic features, with regard to the selection mechanisms linked to action control (Allport, 1987). This make sense, given that animals have evolved neural information processing systems to facilitate interaction with the environment, thereby maximizing its probability of survival and reproduction. Primates and humans both recognize that, to attain this goal, they must extract appropriate information about the environment via perceptual systems and in a form that can be deployed to guide actions.

1.1.3 Insects

Animals which are lower in the evolutionary scale than vertebrate, such as insects, share with higher animals, such as primates, the need to interact with the environment and to select specific information for the control of action. Despite this, there are no data in available literature regarding the mechanisms of selection for action in insects as those outlined above for humans and non-human primates. In other words, no one knows whether irrelevant non-target stimuli can attract the attention of invertebrate animals during the performance of a goal-directed action and in so doing, influence the motor commands associated with that action.

The current thesis attempts to further investigate the question of selective attention in insects (Nityananda, 2016) with a specific slant on the control of action. To date, there are only few studies in the literature which have approached the attention-like processes in insects. In these studies, attention is viewed as essentially a perceptual problem with the aim to protect the sensory system from a crowded and chaotic stimulation. Although, this might be one of several functions that selective attention serves, it must be mentioned that the

need for selection arises especially when animals are required to act rather than perceive. With this in mind, a definition of attention as a process serving the selection for action assumes also in insects a meaning closer to a function entails selection and inhibition of actions rather than perceptions as suggested by higher animals.

Although not framed within the selection-for-action theory, insects put in place action selection and action inhibition mechanisms. For example, the fruit fly *D. melanogaster* has the ability to select two different kinds of visually evoked escape responses which are performed to avoid looming predator attacks (von Reyn et al., 2014). Particularly, a long take-off duration with the fully raising of wings occurs when the looming stimulus approach slowly. On the contrary, a short take-off duration without the raising of wings occurs when looming stimulus is faster, advantaging speed for survival. The computation for selection of the escape mode is based on two excitatory components, to wit, one encoding the angular size and the other the angular velocity of the looming stimulus (von Reyn et al., 2017). The integration of size and velocity increases the probability that a fly deploy a short take-off duration during a fast predator attack whereby saving time is essential for survival.

To study this kind of action selection mechanisms, several studies have employed a sophisticated flight simulator where a fruit fly is tethered to a pin and positioned inside a virtual surrounding environment which can operate in two modes, that is, the visual surrounding pattern can rotate according (i.e., close-loop) or independently (i.e., open-loop) to the fly's intended yaw responses in the horizontal plane (Götz, 1964; Heisenberg & Wolf, 1984; Wolf & Heisenberg, 1991). By using a combination of such simulator with an infrared light beam as source of heat for flies conditioning, the action selection mechanism has demonstrated also to be tuned with the relative salience of competing visual stimuli (Liu et al., 2006). Flies can make a value-based choice when they are trained in the flight simulator to associate heat punishment with one of two visual bars characterized by different position and colour (i.e., classical conditioning) (Zhang et al., 2007a). Furthermore, even without learning based on classical conditioning, flies can select specific action related to the intrinsic features of a stimulus, either showing

attraction towards it or idiosyncratically repulsing it (Maimon et al., 2008; Grabowska et al., 2018). In particular, flies are attracted, like many other insects, towards long vertical stimuli, whereas they show aversion to small square stimuli. These studies show how fruit flies are able to discriminate visual stimuli and to consequently select the appropriate action via visual attention-like process (van Swinderen, 2011).

Visual attention can be primarily subdivided in two distinct processes (Corbetta & Shulman, 2002). The top-down processing describes the flow of communication from 'higher' to 'lower' centres, conveying information come from previous experience rather than sensory inputs. Instead, the bottom-up processing proceeds unidirectionally from the sensory inputs, through perceptual computation, to the motor output without involving feedback information flowing from 'higher' to 'lower' centres.

Along these lines Wolf and Heisenberg (1980) defined as 'visual attention' the ability shown by flies to restrict the yaw response towards one of two moving objects inside a stationary flight simulator. They demonstrated the existence of a bottom-up attentional processing (Heisenberg & Wolf, 1984). An idea that has been recently corroborated by Sareen and colleagues (2011). By means of a cueing task, these authors demonstrated that when one of two competing vertical stripes was placed in front of flies and oscillated for 5 s prior to the displacement of both stripes, flies responded preferentially with a yaw response polarity corresponding to the displacement of the stripe on the cued side, indicating that the cue guided attention in a top-down manner (Sareen et al., 2011). This study also tested the delay between the presentation of the cue and the displacement of stripes, finding that the cue attracted the attention significantly to its side even after a delay of 2 s, whereas its effect was no longer significant at a delay of 5 s. The guidance of attention to one side was not compromised even if the cueing effect was carried out by an extra stripe (i.e., cueing stimulus) spatially separated from the displaced stripes (i.e., test stimuli). The focus of attention was still effective at an angular distance within a window of ±20 deg around the test stimulus but not with larger distances. It is noteworthy that the sudden appearance of a very salient visual stimulus (i.e., a distractor) had the power to override the

attentional restrictions, as expected in term of a bottom-up attentional processing. Finally, this study remarked how the cueing effect was only effective in the lower visual field of the fly. This aspect is intuitively explainable by the need for a fly to pay attention to the objects positioned below like food, specific landmarks and predators which attack from below, such as robber flies and dragonflies (Sareen et al., 2011). The lasting of the cueing effect, once the cue has disappeared, has been proposed to rely on the signalling of dopamine in the α/β_p compartment of the mushroom bodies (MBs) suggesting a kind of working memory underlying such process (Koenig et al., 2016a).

Taking advantage of the evidence concerned with the fly's ability to shift the focus of attention endogenously, it has been observed that flies keep the focus of attention for up to 4 s at the location where a previous stimulus had elicited a fly's behavioural response (Koenig et al., 2016b). Specifically, when flies faced a series of 60 simultaneous displacements (i.e., front-to-back) of two lateral stripes symmetrically positioned at an angular distance of ±45 deg with respect to the centre, the choice of response polarity (i.e., either right or left stripe) was not exclusively random but seemed to follow a mechanism that favours the formation of chains so that the likelihood for the same response polarity was increased. However, this was true for time intervals between the two displacements equal or less than 4 s (i.e., 1, 2 and 4 s) but not of 5 s. Differently from the visual cueing effect previously presented, here there was no cueing involved. For this reason, the authors have discussed this phenomenon as an attentional span that is formally a behavioural after-effect of the fly's action selection process during the last task. Put simply, flies prefer to choose the same response as the previous one if the time interval duration between them is of maximum 4 to 5 s.

In terms of cueing effect, another study reports different results than the study by Sareen and colleagues (2011). Shiozaki and Kazama (2017) have employed a static visual cue (i.e., a dark stripe on a uniform lit background or vice versa), which was presented for 2 s at 60 deg of eccentricity either to the right or to the left of the fly. Following the presentation of the cue, a delay period of 1 s of uniform illumination was presented before a bar choice task consisting in the presentation of two stripes on both sides at ±60 deg in respect to the fly. In this

paradigm, the flies' choice was strongly biased towards the uncued side either in open- or closed-loop and regardless of the contrast of pattern (i.e., dark or bright stripe). The authors have argued that this phenomenon would be consistent with the location hypothesis. According to this hypothesis the cueing effect generates a location-specific activation and this biases the choice towards the bar at the uncued location. Such a hypothesis is reminiscent of the novelty effect, namely the tendency observed in many organisms to preferentially gaze novel objects over familiar ones.

Overall, the studies here presented provide a clear-cut demonstration about the presence in flies of action selection mechanisms mediated by attentional processes. From this literature it also emerges very clearly that more research is needed to investigate these mechanisms in lower animals as flies. Flies can select a specific stimulus in the environment as target for a goal-directed action but it is not known whether irrelevant stimuli have to be inhibited in order to accomplish the main action, and whether this results in an interference effect.

1.2 THE EXPERIMENTAL MODEL: FRUIT FLY

The fruit fly *Drosophila melanogaster* (from the Greek "dew-loving with a black belly"; *D. melanogaster*), a species of phylum Arthropoda, belonging to the order of Diptera and of the family Drosophilidae, is a well-known model organism for biological research. Several researchers, by employing *D. melanogaster*, have addressed complex biological problems such as the molecular mechanisms that control the circadian rhythms (Zehring et al., 1984; Bargiello et al., 1984; Hardin et al., 1990). Although *D. melanogaster* has chiefly been utilized to investigate biological themes (e.g., genetics, development biology and immunology), it has been also considered for neuroscience research (Bellen et al., 2010). By studying *D. melanogaster*, it has been possible to enlarge our knowledge on the comprehension of the nervous system. In this respect, many fly's behaviours, comparable to those of mammals, enlightening important aspects concerned with the organization of the nervous system have been studied. The access to a large set of genetic techniques to manipulate the completely sequenced genome

(Rubin & Lewis, 2000) allowing to identify whatever phenotypes, is one of the factor that determined the success of flies as an experimental model. The homology of the fly genome with the human one (i.e., over 50% of genes) has prompted scientists interested to use flies for the investigation of the molecular mechanisms underlying the physiological processes that once damaged result in neurological disorders. For example, flies have been widely used as model system for investigating human neurodegenerative disorders such as Parkinson's disease, Huntington's disease and Alzheimer (Bonini & Fortini, 2003). Also the psychiatric disorders have been proposed to be suitable issues to be studied in flies (van Alphen & van Swinderen, 2013; Zordan & Sandrelli, 2015).

Furthermore, thanks to the great improvement of the technical tools for investigating the neural circuits in actively behaving animals, the fruit fly is increasingly becoming one of the most powerful model for studying cognitive neuroscience (Haberkern & Jayaraman, 2016; Giurfa, 2013). *D. melanogaster* is an ideal candidate for integrating molecular, behavioural and cognitive levels of study (Grillner et al., 2005b). The impressive 3D brain volume reconstruction at microscopic level of the 100,000 fly's neurons enables an unprecedented mapping of synaptic connectivity extremely useful for speeding up the comprehension about the circuits function (Zheng et al., 2018).

In the next sections I shall outline the functional neuroanatomy of fly with specific reference to three systems which are at the basis of the selection mechanisms for the control of action: the visual system, the motor system and the higher order visuomotor circuits. Together with the neurobiology of these systems the aim of the following sections is to provide an overview of the visuomotor processes at the bases of the flies motor behaviour.

1.2.1 Visual system

Vision is a fundamental sensory system for *D. melanogaster*. Within its ecosystem, the fruit fly needs to detect and interact with specific items. Very often these items are in movement, either in a reafferent (i.e., endogenously determined) manner, such as food spotted on flight, or in an exafferent (i.e.,

exogenously determined) manner, such as a moving conspecific or predator (Egelhaaf, 2006). The behaviours guided by these visual items are all but simple for the fly and require complex computations performed by many visual neurons that progressively integrate the inputs coming from different parts of the visual field. The computations performed by the two fly's eyes, each one covering about 180 deg of visual field, have been a matter of study since a long time and noticeable progress in their identification have been made (Borst, 2009).

The fly visual system is confined for each eye in the so-called optic lobe (containing more than 60% of all neurons) which is composed by the retina and four retinotopically arranged neuropil layers: the lamina, the medulla, the lobula and the lobula plate (Borst, 2014).

Retina

The retina, which is the most external part of the compound eye of fly, consists of about 750 modular units called 'ommatidia'. These ommatidia are like single functionally independent lens, differently to the vertebrate eyes which are non-compound. The angular distance between the optic axes of two neighbouring ommatidia (i.e., interommatidial angle) is of 4.6 deg. For a comparison, the human's fovea, which covers 2 deg of the visual field, have almost 60,000 cones providing a spatial resolution of about 0.01 deg. Therefore, the low number of 'pixels' forming the fly's eyes (i.e., the ommatidia) would lead to conclude that flies have a poor spatial resolution. Despite this there is no reason to assume that fly sees the world in a pixelated manner (Borst, 2009). Indeed, flies have shown to perceive and react to visual displacements of a pattern towards an unexpected direction by as little as 0.1 deg (Heisenberg & Wolf, 1988), suggesting that the functional visual spatial resolution is much higher than the interommatidial angle. Each ommatidium is composed of 20 cells, 8 of which are photoreceptor cells onto which the corneal lens focuses the light for subsequent phototransduction. The 'rhabdomeres' are the light gathering structure of the photoreceptor neurons made of microvilli which contain the opsins. The 8 photoreceptors are subdivided into three main categories regarding their spectral

sensitivity: six outer photoreceptors forming the peripheral rhabdomeres (i.e., R1 – R6) are blue sensitive and surround other two central inner photoreceptors, the distal R7 cells, which form the apical central rhabdomeres, express one of two different ultraviolet (UV) sensitive opsins, while the proximal R8 cells, which form the basal central rhabdomeres positioning below the R7 cells, express a blue-green sensitive opsins (Zuker, 1996). Contrariwise to what occurs in vertebrate, the light activates the fly photoreceptors via photoisomerization leading to the stimulation of phospholipase C and resulting in activation of two distinct Ca^{2+} permeable channels (i.e., TRP and TRPL) which depolarize the photoreceptor membrane potential (Hardie & Juusola, 2015). Interestingly, while the vertebrate photoreceptors require the reconstitution of opsins through enzymatic reactions consuming time, the reconstitution in flies needs simply the exposition to longer wavelength of light. Moreover, the fly photoreceptors respond to single photons with kinetics about 10 to 100 times more rapidly than vertebrate rods, yet still signal under full sunlight.

The R1 – R6 photoreceptors convey motion information. These photoreceptors are a homogeneous group of cells each of which owns the opsin rhodopsin 1 (Rh1), which shows a peak at 478 nm (i.e., light blue colour) and another one in the UV wavelength range (Yamaguchi et al., 2010). The different R1 – R6 photoreceptors have slightly different optical axes but corresponding photoreceptors within neighbouring ommatidia have parallel optical axes and converge upon the same downstream synaptic units, forming a pathway conveying the same spatial information (Agi et al., 2014). This wiring principle has been termed as 'neural superposition' and it is thought to increase the sensitivity under low light conditions, preserving acuity and providing additional parallel input for efficient visual processing of the day-active fast-flying flies. Compromising these photoreceptors, by means of mutations or genetic silencing, it has been severely impaired the motion vision and consequently the motion-driven behaviours (Heisenberg & Buchner, 1977; Rister et al., 2007).

The R7 and R8 photoreceptors instead enable the colour vision and polarization vision. Their impairment does not affect the motion-driven behaviour (Yamaguchi et al., 2008). Along the dorsal margin of the eye, both R7

and R8 of the ommatidia express rhodopsin 3 (Rh3) which is sensitive to short UV wavelength involved in the detection of the electromagnetic-vector (e-vector) orientation of the polarized light (Wernet et al., 2003; Wernet et al., 2012). In these polarized light sensitive ommatidia the rhabdomeres are untwisted and oriented orthogonally to each other, contrary to the colour sensitive ommatidia where the rhabdomeres are twisted. Also in the ventral area of the eye there are polarized light sensitive ommatidia, in which a combination of photoreceptors R1 – R6 as well as R7 and R8 manifest partially untwisted rhabdomeres (Behnia & Desplan, 2015). The ventrally sensitivity remains poorly understood but it might be useful for detecting or avoiding water surface which reflect the polarized light. Polarization of light seems to be analysed by the fly visual system and conveyed to a central fly circuit to enhance the fly orientation ability for long-range flight of the animals with respect to the sun (Weir & Dickinson, 2012; Warren et al., 2018; Giraldo et al., 2018). The remaining part of the retina contains two types of ommatidia called 'pale' (p) and 'yellow' (y). The p-type ommatidia have R7 cells which express the Rh3 or R8 cells which express the blue sensitive rhodopsin 5 (Rh5). The y-type ommatidia have R7 cells which express the long UV wavelength sensitive rhodopsin 4 (Rh4) or R8 cells which express the green sensitive rhodopsin 6 (Rh6). The 30% of the ommatidia are p-type, while the remaining 70% of ommatidia are y-type. The p- and y-type of ommatidia are stochastically distributed throughout the main part of the retina (Rister & Desplan, 2011). Thus, a comparison of different combinations of R7 and R8 photoreceptors within one ommatidium or between ommatidia allow the colour vision in flies.

Lamina

Although in a no strictly retinotopic manner, the modular organization of the retina is maintained in the first neuropil (mostly unmyelinated nerve fibres and glial cell processes densely interwoven), the lamina, where R1 – R6 cells target to approximately 750 independent units, called 'columns' (Fischbach & Dittrich, 1989). Put simply, visual information from adjacent points of the visual field is processed in anatomically neighbouring columns. R1 – R6 cells form the first

direct tetradic histaminergic synapses with downstream neurons involved in motion processing (i.e., L1 – L3 cells and amacrine cell).

In each lamina column, also called 'cartridge', there are 12 distinct types of cells (Tuthill et al., 2013). Eight cells connect the lamina with the medulla: the five lamina monopolar cells L1 – L5, the two centrifugal cells C1 and C2 and the T1 cell. In addition to these cells, there are four wide-field amacrine cells: the two lamina wide-field (Lawf1 and Lawf2) neurons which receive input from the medulla, the lamina tangential (Lat) neuron which connect the central brain with the lamina and the lamina-intrinsic (Lai) neuron. The amacrine (from the Greek "non-long-fibre") cells are characterized by the lack of axonal process (i.e., anaxonal). At the level of the large monopolar cells of the blowfly, *Calliphora vicina*, the histamine released by the photoreceptor cells (i.e., R1 – R6), binding the chloride channel (Cl^-), leads to a strong and transient hyperpolarization of the cells whenever the light hits photoreceptors (Hardie, 1989). Such electrophysiological hyperpolarization is followed by an sustained hyperpolarized component that tend to disappear with increasing light intensity, while is inversed (i.e., depolarization) when the light is switched off (Zheng et al., 2009). The neurotransmitters used by the fruit fly lamina neurons remain largely unknown, even though, by using single-cell transcript profiling, it has been pointed out that the L1 cells are glutamatergic while the L2 and L4 are cholinergic (Takemura et al., 2011). The L4 cells receive exclusively cholinergic excitatory inputs from L2 cells and send feedback to L2, while L5 cells receive glutamatergic inputs from L1 (Mauss et al., 2017a). It is interesting to note that many of such columnar neurons show an incredible similarity with neurons of evolutionary distant dipteran species (Buschbeck & Strausfeld, 1996). On the contrary the axons of R7 and R8 cells run through the lamina without making synapses and terminate in specific layers of the medulla.

Recently, the development of genetically encoded calcium indicators (GECI) for the functional investigation of the neural activity has allowed recording from the lamina cells of fruit flies. The L1 and L2 cells have shown to hyperpolarize transiently in response to luminance changes as seen in the blowfly, while L4 and specially L3 cells have shown less transient response dynamics (Clark et al., 2011;

Silies et al., 2013; Meier et al., 2014). The Lawf2 neurons have shown a large receptive fields and to respond more strongly to low-frequency luminance fluctuations without showing motion selectivity in whole-cell patch-clamp electrophysiological recordings (Tuthill et al., 2014). Genetically silencing of the L1 and L2 cells makes flies blind to the visual motion and at intermediate pattern contrast L1 cells detect the back-to-front direction of motion along the retina while L2 cells mediate front-to-back direction of motion (Rister et al., 2007). Electrophysiological recordings in motion-direction sensitive cells of the lobula plate have demonstrated that when the L1 cells were genetically silenced (i.e., overexpressing of *shibire*^{ts}), the responses to moving bright edges ('ON') were strongly reduced while the responses to moving dark edges ('OFF') were unaffected (Joesch et al., 2010). On the contrary, when the L2 cells were silenced only the OFF responses were reduced. These results indicate that the L1 cells provide the input to an ON pathway while the L2 cells to an OFF pathway (Strother et al., 2014). The functional role of the other lamina neurons is so far uncertain, for example the L3 cells has been proposed to be involved in the colour vision because they make synapses to the Tm5 cells of medulla, on which make synapses also R7 and R8 photoreceptors (Gao et al., 2008).

Medulla

The second neuropil layer of the optic lobe region, the medulla, is composed of about 750 columns, where the R7 (likely GABAergic) and R8 (likely histaminergic) cells for colour vision make the first synapses and the L1 – L5, C2, C3 and T1 cells for the motion vision assemble, forming synapses partnership with each other, at distinct vertical positions in each column (Fischbach & Dittrich, 1989; Bausenwein et al., 1992). Each medulla column houses about 59 different types of cells and all inputs ramify in ten different strata of the medulla (i.e., M1 – M10). The outer six strata, M1 – M6 of the distal medulla, receive inputs from the lamina cells (i.e., L1 – L5), centrifugal cells (i.e., C2 and C3), T1 cell, R7 and R8 photoreceptor cells.

In brief: L1 projects to M1 and M5 stratum; L2 projects to M2; L3 projects to M3; L4 projects to M2 and M5; L5 project to M1 and M5; C2 projects to M1 an M5; C3 mainly projects to M2 and M3 but extends down to M5; R7 projects to M6; and R8 projects to M3.

However, R7 and R8 have their axons always lay adjacent to each other which make synapses distributed over several zones; R7 has terminals also in M5 and few in M1 stratum, while R8 has presynaptic sites in M1, M2 and M3 stratum.

Most terminals also receive input, from other terminals as well as from medulla circuits, possibly at feedback synapses, and thus they are not exclusively presynaptic. For instance, the terminals of the L1 cells make synapses with the L5 and R8 terminals in M1 stratum, whereas L2 cells make synapses with medulla cells in M2 stratum, which in turn send inputs to L4 cells. There is segregation between the pathways of L1 and L2 which are connected only by the two centrifugal cells C2 and C3. At this level an organization of parallel pathways might supply different functions concerned with the detection of form, polarized light, UV, colour and motion processing (Borst et al., 2010).

The columnar neurons of the medulla are 26 types of transmedullary (Tm) cell within which there are 4 subtypes, 12 medulla intrinsic (Mi) neurons, 13 TmY cells, and 8 distal medulla (Dm) cells (Takemura et al., 2008). In each column these neurons contribute an estimated total of at least 35 actual cells with somata in the medulla layer. The Tm neurons project beyond the medulla, predominantly towards the lobula layer, the Mi neurons connect the outer strata of the distal medulla with the inner strata of the proximal medulla and TmY neurons projections bifurcate to reach both the lobula and the lobula plate layers.

The colour vision conveyed by the R7 and R8 photoreceptors have emerged to make synapse in several medulla neurons as candidate elements of the neuronal circuit for the chromatic information processing. Two very similar medulla cells, Tm5a and Tm5b are postsynaptic to R7 cells while Tm5c and Tm20 are postsynaptic to R8 cells (Melnattur et al., 2014). Tm5a, Tm5b, Tm5c and Tm20 act in parallel as redundant pathways for colour vision.

The motion vision conveyed by the L1 pathway is then sent to the M10 stratum, where the dendrites of the T4 cells branch while the motion information from

the L2 pathway is sent to the stratum 1 of the lobula where the dendrites of T5 cells ramify (Fig. 1.1). In pathways 1, L1 cells make synapses to T4 cells via Mi1 and Tm3 cells of medulla while the L3 make synapses to T4 via Mi9 (Takemura et al., 2013; Takemura et al., 2017). In pathway 2, L2 (and L4) cells make synapses to T5 cells via Tm1, Tm2 and Tm4 cells while L3 cells make synapses to T5 via Tm9 cells of the medulla (Shinomiya et al., 2014). Each medulla column targets four morphologically different subtypes of T4 cells (T4a – T4d) as well as four subtypes of T5 cells (T5a – T5d). Such different subtypes of T4 and T5 neurons responds specifically to one of the four cardinal directions of motion (i.e., up, down, left and right) (Behnia & Desplan, 2015).

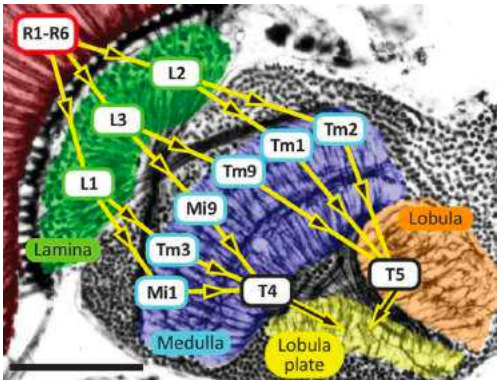

Fig. 1.1 Visual motion pathways. The four optic neuropils: lamina, medulla, lobula and lobula plate. Visual information encoded by R1 - R6 are then conveyed to T4 and T5 cells via the interneurons of the lamina and medulla. Image modified from Takemura et al., 2017.

Lobula

The third neuropil layer of the optic lobe region, the lobula, is subdivided in six different strata (i.e., Lo1 – Lo6). Axons from Tm1 and Tm9 have greatest overlap with dendrites of T5 cells in the Lo1 stratum. Instead, axons from Tm2 have such overlap in the Lo2 stratum, while Tm4 cells extend their terminals from Lo1 deeper to Lo4 (Shinomiya et al., 2014). Imaging and electrophysiological recordings confirmed the segregation of the two pathways involved in visual motion where pathway 1 conveys the light ON information via Mi1 and Tm3 cells

which are important for contrast computation (Bahl et al., 2015), while pathway 2 conveys the light OFF information via Tm1 and Tm2 cells (Behnia & Desplan, 2015). Thus, the first pathway appears to act as the delayed and non-delayed arms of a moving light edge while the second one plays an equivalent role for a moving dark edge.

Lobula plate

The fourth neuropil layer of the optic lobe region, the lobula plate, is subdivided in four different strata (i.e., Lop1 – Lop4). These strata are composed by the presynaptic terminals of T4a – T4d and T5a – T5d cells making each stratum of the lobula plate specifically sensitive to one direction of motion. Lobula plate is organized such that adjacent strata represent opposite directions of motion. Thus, both cells T4 and T5 receive cholinergic inputs and then make excitatory synapses in all four strata with the dendrites of the lobula plate tangential cells (LPTCs) providing wide-field motion input (Behnia & Desplan, 2015). Furthermore, T4 and T5 send input also to inhibitory interneurons, called lobula plate intrinsic (LPi) cells, which convey an inhibitory glutamatergic signal to LPTCs expressing a glutamate-gated Cl^- channel in the neighbouring motion-opponent stratum. Therefore, LPTCs integrate two sources of local, direction-selective information: direct excitation from ON and OFF selective T4 and T5 cells in every lobula plate stratum and indirect inhibition from bi-stratified LPi cells activated by neighbouring T4 and T5 terminals (Mauss et al., 2017a). The silencing of T4 and T5 cells determines the abolishment of the motion response in the LPTCs (Schnell et al., 2012). Moreover, the same neurons blocking have shown to make flies completely blind to visual motion when tested on a treadmill setup (Bahl et al., 2013). The LPTCs are mainly subdivided in two types: the horizontal system (HS) cells and the vertical system (VS) cells (Borst, 2014). The dendrites of the HS cells are confined to the most frontal stratum of the lobula plate, whereas the dendrites of the VS cells branch in the most posterior stratum. Basing on the dendrites location the HS cells can be categorized in northern (HSN) HS, equatorial (HSS) HS and southern (HSS) HS (Schnell et al., 2010).

Whereas, at least six VS cells (VS1 – VS6) have been identified (Joesch et al., 2008).

Anatomical studies in the blowfly *Calliphora vicina* (called also *C. erythrocephala*) have shown that HS and VS cells are gap junction-coupled to the neck motor neurons (Strausfeld & Bassemir, 1985; Haag et al., 2010; Wertz et al., 2012). The HS and VS cells are thought to drive the optomotor response elicited by the wide-field visual motion. Indeed, inactivation of these cells through genetic mutation that reduces the size of the entire lobula plate has shown to strongly affect the optomotor turning reactions (Heisenberg et al., 1978). Moreover, selective optogenetic activation of the HS cells elicits robust yaw head movement and yaw turning responses in tethered flying and walking fruit flies (Haikala et al., 2013; Busch et al., 2018). The HS cells depolarize in response to a pattern moving front-to-back in respect to the fly gaze and hyperpolarize during opposite back-to-front motion (Schnell et al., 2010). The VS cells depolarize in response to a pattern moving downward and hyperpolarize during opposite upward motion (Maimon et al., 2010). Recent electrophysiological recordings have confirmed that the HS cells respond strongly to yaw and weakly to pitch and roll; the VS1-3 cells respond strongly to pitch and roll but weakly to yaw; while the VS4-6 cells respond strongly to roll with intermediate responses to yaw but almost nothing to pitch (Kim et al., 2017a). Interestingly, the same trend of the cells response to yaw movement of a visual panorama in terms of magnitude, that is, strongest depolarization response in HS, intermediate in VS4-6 and weakest in VS1-3, it has been highlighted for the hyperpolarization response during a fast contraversive turning (i.e., saccade-related potentials) which it seems owed to the silencing of the cells by means of a motor efference copies (Kim et al., 2017a; Kim et al., 2015).

Finally, the HS and VS cells have shown to be modulated by the locomotion state of the fly increasing their response during walking and flying (Chiappe et al., 2010; Fujiwara et al., 2016; Maimon et al., 2010). Such an effect is mediated by the octopamine released during motor activity (Suver et al., 2012). Octopaminergic neurons increase the excitability of the Mi4 cells and sustain the

behavioural responses to fast-moving but not slow-moving visual stimuli in walking flies (Strother et al., 2018).

Optic flow response

D. melanogaster exhibits a large repertoire of visually guided behaviours (Heisenberg & Wolf, 1984). The ethological function of some these behaviours remain unclear while appear to have a specific significance in many others. For example, the aim of the tendency shows by flies to approach a light source called phototaxis (Carpenter, 1905), one of the first visually guided behaviours described, is nowadays still unknown (Gorostiza et al., 2016). Amongst those with a clear function instead, one of the most important is the visual course control for stabilizing flight and walking to counteract external perturbations (Götz, 1964; Götz & Wenking, 1973; Götz, 1975). Since the weight of a typical *D. melanogaster* is approximately of 1 mg and it can reach a forward speed of 80 cm s^{-1}, an abrupt gust of wind, for instance, can easily disturbs the course of flight (Dickinson & Götz, 1996). For these reasons, the fly control behaviour is mostly based on the wide-field optic flow, which is a fundamental source of visual motion information to perform smooth manoeuvre and to correct the velocity of flight.

The optomotor response, that is the reflexive behaviour exhibited by flies in attempting to turn in the same direction of a rotating visual pattern, is the most studied. It has been firstly demonstrated by using a simulator in tethered flying and walking *D. melanogaster* (Götz, 1964; Götz & Wenking, 1973). This behavior is also present in freely behaving flies, suggesting its independence from the type of locomotion and experimental setup (Götz, 1975; Mronz & Lehmann, 2008). Moreover, such a response is not exclusively related to yaw (i.e., rotation around the vertical body axis), but occurs also in pitch (i.e., rotation around the transverse body axis) and roll (i.e., rotation around the longitudinal body axis) behaviours (Blondeau & Heisenberg, 1982). The selective direction signal of visual motion was elegantly investigated in a seminal study conducted by Hassenstein and Reichardt (1956). These authors developed a model for elementary motion

detection, called Hassenstein-Reichardt model, by studying the optomotor response of a beetle *Chlorophanus viridis* walking on a spherical Y-maze that was light enough to be held and moved by the beetle legs. By counting rightward and leftward turnings they assessed the tendency showed by beetles to turn according to visual surrounding movement in order to maintain a straight heading in spite of the false perception of a reafferent motion in the opposite direction determined by the wide-field optic movement. Basically, the model surmises that luminance signals are subtracted by two local mirror-symmetrical subunits which apply two different temporal filters, that is, a low- and a high-pass filter. A 2D array of such local elementary motion detectors (EMDs) throughout the eyes is thought to provide the optomotor response by spatially integrating the output of all EMDs. As a corollary of the model, some predictions have been advanced and verified in the optomotor response of *D. melanogaster*. For example, response strength increased with increasing of pattern contrast; response velocity optimum; and grating patterns with different spatial wavelength show different velocity optima (Borst, 2014). In sum, together with the proprioceptive inputs, optomotor response guarantees a straight path of locomotion compensating unintended turnings. Specifically, the reflexive steering responses syndirectional with the wide-field optic flow allow eventually the fly to correct possible unwanted reafferent movements in order to carry out the programmed path. The fly optomotor response can be compared to the human optokinetic nystagmus which stabilizes the eye during movement (Büttner & Kremmyda, 2007). As a consequence of the optic flow, regulating the angular velocity along the retina of the environment image, flies control also the flight speed as it has been shown in bees (Srinivasan & Zhang, 2004; Fry et al., 2009; Creamer et al., 2018). In other words, flies equate the overall optic flow on their eyes to move straight and adjust their speed. Flies show changes in the horizontal acceleration in response to changes in the ventral optic flow velocity but, surprisingly, they do not exhibit change in altitude as posited by an altitude regulator model (Straw et al., 2010). Rather, they track the height of the horizontal edge as it changes over time to adjust their altitude. Anyway, the wide-field vertical motion is stabilized by flies via changes in climb rate (Götz, 1968) similarly to the syndirectional turnings of

the optomotor response during horizontal motion (Götz, 1964). Nevertheless, unlike edge fixation, such reflex due to vertical optic flow would stabilize altitude only against perturbations without specifying the height of the flight.

In some types of behavioural assay, it has been shown how flies move in the opposite direction with respect to the moving visual pattern. For example, when a group of free walking flies is inserted in a 'hallway' arena and then subjected to a moving grating pattern, flies move against the direction of the grating motion (Zhu et al., 2009). Particularly, in response to centrifugal motion, flies quickly converge at the center, while in response to centripetal motion, flies segregate equally to the two ends of the hallway. This behaviour might be somehow consistent with the control effects determined by the vertical optic flow. Taking into account that in this setup the flies are contained within a clear acrylic tube in the center of a three-sided visual hallway, the fact that flies can see the visual grating beneath might determine a sort of movement regulator for walking based on the vertical optic flow.

Smooth pursuit behaviour

Another fundamental visually guided behaviour in flies is the smooth pursuit behaviour, also known in flies as 'fixation' (i.e., the pursuit of a specific target moving with respect to a background).

The wide-field optic flow discussed in the previous section represents a background onto which can be superimposed the relative motion of a visual object. Animals would keep gaze still on an object during fixation to avoid the blur that results from the long response time of the photoreceptors (Land, 1999). Blur begins to degrade the image at a retinal velocity of about 1 receptor acceptance angle per response time. Thus, object velocities that overcome the ratio between receptor response time and receptor acceptance angle are not well perceived and require fixation.

Flies require tracking of items to navigate within the environment in order to attain specific aims, such as chasing of a conspecifics for mating (Land & Collett, 1974). Fixation behaviour has been largely studied in flies which show a tendency

to keep a visual object in front of them. Reichardt and Wenking (1969) employed a close-loop flight simulator coupling the online output measures from a torque meter, on which a *Musca domestica* fly was rigidly tethered, to a visual surrounding landscape consisting of a vertically oriented stripe. In such a way, the fly was enabled to control its visual input. By using this setup, they demonstrated how the flies preferred to keep the stripe in front of them. Subsequently, in a theoretical approach of the fixation phenomenology, Poggio and Reichardt (1973) described the stochastic fluctuation of the stripe caused by the symmetric yaw torques of flies and the asymmetric optomotor response to the stripe rotation, between progressive (i.e., front-to-back) and regressive (i.e., back-to-front), as the necessary requirements for the smooth fixation. Specifically, in open-loop configuration the progressive rotation of a black stripe from front to back in respect to fly heading results in a stronger yaw response than the regressive rotation from back to front. This imbalance response, which provides to flies the opportunity to push the stripe towards the front, would be based on a linearized mathematical description of two terms regarding the stripe: angular position and velocity. Although some investigators have stated that the motion-direction sensitive cells cannot provide position information, according to Poggio and Reichardt (1973) this argument cannot be accepted since it is obvious that asymmetrically responding motion detectors may provide the necessary requirements for position information. Moreover, these authors described with the 'superposition principle' the fly's response in a composite visual panorama, consisting of a collection of stripes, whereby the turning tendency is elicited by each stripe independently.

The fixation has been studied in walking flies too. Horn and Wehner (1975) presented to fruit flies two stripes on a plexiglass drum surrounding an open circular arena of 20 cm diameter where in they were free to walk. Once flies got access to the arena by means of a hole positioned at the centre of the arena, they were faced with two stripes which could be separated by different angular distances. Flies were free to choose the preferred direction and their position was determined by recording the angular wedge (72 wedges of 5 deg width composed the entire arena) they crossed at a distance of 3 cm from the centre of the arena.

If the angular distance between the stripes was less than 60 deg, in average flies preferred to move along the direction corresponding to the bisector of the angle between the stripes. Conversely, if angles greater than 75 deg were considered, flies showed to chose one of the two stripes, resulting in a distribution of flies' orientations with two maxima peaks matching the angular position of the two stripes. Either dark stripes on a bright background or bright stripes on a dark uniform induced the same preference response. The authors explained this behaviour as the superposition of two turning tendency functions (with peak at 30 deg) phase shifted depending on the angle subtended by the stripes in compliance with the superposition principle of Poggio and Reichardt (1973). This interpretation was based on an indirect measure of the turning tendency function because of a single flies' position recording, hence interaction effects due to the angular distance between the stripes might be an alternative explanation. For example, Reichardt and Poggio (1975) argued that a pure superposition principle would not hold for angular distances up to 80 deg because the effect produced in the visual system comes out to be a nonlinear inhibitory interaction. The lateral inhibition, which decreases with the increase of the angular distance between the stimuli, would play an important role in the mechanism of spontaneous pattern preference (Horn, 1978). As matter of fact, when freely walking flies are subjected to the so-called 'Buridan's paradigm', a fascinating innate behaviour emerges (Bülthoff et al., 1982; Götz, 1980). Namely, inside an arena with only two inaccessible opposite dark stripes (i.e., at angular distance of 180 deg) on a bright background as surrounding landscape, flies typically continue to run back and forth between these two opposing stripes, alternating fixation and anti-fixation behaviours. This phenomenon has been compared to the regularity and persistence of ambiguity effects typical of the multistable perception, such as the reversal of perspective depth of a Necker cube (Bülthoff et al., 1982).

Saccadic response

The fruit fly locomotion is mainly characterized by two components: straight path sequences interspersed with rapid changes in heading termed 'body-

saccades' which resemble the human eye saccades (Heisenberg & Wolf, 1979). In free flying flies, such saccades have approximately an amplitude of 90 deg and a duration of less than 100 ms (Tammero & Dickinson, 2002). In magnetically tethered flies, the average amplitude of saccades is of 35 deg performed in 80 ms and, as in free flight and rigidly tethered flies, saccades are triggered by the image expansion of a pattern or a looming object similarly to the stimuli that evoke landing or escape responses (Tammero et al., 2004; Bender & Dickinson, 2006).

By interpreting this behaviour on the basis of the EMDs array, the asymmetry in output owed to the expansion provides the direction of the saccade, but not its amplitude. Indeed, once initiated, visual feedback does not appear to influence the saccade kinematics further. Such all-or-none event cannot be explainable with the linear models of flight control based on the optomotor equilibrium (i.e., motoric compensation of moving visual pattern).

It has been shown how saccades account for at least 80% of total change in heading during free flight and that an aversive saccade to avoid the collision with a post is evoked when it subtends a retinal size of about 33 deg (van Breugel & Dickinson, 2012). Likewise, during landing flies actively turns towards a stationary post via a directed saccade without a specific retinal size, begin to decelerate computing both the size of the post and its rate expansion on the retina (i.e., 10-20 cm from the post covering a retinal size of 5-10 deg) and, finally, extend their leg when the post reaches in average a threshold retinal size of about 60 deg (van Breugel & Dickinson, 2012).

In the evading response of a looming object, flies perform banked turn consisting of a rapid rotation about yaw, roll and pitch axes followed by an active counter-rotation to damp the manoeuvre (Muijres et al., 2014). This change in heading appears five times (5300 deg s^{-1}) as fast as during the voluntary (1000 deg s^{-1}) saccadic turns (Muijres et al., 2014).

During evasive manoeuvres, which have to favour quick heading changes, the yaw is poorly controlled in the early phase requiring later angle correction, whereas during voluntary body saccades the yaw correction is better coordinated so as to restrict retinal slip to a brief period (Muijres et al., 2015). These two dynamics of maneuverer are remarkably stereotyped regardless the variation in

the size, degree and speed of the saccade. However, they are different enough to suggest that distinct motor programs produce them.

Recently, an intriguing study has investigated the features of saccade compared to smooth pursuit movement in magnetically tethered flies free to rotate about the yaw axis (Mongeau & Frye, 2017). The authors have studied the different dynamic between saccadic and smooth flight movements generated by fixation of a rotating bar (i.e., bar-fixation) or by wide-field optic flow, wondering whether flies can tune catch-up saccade commands for object fixation or optomotor tracking. The results they have found suggest that the wide-field optic flow controller for the optomotor smooth compensation would trigger also the optomotor saccade by a threshold in the temporal integral of retinal slip motion (i.e., based on the velocity controller). On the contrary, the small-field bar-fixation saccade would not be triggered by a threshold in the absolute retinal position but rather by a threshold in the temporal integral over narrow space between the bar position and visual midline (i.e., a relative bar position) with an offset of approximately 45 deg. Accordingly, the authors have proposed a hybrid control system which would contain two different components: a wide-field optic flow integrating component and a saccade trigger component for object fixation which might be based on the small object sensitive neurons (i.e., LC10 and LC11) discovered in the lobula layer (Keleş & Frye, 2017; Ribeiro et al., 2018).

Spontaneous saccades, that is, saccades which are not tied to any obvious external stimulus, have shown to be shorter, faster and larger in amplitude than the bar-fixation saccades (Mongeau & Frye, 2017). Although, by using complex searching algorithms applied in free flying flies to automatically categorize the components of locomotion, it has been found that the 93% of the saccades are visually, rather than spontaneously, triggered (Censi et al., 2013). The body saccades are also performed by walking flies, where they separate rotational from translational movements by quickly turning their bodies by 15 deg in about 100 ms (Geurten et al., 2014). Walking flies can also move their heads by up to 20 deg in respect to their bodies, but they do not turn its head relative to its body during saccadic turns.

1.2.2 Motor system

As in vertebrates (Kiehn, 2016), *D. melanogaster* needs to integrate the information coming from many sensory inputs in an anterior (or cerebral) ganglia and to convey such computations downstream towards the posterior ganglia (i.e., the nerve cord) where the commands are then implemented in the movements of legs and wings. The neural circuits which compose the posterior nerve cord of the central nervous system (CNS), known as ventral nerve cord (VNC) because of its ventral position, process higher order information in order to generate independent motor outputs for controlling and coordinating sequences of muscles contractions. Noteworthy, some movements, such as walking or taking off for flight, can be executed even when the brain is removed, indicating that the circuits in the nerve cord generate autonomous rhythmic motor outputs (Harris et al., 2015). These motor rhythms, which require highly coordinated contractions of a large number of muscles in a quite dynamic way, have shown to be generated by the so-called 'central pattern generators' (CPGs). The CPGs are specialized networks in the CNS which can intrinsically produce rhythmic motor outputs upon continuous activations performed by the brain or other region of CNS (Bidaye et al., 2018). The command inputs from the brain are combined with the CPGs and the resulting outputs are in turn affected by the sensory feedback. The interplay between CPGs, sensory signals from the legs and the coordinated influences between legs can explain most of the features related to the stepping and walking behaviours in insects. Nevertheless, the role played by the brain remains fundamental for the integration of visual, chemosensory and proprioceptive inputs during the execution of such motor outputs (Frye & Dickinson, 2004; Lehmann & Bartussek, 2017).

Ventral nerve cord

The VNC is composed by a large number of neurons that can be classified according to their function and morphology: the local interneurons (INs) modulate and generate rhythmic motor outputs; the ascending neurons (ANs)

convey information from the VNC to the brain; the descending neurons (DNs) relay information from the brain to the VNC; the sensory neurons (SNs) send information from the wings, legs and halteres to VNC; and the motor neurons (MNs) make synapses onto muscles for causing muscle contractions (Venkatasubramanian & Mann, 2019).

The VNC is dominated by four thoracic neuropils that correspond to the three thoracic segments (i.e., T1-3) and one fused posterior abdominal ganglia: prothoracic, mesothoracic, metathoracic and abdominal neuropil. Moreover, between the prothoracic and mesothoracic neuropils there are other two small neuropils: the accessory mesothoracic neuropil, which mostly receives wing sensory afferents and the tectulum, which controls the flight and other wing-related behaviours.

The post-embryonic neurogenesis of the VNC arise from 25 distinct neuroblasts progenitors whose development determines 33 hemilineages which segregate in 16 anatomically distinct neuropils, likely representing also functionally distinct modules that contribute to specific motor outputs (Namiki et al., 2018; Venkatasubramanian & Mann, 2019).

Descending neurons

In *D. melanogaster* it has been estimated that ~3,600 fibres traverse the cervical connective which has on average a diameter of 35 μm (Coggshall et al., 1973). Hsu and Bhandawat (2016) have recently provided the first comprehensive description of the fruit flies DNs identifying ~1,100 of these tracts as fibers whose cell bodies are DNs distributed across 6 clusters in the brain, while the remaining ~2,500 would be ANs which convey motor and sensory inputs from the posterior ganglia to the brain. Three clusters of cell bodies belonging to DNs are localized in the anterior portion of the brain: the anterior optic tubercle (AOTU) cluster located lateral to vertical lobe of MBs and medial to AOTU; the anterior ventrolateral protocerebrum (AVLP) cluster located between AVLP and antenna lobe (AL); and the periesophageal (PENP) cluster located between PNEP and AL (Ito et al., 2014; Hsu & Bhandawat, 2016). Whereas, the other three clusters are distributed more

posteriorly: the pars intercebralis (PI) cluster is located dorsally and between the two hemispheres forming a sort of autonomic nervous system; the gnathal ganglia (GNG) cluster also known as subesophageal ganglion, which is the largest cluster positioned ventrally to the cerebral ganglia; and the superior medial protocerebrum (SMP) cluster which encompasses the posterior superior medial protocerebrum, the superior intermediate protocerebrum, the posterior lateral protocerebrum (PLP), the inferior bridge (IB) and the superior clamp (Hsu & Bhandawat, 2016). The authors have also differentiated the DNs on the basis of the neurotransmitter they release highlighting DNs for all the chemicals tested: acetylcholine, GABA, glutamate, serotonin, dopamine and octopamine (Hsu & Bhandawat, 2016). The 38% of DNs are excitatory cholinergic neurons, the 37% are inhibitory GABAergic neurons, the 6% are glutamatergic and the 3% are serotoninergic. In contrast to vertebrate DNs, which are mostly excitatory, fruit flies DNs express equally excitatory and inhibitory neurotransmitters. These two opposite pathways might be necessary for the control of the two types of locomotion that flies can adopt: flying and walking.

More recently Namiki and collaborators (2018) have identified 190 bilateral pairs of DNs (380 DNs total) and created a library of genetically engineered flies which strictly target 133 of these DNs in order to understand their anatomical and functional organization. By means of cluster analyses aimed at grouping similar items, they have determined two different pathways connecting specific regions of the brain to each of two motor neuropils associated with a specific form of adult fly locomotion. A pathway of DNs linking the posterior slope to the wing neuropil in VNC would maintain flight and inhibit walking, whereas another pathway linking the GNG to the leg neuropil in VNC would maintain walking and inhibit flight (Namiki et al., 2018). Specifically, the first pathway of DNs connects the posterior slope (PS), inferior (IPS) and the superior (SPS), to the dorsal neuropil of the VNC, in which the neck/wings/halteres neuropil can be found. In the second pathway, the DNs connect the GNG to the ventral neuropils of the VNC carrying information to the leg neuromeres. A third pathway connects a large number of brain neuropils to the tectulum which is involved in behaviours

requiring sensory integration and motor coordination of both leg and wings such as looming-evoked escape take-off or courtship (Namiki et al., 2018).

An analysis of the expression based pattern on different reporters for cell membrane and synaptic boutons have allowed distinguishing input and outputting sites of these DNs. Of the 41 neuropils composing the brain, 28 were innervated by DNs, the largest region innervated was the GNG and the largest number of inputs was identified in the IPS (Namiki et al., 2018). The input regions have been clustered in two main groups: the first group includes dendrites in a set of posterior neuropils (i.e., PLP, SPS, IPS, epaulette, vest, lateral accessory lobe) which receive inputs from the lobula plate (PLP, SPS and IPS) and the central complex (lateral accessory lobe); whereas the second group includes dendrites in wedge, gorget, AVLP and posterior ventrolateral protocerebrum (PVLP) which receives the bulk of optic projections from the lobula. The DNs with dendrites in GNG have shown to receive almost no input from other neuropils. Instead, regarding the output sites in the VNC, two clusters have been detected: one targeting the three ventral segmental pairs of leg neuromeres and another one targeting the three dorsal neuropils associated with the neck, wing and halteres residing respectively in T1, T2 and T3 segment. Since the 78% of DNs have shown output in the GNG, their role might be to inhibit the walking promoting DNs receiving input in this region (Namiki et al., 2018). In turn this might signify that they send significant information to the GNG after receiving input from other neuropils of the brain (e.g., posterior slope) and before sending the information in VNC (i.e., dorsal neuropil). Support to this connections comes from the desert locust *Schistocerca gregaria* which maintains walking even without the cerebral ganglia and the spontaneous bouts are prolonged (Kien, 1983). Whereas in the cockroach *Periplanatea americana*, the walking activity is reduced and the flight duration is prolonged after a lesion or reduced neural activity in the subesophageal ganglion (Gal & Libersat, 2006; Kaiser & Libersat, 2015). Because the GNG also receive inputs from ANs conveying a somatotopic sensory map (Tsubouchi et al., 2017), the integration within the GNG of inhibitory inputs from the DNs innervating the cerebral ganglia and the afferent

sensory inputs might be essential for the selection of the specific locomotion type to employ.

The DNs are the exclusive routes that drive the computations underlying the planning of goal-directed actions to their execution. Their activity plays a fundamental role in the interaction with the environment because they are responsible for the initiation or modification of the motor rhythmicity performed by CPGs, without specifying the details of the motor actions. Despite the important role played by DNs, very little is known about their functions and only recently some efforts have been put in the comprehension of their functional organization at cellular level (Suver et al., 2016; Cande et al., 2018). Nevertheless, the functions of some DNs such as the giant fibre interneurons (GFs), the moon walker descending neurons (MDNs) or the pIP10 descending neurons have been well characterized (Bidaye et al., 2014; von Philipsborn et al., 2011; von Reyn et al., 2014). The activation of GFs, for example, is sufficient to elicit a specific coordinated take-off response in which the GFs' axons, terminating on the jump muscle MNs and other INs, drive a stereotyped contraction of the tergotrochanteral muscles (TTMs) and dorsal longitudinal wing depressor muscles (DLMs) (von Reyn et al., 2014). Interestingly, two visual types of neuron have been shown to project to the GFs providing the features necessary for detecting an approaching objects and driving an escape take-off (von Reyn et al., 2017; Ache et al., 2019; de Vries & Clandinin, 2012). The lobula columnar type 4 visual projection neurons (LC4) encode the angular velocity of a looming object whereas the lobula plate/lobula columnar type 2 visual projection neurons (LPLC2) provide the angular size of the object. A model summing a linear function of angular velocity and a Gaussian function of angular size reproduces the GFs escape response dynamics and predicts the peak response time (Ache et al., 2019).

Motor neurons

Notwithstanding the huge manoeuvrability of fruit flies, the number of motor neurons (MNs) involved in the control of flight (i.e., ~24 MNs) corresponds

roughly to the number of muscles controlling the wings (Ikeda & Koenig, 1988; Harcombe & Wyman, 1977). For example, fruit flies and hummingbirds share a quite similar aerodynamic agility but surprisingly fruit flies need much less MNs to control such a complex behaviour (Dickinson & Muijres, 2016; Donovan et al., 2013). In general the muscles of arthropods are innervated by few MNs (i.e., 1-3 MNs) if compared to other animals. A human limb is innervated by ~50,000 MNs while a fly limb by 1000 times less neurons which drive the muscles force by activating individual muscles in graduated manner (Hsu & Bhandawat, 2016). However, in comparison to this three-orders of magnitude difference in the number of MNs between vertebrates and invertebrates, the ratio between the number of INs in the body ganglia and the one of the MNs is much more similar, meaning that spinal circuits are equally complex. Recently, O'Sullivan and coworkers (2018) have dissected the functional role of the MNs involved in flight and male courtship song, pinpointing in almost all the tested MNs the ability to control at least one of the two main song modes: the pulse song, consisting of trains of single wing beats with frequency around 200 Hz and the sine song, generated by the continuous wing oscillations for several seconds with a frequency of 150 Hz. The basalare 2 MN was the only one involved exclusively in the flight ability, other 8 MNs were instead involved in both courtship song and flight, whereas the pleurosternal 1 MN was the only one involved in the pulse-specific phenotype.

A *D. melanogaster* is able to beat its wings more than 200 times per second and the aerodynamic of its flight may be described by the friction between wings and surrounding medium (i.e., viscosity of air) and the inertia of the body (i.e., resistance to any change in its velocity) (Zanker, 1990). However, by using high-speed video recordings of free flight manoeuvres it has been indicated that even in small insects such as *D. melanogaster*, the torques created by the wings act mostly to overcome the body inertia and not the friction (Fry et al., 2003). The negligible effect of the friction would be evident during saccade, where the necessity of a counter-torque to terminate the rotation of the body would not be required to overcome the viscous forces acting on the body. Indeed, at the onset of saccades, the outside wing tilts back and beats with a greater stroke amplitude

than that of the inside wing and after 12.5 ms the condition reverse according to the need to generate a counter-torque deceleration. Other authors have argued that the friction contributes about 100 times more than the body alone to the yaw turning behaviour in *D. melanogaster* because it determines both the precision with which the animal needs to control the torque around its vertical axis and potentially also the need for sensory feedback from organs such as the halteres (Hesselberg & Lehmann, 2007). The large asynchronous indirect flight muscles (A-IFMs) generate the back and forth wings motion by stretch-activated oscillations, whereas the smaller steering muscles control flight by wing hinge reconfigurations of the thoracic oscillator (Lehmann & Bartussek, 2017). Interestingly, the dendrites of MNs innervating the A-IFMs reside in the most dorsal portion of the wing neuropil, whereas the dendrites of MNs innervating the steering muscles reside primarily in the ventral layer of wing neuropil (Namiki et al., 2018). Recent Ca^{2+} imaging recording of the steering muscles during visually mediated responses have revealed that each anatomical group is equipped with a phasic muscle capable of generating large transient changes in wing motion and small active tonic muscles that allow continuous graduated regulation (Lindsay et al., 2017). These two systems (i.e., phasic and tonic) would receive descending convergent input from two pathways, one that mediates spontaneous feedforward-based rapid and large steering manoeuvres and another that mediates feedback-based compensatory fine-scale adjustment.

In walking, *D. melanogaster*, as the vast majority of animals able to legged locomotion on land, has to push its six legs against the ground producing an equal and opposite ground reaction force. Humans for example, vaulting up and over each stiff leg making an inverted pendulum, transform the kinetic energy in the first phase into gravitational potential energy which is recovered as the bodies fall forward or downward in the second phase (Dickinson et al., 2000). In other words, kinetic and gravitational potential energy is temporarily stored as elastic strain energy in muscles, tendons and ligaments for the subsequent recovery during the propulsive phase. In insects, which are sprawled-posture animals, the lateral energy exchange fulfils the same function, that is, energy storage and recovery may occur within the horizontal plane, orthogonal to the

direction of motion. The legs push laterally and determine a robust gait which can be regulated as the animal changes speed, moves over uneven ground or changes its heading by modifying the force of a single leg (Domenici et al., 1999). The walking behaviour in *D. melanogaster* is quite flexible and the neural controller producing inter-leg coordination is not restricted to a fixed motor pattern rather than it generates distinct neural programs. Unlike vertebrates which suddenly switch from one gait to another, flies rely on a continuum of gait patterns that correlate with walking speed (Mendes et al., 2013). Flies show tripod coordination at high speed, tetrapod coordination at medium speed and at very low speed the walking is often accomplished by simultaneous stance phases of five legs while only a single leg is in swing phase at a time (Wosnitza et al., 2013). Since each muscle of the flies' forelegs (i.e., T1 segment) is innervated by 53 MNs derived from 11 independent neuroblasts (Baek & Mann, 2009), it is likely that different subsets of MNs play different roles in the walking speed. Recently, the leg motion has been proposed to be controlled by at least two different descending systems, one which likely contacts premotor leg circuits for controlling the proximal leg joints, and another one which has the opportunity to control the MNs innervating the muscles spanning all leg joints (Namiki et al., 2018). Afferent information conveyed by different types of SNs, such as the chemosensory (i.e., gustatory receptors of sensilla) and the mechanosensory receptors (i.e., bristle, hair plate and campaniform sensilla) that include the proprioceptive chordotonal organs (Tuthill & Wilson, 2016; Montell, 2009), project to the leg neuromeres affecting the descending information. For example, the proprioceptive sensory feedback (Sherrington, 1906), that is the sense of self-movement and body position, is important for the motor control (Mamiya et al., 2018). However, disruptions of this sensory feedback compromise the parameterization of steps and the walking precision, especially at low speed but they do not interfere with the ability to execute coordinated gait (Mendes et al., 2013).

1.2.3 Integration circuits: the central complex

In order to implement beneficial behavioural actions the stimuli from the outside world have to be computed by CNS through neural code at the level of intersection between sensory and choice information (Panzeri et al., 2017). As outlined above, in fly's brain there are neuropils for visual and motor processing. The high-order structure of the fly's brain, whereby the integration between visual and motor systems is likely to be achieved, lies in the central brain, a highly conserved structure across insect species. More specifically, it would be an ensemble of neuropils located along the midline of the protocerebrum termed as central complex (CX) (Strausfeld, 2012). In support of its integrative role for the accomplishment of high cognitive functions, the CX is characterized by widespread functional connections across the brain and none DNs have been found in it (Mann et al., 2017; Namiki et al., 2018). The CX receives mostly visual inputs, although not exclusively, and it would integrate information coming chiefly from two orthogonal functional pathways which cross each other: the spatial azimuthal direction (i.e., where) and the visual object information (i.e., what) (Pfeiffer & Homberg, 2014).

Interestingly, the CX has been proposed resemble the vertebrate basal ganglia from a structural and functional perspective (Strausfeld & Hirth, 2013b). Both these structures share several genes involved in their development, as well as the function of selection and maintenance of behavioural actions. According to Fiore and collaborators (2015), CX (in particular the ellipsoid body) and basal ganglia are ideally positioned for action selection, because of their anatomical location being downstream of sensory inputs and upstream of motor outputs. Moreover, dysfunctions of these structures similarly result in behavioural impairments which span from motor and memory abnormalities to attention and sleep disturbances (Strausfeld & Hirth, 2013b).

STRUCTURAL PROPERTIES The CX is composed by four neuropils: the dorsocaudal protocerebral bridge (PB); the rostroventral central body, which in turn is subdivided in an upper division called fan-shaped body (FB) and in a

lower division called ellipsoid body (EB); and the noduli (NO) which are two globular neuropils attached below the central body (Hanesch et al., 1989). A putative fifth neuropil called asymmetrical body (AB), has been recently located ventrally to the FB and dorsally to the NO (Wolff & Rubin, 2018).

The neurons constituting these four neuropils are characterized on the basis of the differences in arborisation patterns. Three main categories of cells can be distinguished: columnar neurons, which are small-field cells connecting different neuropils or regions of the same neuropil (typically running dorsoventrally in a columnar fashion); tangential neurons, which are large-field cells forming strata perpendicular to the columns generally within one neuropil such as FB or EB; and pontine neurons. The latters are interneurons linking arborisation domains in two different slices or layers of the same neuropil.

The appearance of the CX along development is identifiable in the third instar larva implying a functional role for the adult brain. The PB and the FB are the first structures to develop in their immature form, then the noduli and finally the EB (Young & Armstrong, 2010a). The fact that the later development of the EB matches the compound eyes differentiation reveals a close relationship of this structure with the visual system (Homberg, 2008; Pfeiffer & Homberg, 2014).

FUNCTIONAL PROPERTIES Studies on the functional role played by the CX have highlighted an engagement in processes such as locomotor control, visual memory, place learning and homeostatic sleep (Strauss, 2002; Neuser et al., 2008; Rieche et al., 2018; Ofstad et al., 2011; Liu et al., 2006; Ueno et al., 2012; Donlea et al., 2014; Donlea et al., 2018). Comparing the data on *D. melanogaster* with data from other different insects (e.g., honeybee, cockroach, cricket, desert locust and monarch butterfly), the CX seems to be linked to the space representation for navigation and to the spatial features for motor control (Heinze, 2017).

Strauss and Heisenberg (1993) studied the effect on the flies walking of mutations that affected the morphological characteristics of the CX showing in mutants decreased levels of activity, shorter activity duration and lower speed compared to wild-type flies. Martin and colleagues (1999) by using a binary

system to target the synaptic blocking of specific networks of the CX showed that these compromised flies did not change the frequency of walking bouts initiation but the duration of these walking bouts were reduced. Overall, the CX results to be a high-order centre for motor control likely involved in the tuning of the action response according to the surrounding visual environment.

Although there are not DNs which connect directly the CX to the VNC, other neuropils might take part in the information flow towards the motor centre. The lateral accessory lobe (LAL) is the major projection region from the CX and it is an important hub in relying action control (Stone et al., 2017; Shih et al., 2015). Nevertheless, the LAL is innervated by few DNs, while other regions such as PS, PVLP and anterior mechanosensory motor centre (AMMC) are innerved by many DNs. In insect such as silk moths the connections between LAL and PS have been extensively described (Namiki & Kanzaki, 2016). Only connectomics studies in *D. melanogaster* have suggested such LAL-PS structural connectivity (Chiang et al., 2011; Shih et al., 2015) besides a pair of neurons connecting PB, LAL and PS (Wolff & Rubin, 2018).

Data regarding the functional connectivity within the CX and between CX and other putative neuropils for motor controlling are starting to emerge (Franconville et al., 2018). Thus, the command outputs for motor control would rely on a pathway involving the processing of the CX which, sending inputs to the LAL in turn connected to the PS, communicates to the motor centres via DNs.

Different dopaminergic clusters of modulatory neurons innervate the CX regulating forms of arousal which can be distinguished depending on the targeted neuropils. The six major clusters of dopamine neurons (i.e., PAM, PAL, PPM1/2, PPM3, PPL1 and PPL2) might play different role acting on specific circuits (Friggi-Grelin et al., 2003). The ventromedial posterior protocerebral dopaminergic neurons (PPM3) seem to be the only innervating the EB implying that a specific role upon this neuropil should be played by that specific dopamine neurons (Kahsai & Winther, 2011). For instance, the PPM3 neurons modulate the tangential neurons innervating the EB via Dop1R1 receptors increasing the flies locomotor activity (Kong et al., 2010). The dopamine modulation of the EB tangential neurons has also shown to be involved in the startle-induced response

(Lebestky et al., 2009). In flies bearing a mutated form of the Dop1R1 receptor, the repetitive startle-induced arousal is enhanced and the rescue of the dopamine receptor in the EB tangential neurons specifically restore a normal arousal without affecting the nocturnal hypoactivity shown by these mutants (Lebestky et al., 2009). It means that PPM3 neurons contribute to some behaviours but not others. Along with this, the dorsolateral posterior protocerebral dopaminergic neurons (PPL1) which innervate the dorsal part of the FB (dFB) have been identified as sleep inhibiting neurons (Liu et al., 2012; Pimentel et al., 2016).

Protocerebral Bridge

The PB is a caudal neuropil located between the two calyces of the MBs that resembles handlebars-shaped moustache with the lateral parts bent postero-ventrally and the middle part bent antero-ventrally (Hanesch et al., 1989). The PB is vertically divided into distinct units called glomeruli. By using classical staining and immunostaining techniques[1], 16 glomeruli along the PB, 8 on each side of the midline have been recognized (Young & Armstrong, 2010b; Hanesch et al., 1989; Lin et al., 2013a). Wolff and colleagues (2015), by employing the multicolour flp-out technique (MCFO)[2], have revealed 18 rather than 16 glomeruli in the PB, 9 per hemisphere numbered progressively (G1-9) starting from the midline. These glomeruli are formed by the arborisations of small-field columnar neurons whose branches populate only a single glomerulus. Different types of small-field neurons form distinct groups of functional columnar neurons and none of these groups innervate all 18 glomeruli, indeed they usually arborize in either G1-8 or G2-9 of each hemisphere. These two categories respect a basic wiring principle with the anatomically "downstream" neuropils on which they send or from which they receive input. That is, neurons innervating the most lateral four glomeruli of the PB in each hemisphere stay ipsilateral in the second neuropil (e.g., FB or EB)

[1] Golgi staining, immunostaining technique with discs large antibody which labels septate junctions and nc82 antibody which recognizes the Bruchpilot protein (i.e., a protein localized in the presynaptic active zone) combined with the green fluorescent protein (GFP).

[2] This technique labels neighbouring cells in a spectrum of colours allowing to visualize single neurons in small populations and providing an high spatial information.

while they cross to the contralateral side in the third neuropil (e.g., LAL or NO). On the contrary, the neurons innervating the most medial four glomeruli of the PB decussate already at the level of the second neuropil.

The branches of some small-field neurons span neighbouring glomeruli, contiguous or distant from the primary site receiving the most extensive innervation. Such multi-glomerular neurons may have both spines and boutons in the PB and usually they extend unilaterally rather than bilaterally. Unusual types of PB innervating neurons are cells which project ipsilaterally and contralaterally. For instance, one of these cells types has an ipsilateral presynaptic site which occupies multiple glomeruli of the PB and a contralateral extensive bifurcated dendritic branch which innervates the IB and the SPS (PB_{G2-9}.b-IB.s-SPS.s)[3]. Another unusual class of neurons are local interneurons with neurites that seem to receive information distributed within the PB and then to send input within specific glomeruli. For example, a type of these cells has a mainly dendritic arborisation spanning the G1-9 of both hemispheres and only two clusters separated by 7 glomeruli of presynaptic boutons (PB18.s-Gx.Δ7Gy.b). Among the cells type which provide input to the PB it is interesting to mention two types of neurons. The first type innervates presynaptically half of the PB (with 25-40 boutons) extending from G2 to G9 although G1 is occasionally innervated by a single bouton and postsynaptically the ipsilateral SPS ($PB_{G1/2-9}$.b-SPSi.s). While the second type innervates with dendritic branches the LAL and the PS, and then deliver information to the PB with a dense arborisation of boutons in all 18 glomeruli (PB.b-LAL.s-PS.s).

Lesion, electrophysiological and imaging experiments have confirmed a role for the PB in the control of the walking step-length, in the localization of a visual target for directional movement and in the sunlight navigation (Giraldo et al., 2018; Green et al., 2017; Triphan et al., 2010). The PB has also been likened to the mammalian basal ganglia because of five shared characteristics: 1) motor control and sequencing; 2) modulation of anticipation and visual attention; 3) substantial dopaminergic innervation; 4) recurrent anatomical loop motif and 5) expression

[3] In this nomenclature the uppercase letters defined the neuropil while the lowercase letters after the dot defined either spines (.s) or boutons (.b) (Wolff et al., 2015).

of similar genes for the cell fate determination in the embryonic precursors (Lin et al., 2013a).

Fan-shaped Body

The FB is located caudally to the EB and it represents the largest neuropil of the CX. It is subdivided vertically into eight columns, called segments, according to the regular arrangement of bundles of medium-sized fibres from the PB (Lin et al., 2013a). Along the rostro-caudal axis the FB has four shells which can be delineated on the basis of the extent and positions of small-field arborisations (Hanesch et al., 1989). The most prominent subdivisions of the FB are eight horizontal layers identifiable on the basis of quality, texture and intensity of immunolabeling of active zones (Young & Armstrong, 2010b). However, a higher resolution map of the FB layers by using the MCFO technique has highlighted at least nine layers numbered progressively from the ventral to the dorsal part (Wolff et al., 2015). The columnar organization of the FB, drawn by the projections to the PB, seems to be restricted to the layers 1 through 5 ($PB_{G1\text{-}7}$.s-FB*l*2.s-LAL.b-cre.b; $PB_{G1\text{-}8}$.s-FB*l*3,4,5.s.b-ROB.b). On the contrary, other FB neurons (i.e., tangential neurons) do not have projections to the PB and are not organized in columns. A more fuzzy columnar arrangement in which wider arborisations extend horizontally is evident in layers 4 through 8 (with some exceptions) compared to the layers 1-3 (PB.s-FB*l*6.b.*l*3.s-V GA.s.b). An extreme case is the layer 9 which is not organized in columns and the neurons arborizing in this layer have processes that extend throughout at least half layer (Wolff et al., 2015). In the FB were also found the four abovementioned pontine neurons which connect the FB segments on both sides of the midline, adjacent segments or horizontal layers (Young & Armstrong, 2010b). Despite the columnar organization, in layer 2 and 3 the boundaries are not so restrictive because the neuronal arborisation from neighbouring columns may overlap ($PB_{G2\text{-}9}$.s-FB*l*2.b-NO_3A.b; $PB_{G2\text{-}9}$.s-FB*l*3.b-NO_2D.b; $PB_{G2\text{-}9}$.s-FB*l*3.b-NO_2V.b). A clear columnar organization is instead evident in layer 1, where the ventral margin forms seven distinguished teeth-shaped of a cog with additional two elusive teeth not visible

by means of immunostaining (Wolff et al., 2015). These seven main teeth are each one formed by two of sixteen small-field columnar neurons (one ipsilateral and one contralateral) afferent to FB and efferent from the most lateral glomeruli of the PB (8 for each side). The remaining two columnar neurons, efferent from the most central glomeruli of the PB, are afferent to the two lateral elusive teeth ($PB_{G2\text{-}9}$.s-FB*l*1.b-NO_3PM.b).

The communications among neuropils of the CX are quite restricted and the neurons connecting the PB to NO arborize only in the layers 1-3 of the FB. Specifically, the layer 1 of the FB communicates directly with the NO_3M and NO_3P, the layer 2 exclusively with the NO_3, whereas layer 3 with the NO_2. Thus, NO_2 and NO_3 work together with the FB to elicit a behaviour depending on the information coming from the PB.

Weir and Dickinson (2015) have recorded the Ca^{2+} imaging activity of the FB in response to different visual stimuli during flight. They have found that the three most ventral layers of the FB and the closely related NO were unresponsive to visual stimuli in quiescent flies but became responsive when flies started to fly. This response would be consistent with the role played by the FB in controlling flight heading along the horizontal plane. Interestingly, the responses in FB during flight were independent from motor output, meaning that the activity of the FB would be unrelated to efference copy or sensory reafference. Contrary to FB, the PB responded to visual stimuli even when the fly was not flying though its baseline activity increased during flight in the absence of any stimulus. Similarly, the EB responded to visual stimuli regardless the animal was flying or not and its responses were stronger for visual stimuli presented in the ipsilateral visual field.

Neurons in the dorsal and in the ventral layer of the FB have been shown to house memory trace for pattern parameters linked to the elevation and the contour orientation of visual objects respectively (Liu et al., 2006). Moreover, these neurons have shown to form a short-term visual memory through the expression of the Rutabaga protein, which is a type 1 adenylyl cyclase regulated by Ca^{2+}/calmodulin and G-protein (Liu et al., 2006).

Ellipsoid Body

The EB is a donut-shaped (i.e., a toroid) neuropil positioned rostrally to and partially embedded in the FB with a central hole, called EB canal, pointing slightly dorsally when viewed from the front (Hanesch et al., 1989). It means that the EB is tilted so as the ventral half of the donut is the most rostral portion and the dorsal half is the most caudal one. Along the rostro-caudal axis (i.e., sagittal plane) the EB has been divided in shells (anterior, medial and posterior) or rings (anterior and posterior) while along the radius of the toroid these rings have been called layers because of the stratified configuration they assume in the coronal plane (Hanesch et al., 1989; Young & Armstrong, 2010b; Wolff et al., 2015). However, these different divisions based on the 2D anatomical planes, refer to single 3D domains innervated by characteristic concentric arborisations (i.e., likewise rings) of different diameters/depths belonging to the tangential neurons and by circular sectors glomeruli (i.e., likewise slices of a pie) belonging to the columnar neurons.

TANGENTIAL NEURONS The tangential neurons convey information from the lateral neuropils towards the different layers of the EB. They have been termed 'ring neurons' because of the shape of their arborisations around the EB canal.

Two main types of ring neurons can be identified: the R-neurons which represent the vast majority with their perikarya located in a cluster dorsolaterally to the AL; and the ExR-neurons which are ring neurons with extensive arborisations also outside of the EB (Hanesch et al., 1989). R-neurons project their axons to distinct layers of the EB. They have typically short globular dendrites, called microglomeruli, in the bulb (BU) which is a compartment (previously called lateral triangle) of condensed synaptic complexes lateral to the toroid (Pfeiffer & Homberg, 2014). On the basis of the layers innervated by the R-neurons, four distinct subtypes of neurons numbered progressively from the centre to the periphery of the toroid (R1-4) were classified (Hanesch et al., 1989). The arborisations of the R1-3 neurons are directed from the EB canal outward,

whereas those of the R4 neurons are directed from the periphery inward. The technical development of microscopes able to provide high-resolution images at multiple depths of the samples, enabling the 3D reconstruction of the anatomical structures, has revealed a more complex organization of the EB. Omoto and collaborators (2018) have recently employed up-to-date techniques[4] to image a whole raft of fly lines expressing in specific neurons of the EB. The authors have distinguished and termed five different domains of the EB: the anterior domain (EB_a), corresponding to the previous R2 neurons and involved in the regulation of sleep homeostasis (Liu et al., 2016); the inner and outer central (EB_{ic} and EB_{oc}) domains; and the inner and outer posterior (EB_{ip} and EB_{op}) domains. Based on the innervation patterns involving one o more of these domains, Omoto and colleagues have identified eleven R-neurons and four ExR-neurons. The R-neurons have been classified in: R1 neurons with branches in the EB_{op} and EB_{ip}; R2 neurons with arborisations in the EB_{oc}; R3 neurons with projections to distinct regions within the EB_{ic} and EB_{ip} which have been further divided in five subclasses ($R3_d$, $R3_m$, $R3_a$, $R3_p$, $R3_w$) depending on the extension reached by the branches (i.e., distal, medial, anterior, posterior and wide) along the transverse plane; R4 neurons with axonal ramification embracing the periphery and projecting centripetally which have already been subdivided in $R4_d$ and $R4_m$ on the basis of the boundary defined by their terminal tufts into the EB_{oc} (i.e., distal or medial); R5 neurons with short terminal branches in the EB_a; and R6 neurons with short ramifications that extend anteriorly into the EB_{op}. The ExR-neurons instead have been classified in: ExR1 neurons, already described and recently dubbed as 'helicon cells' (Donlea et al., 2018), with fibre innervating the EB_a, FB, and gall (GA) region of the LAL; ExR2 neurons, already described as for the ExR1, which may correspond to the PPM3 dopaminergic neuron (8-9 cells); ExR3 neurons which may correspond to the posterior medial protocerebrum dorsal (PMPD) serotoninergic neurons which ramify in the EB_{ic}, dorsal layers of the FB, bilaterally to the BU and ipsilaterally to the LAL, crepine (CRE) and SMP; and ExR4 neurons with perikarya in the rostral cellular cortex which innervate the

[4] MCFO technique and immunostaining with the global marker N-cadherin antibody which recognizes the cell-cell adhesion protein N-cadherin.

EB_{op} (they may correspond to the ExR2 as described by Hanesch et al., 1989), GA and LAL. Intriguingly, there are three different types of PPM3 neurons depending on the neuropils targeted: the PPM3-EB neurons innervate the EB, BU and LAL with thin and highly branched axonal terminals in the EB_{op}; the PPM3-FB neurons arborize in the ventral layers of the FB (FB*l*2-3) and in the intermediate noduli (NO_2) with some branches in the LAL overlapped to those of the PPM3-EB; and PPM3-LAL neurons with bilateral projections to the lateral surface of the LAL. The different domains of the EB are also associated to three main subdivisions of the BU, the anterior (BU_a), the superior (BU_s) and the inferior (BU_i) bulb (Omoto et al., 2018). Moreover, BU_s and BU_i could be further divided into the anterior and the posterior domains ($_{a\text{-}p}BU_s$ and $_{a\text{-}p}BU_i$). Topographically organized visual inputs to the ring neurons are conveyed by the tubercular-bulbar (TuBu) neurons which project from the AOTU to the BU (Omoto et al., 2017). The visual information is conveyed to the AOTU by the projections of the medulla-tubercular (MeTu) neurons which receive visual input from the medulla (Omoto et al., 2017). Ca^{2+} imaging recording from the BU of $R4_d$ (~7/20) and $R4_m$ (~14/20) neurons[5] in behaving flies showed distinct microglomeruli tuned to specific horizontal orientation of a visual stimulus and with a preference response to a vertical bar (Seelig & Jayaraman, 2013). These neurons respond regardless the contrast of the bar or the walking state of the flies and the vertical preference is due to the peculiar organization of their visual receptive fields. Each neuron covers 90 deg of the visual field and it responds to a central excitatory region flanked by two inhibitory ones. The R1 (targeted by c105 driver line), $R3_d$ and $R3_p$ neurons (targeted by c232 and 189y drivers) have also demonstrated to play a central role in the detour paradigm used to investigate visuospatial working memory (Neuser et al., 2008; Rieche et al., 2018). Basically, in this paradigm a fly walks back and forth between two stripes (i.e., 'Buridan's paradigm') and at a certain time is required to change its path according to the perpendicular shift of one of the two stripes. Once the fly has adopted the new path to reach the stripe in the new position, within one second both stripes

[5] In this study were used the c232 driver line targeting $R3_d$, $R3_p$ and $R4_d$ and EB1 driver line targeting R_2 and $R4_m$ (Seelig & Jayaraman, 2013).

disappear. Upon a uniform illumination of the visual surrounding environment, wild-type flies remember the position of the original stripe prior to the shift and re-adopt the original heading, whereas flies with silenced R1 or $R3_d$ and $R3_p$ neurons do not. In an ingenious heat maze paradigm developed to study the visual place learning, a group of flies learned to associate the position of a "pleasant" specific cool tile in an "unpleasant" hot surface using the position of a visual pattern surrounding the flies (Ofstad et al., 2011). In this paradigm, the $R3_m$ neurons (targeted by R28D01) have shown to be essential in forming and retaining visual place memories to guide selective navigation (Ofstad et al., 2011). In behavioural and Ca^{2+} imaging experiments the R-neurons (R15B07 driver targeting $R3_d$, $R3_p$ and $R4_d$, and R38H02 targeting $R4_m$) have shown not simply to detect retinotopic information but to compute spatiotemporal features and to integrate recent visual history and self-motion which in turn might inform the downstream behaviour (Shiozaki & Kazama, 2017). A bilateral visual stimulation produces the lower response in the R-neurons when the contralateral stimulus is novel and the higher response when the contralateral stimulus has been recently experienced (Sun et al., 2017). The selection of the stimuli would be a linear combination of ipsilateral and contralateral responses of the R-neurons. Specifically, the microglomeruli in the BU_s encode past visual experience and prefer the ipsilateral visual field with unilateral stimulation, whereas those in the BU_i encode self-motion and prefer the contralateral visual field with bilateral stimulation (Shiozaki & Kazama, 2017). By using specific marker to differently target the dendritic (DenMark) and axonal (syt.EGFP) compartments of the ring neurons it has been also defined the putative direction of the information flow (Omoto et al., 2018). In Table 1 is reported a summary of the ring neurons (Omoto et al., 2018) with the corresponding neuropils innervated according to Wolff and collaborators (2015).

Table 1. *Ring neurons*

Domain	Cell type	Driver (GAL4)
R1	LAL.s-EB_{op}.b	R31A12, C105
R2	BU_s.s-EB_{oc}.b	R78B06, c42, EB1
$R3_d$	BU_i.s-EB_{oc}.b	R80C07
$R3_m$	BU_i.s-LAL.s-EB_{ic}.b	R28E01, R28D01
$R3_a$	LAL.s- EB_{ic}.b	R12G08
$R3_p$	BU_i.s-EB_{ip}.b	VT063949
$R3_w$	BU_s.s-$EB_{oc\text{-}ic}$.b	VT057232
$R4_d$	BU_s.s-EB_{oc}.b	R12B01
$R4_m$	BU_a.s-EB_{oc}.b	R59B10
R5	BU_s.s-EB_a.b	R58H05
R6	BU.s-GA.s-EB_{op}.b	VT011965, R18A05
ExR1	$BU_{s\text{-}i\text{-}a}$.s-EB_a.b	R78A01
ExR2	PPM3-EB, PPM3-FB, PPM3-LAL	TH
ExR3	LAL.s-BU.s-FB*l6*.b-EB_{ic}.b	TPH
ExR4	LAL.s-GA.b-EB.b	R14G09

Note. Domains are defined as in Omoto et al., 2018. Cell types define the neuropils innervated with spines (.s) and boutons (.b) as in Wolff et al., 2015.

COLUMNAR NEURONS The columnar neurons which arborize in different circular sectors of the EB send projections also to the PB and to different compartments of the CX maintaining a segregated organization (Hanesch et al., 1989). A main distinction among these columnar neurons can be done depending on the morphological pattern of the arborisations which radially innervates the circular sectors as evident along the coronal plane: the wedge-shaped arborisations (called 'wedges'); and the tile-shaped arborisations (called 'tiles') (Wolff et al., 2015). When the columnar neurons arborize in both PB and EB, the innervation of each wedge or tile comes from one ipsilateral and one contralateral glomerulus of the PB. The arborisations from cells that target the PB alternate with one another in the EB (either wedges and tiles) such that

arborisations from the left glomeruli alternate with those from the right glomeruli (Strausfeld, 1999; Wolff et al., 2015). The wedge-shaped arborisations segment the full radius of the toroid in such a way that resembles entire slices of a pie. They can occupy all the shells of the EB, only the posterior or the medial shell in function of the neuron type. Similarly to many columnar neurons of the FB, the boundaries of a single wedge are not strictly restricted to the own circular sector but they can overlay with neighbouring sectors (Wolff et al., 2015; Hanesch et al., 1989). The tile-shaped arborisations divide the toroid likewise the wedges but differently to them, the tiles are confined on the surface of the posterior shell (Wolff et al., 2015). Moreover, the tiles volumes do not occupy the entire circular sector but only a more central part even larger than the wedges. These two types of innervation patterns have resulted to belong to functionally distinct neurons types.

WEDGES The only neuronal type with arborisations both in wedges and PB arborizes also in the ventral and dorsal part of the GA ($PB_{G1\text{-}8}$.b-EBw.s-D/V GA.b). These neurons are also known as E-PG neurons where, for an abbreviation purpose, the first letter indicates the input neuropil while the following letters indicate the output neuropils (Turner-Evans et al., 2017; Wolff & Rubin, 2018). The other neurons type which has arborisations in the wedges occupies with postsynaptic spines all domains of the EB and with presynaptic boutons an undefined region surrounding the dorsal part of the GA (EB.w.AMP.s-D GA.s.b). The E-PG neurons have spines in all domains of the EB apart from EB_a and boutons in PB and GA, although a mix of post and presynaptic terminals seem to characterized the wedges of these neurons (Lin et al., 2013a; Turner-Evans et al., 2017). The MCFO technique has shown that each one of the E-PG neurons innervates a single glomerulus (G1-8) of the PB and single wedge in the EB. It means that 16 wedges cover the entire EB whereby some cells occupy a full wedge whereas others fill just half a wedge (Fig. 1.2A). Thus, there is a 1:1 correspondence between the glomeruli of the PB and the wedges of the EB. The counting of the E-PG neurons (36-45 cells) has suggested that 2-3 cells target each one of the 16 glomeruli. Seelig and Jayaraman (2015) have recorded the Ca^{2+} imaging activity of

the E-PG neurons in tethered walking flies positioned on an air supported ball which was tracked by means of two optical mouse sensors. The authors have combined this setup with a closed-loop visual stimulation by using a surrounding LED display. The E-PG neurons have shown to encode an internal representation characterized by a 'bump' of Ca^{2+} imaging activity which dynamically arises in the neurons and rotates around the toroid according to the fly's heading (Seelig & Jayaraman, 2015). These neurons have been also termed as 'compass neurons' because they use information from both visual landmark and angular path direction to create a compass-like internal representation of the animal orientation in the environment (Seelig & Jayaraman, 2015; Turner-Evans et al., 2017). The observed shifts of Ca^{2+} activity were also present in total darkness demonstrating the existence of a proprioceptive input channel able to update the heading representation in the toroid in the absence of visual input (Green et al., 2017; Turner-Evans et al., 2017). Even in the absence of self-motion cues the activity of specific wedges maintains a stable representation of the fly's heading in its environment for more than 30 s (Seelig & Jayaraman, 2015). Interestingly, local landmarks rather than self-motion cues appear to determine the position of the Ca^{2+} activity among the wedges (Seelig & Jayaraman, 2015). Indeed, the population vector average (PVA) of the wedges activity estimated for accumulated rotation of the visual cue and for accumulated walking rotation on the ball has shown that the PVA estimation matches more closely the visual cue rotation than the walking rotation (Seelig & Jayaraman, 2015). Moreover, in experiments employing two visual stripes (or more complex visual environment), the Ca^{2+} activity remained locked to a single stripe or switched between competitors with a lower probability (Seelig & Jayaraman, 2015). All these E-PG neurons' features has been interpreted as key dynamics of the so-called 'ring attractor models' (Kakaria & de Bivort, 2017; Seelig & Jayaraman, 2015). The optogenetic activation of a selective region covering about two wedges of the E-PG neurons (i.e., reference location) and the concomitant activation of a region of the same size but in different wedges (i.e., second location) has shown the activity reduction of the first location by increasing the stimulation at the second location (Kim et al., 2017b). The activity reduction of the first region is consistent

with a mutual suppression that ensures a unique activity bump through a simple 'winner-take-all' process (Kim et al., 2017b). By means of the abrupt shift of a visual stripe, as well as with an equivalent optogenetic activation recreated artificially, both the 'global' (i.e., global cosine-shaped interaction among wedges) and the 'local' (i.e., local excitatory interaction) model hypotheses of ring attractor predicted a mixture of jump and flow response around the toroid depending on the strength and width of the shifting input (Kim et al., 2017b). Compared to the global model's prediction, the optogenetic input strength required to induce a jump of the bump was smaller, matching better that one of the local model. Therefore, the neural circuit involving the E-PG neurons would be characterized by a narrow local excitation and a flat long-range inhibition around the ring.

Overall, the discrete bump of activity emerging from the E-PG neuronal network linked to the angular position of a likely fixated object has been considered the most convincing evidence of the neural circuit underlying the visual attention (de Bivort & van Swinderen, 2016).

An anterograde trans-synaptic labelling method called *trans*-Tango [6] has highlighted interesting connections within the EB useful to understand the circuits necessary to generate a representation of heading direction or to guide actions. This technique has revealed that the inner R-neurons such as $R3_d$ and $R3_p$ are characterized by recurrent connectivity which might enable a persistent activity required for visual working memory and that the R-neurons provide direct presynaptic inputs to the E-PG neurons (Omoto et al., 2018). Along with this, reciprocal cell contacts between E-PG and R2/R_{4m} neurons have been predicted by *in silico* simulations aimed at understanding the processes involved in spatial navigation (Fiore et al., 2017). Recently, they have been shown with the GFP reconstitution across synaptic partners (GRASP) system in which two spilt-GFP halves emit fluorescence only when they are reconstituted (Kottler et al.,

[6] In this method a synthetic receptor with downstream signalling pathway is panneuronally expressed. Then, by activating this receptor with specific presynaptic driver leads the pathway to convert postsynaptically this activation into reporter expression. In this manner, the presynaptic neurons labelled by the GFP under UAS control can be visualized in conjunction with downstream postsynaptic neurons labelled by the red fluorescent protein (RFP) under QUAS control (Talay et al., 2017).

2019). These findings clearly suggest that the EB might operate as a critical interface between the visual sensory ring neurons and the motor directional columnar neurons (Fig. 1.2B).

TILES One of the most important differences between wedges and tiles is that the latter are targeted by cells from two glomeruli of the PB rather than just one. It means that 8 tiles with a double width compared to the wedges cover the entire EB because of a 1:2 correspondence between glomeruli and tiles (Fig. 1.2C).

The two types of tile neurons so far identified have boutons in the EB and spines in the PB. Nevertheless, these two types of neurons differentiate because, in addition to the EB, one type of neuron has boutons in the GA ($PB_{G1\text{-}9}$.s-EBt.b-D/V GA.b) whereas the other in the NO_1 ($PB_{G2\text{-}9}$.s-EBt.b-NO_1.b). According to the abbreviation style abovementioned, the first type of neurons is briefly called P-EG neurons whereas the second type is shortened to P-EN (Wolff & Rubin, 2018). The P-EN neurons, which have axon tile-shaped terminals in the EB_{op} domain, are subdivided into two subclasses, one defined as P-EN1 and the other one called P-EN2 (Green & Maimon, 2018). The P-EN1 neurons (targeted by R37F06 driver) encode the fly's turns conjunctively with the angular velocity and in so doing they update the appropriate representation of heading in the E-PG neurons (Turner-Evans et al., 2017). Under this aspect, the P-EN1 neurons would be important for maintaining the E-PG activity peak and stability in complete darkness throughout an indirect positive feedback loop between these two neuronal populations. In contrast to E-PG neurons, which are strongly influenced by visual landmarks, P-EN1 neurons do not seem to respond to visual stimuli. They seem activated by proprioceptive input rather than motor efference. In fact, the angular velocity responses in the PB have shown latency, relative to the fly's turning movement, estimated electrophysiologically in about 150 ms meaning that the activity in P-EN1 neurons is a consequence rather than a cause of locomotion. The P-EN1 activity has also shown to follow the E-PG activity by one glomerulus on both side of the PB (corresponding to about 45 deg in the EB) during fast angular rotation (120-150 deg s^{-1}) and to reverse this lag in the EB where the P-EN1 neurons would drive the E-PG neurons (Turner-Evans et al.,

2017). However, such phase inconsistency between PB and EB activity might be due to the fact that the driver used to target the P-EN1 neurons expresses also in another type of neurons which innervate the PB (i.e., $PB_{G2\text{-}9}$.s-FB*l*3.b-NO_2V.b), determining a possible confounding effect linked to the latter activity (Omoto et al., 2018). As confirmation of this, by using a different driver (VT032906) to target the P-EN1 neurons, unison responses between these neurons and the E-PG neurons have been recorded (Green et al., 2017). Moreover, while the Ca^{2+} imaging activity of the P-EN1 neurons targeted with this driver and that one of the E-PG neurons was in phase with each other, the activity showed by P-EN neurons targeted with another driver was nearly in antiphase. An accurate anatomical analysis has identified such latter neurons as a new subset of P-EN neurons, called P-EN2, with a specific physiological function different from the one of the P-EN1. The P-EN2 neurons (targeted by R12D09 driver) would work as a brake for the E-PG rotation around the toroid started by the P-EN1 neurons (Green et al., 2017). Specifically, the P-EN1 activity increases on the leading edge of the moving E-PG bump, whereas the one of the P-EN2 increases on its trailing edge. The phase of the Ca^{2+} imaging activity (by using GCaMP6m) was delayed of 300 ms relative to the fly's turning movement on the ball in the P-EN2 and E-PG neurons (200 ms by using GCaMP6f) and of 600 ms in the P-EN1 neurons. This paradoxically longer delay for P-EN1 compared to P-EN2 was interpreted as an artefact due to the buffering effect of the GECI levels and not as a biological difference among cell types. Anyway, these neurons have resulted necessary for integrating the fly's heading without visual landmarks and because of their function they have been termed as 'shifting neurons'. Stimulating the P-EN neurons with ATP-gated cation channel $P2X_2$ and recording the Ca^{2+} imaging from the E-PG neurons have demonstrated the peaks relocation to the expected positions confirming the functional connectivity between them (Green et al., 2017).

Noduli

The noduli are distinct in three main components: NO_1 is the most dorsal and smallest nodulus with a triangular shape in sagittal plane; NO_2 is the medial nodulus which protrudes slightly anteriorly than NO_1; and NO_3 is the most ventral nodulus with a more square shape than NO_2 which occupies the largest volume among noduli (Wolff et al., 2015). Apart from NO_1, which probably reflects a dense presynaptic site, subcompartments further characterize the other two noduli. Two subcompartments comprise NO2, a larger dorsal domain (NO_2D) and a smaller ventral domain (NO_2V). Instead three subcompartments compose the NO_3: the largest posterior domain (NO_3P); the smallest medial domain (NO_3M); and the most anterior domain (NO_3A).

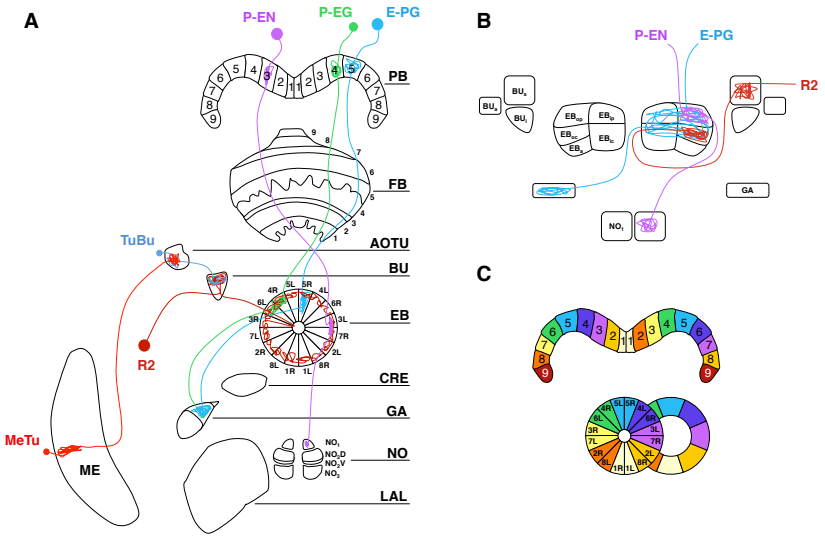

Fig. 1.2. Columnar and tangential neurons innervating the EB. *A*: CX with some columnar neurons: E-PG, P-EG and P-EN neuron. The EB is sectioned according to the wedges formed by the E-PG neurons. A R2 tangential neuron is also depicted, as well as the TuBu and MeTu neurons. *B*: EB domains innervated by the E-PG, P-EN and R2 neurons. *C*: PB glomeruli and EB wedges and tiles innervated by the E-PG and P-EN neurons. Images adapted from Wolff et al., 2015 and Omoto et al., 2018.

1.3 GENETIC TOOLS FOR FLY'S COGNITIVE NEUROSCIENCE

The general advantages which made *D. melanogaster* an attractive animal model, such as the easy and cheap maintenance of flies owed to their small dimensions, high fecundity and short life cycle, have met in more recent years the development of genetic tools for manipulating and recording the fly's brain activity. In the next section I shall present the kind of 'forward' approaches used to mutate flies in order to understand the genetic substrates of their behaviour and the powerful binary systems for expressing in selected tissues. The genetic targeting of specific neural circuits has allowed resolving the anatomical organization of the fly's brain with a high spatial resolution. Then, I shall present the 'reverse' applications of the expression systems. Once targeted the neurons of interest, the binary system enables to express whatever nucleic acid sequence decreasing, increasing or simply manipulating the normal activity of such cells. For instance, by using this system for making flies express specific membrane channels sensitive to some exogenous input, such as light (e.g., the rhodopsin), it is nowadays possible to control at specific time the activity of those neurons. Finally, in a last section I shall introduce a functional imaging application based on the binary system. By making flies express exogenous fluorescent proteins functionally sensitive to the intracellular levels of Ca^{2+} it is possible to obtain read-out of the membrane voltage changes relative to those neurons.

Overall, a high spatial and temporal resolution for exogenous control and endogenous activity recording make these tools worthwhile. Along with complex behavioural analyses, the fruit fly represents for the cognitive neuroscience a great opportunity to crack the neural code (Olsen & Wilson, 2008).

1.3.1 Forward genetic

Currently, fine genetic engineering techniques enable to localize subpopulations of neurons responsible for specific behaviours and to study the underlying molecular mechanisms. Nevertheless this cutting edge tools have contributed to

develop the neuroscientific approaches using flies. This approach is defined as 'forward genetic' because it starts from the phenotype of interest for then move to finding the gene determining that phenotype.

Behavioural neurogenetics

The first systematic approach which opened the door to the modern neuroscience was the so called 'neurogenetics', which focuses on the nervous system effects determined by genetic manipulation (Greenspan, 2008). It began in the 60s and the underlying philosophy was to screen randomly induced mutations in flies for behavioural phenotypes which differed as compared to wild-type flies. The random mutations could be generated by exposing flies to ionizing mutagens such as x-ray, chemical mutagens such as ethyl methanesulfonate or by using biological tools such as transposon elements (i.e., P-elements). Several outcomes were obtainable with these mutagens depending on the type of cell line affected (i.e., somatic or germinal), the entity (i.e., point mutation, genic, chromosomal or genomic) and the type of mutation (i.e., deletion, duplication, inversion, substitution or insertion). In his 'Fly's Room' at the Columbia University, Thomas Hunt Morgan was the first one starting to mutate flies looking for mutants phenotypically evident on the basis of morphological features. In the 1910 he found the first mutant fly bearing white eyes which had mutated what was subsequently named as *white* gene (Morgan, 1910). Since then, although with some exceptions, the research in *D. melanogaster* was mainly dominated by genetic approaches focused on dissecting the principle of inheritance (Bellen et al., 2010). Among those exceptions, two Morgan's students pioneered the approach of linking genes and behaviours. In 1915 Alfred Henry Sturtevant studied genetic variants affecting the courtship behaviour (Sturtevant, 1915), while in 1918 Robert Stanley McEwen studied phototropic and geotropic responses in flies (McEwen, 1918), identifying mutants with poor phototactic response (McEwen, 1925). Only towards the end of 50s, the quantitative genetic analysis applied by Jerry Hirsh to study the individual differences in a geotaxis task (Hirsch, 1959) and the high-throughput

countercurrent technique developed by Seymour Benzer to isolate mutants in a phototaxis task (Benzer, 1967), determined the emerging field of behavioural neurogenetics. However, it is probably the cybernetics research group at the Max-Plank Institute of Biology in Tübingen which provided the most important advance by adopting a novel approach termed 'biological cybernetics'. By using a sophisticated technique (i.e., a flight simulator) developed to test the optomotor response in single flies, Karl Georg Götz highlighted differences in *white* mutants compared to wild-type flies (Götz, 1964). The subsequent contribution of Martin Heisenberg, which employed and improved the flight simulator, represents a milestone in the study of complex behaviours in flies, such as learning, visuomotor responses and attention which has contributed further to the development of the flies' cognitive neuroscience.

Binary systems

During the two decades straddling the 20th and 21st century many genetic engineering techniques have been added to the toolbox available in *D. melanogaster* for investigating for the cognitive neuroscience of flies (Venken et al., 2011; Olsen & Wilson, 2008). The GAL4-UAS binary system represents the most important breakthrough in targeting selective tissues and genes of the fly's body (Venken et al., 2011). The binary system is composed by two elements: the GAL4 driver to localize the expression pattern and the upstream activating sequence (UAS) to which is downstream bound whatever gene to be expressed (i.e., the reporter gene). Both GAL4 and UAS are injected into the flies embryos exploiting the properties of the P-element which is a mobile genetic sequence discovered in *D. melanogaster* able to move or jump inside the genome by means of a 'cut-and-paste' mechanism (i.e., class 2nd of transposon). It has been shown that the P-elements, after being engineered in such a way to contain desired DNA fragments and cloned into plasmids (i.e., vector for P-element), were efficiently capable to transpose stably from extrachromosomal DNA to the fly DNA, correcting mutations (Rubin & Spradling, 1982; Spradling & Rubin, 1982). By applying this technique it become feasible to randomly insert the transgene

coding for GAL4 into the fly genome as well as that one for the UAS sequence with the reporter gene (Fischer et al., 1988; Brand & Perrimon, 1993). The GAL4 is a transcriptional activator from the yeast which it does not do anything inside the organism (can be toxic only at extremely high levels) but when it binds the UAS sequence the transcription of the downstream reporter gene is initiated. The binary expression system entails that a fly line expressing the GAL4 (e.g., male flies) is crossed to another fly line (e.g., female flies) bearing the UAS bound to a reporter gene in order to yield progeny in which that gene is ectopically expressed with a specific pattern. Such pattern of expression is determined by the specific locus of insertion of the GAL4 which defined the subpopulation of cells targeted. To check the expression pattern of a certain GAL4 driver, the mainstream choice is the green fluorescent protein (GFP) from the jellyfish *Aequorea victoria* (Chalfie et al., 1994; Brand, 1995). By means of the GFP as reporter gene bound downstream the UAS, we can obtain images of the expression pattern useful for studying the spatial neural organization or for localizing some other manipulation in that pattern. Improvements of this system have strengthened the expression replicating the upstream UAS sequence and confining on the cell surface the reporter through the fusion of the GFP with the mCD8 transmembrane protein (Lee & Luo, 1999; Pfeiffer et al., 2010).

Whether the P-element jumps within a critical locus, the genetic transformation may be interpreted as a mutation affecting important biological functions, otherwise we can assume that the flies bearing driver or reporter looks like wild-type. The random insertion sites of the plasmids have represented the bigger limit of the P-element system because the position of the insertion can strongly influence the gene expression, complicating the phenotypic analysis. For this reason, a ΦC31 integrase system from phage has been developed for non-random insertion where the plasmid containing the *attB* site and the construct recognizes and integrates into the *attP* containing the docking sites (Groth et al., 2004). Because of the specific site insertion in the fly genome, effects related to the location of the plasmid are not relevant anymore with the ΦC31 integrase and all the fly lines generated in this manner are genetically identical. This new method has been improved increasing the levels of expression and the

translational efficiency by modification of the transcriptional activating domains, codon optimization and mRNA stabilization with 5'-UTR and 3'-UTR sequences derived from viral mRNAs respectively positioned upstream and downstream the reporter gene (Pfeiffer et al., 2010; Pfeiffer et al., 2012). A great research project called 'FlyLight' at Janelia Research Campus has taken to produce a huge library of more than 7,000 transgenic fly lines expressing GAL4 in specific populations of neurons with characterized expression patterns and freely available in a database of images from confocal stacks (Jenett et al., 2012). All these fly lines have been deposited to the Bloomington Drosophila Stock Center (BDSC) which is in charge for their distribution. The strategy behind this project was to construct transgenic lines in which the expression of the GAL4 was driven by a defined DNA sequence containing one or more transcriptional enhancers cloned from genes encoding for transcription factors, neuropeptides, membrane proteins, ion channels, transporter and receptors (Pfeiffer et al., 2008). It means that the expression patterns of these lines are associated to the putative enhancer fragments spanning the flanking regions (length of 3 kb on average) of specific genes. Moreover, highly selective subpopulations of neurons targeted by those lines have been generated as a part of the project by employing the intersectional technique relying on the split-GAL4 binary system (Luan et al., 2006). Analogously to the method used for the GAL4 lines also the split-GAL4 system has been optimized (Pfeiffer et al., 2010). In this system the GAL4 is split into two different hemidrivers: the DNA-binding domain (DBD) and the transcription-activation domain (AD). DBD and AD are driven by separate promoters which in practice correspond to two different driver lines with distinguished expression patterns (i.e., GAL4-DBD and GAL4-AD). Once the two lines have been crossed each other, the resulting progeny will express the GAL4 only in those cells in the intersection between the parental lines, that is where the patterns of the two domains overlap. In those specific cells DBD and AD heterodimerize via leucine zippers and reconstitute a functional activator. The spilt-GAL4 represents an extremely precise tool for the circuitry dissection at high spatial resolution (Dionne et al., 2018). Besides, the multicolour flp-out (MCFO) technique for stochastic cell labelling, which combines GAL4 and Flp recombinase based on the

'flp-out' approach (Struhl & Basler, 1993), has allowed unprecedented neuroanatomy details that can be easily matched with the functional data (Nern et al., 2015).

Different form of drivers have been engineered to control the mechanisms of expression, for instance GAL80 acts as a repressor of GAL4 allowing, when combined together, an intersectional strategies similar to the split-GAL4 for selective patterns expression in non-overlaid regions (Lee & Luo, 1999). A modification of the GAL80, the temperature-sensitive $GAL80^{ts}$, has enabled the temporal control of the GAL4 expression mostly useful to pause its expression during critical phases of development (McGuire et al., 2003). At 19°C the driver line expresses the $GAL80^{ts}$ which inhibits the GAL4, while at 30°C the $GAL80^{ts}$ expression is repressed and the GAL4 is free to bind the UAS permitting the transcription of the gene of interest. Nevertheless, it is noteworthy that the GAL4 expression level per se is increased at 28°C and decreased at 18°C (Mondal et al., 2007). The GeneSwitch is another temporal control method based on the RU486-dependent GAL4 which is effective, enabling the reporter gene expression, only when the fly is fed with the activator RU486, the mifepristone drug (Osterwalder et al., 2001; Roman et al., 2001).

Apart from GAL4-UAS, other binary systems have been developed such as the LexA-LexAop system from the bacterium *Escherichia coli* or the Q-system from the fungus *Neurospora crassa*. In LexA-LexAop system, the LexA protein is fused to the C-terminal activation domain derived from GAL4 or from the viral protein VP16 (GAL80 insensitive) allowing the driving of the reporter gene transcription whose promoter contains LexA operator (LexAop) motifs (Szüts & Bienz, 2000; Lai & Lee, 2006). The LexA-LexAop system has been improved by adding to LexA the human p65 activation domains and an N-terminal nuclear localization signal (11 amino acids) derived from the SV40 large T antigen, whereas by choosing a different LexAop binding site from another LexA target gene it has been reduced the leaky expression (Pfeiffer et al., 2010). However, LexA-LexAop is in general less effective and with a weaker expression pattern than GAL4-UAS. In Q-system, when the transcriptional factor QF binds the QF upstream activating sequences (QUAS), the transcription of the reporter is activated but when QS repressor is

present in the same cell of QF, QS represses QF blocking the reporter expression (Potter et al., 2010). Interestingly, feeding flies with quinic acid can relieve the repression mediated by QS. The advantage for having more binary systems is the possibility to combine them simultaneously in order to target different neuronal populations, for instance, to activate one population and to record from another one in functional connectivity studies.

1.3.2 Reverse genetic

The most common use of the binary systems is probably related to the manipulation of neurons. These system have widely increased the adoption of the 'reverse genetic' approach in which the starting point is a specific gene and the ending point the behaviours to which that gene contributes. A gene of interest may characterize a specific neural circuit and in so doing this approach can afford the functional dissection of the circuitry. Specifically, driving a manipulation in a selected group of neurons, the system allows us to draw a causal process between the biological substrate selected and the phenomenon observed.

Interference

One of the more elegant methods to reduce the gene activity is the RNA interference (RNAi) which produces a post-transcriptional gene silencing (Hammond et al., 2001). Double-stranded RNA (dsRNA) designed for a specific gene and injected into fly embryos silenced the expression of that specific gene (Kennerdell & Carthew, 1998). However, the degradation of the corresponding mRNA that blocks the gene expression (before the translation) interfering with its function was transient and not stably inherited. To overcome this limit, a dsRNA as an hairpin-loop dsRNA was developed under the control of the GAL4-UAS binary system allowing the temporal and the spatial regulation (Kennerdell & Carthew, 2000; Fortier & Belote, 2000; Martinek & Young, 2000). Basically, once the hairpin dsRNA is expressed from the transgene, a complex consisting of the enzyme Dicer-2 and the protein R2D2 which facilitates the selection of one

the two strands, cuts the dsRNA into short interfering dsRNA (siRNA) fragments of 21-23 nucleotide length (Heigwer et al., 2018). Then, the protein Argonaute 2 (Ago2) in turn stabilized by the Hsc70/Hsp90 chaperone system leads to unwind the siRNAs in two single stranded RNA (i.e., the passenger and the guide strand), to the cleavage of the passenger strand and to its ejection (Iwasaki et al., 2010). In the meanwhile, the guide strand is incorporated into the RNA-induced silencing complex (RISC) which occurs when the guide strand pairs a complementary mRNA sequence inducing their cleavage by Ago2 and thus mediating the post-transcriptional gene silencing. The degradation of the target mRNA produces a drastic decrease in the expression of a targeted gene without a complete abolishment. Therefore, the RNAi technique is defined as 'knockdown' method to distinguish it form the 'knockout' procedure in which the gene expression is entirely suppressed. In such a way RNAi allows studying the effects of this decrease highlighting the physiological role of a gene. Based on this technique, genome-wide RNAi collections aimed at targeting all fly genes have been generated (Heigwer et al., 2018). The largest library of RNAi fly lines (i.e., GD) under the UAS control for tissue-specific screens has been yielded by Barry Dickson's laboratory and distributed by the Vienna Drosophila Resource Center (VDRC). The GD library, encompassing 22,270 lines covering 88% of all known protein coding genes in the *D. melanogaster* genome, was constructed by cloning short gene fragments (~300 bp) as inverted repeats downstream of a UAS promoter into P-element in turn injected into flies embryos (Dietzl et al., 2007). The addition of UAS-Dicer-2 has shown to improve the knockdown levels for RNAi transgenes but also to increase the off-target effects (Dietzl et al., 2007). Since the integration sites of P-elements are random, the efficacy level of the knockdown may be variable in these lines. This problem have been tackled by building a transgenic RNAi vector called VALIUM1 (Vermilion-AttB-Loxp-Intron-UAS-MCS) based on the ΦC31 integrase method (Ni et al., 2008). Subsequent improvements of this vector have taken to the development of VALIUM10, which works well without the need of UAS-Dicer-2 because of the *gipsy* insulator sequence that boosts dramatically the level of knockdown, and to generate a library of 2282 lines (759 in VALIUM1 and 1553 in VALIUM10) targeting 2043

genes as part of the TRiP project (Ni et al., 2009). Furthermore, short hairpin dsRNAs (shRNA) containing 21 nucleotides embedded in an endogenous microRNA scaffold (VALIUM20) have resulted an effective alternative for classical dsRNA less prone to off-target effects (Ni et al., 2011). All the TRiP lines are distributed by the BDSC. The advantage of this method is the possibility to compare directly the RNAi lines each other. Recently the VDRC has developed the KK library based on the ΦC31 integrase method. However, it has been found that the *attP* acceptor line (pKC43 vector) used to generate the KK library contains unexpectedly two copies of the vector on the second chromosome resulting in some heterogeneity when crossed with some GAL4 drivers (Green et al., 2014).

Optogenetics

The optogenetics technique refers to the integration of optics and genetics to achieve gain or loss-of-function of temporally defined events within specific living cells (Yizhar et al., 2011; Miesenböck, 2011). It represents the most important advance in the last years among the perturbation methodologies available in neuroscience (Deisseroth, 2015). This technique affords a millisecond-scale control of cell type-specific allowing to understand biological processes in freely moving animals (Deisseroth, 2011).

In a pioneer work, Lima and Miesenböck (2005) introduced the ionotropic purinergic receptor $P2X_2$, which could be activated by caged ATP released by light (Zemelman et al., 2003), under the UAS control. The expression of these channels in dopamine neurons (i.e., by using the TH-GAL4 driver) through the UAS-$P2X_2$ line showed an increase of the locomotor activity after exposure to UV light pulses and a change of the trajectories which crisscrossed the center of the arena (Lima & Miesenböck, 2005). Unfortunately, one of the drawbacks to this system is that the caged ATP must be injected into the flies' haemolymph and then activated by the light. Such a necessary procedure is time consuming and limits the behaviours that can be investigated. However, the advent of the modern genetically encoded channelrhodopsins (ChRs) which are intrinsically

light-sensitive have revolutionized the field (Deisseroth & Hegemann, 2017). The introduction of the ChR1 and especially of the ChR2, initially isolated from the green alga *Chlamydomonas reinhardtii* (Nagel et al., 2002; Nagel et al., 2003), have dramatically increased the experimental degrees of freedom by providing an efficient and straightforward unified component for stimulating the neuronal activity (Nagel et al., 2005; Boyden et al., 2005). The ChR2 is a 470 nm light-sensitive non-selective cation (i.e., H^+, Na^+, K^+ and Ca^{2+}) channel with inward rectification which needs of the *all-trans* retinal as an essential cofactor (Nagel et al., 2003). This channel has been put under the control of the UAS (i.e., UAS-ChR2) and used in adult flies fed with *all-trans* retinal for activating gustatory sensory neurons, dopaminergic modulatory neurons and motor neurons triggering different behaviours with precise temporal control (Zhang et al., 2007b). Engineering of ChR2 construct has increased the expression level and improved the membrane trafficking modifying also the electrophysiological properties. For instance, different variants have shown increase cation conductance or photocurrent amplitude, other have shown faster turn-on and turn-off kinetics, while still others have shown bi-stable mode operation maintaining an open-pore state which enables stable current after light-off and to switch in a close-pore state with red-shifted light excitations (Simpson & Looger, 2018; Deisseroth & Hegemann, 2017). The most powerful version seems to be the 'ChR2-XXL' which shows increased light sensitivity in larvae and adults with reduced dependence on *all-trans* retinal addition (Dawydow et al., 2014). This variant is characterized by an extended open-pore lifetime, elevated cellular expression and enhanced axonal localization. All these features make ChR2-XXL autonomous from the retinal dietary supplementation to depolarize cells and evoke synaptic transmission enabling behavioral control in freely moving flies by using low intensity light (Dawydow et al., 2014). A new green highly light-sensitive (530 nm) ChR from the alga *Stigeoclonium helveticum* has revealed a very fast kinetics and because of that, named 'Chronos' (Klapoetke et al., 2014). Various efforts have been put to identify ChRs that respond with longer wavelength of light. Along with Chronos, another new ChR with long wavelength light sensitivity from the alga *Chloromonas subdivisa* with peak at 590 nm has

been discovered and because of spectral profile called 'Chrimson' (Klapoetke et al., 2014). Compared to the ReaChR (Lin et al., 2013b; Inagaki et al., 2014), another red-shifted chimerical ChR from *Volvox carteri* alga (Zhang et al., 2008), Chrimson (also called CsChrimson) has exhibited redder wavelength sensitivity differing of about 45 nm (Klapoetke et al., 2014). These two red-shifted ChRs (i.e., ReaChR and CsChrimson) have the advantages to penetrate better the cuticle of flies allowing the activation of deeper neurons and to be likely out of the fly's visible spectrum weakly affecting the visual behavioural responses (Grabowska et al., 2018).

The optogenetic silencing of neurons has been more challenge than the activating and it is still developing. A first silencing method was achieved with the halorhodopsin NpHR, a 570 nm light-sensitive anion (i.e., Cl^-) pump from the archaebacteria *Natronomonas pharaonis* (Gradinaru et al., 2008). Due to the weak Cl^- current permitted by NpHR, improvements of the light-sensitive silencers have taken to develop the archaerhodopsin Arch (an outward proton pump) and the cruxhalorhodopsin (an Cl^- inward pump) Jaws (Chow et al., 2010; Chuong et al., 2014). Strikingly, the replacement of the negatively charged glutamate amino acid in position 90 of the ChR2 protein with a positively charged residue produced a Cl^- inward conduction generating light-sensitive anion channel called ChloC (Wietek et al., 2014). Two anion channelrhodopsins (GtACRs), GtACR1 and GtACR2, have been recently discovered from the cryptophyte alga *Guillardia theta* (Govorunova et al., 2015). GtACRs conduct anions completely excluding protons and larger cations hyperpolarizing the cell membrane. Moreover, the GtACRs respond rapidly, require low light intensities for activation and comprise both cyan-sensitive channel (GtACR1, peak at 515 nm) and blue-sensitive channel (GtACR2, peak at 470 nm). These channels have also been expressed in flies successfully inhibiting neural systems involved in locomotion, wing expansion, memory retrieval, gustation and visual motion mediated by T4/T5 cells (Mauss et al., 2017b; Mohammad et al., 2017). Nevertheless, the development of a new blue-light-sensitive K^+ channel 1 (BLINK1) represents likely the most promising solution to the several limits affecting the Cl^- channels or pumps (Cosentino et al., 2015).

1.3.2 Functional imaging

To record the functional neural activity by exploiting the binary systems, various kinds of sensors which can be defined as genetically encoded functional indicators have been developed in the last twenty years (Martin, 2012). Among these indicators, the genetically encoded calcium indicators (GECIs) are the most popular ones. GECIs are protein-based sensors which interacting with Ca^{2+} enable the emission of a single split fluorophore allowing a read-out of the cellular activity (Looger & Griesbeck, 2012). An action potential firing leads to Ca^{2+} inward through voltage gated Ca^{2+} channels located on the cell membrane as well as synaptic inputs directly gate Ca^{2+} through neurotransmitter gated ion channels such as NMDA and nicotinic receptors (Kandel et al., 2013). With this in mind, advances in GECIs engineering has taken to generate the well-known GCaMP (also called G-CaMP) sensor (Nakai et al., 2001). GCaMP is a chimeric protein consisting of a GFP with modified N- or C-termini fused to the Ca^{2+}-binding protein Calmodulin (CaM). In the presence of Ca^{2+}, a structural rearrangement of the sensor occurs closing up the GFP barrel and dramatically increasing the fluorescence output. GCaMP was also put under UAS control (i.e., UAS-GCaMP) and coupled with a two-photon imaging system highlighting distinct spatial patterns of activation in the AL depending on the odour perceived (Wang et al., 2003). The recording of the amount of light emitted by GCaMP (i.e., 509 nm emission), which can increase or decrease the fluorescence on the basis of the Ca^{2+} bound, requires exciting the GFP (i.e., 489 nm excitation). Baseline fluorescence serves as reference for computing the ratio with the activity-resting difference ($\Delta F/F_0$). Therefore, changes in fluorescence through a differential imaging method are related to changes in neural activity. Simultaneous *in vivo* electrophysiological recording and two-photon imaging of GECIs have determined how the $\Delta F/F_0$ correlates with particular voltage changes or calcium-sensitive chemical dyes (Hendel et al., 2008; Jayaraman & Laurent, 2007). However, absence of $\Delta F/F_0$ changes cannot always be interpreted as signs of no activity, since GCaMP often fails to capture single action potentials or it can miss brief high instantaneous rates of activity. A development of GCaMP (i.e., UAS-

GCaMP3) has been used for monitoring neural circuits activity in intact walking flies during visual stimulations (Chiappe et al., 2010; Seelig et al., 2010). Through rational design and structural-based mutagenesis a sixth family of ultrasensitive GCaMP (i.e., GCaMP6) has been developed increasing the total $\Delta F/F_0$ in response to Ca^{2+}, its binding affinity and the velocity of turn-on and turn-off kinetics (Chen et al., 2013). The simultaneous GECIs imaging and electrophysiological recording in presynaptic boutons of the fly neuromuscular junction (NMJ) and in AL neurons has shown that $\Delta F/F_0$ changes of GCaMP6 are more sensitive and/or faster (rise time of 50-75 ms) than other GCaMP variants being able in some conditions to follow single action potentials (Chen et al., 2013). An optimization of GCaMP6 has taken to a new version, the jGCaMP7, with improved detection of individual spikes (jGCaMP7s and jGCaMP7f), imaging of deep neuropils (jGCaMP7b) and which may allows the recording of larger population of neurons (Dana et al., 2019).

Another interesting GECI named CaMPARI (calcium-modulated photoactivable ratiometric integrator) has demonstrated its utility in recording the neural activity during a specific time window by supply of photoconverting light which efficiently and irreversibly makes a green-to-red conversion allowing a temporally precise 'activity snapshot' of large tissue volume (Fosque et al., 2015).

New red-shifted GECIs have been developed as well, including jRGECO1 based on the fluorescent protein mRuby and jRCaMP1 based on the fluorescent protein mApple (Dana et al., 2016). jRGECO1 has shown a sensitivity comparable to GCaMP6 and a faster kinetics than jRCaMP1. This latter, although the lower sensitivity, has not shown photoswitching after illumination with blue light making it more suitable for experiments which combine optogenetic stimulations. These red-shifted GECIs own the advantage of reduced scattering and absorption in tissue consequently reducing the phototoxicity. However, they both have shown smaller maximal $\Delta F/F_0$ changes compared to GCaMP6 (Dana et al., 2016).

Alternatives to GCaMP include the ratiometric Ca^{2+} sensors based on the Föster resonance energy transfer (FRET) such as Cameleon, Camgaroo and TN-

XXL, where Ca^{2+} binding induces a change in fluorescence from one wavelength to another (Yu et al., 2003; Mank et al., 2008; Fiala et al., 2002). One promising alternative to the GCaMP is the chimeric protein GFP-Aequorin, a bioluminescence reporter that integrates activity over longer timescales (Baubet et al., 2000).

In jellyfish *Aequorea victoria*, the chemiluminescent Ca^{2+}-binding protein Aequorin is associated with the GFP for permitting the bioluminescence signal upon the Ca^{2+} stimulation. A chemiluminescence resonance energy transfer (CRET) between Aequorin and GFP is at the basis of the bioluminescence process. This CRET has been exploited engineering a construct of the two proteins fused together as a GECI (Baubet et al., 2000; Rogers et al., 2005). Specifically, the binding of Ca^{2+} to Aequorin produces chemiluminescence (470 nm) through the cofactor coelenterazine (i.e., a luciferin light-emitted molecule) contained in it (Shimomura et al., 1990). In order to become active, the recombinant Aequorin (i.e., the apo form of it) expressed in cells or living animals has to be reconstituted by the coelenterazine. The coelenterazine is membrane permeable and it can be supplied extracellularly for the regeneration of the intracellular photoprotein (Shimomura, 1997). Once the Ca^{2+} binds the Aequorin, it changes its conformation resulting in the oxidation of coelenterazine and emission of a single photon. Whether Aequorin and GFP are fused together, the latter absorbs the single photon via CRET and in turns emits green light (510 nm). The GFP-Aequorin is a bi-functional reporter because its expression pattern can be visualized by GFP, while Ca^{2+} activity can be measured by bioluminescence. Compared to the Aequorin alone, the GFP-Aequorin affords an increase of light emitted which can be detected by using a photon counting technique based on electron-multiplying charge-coupled-detector (EMCCD) camera fitted onto a microscope (Rogers et al., 2008). This reporter has been put under UAS control (i.e., UAS-G5A) and used to record different neural structures in flies (Martin et al., 2007; Lark et al., 2017; Minocci et al., 2013; Murmu et al., 2010). The main advantage of this system relies on the fact that the optical detection of bioluminescence does not require light excitation and is therefore less invasive than GCaMP avoiding photobleaching, phototoxicity and

autofluorescence (Martin, 2008). However, the main drawback is lower background signal which makes difficult to known when specific cells are active (Simpson & Looger, 2018).

2 EXPERIMENTS

In this chapter I shall report a series of studies aimed at investigating the selection for action mechanisms in *D. melanogaster* and at testing whether it has the ability to inhibit irrelevant information for the control of goal-directed actions. Furthermore, the neural mechanisms which might be involved to this endeavour will be presented as well.

2.1 ACTION-BASED ATTENTION

The mechanism of action selection is a widely shared fundamental process required by animals to interact with the environment and adapt to it. A key step in this process is the filtering of the "distracting" sensory inputs which may disturb action selection. Because it has been suggested that, in principle, action selection may also be processed by shared circuits in vertebrate and invertebrates I wondered whether invertebrates showed the ability to filter out "distracting" stimuli during a goal-directed action, as seen in vertebrates. In this first experiment, action selection was studied in wild-type *Drosophila melanogaster*, by investigating their reaction to the abrupt appearance of a visual distractor during an ongoing locomotor action directed to a visual target.

2.1.1 Introduction

Adaptive behaviour utilizes neural information processing systems to allow interaction with the environment so as to maximize the probability of survival and reproduction. A key feature of this behaviour in mammals is its selectivity. Relevant information has to be extracted by perceptual systems in a form that can be used to select the most appropriate action for the specific behavioural task

(Cisek, 2007). Selection mechanisms, on their side, have to block the many actions evoked by sensory inputs, except for the selected one. In the absence of these mechanisms, chaotic behaviour is consequent (Riddoch et al., 2000).

In humans and primates, selection mechanisms are associated with selective attention (Tipper et al., 1998; Castiello, 1999). The goal of selective attention is to provide sensory information that couples perception to action by selecting which object will be the target of the action and which action to use to reach the goal. However, under such conditions, information from non-target objects "interferes" with the action directed towards the relevant target. The abrupt appearance of a distracting flanker non-obstacle object creates a perceptual representation of the "distracting" object and attention is directed to it. This additional representation creates a conflict with that representing the original target object, resulting in a competition for access to higher processing levels, and producing an alteration of the kinematics of the movement directed towards the original target (Castiello, 1999).

Visual attention systems appear to operate by mapping out relevant perceptual aspects of the environment and translating them into an appropriate action also in invertebrates (Nityananda, 2016). Similar mechanisms were observed in honeybees (Paulk et al., 2014), and in *D. melanogaster* (Sareen et al., 2011) where selective attention was deployed to optimize behavioural choices.

On the other hand, to date, in invertebrates, there are no data regarding the role of "distracting" information, in the form of the sudden appearance of a competing visual stimulus, and whether it interferes with the engaged action towards a target.

Adapting a paradigm used in humans and primates (Sartori et al., 2014; Tipper et al., 1998), here I tested if flies engaged in a motor program to reach a target, were affected by the appearance of a distractor stimulus in a way congruent with an action-centred attention theoretical framework. In my modified 'Buridan paradigm' a distractor stripe (with respect to the fly's visual field) was presented while the fly was already moving towards another target stripe (Bülthoff et al., 1982; Neuser et al., 2008; Strauss & Heisenberg, 1993). I hypothesized that the appearance of the distractor might determine three possible scenarios: (i) if the

presence of the distractor does not alter the originally programmed direction of locomotion, then the fly's movement should proceed in the direction of the target, with no significant changes in the locomotion trajectory; (ii) if the presence of the distractor is inhibited in order for the fly to proceed in the originally planned direction, then some evidence of this inhibitory process might be detectable in the form of slight perturbations in the original locomotion trajectory; (iii) if the presence of the distractor determines the initiation of an alternative motor program, which has the power to override the original one, then a dramatic change in direction towards the distractor should be evident.

I found that flies deployed an inhibitory mechanism operationalized in the form of trajectory changes without significantly interfering with the kinematics of the original target-bound action.

These results raise interesting considerations regarding the nature of the selection-for-action mechanism in *D. melanogaster* and provide new data in support of an attention-like behaviour. In particular, flies appear to inhibit the response towards a novel stimulus in order to complete an already activated motor program, in line with what has already been observed in humans and primates.

2.1.2 Methods

Animals

The experiments were performed on 22 adult wild-type fruit flies (*Drosophila melanogaster*; Oregon-R strain). All flies were reared on standard cornmeal-sucrose-yeast medium at 22°C in a 12 h light/12 h dark cycle at 60% relative humidity. Fly crowding was controlled (20-30 flies each vial). Only individual 2-5 day-old male flies were used. For the experiment, flies were not previously starved. All experiments were conducted between zeitgeber time 2 and 4 at room temperature 22-23°C.

Experimental setup

To test how flies respond to the sudden appearance of a distractor stripe while freely walking toward a target stripe, I modified the 'Buridan paradigm' in which a stripe, termed "distractor", was laterally presented (with respect to the fly's visual field) while the fly was moving towards one of the two opposing stripes, from now on called "targets", which constitute the classical version of the paradigm. The two opposing "Buridan" stripes, differently to the distractor, were present during the entire experimental session. To test how flies respond to the abrupt appearance of the distractor during the free walking behaviour, I employed a cylindrical led-emitting-diode (LED) modular display positioned around an open arena (Reiser & Dickinson, 2008). Such a display consisted in 48 (12 width x 4 height) LED panels emitting green light (520 nm), each composed by an 8 x 8 array of LEDs (IO Rodeo Inc, Pasadena, CA, USA). A custom-designed transparent arena in which the flies were placed during the experiments, made of 3D-printed resin (iMaterialise HQ, Leuven, BE, EU), was placed within the cylindrical LED display. The arena (3.5 mm height at the centre and 109 mm diameter) was designed so as to (i) confine flies in 2D space, (ii) not allow the flies to reach the edge of the arena and (iii) to impede flight by means of a glass 'ceiling' (Simon & Dickinson, 2010). The arena was backlit by an infrared (IR) LED array source (LIU850A, Thorlabs Inc, Newton, NJ, USA) and the IR light was diffused using paper diffuser films placed between the IR light source and the arena. A CCD camera (Chameleon 3, FLIR System Inc, Wilsonville, OR, USA) with 1288 x 964 pixel resolution, fitted with a 2.8-8 mm varifocal lens (Fujifilm, Tokyo, JP) and an 850 nm band pass filter (MidOpt Inc, Woodwork Lane Palatine, IL, USA) was mounted 36 cm above the arena in order to record fly locomotion. Videos of flies moving in the arena were recorded at 21 frames s^{-1}, following selection of a 700 x 700 pixel region of interest which included the entire arena. In order to allow the experimenter to visually observe all events occurring within the arena (including whether visual patterns were being correctly displayed) an HD webcam (C310, Logitech, Lausanne, CH, EU) was also mounted alongside the infrared camera. The LED display was mounted on a

metal plate docked to a stainless steel pillar which allowed to rotate and lift the display, thus facilitating the loading of the arena, before positioning it within the LED cylinder. A custom-designed and homemade table of poly (methyl methacrylate) supported the arena. Display, arena and cameras with their supports, were fixed to an aluminium breadboard (Thorlabs Inc, Newton, NJ, USA). The whole setup was then positioned on an anti-vibration table, placed inside a wooden cage and covered with heavy black fabric to ensure complete darkness (Fig. 2.1A).

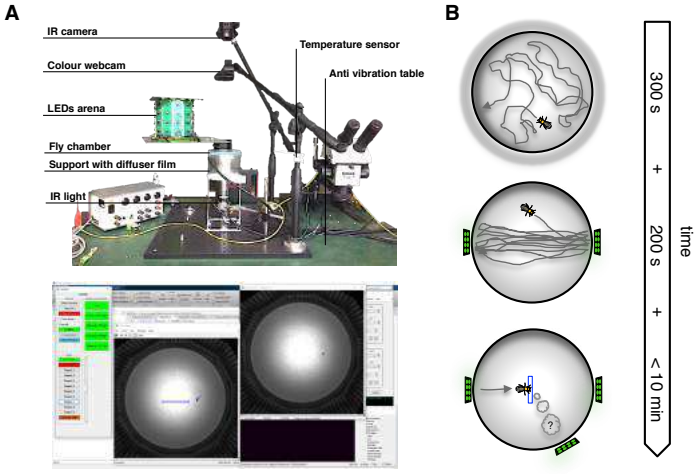

Fig. 2.1. Experimental setup and procedure. *A*: on the top, image showing the main components of the setup utilized in the experiment described in the paper. At the bottom, screenshot of the MATLAB custom GUI developed in our laboratory. *B*: cartoon showing the three phases involved in each experiment. Starting from the top: (1) acclimatization period in complete darkness for 300 s; (2) two opposing bright green stripes were switched on and the behaviour was recorded for 200 s; (3) behavioural task consisting in the random presentation of a distractor stripe at 60 deg whenever the fly crossed a virtual central window (blue rectangle). Behavioural task lasted maximum 10 min, after which the fly was removed regardless the number of trials performed.

Software and management

The cylindrical LED display was controlled using MATLAB (MathWork Inc, Natick, MA, USA) scripts (Reiser & Dickinson, 2008). The MATLAB Image Acquisition Toolbox was used for video recording. Furthermore, in order to

detect the position of the fly's head in a specific spatial location (i.e., inside the virtual central window within the circular arena) and activate the necessary visual patterns on the LED display accordingly, I implemented a system for real time tracking using the FAST (Features from Accelerated Segment Test) method (Rosten & Drummond, 2006) provided by the MATLAB Computer Vision System Toolbox. Online tracking analysis, video recording and control of the LED arena were integrated into a single custom GUI (Graphical Unit Interface), providing a unified software environment to manage all experimental variables. All the scheduled events involved in each experiment were automatically controlled by means of custom scripts which could be launched by the user-friendly GUI (Fig. 2.1A).

Procedure

Flies were individually loaded into the arena and were left to adapt in complete darkness for 5 min. Individuals were then subjected to a 'Buridan's paradigm', by illuminating two opposing bright stripes (i.e., the targets) of 4 x 16 LEDs (width x height) each one covering 15 deg width and 60 deg height of the fly's visual field when observed from the centre of the arena. The classical interpretation of the phenomenon underlying this paradigm refers to the alternation between fixation and anti-fixation of attractive landmarks represented by contrasting stripes on a uniform background (Maimon et al., 2008; Bülthoff et al., 1982; Reiser & Dickinson, 2008; Horn & Wehner, 1975). Preliminary experiments which I conducted have showed a more robust fixation response to the 'Buridan's paradigm' in individuals tested with bright stripes on dark background and, therefore, I decided to run the experiments with this configuration. In this experiment, individual fly locomotion consisting in the fly continuously running to and fro between two opposing bright targets, was initially recorded for 200 s. Flies which did not exhibit this behaviour were not considered further (Kain et al., 2012). At this point the behavioural task-proper was initiated. While the fly was still performing the 'Buridan paradigm', the distractor of the same dimensions as the targets, was presented for 1 s when the fly crossed a virtual

central window (27 mm x 3.6 mm) of the arena while running toward one of the original targets (Neuser et al., 2008). The distractor appeared to the right of the fly at an angle of 60 deg. The sequence of trials (i.e., distractor on or off) was randomly determined and counterbalanced across and within flies. Each fly performed the task for a maximum of 10 min, after which it was removed to avoid fatigue-determined bias (Fig. 2.1B).

Off-line tracking

To obtain an extensive characterization of the fly's 2D position with its body orientation (which was not detected by the real time tracking system), I tracked the fly's positions off-line by using the CTRAX open source software (Branson et al., 2009). Errors occurring during the tracking were corrected manually using appropriate MATLAB scripts (CTRAX, FixErrors Toolbox) (Branson et al., 2009).

Data pre-processing

The files obtained following the off-line tracking analysis were imported into R software (R Development Core Team, 2017) for analysis with custom scripts. Only data from tracks in which single flies were directed towards the target were selected (i.e., all tracks in the opposite direction were removed). Table 1 summarizes these data.

Table 1. *Data summary*

Condition	No.	Velocity, mm s^{-1}	Distance, mm
no distractor	57	8.61±5.56	43.05±18.17
distractor	33	8.22±5.88	41.10±19.17

Note. Average ± SD. No.= number of tracks.

Statistical approach

Repeated measures analysis of variance (rANOVA) was conducted using the *afex* R package (Singmann et al., 2018). Linear Mixed Effects (LME) models computed by using the *lme4* R package (Bates et al., 2014), were employed to compare two shifting models, with or without the experimental manipulation as predictor. For model selection I used the Bayesian Information Criterion (BIC) (Schwarz, 1978).

2.1.3 Results

As a first step, I checked whether the path length and the initial position of flies along the y-axis, x-axis, their orientation and velocity, were uniformly distributed (Fig. 2.2A), to rule out any influence by these variables on the subsequently measured trajectories. None of these variables showed significant differences between the two conditions (for path length: $F_{(1, 88)} = .23$, $\eta^2 = .003$, $p = .63$; for y-axis: $F_{(1, 88)} = 2.61$, $\eta^2 = .03$, $p = .11$; for x-axis: $F_{(1, 88)} = .01$, $\eta^2 < .0001$, $p = .94$; for orientation: $F_{(1, 88)} = .07$, $\eta^2 = .0008$, $p = .79$; and for velocity: $F_{(1, 88)} = 2.77$, $\eta^2 < .03$, $p = .10$). It means that flies owned the same initial parameters regardless of the experimental condition.

Visual inspection of the average flies' position along the y-axis through time showed a slight lateral shift in the presence of the distractor with respect to its absence (Fig. 2.2B). For a more accurate understanding of this behaviour, I focalized the analysis on the first two seconds of each trial, that is, during the distractor appearance and during the period of one second after the distractor was turned off. I decided to extend this analysis beyond the period of distraction (i.e., 1 s) because the peak of lateral shift was evident at 2 s after the distractor onset. Since I was interested in the level of interference determined by the distractor, I linearly modelled the flies' position along the y-axis to understand how much flies changed their heading within this time window (rectangular window in Fig. 2F). I tested and compared two models, one with an interaction parameter between time and condition and the other with only time as a parameter (Table 2).

Table 2. *Models selection*

Model	Df	BIC
$Y_{ij} = \beta_0 + \beta_2 X_{1i} \cdot D_{2i} + \lambda_i + \epsilon_{ij}$	5	20604.52
$Y_{ij} = \beta_0 + \beta_1 X_{1i} + \lambda_i + \epsilon_{ij}$	4	20604.70

Note. Y_{ij}: shift along y-axis; X_1: time; D_2: condition; λ_i: random effects; ε_{ij}: error.

The model with the lower BIC value, turned out to be the one with the interaction parameter (top left inset of Fig. 2.2C for fixed effect and Fig. 2.2D for random effect). The model shows that in the first two seconds of recording, the flies shifted slightly (4.42 deg) towards the distractor (Fig. 2.2C). Bootstrapping of the values related to the interaction parameter for each of the two conditions showed that the final distributions of the values shown by the distractor and no distractor conditions did not overlap, implying a statistically significant difference between the two conditions ($p < .0001$). This basically means that, on a frame-by-frame basis, the flies showed a significantly greater lateral shift in the presence of the distractor than in its absence.

Overall, these results show that flies reacted to the distractor in a way which clearly indicates that they acknowledged its presence, nonetheless maintaining their course towards the original target.

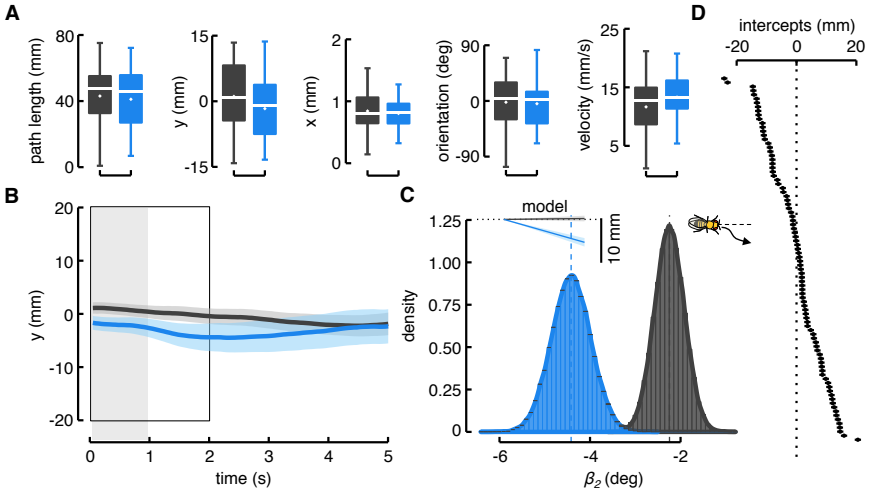

Fig. 2.2. Initial variables and distractor effect. *A*: starting from the left: boxplot of the path length in the two condition ($F_{(1, 88)} = .23$, $\eta^2 = .003$, $p = .63$); boxplot of the initial flies' position along the y-axis ($F_{(1, 88)} = 2.61$, $\eta^2 = .03$, $p = .11$); boxplot of the initial flies' position along the x-axis ($F_{(1, 88)} = .01$, $\eta^2 < .0001$, $p = .94$); boxplot of the initial flies' orientation ($F_{(1, 88)} = .07$, $\eta^2 = .0008$, $p = .79$); boxplot of the initial flies' forward velocity ($F_{(1, 88)} = 2.77$, $\eta^2 < .03$, $p = .10$). Box defines first (Q1) and third (Q3) quartiles; bold horizontal white line is the median; white small rhombus is the mean; whiskers define the lowest value still within 1.5 interquartile range [i.e., 1.5×(Q3–Q1)] of the lower quartile and the highest value still within the 1.5 interquartile range of the upper quartile. *B*: plot of the lateral shifting along y-axis performed by flies distinguished for condition. Average shifts (thick lines) and raw shifts (thin lines) per time. The shadow regions around the average represent SE. The shadow rectangle in light grey represents the 1 s period of distractor appearance. The black window represents the time interval I used for modelling. *C*: distribution of 100,000 bootstrapped model parameter values regarding the interaction between time and condition. The parameter was converted in degrees by means of the equation reported in x-axis. It basically shows that frame-by-frame the lateral shifting increases more for distractor than no distractor condition. Moreover, the two distribution show almost no overlapping which, in the classic frequentist perspective, implies a statistically significant difference between the two conditions ($p < .0001$). On the top left, the inset shows the shifting modelled for condition, while the inset on the right shows a cartoon of the fly shifting consistent with distractor position. *D*: plot of random effect of the model. Dots represent each trial (known as BLUPs, Best Linear Unbiased Predictions) while the horizontal lines crossing dots corresponds to the SD. Colour coding for all graphs: black corresponds to the no distractor condition, whereas blue to the distractor condition.

2.1.4 Discussion

The primary aim of this study was to evaluate if, as observed in humans and primates, the abrupt presentation of a distracting flanker non-obstacle object to fruit flies, would influence the already-engaged locomotor action towards the original target. The results indicate that the onset of the distractor seems to capture the attention of flies, initially inducing a significant shift in their trajectory in its direction if compared to what occurs when no distractor was presented. This implies that flies acknowledged the presence of the distractor.

It has been already shown that invertebrates exhibit attention-like responses. In particular, freely moving insects display selective visual attention (Collett & Land, 1975; Giurfa, 2013; Nityananda, 2016; van Swinderen, 2011). Although it appears that attentional processes in invertebrates are elicited exogenously via bottom-up mechanisms, there is also evidence suggesting higher order modulation of attention via top-down mechanisms (Nityananda, 2016).

This data confirmed that the abrupt onset of a flanker "distractor" evoked a bottom-up attentional response in flies. Indeed, the observed reaction following the presentation of a distractor suggests that the sudden appearance of a distractor in the fly's visual field evoked changes in the motor responses. Recently, by employing a 'Buridan's paradigm' version comparable to mine in freely walking flies, it has been shown how the presence of distractors evoke the flies' distractibility (Kirszenblat et al., 2018). However, this experiment did not address selective visual attention by exploring it from the point of view of the sensory input, rather whether, once a visual target has been selected for an action implementation, the motor program may be affected by the processing of a distracting visual input. This question is embedded in the selection-for-action theory, according to which to minimize the action-interference effects, the information has to be inhibited from the motor perspective (Allport, 1987).

Consistent with this theory, this data showed that flies changed their trajectories only partially towards the distractor, as evident in the trajectory angle of 4.42 deg compared to the distractor angulation of 60 deg. Flies remained much closer to the target during the distraction and then, once the distractor

disappeared, they finalized the original target-oriented motor program. This process would correspond to the formation of an additional motor representation for the "new object" conflicting with that already active for the target object. At this point it is reasonable to surmise that a top-down mechanism would be required to solve the conflict and select the right action. Namely, flies deployed an inhibitory mechanism operationalized in the form of trajectory changes in order to maintain the original target-bound action.

As previously found for humans and primates, the sudden appearance of a distractor object reaches a level of relevance similar to that of the target, activating a competition between the actions evoked by the target and the distractor. In other words, each object generates a parallel kinematic plan for action, determining an interference between "the intended but not-executed" action towards the distractor, and the "intended and executed" action towards the target. The level of interference is proportional to the visual salience of the distractor (Castiello, 1999; Castiello, 1996). Specifically, a perceptuomotor representation for the "new object", which conflicts with that already active for the target, generates a competition for higher levels of processing. This results in an alteration of the kinematics of the engaged action towards the target (Castiello, 1999).

Notwithstanding my interpretation, one particular concern is that this behaviour could simply be due to phototaxis (McEwen, 1918). However, since i) the distractor is of exactly the same size and luminosity as the original target (i.e., it is a visual object which elicits fixation, as is the case for the original target; see Materials and methods), and ii) the ensuing motion of the flies is still directed towards the original target (i.e., it is not the case that the new trajectory is directed towards a point situated midway between the target and the distractor, as expected in the case of phototactic response) (Fraenkel & Gunn, 1961); suggests that the observed response of the flies was rather a consequence of their attention being temporarily captured by the flanker, before being inhibited.

Given the importance of action selection mechanisms in animal behaviour, I believe that the novel evidence here presented for such phenomena in a highly tractable model organism such as *D. melanogaster*, provides an important basis

for a more detailed exploration of the relationship between environmental stimuli and motor responses, as well as of the neural circuitry involved in the visuomotor integration underlying such processes.

It is currently unclear whether flies and humans independently evolved selection-for-action mechanisms, or whether they share the same mechanisms through a common ancestral neural circuit subserving this process. It has however been suggested that the vertebrate basal ganglia and the arthropod central complex share an evolutionarily conserved developmental genetic program and that these two neural structures may also share an involvement in the selection and maintenance of actions (Strausfeld & Hirth, 2013b). This an interesting issue that I further investigated in the third experiment.

2.2 RESPONSE TO A PERTURBATION DURING WALKING

In this study I used the same paradigm as for the previous experiment except that the number of conditions was increased and the exposure time of the distractor was manipulated. I tested how flies react to the appearance of visual distractors presented at different angular distances while they were aiming to a target.

2.2.1 Introduction

Visuomotor control is an important process through which animals interact with the environment. The first step of this process entails visual awareness of what is happening in the surroundings by directing gaze towards a salient stimulus.

The two most relevant mechanisms underlying visual control are *saccades*, rapid eye movements which are used to correct the visual axis with respect to a target and *pursuits*, slow eye movements which are used to smoothly stabilize a moving target onto the fovea (Land, 1999).

In humans, saccades and smooth pursuits eye movements have been historically thought to rely on two distinct neurophysiological and neuroanatomical systems, namely the position and motion systems, but increasing evidence suggests a great deal of overlap between them (Orban de Xivry & Lefèvre, 2007). Therefore, it has been suggested that saccades and pursuit might be different outcomes of a single sensorimotor process, based on a unified neuronal circuit, for visual tracking (Orban de Xivry & Lefèvre, 2007).

D. melanogaster not only has the ability to track a visual stimulus by using either smooth pursuit or saccade responses, but also to discriminate a visual stimulus on a moving wide-field background, suggesting two independent components. The first one sensible to elementary motion (i.e., velocity-dependent EMDs), on which is also based the optokinetic reflex, and the second one to higher-order figure motion (Aptekar et al., 2012). However, whether in fruit flies there is one or two different circuits driving saccades and smooth pursuit responses is still a matter of debate. By using the neurogenetics silencing

of the T4 and T5 cells in tethered walking flies, the motion and the position "systems" have been separated at both behavioural and neuronal levels (Bahl et al., 2013). An optomotor control mechanism based on the motion vision, which operates only with luminance information, would allow the smooth pursuit behaviour of an object, while a position mechanism would permit the object detection and the rapid gaze orientation towards it (i.e., saccadic response).

Furthermore, recent results in flying flies, suggest that catch-up body saccades are triggered by a separate parallel controller, as compared to velocity (with the former being based on a time integral of the visual stimulus position error) (Mongeau & Frye, 2017). This implies that a position system for computing the angular error of a discrete visual stimulus (i.e. a contrasting vertical stripe) would be distinct from the motion system for detecting the velocity of a stimulus.

Conversely, in blowflies of the genus *Lucilia*, catch-up saccades and smooth pursuit body responses seem to rely on a single sensorimotor system encoding for both position error (i.e., angle) and target motion (i.e., velocity) (Boeddeker & Egelhaaf, 2005). Moreover, a formal separation of the two systems might not have a corresponding separation at the neuronal level (Poggio & Reichardt, 1973; Boeddeker & Egelhaaf, 2005; Poehlmann et al., 2018). Along these lines, it has recently been shown how the well-known asymmetric optokinetic mechanism (based on the input of T4/T5 cells to the lobula plate), which is at the basis of visual motion perception for flight body stabilization in *Drosophila melanogaster*, could mediate the responses associated to position as well as the responses which are associated with motion (Fenk et al., 2014; Poehlmann et al., 2018).

In this study, I attempt to identify the mechanisms underlying visuomotor control in freely walking flies by introducing a visual interference during an ongoing walking activity. The questions I wish to address are: (i) does the visual surrounding environment drive the locomotor activity of flies passively depending on the optokinetic response (i.e., a motion-based system) or (ii) are flies able to represent the position of a landmark through active fixation (i.e., a position-based system) and put in place a response inhibitory mechanism for novel incoming stimuli?

To answer these questions I exploited the fixation behaviour induced by the 'Buridan's paradigm' which is thought not to involve the motion-direction integrating cells (i.e., HS and VS cells), even though greater accuracy is gained with a perfectly working motion-direction system (Bülthoff et al., 1982; Heisenberg et al., 1978). I tested how the abrupt presentation of a lateral bright stripe to flies already engaged in walking between pre-existing opposing stripes would determine motor adjustments in terms of turning reaction and spatial trajectories.

I hypothesized that the position system would be more prominent than the motion system since the paradigm used seems to marginally involve the motion system. My prediction was that flies should display a behaviour consistent with a mechanism involving attention towards the originally presented bright stripe and the consequent inhibition of the new abruptly presented lateral stripe (Frighetto et al., 2019). In other words, I expected that flies would filter out the distraction through a mechanism based on the position system and in such a way consistent to a reactive inhibition model (Houghton & Tipper, 1994; Tipper et al., 1997). In this view flies would display a slight drift in their trajectory towards the distractor when the latter is presented at greater angle with respect to the target, because in this condition the distractor would represent a weaker interference with respect to the original target (i.e., weaker inhibition). Whereas, I expected only a slight drift away from the distractor when the latter is presented at a smaller angle with respect to the target because in this case the distractor would represent a higher interference with respect to the original target (i.e., stronger inhibition).

2.2.2 Methods

Animals

Similarly to the previous study, the experiments were performed on 21 young adult male flies of 2-5 day-old from the wild-type Oregon-R strain (for further details see Frighetto et al., 2019).

Experimental setup and software management

The setup and software management were similar to those used in the previous section of this chapter.

Procedure

For each recording, a single fly was loaded into the arena by using a mouth aspirator and was left to adapt in darkness for at least 5 min. The individual was then subjected to a 'Buridan's paradigm' and recorded for 200 s. Flies which did not exhibit this regularity in the alternation between fixation and anti-fixation (i.e., remained still or roamed at random) were not considered further (Kain et al., 2012). After this "selection phase", the behavioural task-proper was initiated. While the fly was still running towards one of the target bright stripes, a new bright distractor stripe was presented at the moment the fly crossed the midline of the arena (a modified detour paradigm; Neuser et al., 2008). The distractor was presented for a period of 3 s starting from the fly crossing of a virtual central window (27 mm width and 3.6 mm depth; Fig. 2.3) along the x-axis connecting the two "Buridan" bright stripes. Simultaneously, the camera was triggered and the video acquisition was extended for 2 s after the distractor was turned off. Distractor stripes had the same dimensions as the pre-existing target stripe and could appear to the right or to the left, at an angle of either 30 or 60 deg, with respect to an ideal line connecting the opposing target stripes. Each one of the four distractors conditions (left or right at 30 or 60 deg), in addition to the absence of a distractor was presented seven times to the fly (i.e., 5 conditions multiplied by 7 times). Thus, the entire experiment ended when all five conditions had been randomly presented (seven times) for average experiment duration of 30 min.

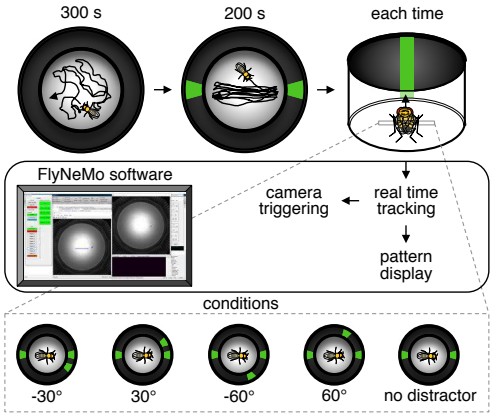

Fig. 2.3. Experimental design. Starting from the top left, the image shows the procedure employed in the study. Each experimental session was composed by three phases: (1) acclimatization period in complete darkness for 300 s; (2) two opposing bright green stripes were switched on and the behaviour was recorded for 200 s; (3) behavioural task consisting in the random presentation of a distractor stripe whenever the fly crossed a virtual central window (light grey rectangle). On the middle left, screenshot of the FlyNeMo GUI with its pipeline to the right which allowed us the real time tracking of the fly, the sending the visual pattern to the display and the triggering of the camera for video recording. On the bottom the five conditions which could be randomly triggered, from the left to the right: distractor at 30 deg to the right; 30 deg to the left; 60 deg to the right; 60 deg to the left; no distractor presentation. Each condition had to be presented 7 times and once all conditions reached this value the experiment automatically ended. Movements to the right were categorized with negative sign while the ones to the left with positive sign. Behavioural task lasted on average 45 min.

Off-line tracking

An extensive definition of the fly's 2D position and body orientation were obtained by tracking the flies off-line with the CTRAX software (Branson et al., 2009).

Data pre-processing

Once corrected the files related to the tracking data (since some errors could be made by CTRAX) and transformed into .txt, the files were imported into the integrated development environment RStudio (RStudio Team, 2017) for R programming language (R Development Core Team, 2017), in order to pre-process and analysis data by means of custom scripts. A suite of kinematic indices

(i.e., velocities and accelerations) was computed as well as movement time and the distance travelled by flies. For the trajectory analysis, only data from tracks in which flies were directed towards the target were selected (i.e., all tracks in the opposite direction were removed). The tracks considered for the analysis were selected on the basis of two criteria, the minimum path length had to be longer than 10 mm and the path had to reach the periphery of the arena (i.e., 40 mm at least) in 3 s. These criteria were used to obtain trajectories aimed at the final endpoint near the edge of the arena (of 45 mm radius) and to avoid interference arising from flies stopping. After filtering, the distances travelled by flies were normalized with a feature scaling method $d' = (d - d_{min})/(d_{max} - d_{min})$; where d is the original distance travelled and d' the normalized one. For each normalized distance value, the lateral drift value, from now on y – along the axis orthogonal to the line connecting the two stripes of the 'Buridan's paradigm' (i.e., x-axis), was selected and in so doing, the normalized trajectory reconstructed. For saccade detection I used an automatic routine to find out yaws with velocity threshold above 200 deg s^{-1} and duration longer than 95 ms (Geurten et al., 2014). A summary of the data frame is reported in Table 3.

Table 3. *Velocity, distance and movement time with respect to the conditions*

Condition	No.	Velocity (mm s-1)	Distance (mm)	Movement time (ms)
no distractor	61	20.42±6.20	42.81±4.44	2097±443
30°R	79	20.89±7.24	40.46±3.53	1937±423
30°L	81	21.20±6.17	41.05±3.55	1936±359
60°R	55	20.44±6.38	41.24±5.56	2018±419
60°L	62	20.63±6.64	42.36±4.82	2054±399

Note. Average ± SD. No.= number of tracks.

Statistical analyses and simulation

To understand which predictors explained the trajectories taken by the flies in the presence of distractors, I tested a series of LME models using the R package

lme4 (Bates et al., 2014). I used LME because such models allow the adjustment of estimates for repeated sampling (i.e., more than one observation arises from the same fly) and for imbalance in sampling (i.e., some flies are sampled more than others). LME also allows to take into account the experimental variation (i.e., variation among flies or among other groupings variables) and to avoid the harmful effects of averaging, since this tends to remove variation (McElreath, 2016). Subsequently, the LME models were compared in order to select the best one (i.e., the best fit to the data). For model selection I used the Bayesian Information Criterion (BIC) also known as the Schwarz information criterion or Schwarz's BIC (Schwarz, 1978), an index that measures the efficiency of the model in terms of data forecasting. Since BIC tends to favour models with fewer parameters than the related AIC (Akaike Information Criterion), thus penalizing the likelihood results through overfitting, I preferred the former. In case of comparison between a null and an alternative model I used an approximation of the Bayes Factor (BF) calculated as $BF \approx e^{(-\frac{\Delta BIC}{2})}$, where $\Delta BIC = BIC_{(\text{null model})} - BIC_{(\text{alternative model})}$, which gives us a value about how much more plausible is one model compared to the other one. Analysis of variance (ANOVA) computed by using the R package *afex* (Singmann et al., 2018) and pairwise post hoc comparisons adjusted with the Tukey method were also used under the null hypothesis that the sample distributions belonged to the same population. To compute repeated measures correlations I used the R package *rmcorr* (Bakdash & Marusich, 2017). Simulations of the polynomial trajectories, based on a custom algorithm which took into account parameters linked to the flies' initial position as input, were also preformed in RStudio (RStudio Team, 2017). A system of simple trigonometric equations was solved within an iterative procedure with repetitions corresponding to the percentage steps of the normalized trajectories which matched distances travelled by flies computed on the basis of an average velocity. For each step a pseudo-random number from a uniform distribution (-15, 15 deg) was added to the orientation value in order to generate background noise.

2.2.3 Results

Trajectories effect

To verify my hypotheses, as a first step, I investigated how flies responded to the appearance of the distractor in terms of trajectories. Before doing so, to confirm the null hypothesis, I checked the distributions among conditions (where "condition" refers to the presence/absence and position of the distractor) of the position and the orientation of flies at the beginning of each trial (i.e., t0) when they crossed the virtual window triggering the video recording and the distractor appearance (Fig. 2.4A). Moreover, I tested the final values (i.e., t1) of the radius owned when flies reached the periphery of the arena (i.e., at least 45 mm) and the forward velocity at t0 among conditions to rule out any influence of them. None of such variables at t0, position along the y-axis (Fig. 2.4B), position along the x-axis (Fig. 2.4C), orientation (Fig. 2.4D), radius reached at t1 (Fig. 2.4E) and forward velocity at t0 (Fig. 2.4F) showed significant differences among the conditions, confirming the null hypothesis. I next conducted LME modelling of the trajectories (Fig. 2.4G, H, I) testing seven different models. BIC was computed for each model and the resulted values used for selecting the best model (Table 4).

Table 4. *Models selection*

Model	Df	BIC
$Y_{ij} = \beta_0 + \beta_1 D_{1i} X_{1i} + \beta_2 X_{2i} + \beta_3 X_{3i} + \lambda_i + \epsilon_{ij}$	10	37876.24
$Y_{ij} = \beta_0 + \beta_1 D_{1i} X_{1i} + \beta_2 X_{2i} + \beta_3 X_{3i} + \beta_4 X_{4i} + \lambda_i + \epsilon_{ij}$	11	37888.99
$Y_{ij} = \beta_0 + \beta_1 D_{1i} X_{1i} + \beta_3 X_{3i} + \lambda_i + \epsilon_{ij}$	9	37997.51
$Y_{ij} = \beta_0 + \beta_1 D_{1i} X_{1i} + \beta_2 X_{2i} + \lambda_i + \epsilon_{ij}$	9	38275.39
$Y_{ij} = \beta_0 + \beta_1 D_{1i} X_{1i} + \lambda_i + \epsilon_{ij}$	8	38295.39
$Y_{ij} = \beta_0 + \beta_1 D_{1i} X_{1i} + \beta_5 X_{5i} + \lambda_i + \epsilon_{ij}$	9	38302.24

Note. Y_{ij}: drift along y-axis; D_1: conditions; X_1: normalized distance; X_2: initial orientation; X_3: initial position along y-axis; X_4: initial forward velocity; X_5: initial position along x-axis; λ_i: random effects; ε_{ij}: error.

By using this approach the best fit model (the one with the lowest BIC value) was the one that considered the interaction between normalized distance and conditions in addition to the parameters of initial orientation and position along the y-axis. Distinct left and right slopes (depending on the type of distractor presented) characterized the linear trajectories as a function of the interaction parameters (distance and condition), while the absence of any overlap between the confidence intervals implies a statistically significance difference between them (Fig. 2.4H). The average trajectories of the flies shifted coherently with the position of the distractor, so that the greater the angle of appearance of the distractor with respect to the original trajectory, the farther the shift of the path of the flies in the direction of the distractor. However, the shifts in the trajectories did not appear to be related to the absolute angular distance of distractors from the target, but seemed to depend more on the initial (i.e., at t0) position and orientation of flies (i.e., position angular error) (Fig. 2.4J). This means that flies were attracted by the distractor independently from its location (i.e., 30 or 60 deg). Therefore, what I expected to be (i.e., distractor at 60 deg) and not to be (i.e., 30 deg) attractive, determined different responses. For distractors at 30 deg, the response of flies resembled the observation by Horn and Wehner (1975), who reported that flies showed a preference of movement in a direction midway between two stripes, when the flies start with random stationary orientations. Nevertheless, my observations show that, although the flies adopted a trajectory lying in between the distractor and the target, the resulting path was closer to the latter (Table 5).

Table 5. *Coefficients of the best model*

Parameter	Estimate	Std. Error	t value
orientation, t0	0.1757	0.0135	12.9798
y,t0	0.8831	0.0310	28.4529
no distractor	0.0310	0.0173	1.7931
30°R	-0.4120	0.0152	-27.0590
30°L	0.4676	0.0150	31.1003
60°R	-0.5449	0.0182	-29.9942
60°L	0.6619	0.0171	38.6347

Instead, for distractors at 60 deg, flies adopted an average trajectory which tended to drift towards the distractor in a more pronounced manner than in the case of the distractor at 30 deg, meaning that the 60 deg distractor attracted the flies, but not as much to determine dramatic changes in the trajectory path. The data also argue against these responses being determined by phototaxis, since if this were the case, I should have consistently observed trajectories midway between the target and the distractor for both angular distances tested (Fig. 2.4K).

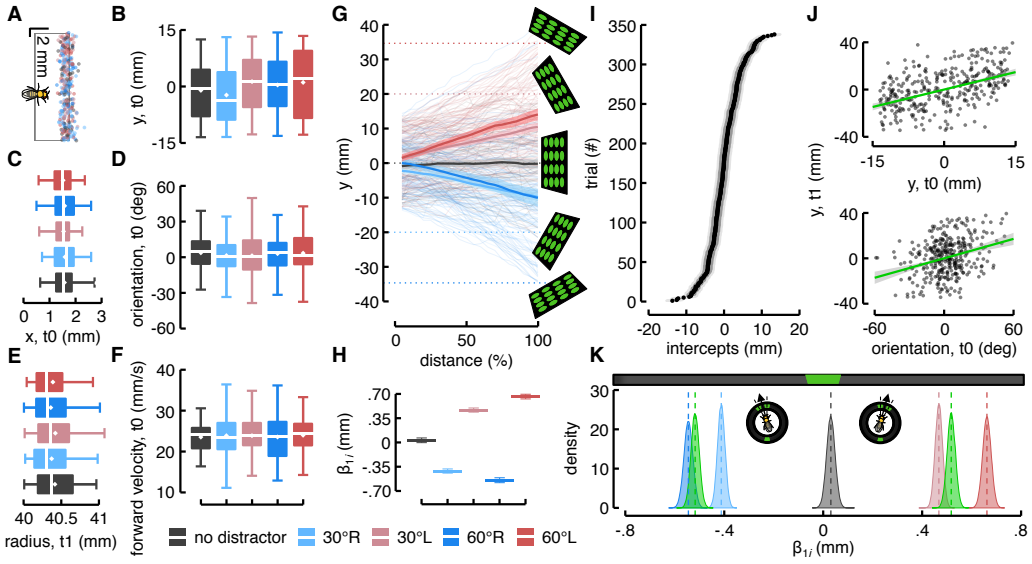

Fig. 2.4. Trajectories effects and modelling. *A*: scatter plot of the position owned by flies when they crossed the virtual window (black rectangle) triggering the video recording and the distraction. *B*: boxplot of the initial flies' position (i.e., t0) along the y-axis ($F_{(3, 50)} = 1.72$, $\eta^2 = .06$, $p = .17$). *C*: boxplot of the flies' position along the x-axis at t0 ($F_{(3, 54)} = 1.19$, $\eta^2 = .04$, $p = .32$). *D*: boxplot of the flies' orientation at t0 ($F_{(3, 47)} = .52$, $\eta^2 = .02$, $p = .66$). *E*: boxplot of the radius reached by flies at t1 ($F_{(4, 58)} = 1.18$, $\eta^2 = .05$, $p = .33$). *F*: boxplot of the flies' forward velocity at t0 ($F_{(3, 49)} = .39$, $\eta^2 = .008$, $p = .77$). *G*: plot of the lateral shifting along y-axis performed by flies distinguished for conditions. Average shifts (thick lines) and raw shifts (thin lines) per distance. The shadow regions correspond to SEM. The dotted lines (coded by colours) show the position of the distractors along the y-axis. *H*: estimated parameters of the fixed effect referred to the interaction between distance and condition with corresponding confidence intervals (parametric bootstrap intervals of 10,000 simulations) at 97.5% level. *I*: plot of random effect. Dots represent each trial (known as BLUPs, Best Linear Unbiased Predictions) while the horizontal lines crossing dots corresponds to the SD. *J*: on the top, correlation between the flies' position along the y-axis at t0 and the ones at t1 ($r_{rm} = .47$, $df = 316$, $p < .0001$); on the bottom, correlation between the flies' orientation at t0 and the flies' position along the y-axis at t1 ($r_{rm} = .33$, $df = 316$, $p < .0001$). *K*: distribution of 100,000 bootstrapped model parameters values regarding the interaction between distance and condition compared to simulated parameters in green referred to trajectories midway between target and distractor due to phototactic behaviour. Only distributions of simulated phototactic parameters for distractors at 30 deg are depicted because the values referred to distractors at 60 deg are so laterally shifted to be outside the figure. For distractor at 30 deg the distributions show overlapping between the model and phototactic simulated parameters, which, in the classic frequentist perspective, implies a no statistically significant difference between the two conditions. However, for distractor at 60 deg no overlapping are evident, meaning that the flies' responses were not due to phototaxis. As reported on the bottom of the panel, colour coding for all graphs: black corresponds to the no distractor condition; light blue to distractor at 30 deg to the right; light red at 30 deg to the left; blue at 60 deg to the right; red at 60 deg to the left.

Orientations effect

Modelling of the orientations initially adopted by the flies at the onset of the distractor stimulus showed a behaviour consistent with the trajectory models. Profiles of the average orientation showed shifts according to the angular position of the distractors (Fig. 2.5A). Interestingly, such orientations never lined up with the exact distractor position, but rather pointed towards a position midway between the target and distractor (in the case of 30 deg distractors) or to an orientation closer to the target in the case of the 60 deg distractors. I compared different models, as done in the case of the trajectories, and the best model was perfectly consistent with the one chosen for the trajectories. That is, a model consisting in an interaction parameter (between orientation and normalized distance), plus the parameters related to orientation and position along the y-axis at t0 (Fig. 2.5B, C, D). Looking at the orientations adopted by flies at t1, it is interesting to observe how two different clusters emerge in the case of distractors appearing at 60 deg, either to the right or to the left, in which the major distribution peak remains around the zero (i.e., in the direction of the original target), while minor peaks appeared to be centred at ± 60 deg (Fig. 2.5E). This suggests that one group of individuals ended their trajectories with an orientation towards the target, whereas another group's trajectories were in the direction of the distractor.

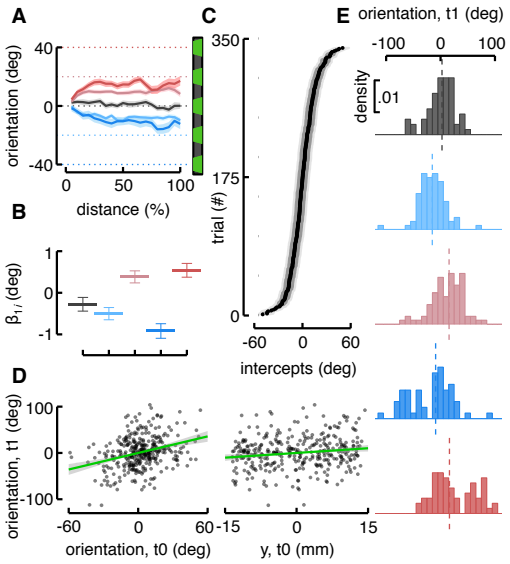

Fig. 2.5. Orientations effects and modelling. *A*: average profile of the flies' orientation along distance travelled distinguished for conditions. The shadow regions represent SEM. The dotted lines (coded by colours) show the angular position of the distractors. *B*: estimated parameters of the fixed effect referred to the interaction between distance and condition with corresponding confidence intervals (parametric bootstrap intervals of 10,000 simulations) at 97.5% level. *C*: plot of random effect. Dots represent each trial (known as BLUPs, Best Linear Unbiased Predictions) while the horizontal lines crossing dots corresponds to the SD. *D*: on the left, correlation between the flies' orientation at t0 and the ones at t1 (r_{rm} = .33, df = 316, p < .0001); on the right, correlation between the flies' position along y-axis at t0 and the flies' orientation at t1 (r_{rm} = .14, df = 316, p = .008). *K*: distribution of the orientations owned by flies at t1 per condition. The dashed lines correspond to the mean. In all images of the panel the colour-coding is as previously described (see Fig. 4).

Kinematic indices

Since, both in the case of the trajectory- and orientation-modelling, the best model took into account not only the effect of the distractor presentation but also the initial state of the flies, it could be argued that there is an absolute re-orientation effect which results in the animals taking on a new path regardless of where they are along the trajectory. This in turn suggests the presence of a mechanism which can adjust the heading by a certain number of degrees, independently of the angular error (referred to the distractor) exhibited by the flies at t0. To verify whether this might be the case, I investigated a few

kinematics indices at a time immediately after the distractor appearance (i.e., within 1 s). I looked at the forward velocity and acceleration in order to rule out any biasing effect due to these forward components. Such components did not show any difference among conditions (Fig. 2.6A). On the contrary, angular velocity and acceleration showed peaks consistent with the position of the distractor at around 150 ms following its appearance (Fig. 2.6B). These peaks lend support to the idea of a fixed heading-correction mechanism being involved in determining the response of the flies. However, by comparing the amplitude of these early changes in direction with the angular errors displayed by flies at t0, I found these two quantities to be significantly correlated for the distractors located to the left of the target (Fig. 2.6C), suggesting that the amplitudes of the early changes in direction were tuned to the angular errors. The correlations between angular errors and angular velocities were not so strong, while angular velocities and amplitudes of heading changes were highly correlated (Fig. 2.6C). In sum, within the same time window, greater angular errors elicited greater angular corrections identifiable also by increased angular velocities. These results do not confirm the idea of a fixed amount of correction independent of angular errors. Rather, these data suggest that flies responded to the distractors by correcting their heading with respect to the angular position of the distractor in order to fixate it. To some extent flies appear able to see and compute the position of the distractors by means of a proportional adjustment in their orientation even without a frontal view of the distractors. I also wondered whether the forward velocity at t0 could modulate the angular velocity, but no significant correlation between these two parameters was found (Fig. 2.6D). Finally, the early turnings tuned to the angular error resembled a “body saccade” based on a position system since, due to the high velocity with which this process occurs, it does not appear to be compatible with a behaviour depending on the motion of the distractor along the retina. Although, compared to the previous definition of spontaneous body saccade in walking flies, in my case the early changes in direction were slower and lasted longer. For this reason, I analysed the number, the amplitude and the velocity of the body saccades in order to understand if there were any observable differences between the conditions in

the presence or absence of the distractor (Fig. 2.6E). By comparing two models considering or not the condition as a predictor, I found that the latter one (i.e., the null model) was much more plausible than the former one for the number (BF ≈ 27367.39) and the amplitude (BF ≈ 6.73) of body saccades, while their angular velocities were better explainable taking into account the conditions (BF ≈ 839.38). It means that higher velocities than when no distractor was sent, characterized the saccades performed towards distractors at 60 deg. Thus, the early changes in direction tuned to the position of distractor would seem to be a case of body saccade driven by an external visual stimulus aimed at obtaining more information about the distractor (i.e., a fixation saccade).

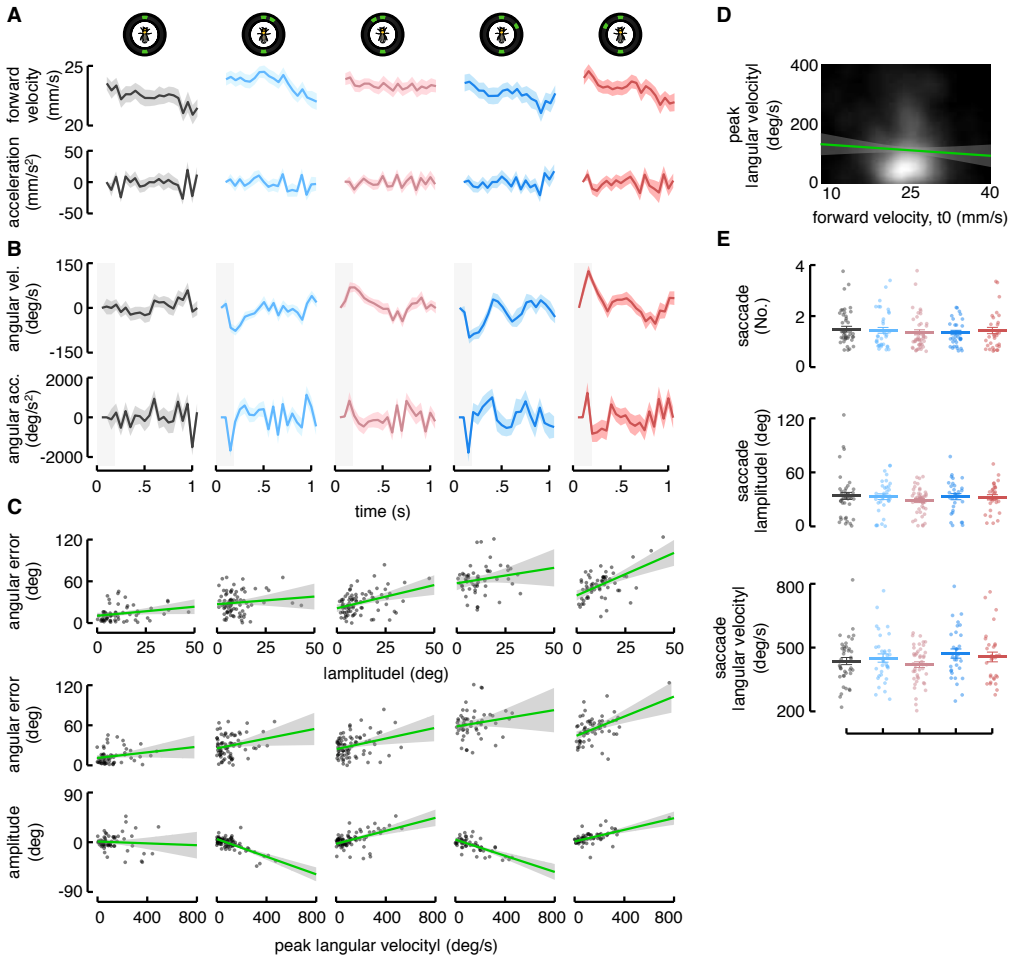

Fig. 2.6. Kinematics indices. *A*: on the top, average profile of the flies' forwards velocity per condition within the first second. On the bottom, the one of the flies' acceleration per condition. The shadow regions around the average profile represent SEM. *B*: on the top, average profile of the flies' angular velocity. On the bottom, the one of the flies' angular acceleration. The grey shadow rectangles represent the first 150 ms after the distractor appearance during which the angular velocities reach the amplitude peak. *C*: on the top, correlation between the amplitude peak of heading changes at 150 ms and the angular error at t0 (no distractor: r_{rm} = .08, df = 40, p = .63; 30°R: r_{rm} = .14, df = 57, p = .26; 30°L: r_{rm} = .33, df = 59, p = .009; 60°R: r_{rm} = .30, df = 35, p = .07; 60°L: r_{rm} = .46, df = 41, p = .002); on the middle, correlation between the amplitude peak of angular velocity at 150 ms and the angular error at t0 (no distractor: r_{rm} = .10, df = 40, p = .53; 30°R: r_{rm} = .24, df = 57, p = .06; 30°L: r_{rm} = .26, df = 59, p = .04; 60°R: r_{rm} = .23, df = 35, p = .18; 60°L: r_{rm} = .23, df = 41, p = .15); on the bottom, correlation between the amplitude peak of angular velocity and the amplitude peak of heading changes (no distractor: r_{rm} = -.03, df = 40, p = .83; 30°R: r_{rm} = -.69, df = 57, p < .0001; 30°L: r_{rm} = .60, df = 59, p < .0001; 60°R: r_{rm} = -.41, df = 35, p = .01; 60°L: r_{rm} = .38, df = 41, p = .01). *D*: density plot with correlation between the forward velocity at t0 and the amplitude peak of angular velocity (r_{rm} = -.11, df = 40, p = .48; 30°R: r_{rm} = .13, df = 57, p = .30; 30°L: r_{rm} = .03, df = 59, p = .82; 60°R: r_{rm} = -.15, df = 35, p = .38; 60°L: r_{rm} = .20, df = 41, p = .19). *E*: on the top, jitter plot of saccades number per condition (thick lines with error bars correspond to mean ± SEM); on the middle the one of saccades amplitude; on the bottom, the one of saccades angular velocity. The colour-coding in the panel is as previously described (see Fig. 4).

Simulations

If flies saw and somehow fixated the distractors, even though the latter were not presented frontally, why would the flies remain 'loyal' to the initial parameters? A parsimonious explanation considers the possibility that flies may have been passively driven by both environmental visual stimuli (i.e., target and distractor) based on their motion on the retina. On the appearance of the distractor, flies would add this visual motion information to that already present from the target. Both these retinal slip motions would lead to a compensatory turning behaviour. This represents a well-known response based on the optokinetic reflex, which is also the main mechanism for smooth pursuit stabilization (Fig. 2.7A). The initial angular error displayed by the fly (with respect to the distractor position) would not constitute negligible variable, but it would be a starting point for the step by step motor adjustments required in order to reduce the angular error. In an attempt to clarify this issue, I simulated the trajectories of flies by using an algorithm which considered (for each trials) the fly position along the y-axis at t0, orientation at t0, as well as the distractor and target positions relative to the fly. Since forward velocity did not contribute explanatory power to the model and it did not show differences among conditions, for all trials I used the same average forward velocity profile. Basically, the algorithm compensates, for each step of the normalized distance, the angular distance produced by the stimuli as they move along the retina (i.e., slip motion) with a corresponding change in direction. Furthermore, I added pseudo-random noise to the change in direction in order to obtain a more realistic representation of the process. In this way I obtained average trajectories which closely followed the ones represented by the real data (Fig. 2.7B). I then tested the reliability of the simulation by putting together all the real and simulated data, fitting them with the previously identified best LME model and trying to detect the hypothesized stratification. Using a model selection process based on BIC I compared two LME models, one with the addition of a predictor to distinguish real data from the simulation data and the other one lacking this predictor. I found that the best model was the one that contemplated the distinction predictor (Table 6).

Table 6. *Monomodal optokinetic simulation*

Model	Df	BIC
$Y_{ij} = \beta_0 + \beta_1 X_{1i} D_{1i} + \beta_2 X_{2i} + \beta_3 X_{3i} + \beta_4 D_{4i} + \lambda_i + \epsilon_{ij}$	11	76976.78
$Y_{ij} = \beta_0 + \beta_1 X_{1i} D_{1i} + \beta_3 X_{3i} + \beta_4 X_{4i} + \lambda_i + \epsilon_{ij}$	10	76985.60

Note. Y_{ij}: shift along y-axis; X_1: normalized distance; D_1: conditions; X_2: initial orientation; X_3: initial position along y-axis; D_4: simulation; λ_i: random effects; ε_{ij}: error.

This result suggests that the response of the flies depends upon more than just an optokinetic mechanism. Thus, some flies respond by stabilizing their heading based upon the retinal slip motion generated by both stimuli, while other flies stabilize only the distractor, without paying any further attention to the target.

Hence, in view of the previous observation that, in the case of the 60 deg distractor, two different clusters of orientations were identifiable at t1 (Fig. 2.5E), I carefully looked at the distributions of the positions of the flies along the y-axis. As the modulus of the medians of such positions at t1 were similar among conditions, and that they were all included in an interval between 11 and 12 mm, I decided to split the data according to the mean of these absolute values, which is 11 mm (Fig. 2.7*C*). This data splitting produced an imbalance in the number of trajectories available for analysis in favour of those ending outside the range of ± 11 mm starting from the centre of the target (which was ± 8 mm wide) (Fig. 2.7D). However, the heat map depicting the residency of flies at t1 shows the sense of this arbitrary manipulation of data, especially for the distractor at 60 deg (Fig. 2.7E). Flies which ended their movement close to the target at t1 (i.e., within ± 11 mm) could be those that were influenced by the slip motion generated by both the target and distractor whereas flies which ended their movement farther (i.e., > 11 mm) could be those that were influenced only by the distractor slip motion (Fig. 2.7F).

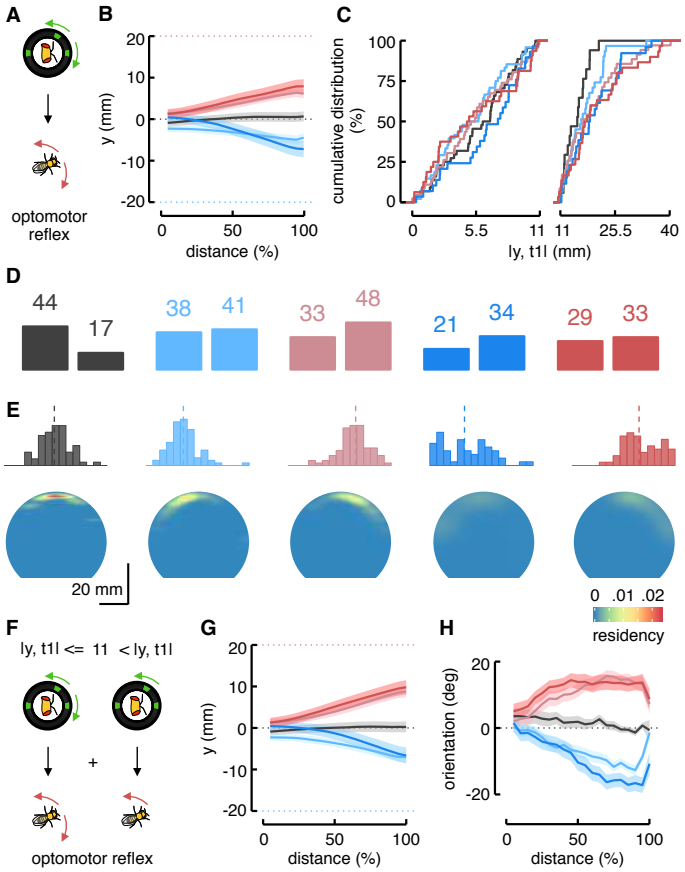

Fig. 2.7. Simulations. *A*: cartoon of the retinal slip motion compensation mechanism which might be underlying flies' behaviour in our paradigm. *B*: average profile of the lateral shifting along y-axis per conditions simulated with the an algorithm based on the retinal slip motion compensation as in *A*. The shadow regions correspond to SEM. The dotted lines show the position of the 30°R (light blue) and 30°L (light red) distractors along the y-axis. *C*: on the left, cumulative distribution of the flies' position along y-axis at t1 within ±11 mm around the centre of the target; on the right, cumulative distribution of the flies' position along y-axis at t1 which shifted >11 mm from the centre of the target. *D*: bar plot representing the number of trials per condition in the two groups generated by the data splitting based on the flies' position along y-axis at t1. *E*: on the top, distribution of the flies' position along y-axis at t1 per condition. The dashed lines correspond to the mean; on the bottom, density plot of the flies' residency at t1. *F*: cartoon of two different mechanisms regarding the retinal slip motion compensation which might be underlying responses of flies to our paradigm. On the left, compensation considering both target and distractor which would be underlying behaviour of flies ending within ±11 mm along y-axis at t1; on the right, compensation considering only distractor which would be underlying behaviour of flies ending >11 mm along y-axis at t1. *G*: average profile of the lateral shifting along y-axis per conditions simulated with the an algorithm based on the retinal slip motion compensation as in *F*. The shadow regions correspond to SEM. *H*: average profile of the orientations per conditions simulated with the an algorithm based on the retinal slip motion compensation as in *F*. The shadow regions correspond to SEM. The dotted lines show the position of the 30°R (light blue) and 30°L (light red) distractors along the y-axis. The colour-coding in the panel is as previously described (see Fig. 4).

I also simulated these trajectories, but this time I considered the kinematics exhibited by the flies at the beginning of each trial with two different algorithms which depended on the distance the flies reached along the y-axis at t1. Pooling the trajectories obtained by using this approach, the average trajectories reproduced the real situation more faithfully than that the trajectories computed using the previously adopted model (Fig. 2.7G). Moreover, although the slopes describing the average orientation profiles for the simulated data were less pronounced than those describing the real data (likely as a result of the early body-saccade), they nonetheless appeared to be rather similar (Fig. 2.7*H*). To test this, I grouped the real and simulated data and compared two LME models which differed by a single dichotomous predictor which identified the pooling. Surprisingly, both from the point of view of the trajectories and the orientations, the best model did not distinguish between the two groups of data, suggesting that the simulation reproduced the real data very faithfully (Table 7).

Table 7. *Bimodal optokinetic simulation*

Model	Df	BIC
$Y_{ij} = \beta_0 + \beta_1 X_{1i} D_{1i} + \beta_2 X_{2i} + \beta_3 X_{3i} + \lambda_i + \epsilon_{ij}$	10	79737.43
$Y_{ij} = \beta_0 + \beta_1 X_{1i} D_{1i} + \beta_2 X_{2i} + \beta_3 X_{3i} + \beta_4 D_{4i} + \lambda_i + \epsilon_{ij}$	11	79747.86

Note. Y_{ij}: shift along y-axis; X_1: normalized distance; D_1: conditions; X_2: initial orientation; X_3: initial position along y-axis; D_4: simulation; λ_i: random effects; ε_{ij}: error.

Bimodal choice

In principle the abovementioned bimodal division was not applied as to separate flies which were interested in the distractor from those which were not, but rather to characterize two possible computations based on the same mechanistic behaviour (i.e., smooth pursuit). If it is true that the trajectories and orientations adopted by flies were explainable by considering the initial angular errors, then the fact that I applied an *a priori* data selection could be questionable. Although

there were significant differences between the two groups of flies in terms of their orientation and position along the y-axis at t0 (suggesting that the position along the y-axis at t1 could be partially predicted by the state at t0), some clarification was still required (Fig. 2.8*A*, B). Firstly, what was no longer obvious was why flies would have to put in place two different computations, as highlighted by our simulation, depending on the angular error they exhibit at t0. Secondly, if our results showing that on detecting the distractor position flies made a saccade-like turning to adjust their heading are true, when and how did the flies decide either to consider both target and the distractor or just the distractor as a goal? To attempt to answer this question I looked at the early angular components of the two groups of flies identified using the bimodal smooth pursuit simulation. When the distractors were presented at 60 deg, both groups an of flies turned evidently towards the distractor within about 250 ms from its appearance, but, rather unexpectedly, the group consisting in flies for which both stimuli constituted the final goal, performed a contrary turn within the subsequent 250 ms (Fig. 2.8*C*). For the distractors presented at 30 deg this phenomenon did not occur in either of the two groups. Furthermore, when the distractor was located at 60 deg, flies showed an a first shared saccade-like turning response (in terms of angular velocity) tuned to the position of the distractor and, once again only in the group consisting in flies for which both stimuli constituted the final goal, a second contrary saccade (Fig. 2.8*D*).

Taken together the above data suggest that although the initial state of the flies at the time of distractor appearance seemed to be sufficient to predict the final trajectory of the individuals, the data also show that a first early component was sufficient to adjust the angular error of flies in both groups to approximately the same extent. However, for reasons which possibly depend indirectly on the initial states, some flies appeared to "decide" within about 250 ms to stabilize either the target or the distractor as visual goals. It seems that instead of adopting a single starting state, flies internally possessed two alternative starting states which were marginally affected by the initial angular error (Fig. 2.8*E*). One such starting state may be seen as being wired to the willingness to adopt a new

goal, while the other could be aimed at maintaining the previously set goal (Fig. 2.8*F*).

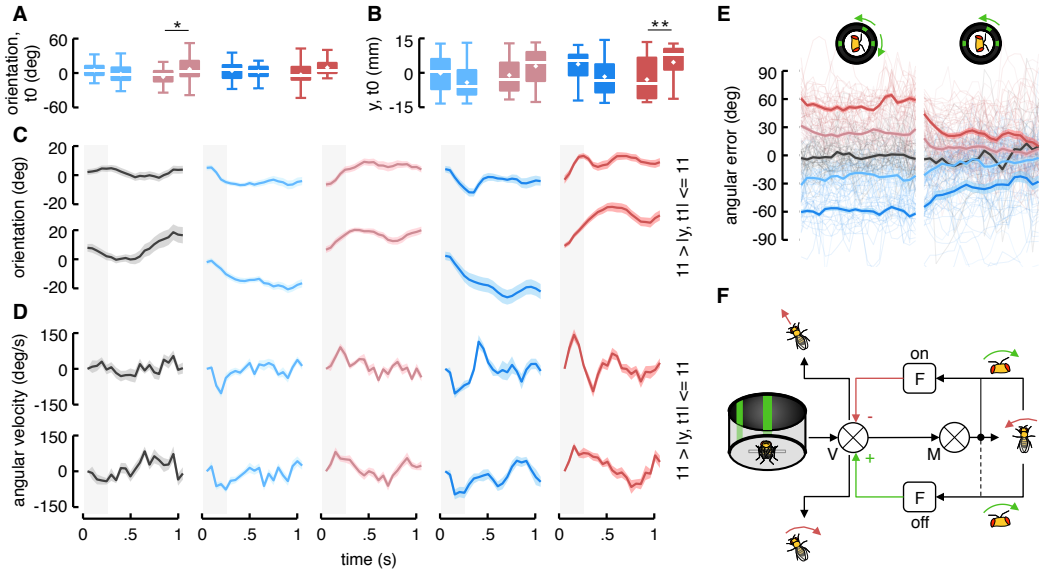

Fig. 2.8. Bimodal choice. *A*: box plot of the flies' orientation at t0 per condition in the two split samples. Respectively, the box plot on the left corresponds to the sample y, t1 ≤ ±11 mm, while the box plot on the right correspond to the sample y, t1 > 11 mm. The model considering the split sample as parameter is more plausible of the one which does not consider it (BF ≈ 70.04). Post-hoc comparisons adjusted with Tukey method show only in the 30°L condition a difference between the two samples (p = .03). *B*: box plot of the flies' position along y-axis at t0 per condition in the two split samples. The box plots refer to the two split samples as in the previous image. The model considering the split sample as parameter is more plausible of the one which does not consider it (BF ≈ 530.35). Post-hoc comparisons adjusted with Tukey method show in the 60°L condition a difference between the two samples (p = .007). *C*: average profile of the flies' orientation within the first second per condition in the two split samples. On the top, the sample y, t1 ≤ ±11 mm; on the bottom, the sample y, t1 > 11 mm. The shadow regions represent SEM. *D*: average profile of the flies' angular velocity within the first second per condition in the two split samples. The profiles refer to the two split samples as in the previous image. *E*: plot of the angular error correction performed by flies distinguished for conditions in the two split samples. Average angular error (thick lines) and raw angular error (thin lines) per distance. On the left, the sample y, t1 ≤ ±11 mm; on the right, the sample y, t1 > 11 mm. The shadow regions correspond to SEM. *F*: cartoon of the proposed mechanism underlying bimodal response of flies in our paradigm based on the efference copy system. Whether the forward prediction is active, as in upper part of the image, then the fly's heading change is maintained. On the contrary, whether the forward prediction is inactive, as in lower part of the image, then the fly's heading change turns back in its initial state. The colour-coding in the panel is as previously described (see Fig. 4).

2.2.4 Discussion

The paradigm employed in this study was aimed at testing the role played by the position system during an action interference effect which would determine an inhibition towards the distractors depending on the level of activation. A stronger influence of the position system compared to the motion one in response to the appearance of the distractors was not confirmed. Along with this, my data do not support the reactive inhibition model (Houghton & Tipper, 1994) at least in the extent hypothesized, although it is most plausible that the levels of inhibition towards the distractors were not as much as wanted. Future manipulations of the target and distractors saliency, for example by means of conditioning paradigms, might disentangle this issue. Nevertheless, a clear-cut distinction between the position and motion systems' contributions has emerged as well as an early mechanism of selection implying the completion of an action directed towards an internal goal.

The nature of fixation behaviour is a long lasting issue in *Drosophila* research. Fixation has been defined as the tendency for flies (most typically in flying individuals in a tethered setup) to maintain a vertically oriented stripe in front of them (Reichardt & Wenking, 1969; Borst, 2014). Stochastic movement of the stripe caused by symmetric yaw torques and an asymmetric optokinetic response to the stripe motion – between progressive (i.e., front-to-back) and regressive (i.e., back-to-front) movements of the stripes – have been considered the necessary requirements for its smooth fixation (Poggio & Reichardt, 1973). Moreover, the response to composite visual panoramas, consisting of a collection of stripes, has been described according to the superposition principle, whereby the flies' response is elicited by the turning tendency linked to each stripe independently (Poggio & Reichardt, 1973). Walking flies faced with two stripes presented concomitantly and separated by an angular distance of less than 60 deg, prefer to move along the direction determined by the bisector of the angle between the stripes (Horn & Wehner, 1975). Conversely, when angles greater than 75 deg are considered, the flies show a distribution of orientations with two maxima directed towards either of the two stripes. This behaviour was described

as the superposition of two turning tendency functions (with a peak at 30 deg), which are phase shifted depending on the angle subtended by the landmarks (Horn & Wehner, 1975).

These conclusions were reached indirectly by measuring the turning tendency function, without considering a position-dependent factor. Here, I recorded the behaviour of freely walking flies in a real closed-loop situation. I was then able to measure the turning tendency function during a distraction paradigm. Our results show that the turning tendency was present at the start of the movement and was tuned to the distractor position and not congruent with the dynamics of a motion detection system. Flies responded by fixating either the target and the distractor or the distractor alone through smooth pursuit behaviour. While for distractors located at 30 deg the superposition principle (Horn & Wehner, 1975) might be compatible with our observations, for distractors located at 60 deg this type of explanation does not appear to hold. Indeed, after an early position-dependent change in direction, two different behavioural choices could be evidenced, allowing the flies to stabilize the visual stimuli differently. For an alternative interpretation, a pure superposition principle would not hold for angular distances up to 80 deg, because the effect produced in the visual system turns out to be a nonlinear inhibitory interaction (Reichardt & Poggio, 1975). A lateral inhibition would play an important role in the determination of a spontaneous pattern; increasing the angular distance between the stimuli, the inhibition decreases (Horn, 1978). Indeed, freely walking flies introduced into a circular open arena with two inaccessible opposing stripes (i.e., 'Buridan's paradigm') are alternatively attracted by them (Götz, 1980; Bülthoff et al., 1982; Strauss & Heisenberg, 1993; Strauss & Pichler, 1998). Although optokinetic responses do not seem to be necessary for such behaviour, a combination of different visuomotor mechanisms guarantees an accurate guidance tuned to the visual environment.

An optokinetic control mechanism, based on visual motion of objects (i.e., closed-loop negative feedback), would allow smooth pursuit behaviour, while a position mechanism would permit an internal spatial representation of external landmarks (i.e., localization). Additionally, what is interesting is the fact that in

motion-blind flies the turning response towards a stationary stripe appearing during an open-loop experiment has the same magnitude as that of wild-type flies in terms of angular velocity and it is remarkably consistent to body saccade-like rotations shown by freely walking flies (Bahl et al., 2013). This supports the interpretation that the early saccade-like response observed in the experiments here presented could be served by circuitry independent from the motion system. The transient dynamics ensuing after the appearance-disappearance of a stripe, as was previously seen in tethered walking flies, could be a side effect of the open-loop paradigms (Bahl et al., 2013). Contrariwise, our results cannot be affected by such a side effect because of the real sensory feedback the flies received. Since flies take less than 100 ms to distinguish an open- from a closed-loop situation, the transient dynamics in the turning response might be due to the lack of reafferent sensory information (Heisenberg & Wolf, 1988). According to control theory, this mechanism corresponds to the forward model, where the future state of a system, the sensory one, is predicted by the current state plus the control signals coming from the motor centres (Webb, 2004). These predictions may be used to anticipate the sensory information sequences (chunks) to which the individual will be subjected during the execution of the action, leading to the silencing of the reafferent sensory input by means of a motor efference copy (von Holst & Mittelstaedt, 1950). In flies, this process commonly refers to a mechanism whereby the retinal slip motion generated by an active body turn (i.e., reafferent motion) towards unexpected moving visual stimuli (i.e., exafferent), is cancelled in order to avoid a consequent reflexive counter-rotation (Heisenberg & Wolf, 1979). This type of modulation has been mainly interpreted as a voluntary action imposed to prevent the flies from becoming passively "stuck" in the same position regardless of the surrounding visual landscape (Heisenberg & Wolf, 1988; Kim et al., 2015). On the other hand, this mechanism is fundamental for both flight stabilization and for the tracking of objects fixated by the flies in the environment, the so-called optomotor-balance (Heisenberg & Wolf, 1979). For example, during flight, a gust of wind may perturb the course of the fly producing a non-predicted exafferent motion (let us suppose, to the right); this perturbation is counterbalanced by an optokinetic reflex involving a body saccade in the same

direction. However, such reafferent motion (i.e., body saccade) produces an equal and opposite full-field motion across the retina to the left. If the reafferent motion were not silenced, a further optokinetic reflex would be elicited, taking the fly back to its initially perturbed position. The same thing would occur for an object moving on the background, although the fixated object remains in a frontal view, the background moves in the opposite direction as compared to the object. This means that reafferent motor control is extremely important during gaze stabilization and pursuit behaviour. Furthermore, under such conditions, it is plausible and parsimonious to envisage such a system as being "constructed" and tuned specifically for the correction of path perturbation, as occurs in mammals (Azim & Alstermark, 2015). An "automatic" mechanism, rather than a "voluntary" one, would seem much more likely since, rapid online correction of a movement requires high speed and accuracy (Gaveau et al., 2014). In other words, it is unlikely that flies, engaged in fixation behaviour would make an overt, aware yaw turn, whenever a small error is perceived between the original heading and the direction of the stimulus. This would require too much time determined by the delay generated by the acquisition of the sensory information and the subsequent decision making process. Although it is true that apparently spontaneous body saccades in magnetically tethered flies are distinguishable from the longer, slower and smaller fixation-bar saccades, suggesting that the former should be extremely fast, it does not tell us anything regarding the origin of the timing for this type of internally triggered events (Mongeau & Frye, 2017). In free-flying flies, using a complex technique based on search algorithms, it has been shown that the majority of body saccades (i.e., 93%) are visually, rather than internally, triggered events (Censi et al., 2013). As flies typically perform their body saccades based on features of visual input, the external environment seems to passively drive them (Bender & Dickinson, 2006). Automatic visuomotor online control would rely on a passive turning tendency reaction elicited by the stimulus (i.e., optokinetic reflex) and on a forward model to predict such a reaction. No voluntary action would be needed for the adjustment, but just motor activity aimed at an external goal (i.e., fixation). Indeed, in primates, an

internal model with its efference copy is cancelled during passive but not during active movement (Brooks & Cullen, 2013).

Does this mean that flies are actually unable to perform internally triggered body saccades or that they are not free to decide whether to respond to an external stimulus? If engaged in fixation behaviour, can they freely decide to react or not to react to a visual perturbation?

In this study I showed how flies may be using an automatic visuomotor controller to stabilize motor behaviour in response to a distracting event. I also revealed how such a controller may be wired to two different states which depend partially on the initial topographic state of the animal. In the early counter-rotation highlighted in a group of individuals during exposure to a distracting stimulus presented at 60 deg, the efference copy may have been "switched off" in order to carry out an action based on a previously established internal goal. Fixation could be differentiated from pursuit behaviour because of the possibility for the former to handle *a priori* action goals. Whereas pursuit would be an automatic mechanism for online movement control, in which the forward model is constantly active, fixation behaviour would be a heading control mechanism which is capable of affecting the state of the forward model. In this scenario voluntary decision might be necessary for fixation/anti-fixation), but not for pursuit behaviour. Put simply, if the fly is engaged in an external fixation goal, the forward model operates by default, while, if the fly is engaged in an internal fixation/anti-fixation goal, the forward model is not operating anymore. Clearly, this hypothesis based on the role of internal-external goals is conceivable if it involves modulation by the motivational state of the fly.

2.3 A PUTATIVE NEURAL CIRCUIT FOR SELECTION AND CONTROL OF ACTION

In the last few years several studies have investigated the neural mechanism underlying spatial orientation in *D. melanogaster*. Convergent results suggest that this mechanism is associated with specific neural circuits located within the CX. Furthermore, such circuits appear to be associated with visual attention and specifically with selective attention processes entailed in action selection.

This work aimed at understanding whether a subset of columnar neurons, the E-PG neurons, is involved in establishing the course control of walking flies in action-interference task based on visual stimuli. As for the previous studies of this thesis I used a modified version of the classical 'Buridan's paradigm' for measuring the level of interference elicited by a distractor upon an ongoing action towards a target. Here, I hypothesize a role by dopamine onto the E-PG neurons which would modulate the activation of a target and the inhibition of distractors via two different types of receptors, respectively Dop1R1 and Dop1R2.

2.3.1 Introduction

Visual inputs provide essential information for the guidance of action not only in "higher" organisms, but also in lower organisms. For instance, *D. melanogaster* relies on vision to avoid predator attacks, to prevent collisions with obstacles or to head efficiently towards salient visual stimuli (Card & Dickinson, 2008; van Breugel & Dickinson, 2012; Maimon et al., 2008). Although the flow of information from the visual to the motor centres represents a fundamental aid for monitoring, refining and selecting actions (Borst, 2014; von Reyn et al., 2014), it needs to be continuously updated given that the presence of sudden unwanted visual inputs may perturb the ongoing action. In such circumstances changes to the originally planned movement have to be made. In the previous section of this chapter I have shown how the flies are able to put in place an inhibitory mechanism, evident along the spatial trajectories, in order to fulfil the goal of an action aimed to a visual target (Frighetto et al., 2019). Here, I hypothesize that

the system devoted to this endeavour lays within the basal ganglia and it might be an evolutionary conserved mechanism existing in flies as well (Strausfeld & Hirth, 2013b; Grillner & Robertson, 2016). The putative neural substrate of an action selection system in flies it has been proposed within an ensemble of modular neuropils located in the central brain, the CX, which is involved in locomotor behaviour (Strauss & Heisenberg, 1993; Martin et al., 1999; Pfeiffer & Homberg, 2014). Particularly, it has been suggested that a doughnut-shaped structure, the EB, is ideally positioned for action selection in the context of spatial navigation (Fiore et al., 2015; Fiore et al., 2017). Recently, using a two-photon Ca^{2+} imaging technique, it has been shown that the E-PG columnar neurons (Wolff & Rubin, 2018), which have dendrites innervating the EB and presynaptic boutons in either the PB or GA brain regions, respond when tracking the orientation of a visual landmark with respect to the fly's position and the fly's heading with respect to an arbitrary position when the fly is in complete darkness (Seelig & Jayaraman, 2015). The dendrites of these neurons are arranged within the EB in a toroidal pattern, anatomically subdivided into16 wedges which can be functionally reduced to 8, since two glomeruli of the PB (7 glomeruli spaced each other) closely innervate adjacent wedges practically forming a singular identity (Wolff et al., 2015). Each wedge responds to a particular direction of navigation through a mechanism corresponding to a ring attractor dynamic which explains how a network with local excitation and global inhibition produce a unique and persistent heading representation (Seelig & Jayaraman, 2015; Kakaria & de Bivort, 2017). Besides, the information concerning visual landmarks is integrated with self-motion information allowing flies to navigate in the environment (Heinze, 2017). The walking direction is updated by the P-EN neurons, having dendrites in PB and boutons either in EB and noduli, which receive inputs from the proprioceptive system in PB (i.e., ~ 150 ms later the fly's turning movement) and then they shift the fly's heading representation in the EB (Green et al., 2017; Turner-Evans et al., 2017). This circuit has been also considered a sort of neural centre for visual attention since it is characterized by a discrete single 'bump' of activity following the presentation of multiple visual stimuli (de Bivort & van Swinderen, 2016). Indeed, the bump of activity in the E-PG neurons is due to a

winner-take-all process and it can travel, flowing or jumping, between two identical visual landmarks or two artificially stimulated regions of the EB remaining locked in a single spot (Kim et al., 2017b). This is reminiscent of a sort of attentional focus (Castiello & Umiltà, 1990; Castiello & Umiltà, 1992) and suggests a unified neurophysiological phenomenon which could form the basis of selection for the programming of locomotion direction.

Furthermore, these neurons, and more in general the EB, might be the neural substrate of a still debated position system which would track an external object permitting the fixation behaviour independently from the optokinetic behaviour which, instead, is permitted by the motion system, a well-characterized system pinpointed in the optic lobe (Bahl et al., 2013). In favour of that, another class of EB neurons, the tangential neurons (also known as R-neurons), which innervate concentric rings within the EB, appear to be retinotopically modulated by visual patterns but not by locomotor states (Seelig & Jayaraman, 2013). These neurons are possibly upstream the E-PG neurons, and convey visual information to the integrator layer for setting motor decisions (Seelig & Jayaraman, 2013). Some R-neurons have been also implicated in visual working memory (Neuser et al., 2008) while others in visual place learning (Ofstad et al., 2011) without showing any modulation associated with the locomotor activity.

Despite the imaging and the electrophysiological recordings from the E-PG neurons, their neurophysiological role in terms of "inverse approach" entailing manipulation of neural activity to understand the real contribution in motor outputs remains quite unclear. Notwithstanding the still ambiguous relationship between the visual and motor system, the E-PG neurons might play a fundamental role in the sensorimotor integration processes underlying action selection and maintenance (Fiore et al., 2015).

To test this hypothesis, I started from the evidence concerned with the ring attractor dynamic supposing that the bump of activity would be facilitated by enhancement of a visual target and inhibition of visual distractors through the dopamine release onto the E-PG neurons. This dopamine modulation would determine a global signal-to-noise ratio increase. Such a filtering mechanism could work via two different subtypes of dopamine 1-like receptors (DopR):

enhancing the activity of a single wedge through the Dop1R1 and inhibiting the global background referred to the other wedges through the Dop1R2.

I tested flies with a downregulation of each one of these two receptors in our action-interference paradigm, aimed at compromising the course control towards a visual target of freely walking flies in response to the appearance of a visual distractor (Frighetto et al., 2019).

I expected that: (i) flies with Dop1R1 downregulation would be more inclined to distraction, and they will tend to change the trajectories in favour of distractors because of the unbalance towards the Dop1R2 receptors; (ii) on the contrary, flies carrying the Dop1R2 downregulation would be less distractible, maintaining themselves more focused to the goal (i.e., the direction of the target) because of the unbalance towards the Dop1R1 receptors.

Finally, to understand the overall outcome of the hypothetical recurrent balance between excitation and inhibition occurring within the circuit, I globally stimulated optogenetically the E-PG neurons during the task. Two possible scenarios were considered: (i) if the hypothetical dopamine modulation was only weakly acting, then a diffused activation all over the doughnut should have taken flies to lose the "compass needle" with consequent scattering of the trajectories; (ii) if the dopamine modulation was strongly working to balance the network, then an over-engagement towards the goal with little changes in trajectories should have been evident as a consequence of the net reinforcement of the bump due to the optogenetic stimulation.

My findings show a striking mechanism in which the dopamine seems to inversely act on the E-PG neurons increasing and inhibiting the circuit via different receptors in order to increase the signal-to-noise ratio aimed at pursuing goal-directed actions.

2.3.2 Methods

Fly stocks

To target the E-PG neurons I used the w^{1118};;P{$y^{+t7.7}$ w^{+mC}=GMR70G12-GAL4}attP2 (BDSC #39552) (Jenett et al., 2012). I checked the expression pattern by using y^1w^*; P{$w^{+mW.hs}$=FRT(w^{hs})}G13 P{w^{+mC}=UAS-mCD8::GFP.L}LL5; (BDSC #5139) as effector transgene encoding fluorescent marker. Downregulation of DopR were performed by means of RNAi constructs which interfere with the expression of Dop1R1 w^{1118};P{w^{+mC}=UAS-Dop1R1^{RNAi}}pKC43; (VDRC #107058/KK) and Dop1R2 w^{1118};P{w^{+mC}=UAS-Dop1R2^{RNAi}}pMF3; (VDRC #3392/GD) (Dietzl et al., 2007; Green et al., 2014). The optogenetic experiments were conducted employing y^1w^{1118};PBac{ $y^{+mDint2}$ w^{+mC}=UAS-ChR2.XXL}VK00018; (BDSC #58374) which carried an amino acid substitution in position 156 of ChR2 protein, a cysteine in place of an aspartic acid (D156C) (Dawydow et al., 2014). Such a substitution has shown to highly increase the protein expression combined with a long open state in the ChR2 kinetics. Interestingly, flies bearing this construct do not require to be fed with the *all-trans* retinal as dietary supplementation to depolarize neurons (Dawydow et al., 2014).

Flies rearing and crossings

The flies were reared on standard cornmeal-sucrose-yeast medium at 22°C in a 12 h light/12 h dark cycle at 60% relative humidity. Virgin homozygous females from the UAS effector lines were selected and crossed with homozygous males from the R70G12 driver line. To be sure that the selected flies were virgin I put five females per vial in a fresh food medium for 3 days and then checked for any fertilized eggs before the adding to the vial of ten young adult males. I left flies mate within the housing vials for 3 days, after that, the vials were emptied from adults waiting to harvest the progeny. Heterozygous flies were then collected and transferred in new vials, obtaining the following genotypes which target the E-PG neurons: (1) UAS-mCD8::GFP/+; R70G12/+ (2) UAS-Dop1R1^{RNAi}/+; R70G12/+ (3)

UAS-Dop1R2^{RNAi}/+; R70G12/+ (4) UAS-ChR2.XXL/+; R70G12/+. Only the flies from the latter genotype (i.e., expressing the ChR2) were kept in a separate box under the same circadian cycle but with the 12 h light period characterized by a red-shifted spectrum of illumination to avoid unwanted neural activation due to wider spectrum of light. A mini-incubator was created by fastening four LEDs (Ledberg, IKEA, Delft, NL, EU) controlled via timer under the lid of a cardboard box (Tjena, IKEA, Delft, NL, EU) and by covering them with red gel filters. Temperature and humidity were regularly monitored within the box. Moreover, all flies were daily inspected to check their healthy state. Whether the flies showed to be in bad shape or the food started to manifest early signs of growing bacteria, flies with their vials were immediately threw away. No fly was treated with antibiotics to recover from infection. Fly crowding was also controlled (about 20 flies in each vial) to avoid competition for food. Flies were kept in their vials until the beginning of the experiment. By using a mouth aspirator they were randomly picked from the vials and directly transferred to the experimental setup. I was not blinded regarding the fly's genotype and no fly was starved or its wings clipped before the experiment. The experimental sessions were conducted between zeitgeber time 2 and 5 at the same temperature (i.e., 22°C). All experiments were performed on 144 adult male flies of 2-5 day-old. This choice was done firstly because males show a "reactivity" component in which they seem more sensitive to new environmental conditions than females which show an higher number of start/stop during the first 2 h of recording (i.e., locomotion is less sustained) and secondly because virgin or mated females show differences in the distance travelled with the first ones which travel farther than the second ones (Martin, 2004). Therefore, using males I easily skipped this avoidable variability.

Experimental setup

The setup and software management were similar to those described in the previous section of this chapter. However, to perform the optogenetic experiments I implemented the setup with two arrays each one composed of four

LEDs (SP-08-B3 Rebel LED - 168 lm, Luxeon Star LEDs, Lethbridge, AB, CA) emitting a wavelength range of light from 460 to 485 nm and positioned 27 cm above the fly chamber (Fig. 2.9A). These two arrays were mounted laterally to the camera for video recording (Chameleon 3, FLIR System Inc., Wilsonville, OR, USA) which was placed 30 cm above the arena allowing a spatial density of 5.05 pixels per mm. To increase the thermal exchange surface and maintain low temperature, the LEDs arrays were placed on aluminium heat sinks (3741 series, Aavid Thermalloy, Bologna, IT, EU). Each LEDs array was fixed with a clip holder on a metal gooseneck post (APM15 and APM60BK, Proel, S'Omero-Teramo, IT, EU) in turn mounted on the shared platform for all components through a post base (PB2, Thorlabs Inc, Newton, NJ, USA). The LEDs were wired in a circuit on a breadboard and managed by a microcontroller (Arduino Uno Rev3, Arduino, Ivrea, IT, EU). The microcontroller was connected via USB cable to the PC and its management integrated in the FlyNeMo software developed in MATLAB (MathWork Inc., Natick, MA, USA) for the control of all experimental variables. The wavelength and the intensity of 3.5 $\mu W/mm^2$ (PM16-120 Photodiode Sensor, Thorlabs Inc., Newton, NJ, USA) emitted by the LEDs efficiently activated the neurons expressing the ChR2 (Dawydow et al., 2014).

GAL4 expression pattern

To identify the most suitable driver line for our experiments, I screened by eyes the expression patterns of a whole raft of GAL4 imaging stacks from the FlyLight database (Jenett et al., 2012). Finally, the expression pattern of the R70G12 line was selected as a putative target of dopamine neurons innervating the E-PG neurons and the confocal images downloaded. However, once obtained the line from the BDSC I checked it expression pattern. Five male flies from the UAS-mCD8::GFP/+; R70G12/+ genotype were anesthetized with carbon dioxide gas, immersed in phosphate-buffered saline (PBS) and their brains dissected out under a stereomicroscope using stainless steel forceps (Dumont #5, Fine Science Tools Inc., North Vancouver, BC, CA). Following dissection, the brains were fixed in 4% paraformaldehyde in PBS at a room temperature for 10 min, then washed

three times for five minutes each in PBS and mounted in a drop of Vectashield medium (Vector Laboratories Ltd., Peterborough, UK, EU) on a coverslips. The samples were examined by using a confocal microscope (TCS SP5, Leica Microsystems GmbH, Wetzlar, DE, EU) with 63x/NA1.4 oil immersion objective. Data were acquired at frame size of 1024 x 1024 pixels of dimension 0.21 x 0.21 and z-section thickness of ~1 µm using an 8-bit dynamic range. Maximum intensity projections were generated from the stacks and brightness was optimally adjusted. Fluorescence emission form the 488 nm excitation passed through a 505-550 nm bandpass filter. The visually observation of our confocal stacks confirmed a corrected pattern of expression in the R70G12 driver line as shown in FlyLight database (Fig. 2.9B).

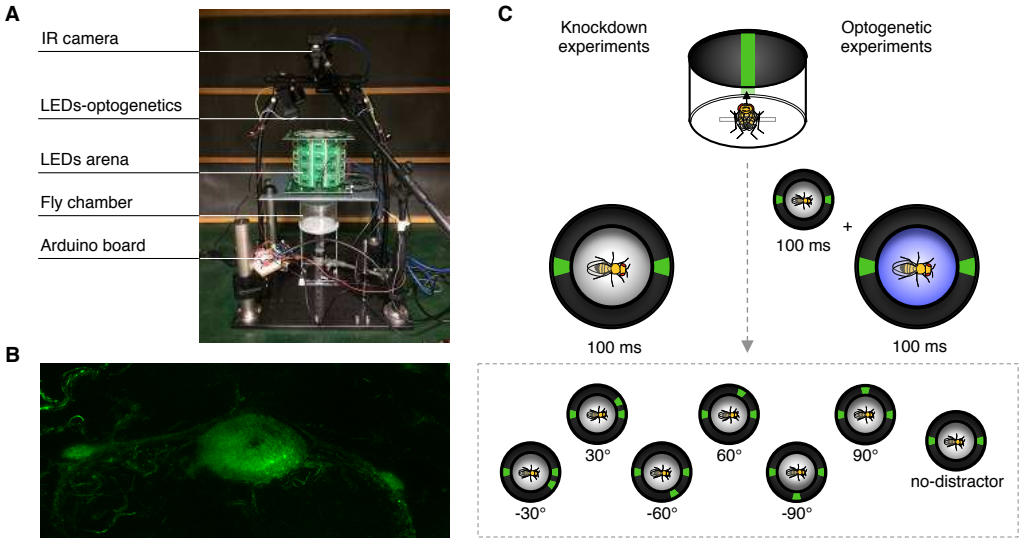

Fig. 2.9. Experimental setup, expression pattern and procedure. *A*: image of the setup upgraded for optogenetics with the main components reported on the left. *B*: expression patter of the UAS-mCD8::GFP/+; R70G12/+. It is manifest the GFP expression within the EB and in the two lateral GA regions belonging to the LAL. *C*: procedure in the knockdown experiments on the left and in the optogenetic experiments on the right. On the left, whenever the fly crossed the virtual window, after 100 ms of delay the fly was presented to one of the conditions reported on the bottom of the image. On the right, after the window crossing, there was a delay of 100 ms, followed by a pulse of blue-light for 200 ms. By straddling the light pulse, one of the conditions reported on the bottom was triggered. Seven conditions, randomly chosen, were considered: a condition in which no distractor was sent and six conditions in which the distractor might be presented to the right or to the left at 30, 60 or 90 deg. Each condition had to be presented 5 times and once all conditions reached this value the experiment automatically ended. Movements to the right were categorized with negative sign while the ones to the left with positive sign.

Procedure for knockdown experiments

The procedure used to test the action-interference effects in flies expressing downregulation of DopR was similar to that one described in the previous section of this chapter except that in the current experiments the distractors could appear randomly either to the right or to the left of the fly at an angle of 30, 60 or 90 deg with respect to an ideal line connecting the opposing "Buridan" stripes. The fly crossing of the virtual window positioned roughly at the centre of the arena (~ 45% of the length connecting the opposing stripes) triggered the video recording of a 550 x 550 pixels region of interest at 30 frames s^{-1} which lasted 5 s. After a baseline collection of 3 frames (i.e., ~ 100 ms later) to obtain a clear indication of the position and orientation of the flies, the distractor was displayed for 3 s. Thereafter, the distractor was switched off waiting for fly crossed again the virtual window. A condition in which no distractor was displayed was also included bringing to a total of 7 conditions. The experiment ended when each condition was presented five times (i.e., 7 conditions x 5 times). By adopting this approach, each fly needed a different amount of time for completing the experiment which had an average duration of 90 min (Fig. 2.9C).

Procedure for optogenetic experiments

For the optogenetic experiments the procedure was similar to that one employed in the knockdown experiments regarding DopR. The only difference was that when the flies crossed the virtual window, after the baseline recording of ~ 100 ms, a blue-light pulse (470 nm wavelength peak) lasting 200 ms was delivered all over the arena depolarizing the E-PG neurons of the ChR2 expressing flies. Straddling the blue-light pulse (i.e., at 100 ms), the visual distractor was displayed as well (i.e., onset 200 ms after the fly crossing of virtual window) for 2.9 s (Fig. 2.9C).

Data processing

As done in previous experiments, I decided to process the video recordings with CTRAX open source software for tracking analysis (Branson et al., 2009) to obtain a larger range of variables related to the fly's spatial properties rather than the x and y-axis position obtained from our online tracking system. The final .mat files, exported from CTRAX, were transformed into .txt files with a custom script and then imported into the integrated development environment RStudio (RStudio Team, 2017) for data processing and statistical analysis. Only data from tracks in which the flies were directed towards the target were considered, meaning that the tracks directed in the opposite direction were not considered in the analysis. Moreover, in addition to this filtering, a minimum path length travelled within the first 3 s (i.e., during the appearance of distractor) was imposed as a cut-off for analysis in which only track lengths greater than 10 mm were included. A summary of the data frame is reported in Table 8.

Table 8. *Data summary*

Group	No. flies	No. trials
Control for knockdown exp.	32	779
E-PG>Dop1R1^{RNAi}	31	801
E-PG>Dop1R2^{RNAi}	31	808
Control for optogenetic exp.	20	442
E-PG>ChR2^{XXL}	30	593

Note. No.= number.

Statistical approach

In order to understand whether the presence of distractors explained the trajectories and the orientation adopted by the flies similarly to those showed in our previous observations I tested the same series of LME models using the R package *lme4* (Bates et al., 2014). Then, following the same approach, the LME models were compared by using the BIC to select the best one (i.e., the most

plausible). The goodness of fit with marginal and conditional pseudo-R^2 were calculated by means of R package MuMIn (Barton, 2019). Analysis of variance (ANOVA) were computed by using the R package *afex* (Singmann et al., 2018) and pairwise post hoc comparisons adjusted with the Tukey method by using the R package *lsmeans* (Lenth, 2016). Repeated measures correlation by using the R package *rmcorr* (Bakdash & Marusich, 2017) was also used.

2.3.3 Results

Knockdown experiments

Trajectories

To test the hypothesis related to a modulation of distractibility via DopR, I looked at the trajectories outcomes in UAS-Dop1R1^{RNAi}/+; R70G12/+ flies, from now on briefly called E-PG>Dop1R1^{RNAi} and in UAS-Dop1R2^{RNAi}/+; R70G12/+ flies, from now on called E-PG>Dop1R2^{RNAi}. The control group of these experiments was an artificial group composed by the data merging of parental fly lines (i.e., R70G12-GAL4, UAS-Dop1R1^{RNAi} and UAS-Dop1R2^{RNAi}), which had the same genetic background of the progeny without expressing the combinations of GAL4-UAS transgenes which took to real biological effects. At a first glance, not a great effect seemed to be evident in the average profile of the trajectories (Fig. 2.10A). Then, I fitted the trajectories employing LME models as previously performed. In the former experiments I found that the parameters associated to the initial orientation and position of flies along the y-axis, were important predictors to be considered in the model. Thus, I tested and compared different LME models referred to the shift of the trajectories along the y-axis as dependent variables, considering or not as predictors the velocity, orientation and position owned by flies in the first frame (t0). Hence, the shift along the y-axis over time and distinguished per conditions, which provides an objective and quantitative evaluation of the strength and the extent of tendency of flies to change their trajectories towards the distractors, was considered as an interaction fixed effect

common among models. The stochastic variation in intercepts among trials within flies was considered as random effects for all models. Furthermore, aimed at understanding whether the knockdown of the two subtypes of DopR had caused any effects consistent to our expectation, the independent variables referred to groups was introduced in the model selection process as a three levels interaction together with condition and time. Put simply, such an interaction meant that the shift over time could be more prominent in a group than in others, considering of course the direction of changes related to the conditions. A selected time window, corresponding to the first 3 s (i.e., t0 – t3 during which the distractor was switched on), was selected for modelling because of the greatest effect potentially evoked by the distractors. The best LME model confirmed the roles played by the orientation and position along y-axis owned by flies at t0 (when the distractor was not yet displayed) as predictors of the trajectories (Table 9).

Table 9. *Models selection for trajectories t0 – t3*

Model	Df	BIC
$Y_{ij} = \beta_0 + \beta_1 D_{1i} D_{2i} X_{1i} + \beta_2 X_{2i} + \beta_3 X_{3i} + \lambda_i + \epsilon_{ij}$	26	1282585
$Y_{ij} = \beta_0 + \beta_1 D_{1i} D_{2i} X_{1i} + \beta_2 X_{2i} + \beta_3 X_{3i} + \beta_4 X_{4i} + \lambda_i + \epsilon_{ij}$	27	1282596
$Y_{ij} = \beta_0 + \beta_1 D_{1i} X_{1i} + \beta_2 X_{2i} + \beta_3 X_{3i} + \lambda_i + \epsilon_{ij}$	12	1283407
$Y_{ij} = \beta_0 + \beta_1 D_{1i} X_{1i} + \beta_2 X_{2i} + \beta_3 X_{3i} + \beta_4 D_{2i} + \lambda_i + \epsilon_{ij}$	14	1283429

Note. Y_{ij}: drift along y-axis; D_1: conditions; D_2: group; X_1: time; X_2: initial orientation; X_3: initial position along y-axis; X_4: initial forward velocity; λ_i: random effects; ε_{ij}: error.

By adding the categorical predictor referred to groups in the interaction between condition and time, the plausibility of the model increased compared to the one owned by the model without it (BF$\approx$ 2.79 x 10^{178}). The estimate of marginal (i.e., related to fixed effect) and conditional (i.e., related to fixed plus random effects) pseudo-R^2 of this best model (Table 10) showed a quite good coefficient of determination.

Table 10. *Goodness of fit*

R^2 marginal	R^2 conditional
0.57	0.86

Confidence intervals (CI) estimated for the interaction parameters showed that many of them did not overlap, implying, in the classical frequentist perspective, a statistically significant difference among groups (Fig. 2.10B, C). Nevertheless, taking into account our initial hypothesis, these results did not show clear evidence of distractibility modulated by the Dop1R1 and Dop1R2 receptors in term of trajectories adopted. The general tendency was similar in the three groups. The fact that also the no distractor condition showed a certain amount of variability among groups, and that these differences were comparable to those of distractor conditions, supported the conclusion that they were unlikely related to the genotype. In all groups: (i) when no distractor was presented, the flies continued to run straight towards the target; (ii) when a distractor at 30 or 60 deg to the right or left was presented, the flies shifted the trajectories towards it with an increase from 30 to 60 deg; (iii) when a distractor was presented at 90 deg to the right or left, the tendency of the shift started to be reversed.

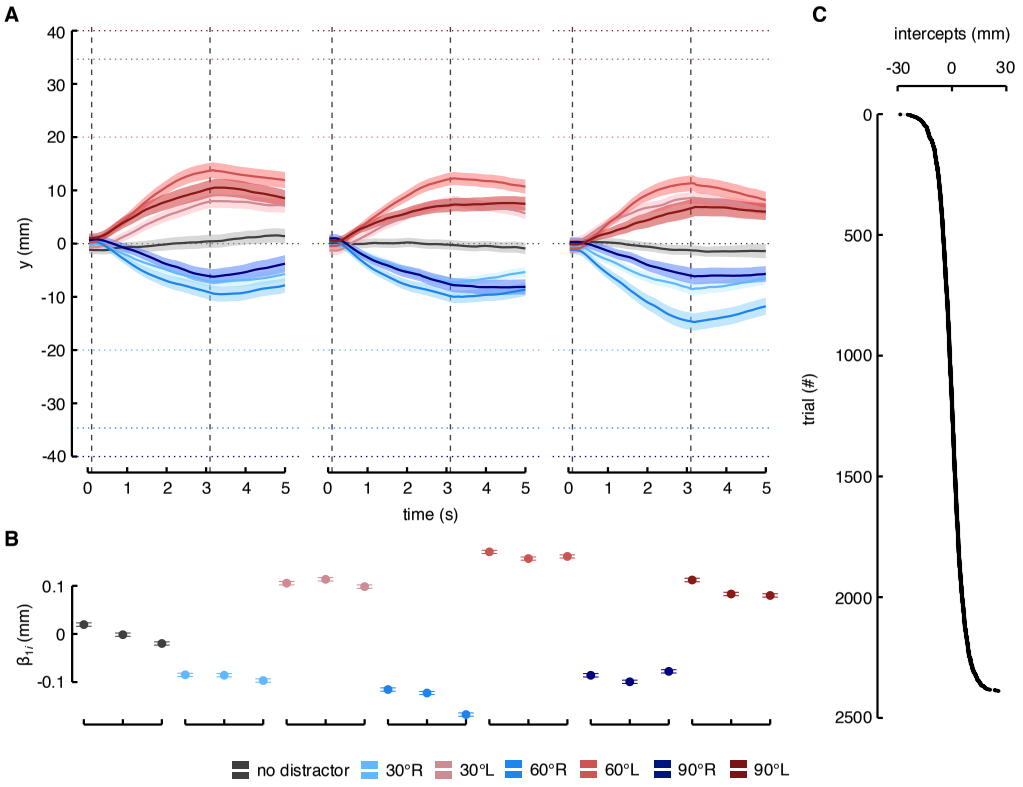

Fig. 2.10. Trajectories in DopR knockdown flies. *A*: plot of the average shift along y-axis per time in the three groups and distinguished for conditions. On the left, the trajectories of the control group, on the middle the ones of the E-PG>Dop1R1^{RNAi}, and on the right the ones of the E-PG>Dop1R2^{RNAi}. The shadow regions around the profiles correspond to SEM. The horizontal dotted lines (coded by colours) show the relative position of the distractors along the y-axis. The two vertical black dashed lines mark respectively along time, the appearance of the distractor at 0.1 s and its disappearance at 3.1 s. *B*: estimated parameters of the fixed effect referred to the interaction between time, condition and group with corresponding confidence intervals (parametric bootstrap intervals of 10,000 simulations) at 97.5% level. From right to left the parameters refer to groups in the same order as in *A*. *C*: plot of random effect. Dots represent each trial (known as BLUPs, Best Linear Unbiased Predictions) while the horizontal lines crossing dots corresponds to the SD. As reported on the bottom of the panel, colour-coding for all graphs: black corresponds to the no distractor condition; light blue to distractor at 30 deg to the right; light red at 30 deg to the left; blue at 60 deg to the right; red at 60 deg to the left; deep blue at 90 deg to the right; deep red at 90 deg to the left.

Orientations

The average profile of orientations showed a clearer distinction among groups than the one concerned with the trajectories (Fig. 2.11A). To better understand such a behaviour I pursued the same approach used for the trajectories, testing different LME models either for t0 – t3 (i.e., distractor was switched on) or t3 – t5

(i.e., distractor was switched off) time windows. A series of LME models were fitted to the flies' orientations in order to obtain the best-fit model explaining the orientation of the flies over time. For the t0 – t3 time window, the best model coincided with the one for the trajectories, confirming that different degrees of changes in orientation among groups were detected (Table 11).

Table 11. *Models selection for orientations t0 – t3*

Model	Df	BIC
$Y_{ij} = \beta_0 + \beta_1 D_{1i} D_{2i} X_{1i} + \beta_2 X_{2i} + \beta_3 X_{3i} + \lambda_i + \epsilon_{ij}$	26	1952433
$Y_{ij} = \beta_0 + \beta_1 D_{1i} D_{2i} X_{1i} + \beta_2 X_{2i} + \beta_3 X_{3i} + \beta_4 X_{4i} + \lambda_i + \epsilon_{ij}$	27	1952448
$Y_{ij} = \beta_0 + \beta_1 D_{1i} X_{1i} + \beta_2 X_{2i} + \beta_3 X_{3i} + \beta_4 D_{1i} D_{2i} + \lambda_i + \epsilon_{ij}$	26	1952463
$Y_{ij} = \beta_0 + \beta_1 D_{1i} X_{1i} + \beta_2 X_{2i} + \beta_3 X_{3i} + \lambda_i + \epsilon_{ij}$	12	1952518

Note. Y_{ij}: drift along y-axis; D_1: conditions; D_2: group; X_1: time; X_2: initial orientation; X_3: initial position along y-axis; X_4: initial forward velocity; λ_i: random effects; ε_{ij}: error.

As already seen in the case of the flies' trajectories, the flies' orientations also changed coherently to the distractor positions for angulation of 30 and 60 deg in all the three groups (Fig. 2.11B, C). The greater were the angle of the distractor with respect to the original target, the farther the flies' orientations changed in direction of the distractor. A general reduction of changes in orientation when a distractor was presented at 30 deg was evident in E-PG>Dop1R2^{RNAi} flies compared to controls, while E-PG>Dop1R1^{RNAi} flies responded likewise the controls. Conversely, at 60 deg the pattern of responses was less clear, with E-PG>Dop1R1^{RNAi} showing a greater change than controls when the distractor was sent to the left, whereas E-PG>Dop1R2^{RNAi} changed more than controls when it was sent to the right. The same pattern, but with inversed polarity was evident at 90 deg, where E-PG>Dop1R1^{RNAi} showed less change than controls (and than condition at 60 deg) for distractor to the left, whereas E-PG>Dop1R2^{RNAi} showed less change than controls (and than condition at 60 deg) for distractor to the right.

For t3 – t5 time window instead, the best model is the one that considers the predictor referred to groups in an interaction with condition, meaning that after the distractor was switched off the changes in orientation were distinguishable depending upon condition and groups (i.e., variation in intercepts) (Table 12).

Table 12. *Models selection for orientations t3 – t5*

Model	Df	BIC
$Y_{ij} = \beta_0 + \beta_1 D_{1i} X_{1i} + \beta_2 X_{2i} + \beta_3 X_{3i} + \beta_4 D_{1i} D_{2i} + \lambda_i + \epsilon_{ij}$	26	1502868
$Y_{ij} = \beta_0 + \beta_1 D_{1i} X_{1i} + \beta_2 X_{2i} + \beta_3 X_{3i} + \lambda_i + \epsilon_{ij}$	12	1503279
$Y_{ij} = \beta_0 + \beta_1 D_{1i} X_{1i} + \beta_2 X_{2i} + \beta_3 X_{3i} + \beta_4 D_{2i} + \lambda_i + \epsilon_{ij}$	14	1503294
$Y_{ij} = \beta_0 + \beta_1 D_{1i} D_{2i} X_{1i} + \beta_2 X_{2i} + \beta_3 X_{3i} + \lambda_i + \epsilon_{ij}$	26	1503317

Note. Y_{ij}: drift along y-axis; D_1: conditions; D_2: group; X_1: time; X_2: initial orientation; X_3: initial position along y-axis; X_4: initial forward velocity; λ_i: random effects; ε_{ij}: error.

In particular, controls re-oriented themselves towards the original target much more than E-PG>Dop1R2^{RNAi}, which, in turn, re-oriented more towards the target than E-PG>Dop1R1^{RNAi} (Fig. 2.11D). To sum up, a part from E-PG>Dop1R2^{RNAi}, which remained closely orientated to the target during the appearance of distractors at 30 deg, all three groups responded quite similarly by changing their orientation towards the distractors. However, as evident after distractors disappearance (i.e., t3 – t5), E-PG>Dop1R1^{RNAi} seemed to remain docked to the orientation engaged during distraction (i.e., t0 – t3) while E-PG>Dop1R2^{RNAi} and controls seemed to re-orient turning back towards the original target.

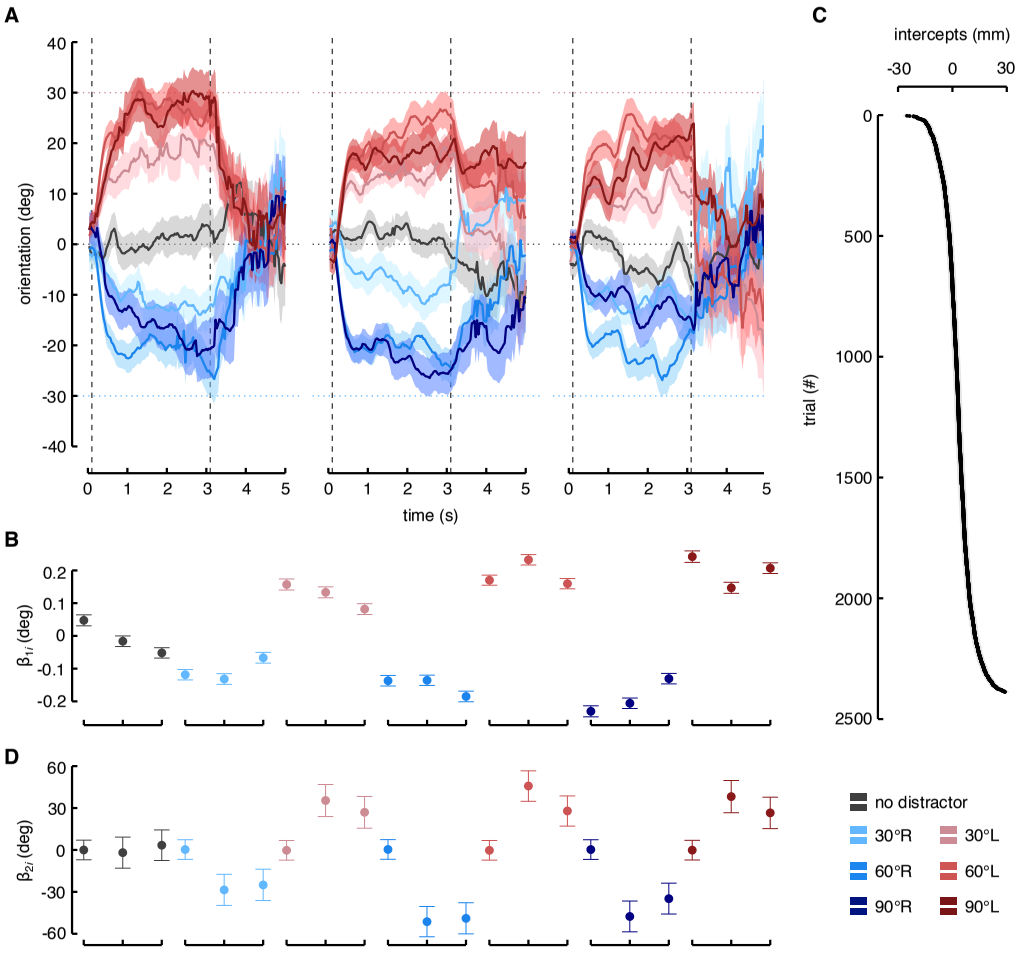

Fig. 2.11. Orientations in DopR knockdown flies. *A*: plot of the average orientation per time in the three groups and distinguished for conditions. The groups are represented as in the previous figure, from right to left: controls, E-PG>Dop1R1^{RNAi} and E-PG>Dop1R2^{RNAi}. The shadow regions around the profiles correspond to SEM. The dotted lines show the angular position of the distractors at 30 deg. The two vertical black dashed lines mark respectively along time, the appearance of the distractor at 0.1 s and its disappearance at 3.1 s. *B*: estimated fixed effect for the model confined to the time window t0 – t3. The parameters refer to the interaction between time, condition and group. The error bars correspond to confidence intervals (parametric bootstrap intervals of 10,000 simulations) at 97.5% level. *C*: plot of random effect of the model confined to time window t0 – t3. Dots represent each trial (known as BLUPs, Best Linear Unbiased Predictions) while the horizontal lines crossing dots corresponds to the SD. *D*: estimated fixed effect for the model confined to the time window t3 – t5. The parameters refer to the interaction between condition and group. The error bars correspond to the bootstrapped confidence intervals as in the previous image. Colour-coding, as previously described, is reported on the bottom right.

Forward velocity

Looking at the forward velocity, the E-PG>Dop1R2^{RNAi} flies exhibited a lower velocity compared to the other two groups (Fig. 2.12A). Controls and both knockdown groups of flies had a comparable velocity profile before t3 which decreased during the display of distractor. Moreover, controls and E-PG>Dop1R1^{RNAi} flies did not show differences after t3, when the distractor was turned off, showing to increase the velocity. Surprisingly, E-PG>Dop1R2^{RNAi} showed a sharp peak of velocity about 100 ms after the distractor was switched off (Fig. 2.12B). This peak was present only in the distractor conditions and its amplitude seemed to be inversely correlated to the angle of distraction (i.e., the greater was the peak amplitude, the smaller was the angle subtended by distractor). I correlated the peak amplitudes with the degrees of error, which represent a measure of how far the flies' orientation were from the angulation of the corresponding distractor, confirming such correlation (Fig. 2.12C).

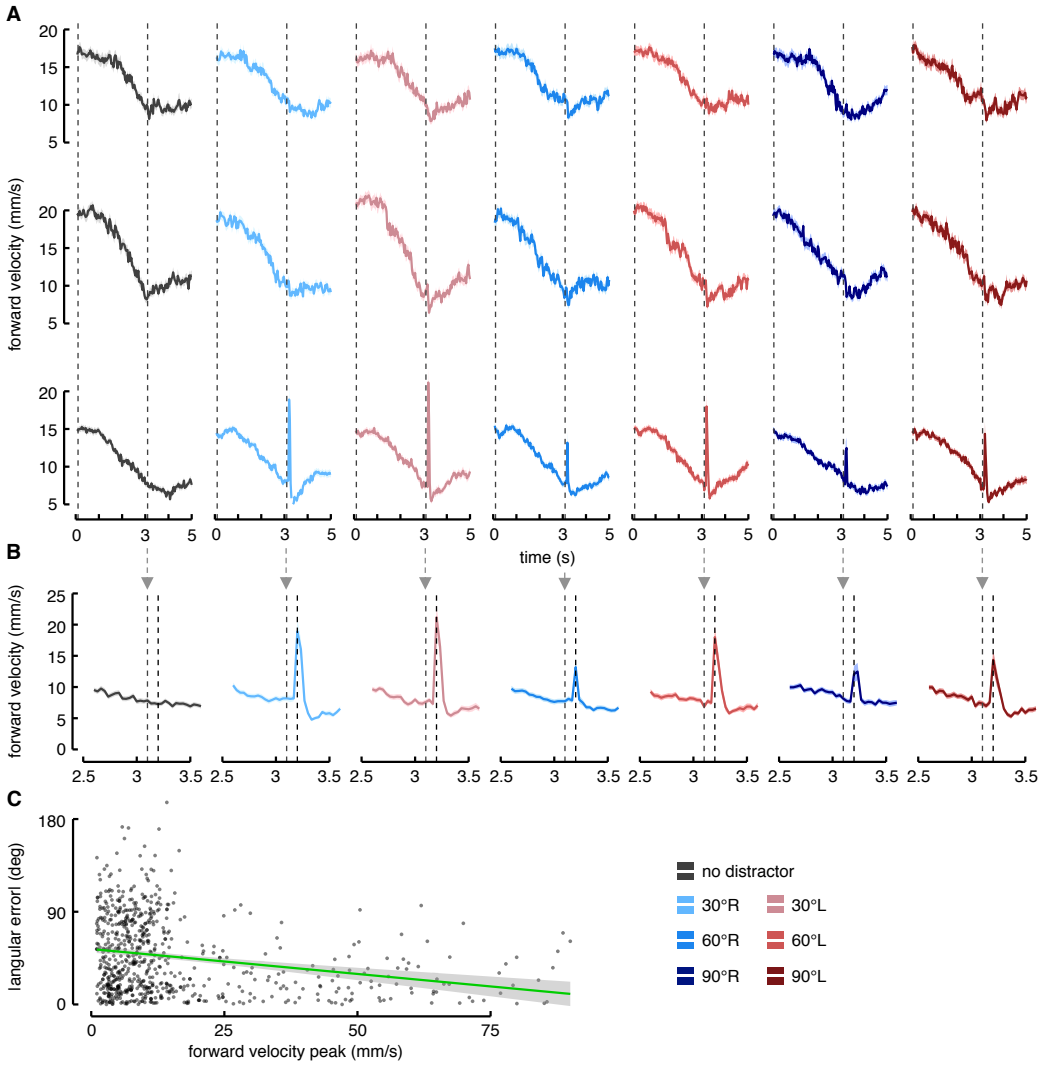

Fig. 2.12. Forward velocity in DopR knockdown flies. *A*: average profile of the flies' forwards velocity per condition along time. On the top the control group; on the middle the E-PG>Dop1R1^{RNAi}; on the bottom the E-PG>Dop1R2^{RNAi}. The shadow regions around the average profile represent SEM. The two vertical black dashed lines mark respectively along time, the appearance of the distractor at 0.1 s and its disappearance at 3.1 s. *B*: enlargement of the time window between 2.5 and 3.5 s showing the forward velocity peak in the E-PG>Dop1R2^{RNAi} ($F_{(2, 91)} = 22.17$, $p < .0001$; ctrl - E-PG>Dop1R1^{RNAi} $p = .81$; ctrl - E-PG>Dop1R2^{RNAi} $p < .0001$; E-PG>Dop1R1^{RNAi} - E-PG>Dop1R2^{RNAi} $p < .0001$). The two vertical black dashed lines mark respectively the disappearance of the distractor at 3.1 s and the velocity peaks at 3.2 s. *C*: correlation between the forward velocity peaks at 3.2 s and the angular error owned by flies at 3.1 s in E-PG>Dop1R2^{RNAi} ($r_{rm} = -0.23$, $df = 675$, $p < .0001$). Colour-coding is reported on the bottom right.

Angular velocity

In the light of our previous observations that have shown how wild-type flies were able to perform "body saccade" towards visual stimuli within the first 250 ms after the distractor onset, I thought to look at the same kinematic dynamic in order to understand whether the downregulation of DopR had affected the early mechanisms associated to the focus of attention (Fig. 2.13A). Coherently to my expectation, E-PG>Dop1R2^{RNAi} flies showed smaller peaks of angular velocity compared to E-PG>Dop1R1^{RNAi} and controls (Fig. 2.13B). Besides, a delay in the peaks was evident as well, especially in the condition at 60 deg. Subsequently, looking at the angular velocity when the distractor was turned off, the scenario completely reversed with the E-PG>Dop1R2^{RNAi} which showed higher angular velocity peaks temporally consistent to the ones of forward velocity (Fig. 2.13C). These peaks owned a direction opposite to the distractor, meaning that E-PG>Dop1R2^{RNAi} abruptly performed a body saccade towards the original target. On the contrary, the angular profile of the E-PG>Dop1R1^{RNAi} appeared much less affected by the switching off of the distractors.

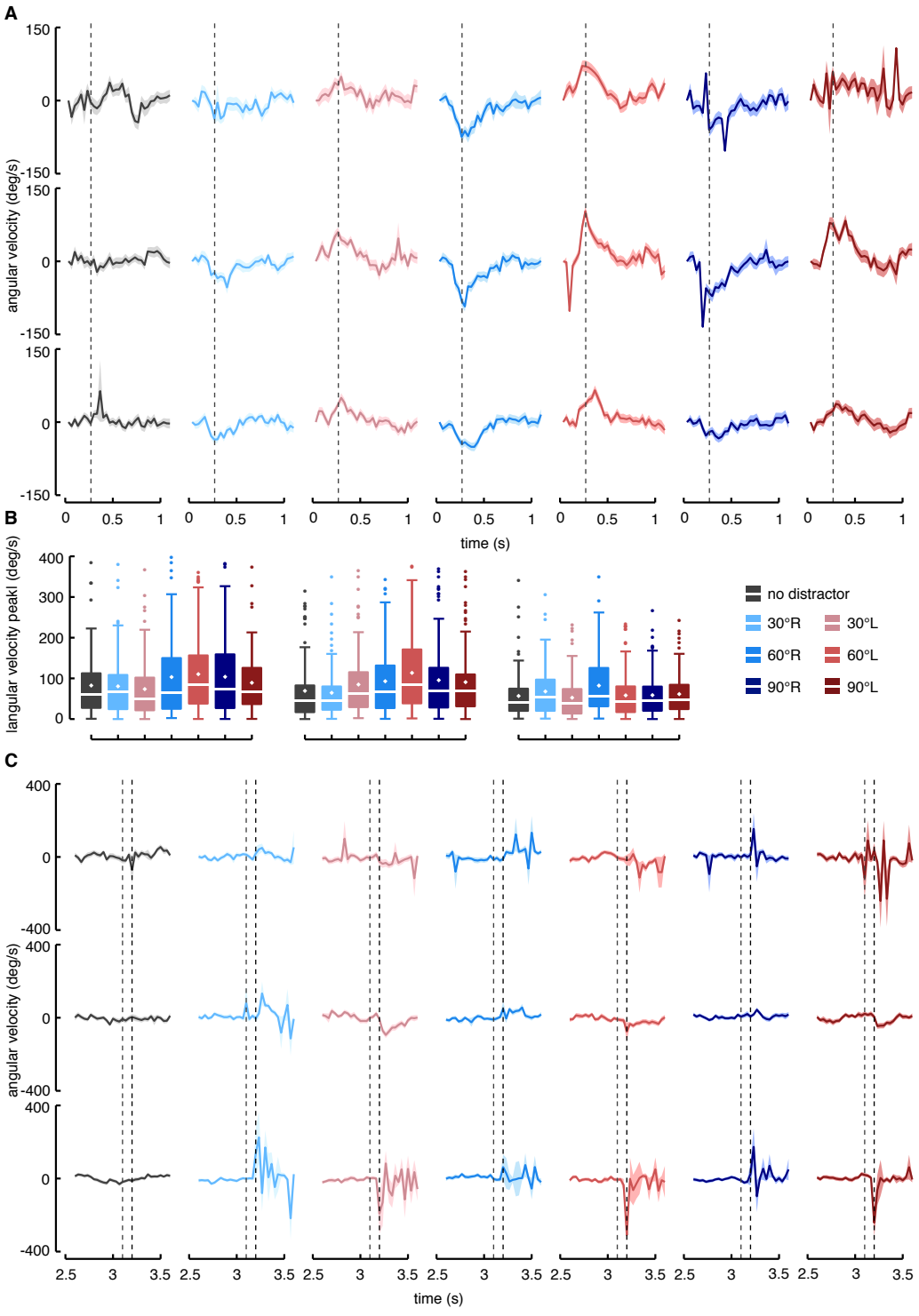

Fig. 2.13. Angular velocity in DopR knockdown flies. *A*: average profile of the angular velocity. The vertical black dashed lines mark the peak of angular velocity at 250 ms. *B*: boxplot of the angular velocity peak ($F_{(2,\ 91)}$ = 21.56, p < .0001; ctrl - E-PG>Dop1R1^{RNAi} p = .67; ctrl - E-PG>Dop1R2^{RNAi} p < .0001; E-PG>Dop1R1^{RNAi} - E-PG>Dop1R2^{RNAi} p < .0001). *C*: average profile of the angular velocity. Starting from the left, the first dashed lines mark the distractor switch-off at 3.1 s while the second one the peak of forward velocity at 3.2 s evident in the E-PG>Dop1R2^{RNAi} ($F_{(2,\ 91)}$ = 51.23, p < .0001; ctrl - E-PG>Dop1R1^{RNAi} p = .66; ctrl - E-PG>Dop1R2^{RNAi} p < .0001; E-PG>Dop1R1^{RNAi} - E-PG>Dop1R2^{RNAi} p < .0001). Colour-coding is reported on the middle right.

Optogenetic experiments

Trajectories

To better understand the putative role played by the E-PG neurons in the selection of action, I thought to briefly activate (i.e., for 200 ms) the circuit overall by means of optogenetic technique during an early phase straddling the distractor onset. These experiments were performed on UAS-ChR2.XXL/+; R70G12/+ flies, from now on called E-PG>ChR2^{XXL} and on an artificial control group composed by the ensemble of the two parental fly lines (i.e., R70G12-GAL4 and UAS-ChR2.XXL). Looking at the average profile of the trajectories was evident in both groups that, compared to the knockdown experiments, the flies remained much closer to the original target (Fig. 2.14A). By modelling the trajectories as previously done during t0 – t3 time window, differences were detected between the two groups, meaning that the optogenetic activation of the E-PG neurons affected the trajectories adopted by flies (Fig. 2.14B, C). The E-PG>ChR2^{XXL} appeared to shift less in the condition at 60 deg and more in the one at 90 deg than controls. However, I suspected also that a common bias due to the blue-light pulse was responsible of the anomalous straight paths in both groups.

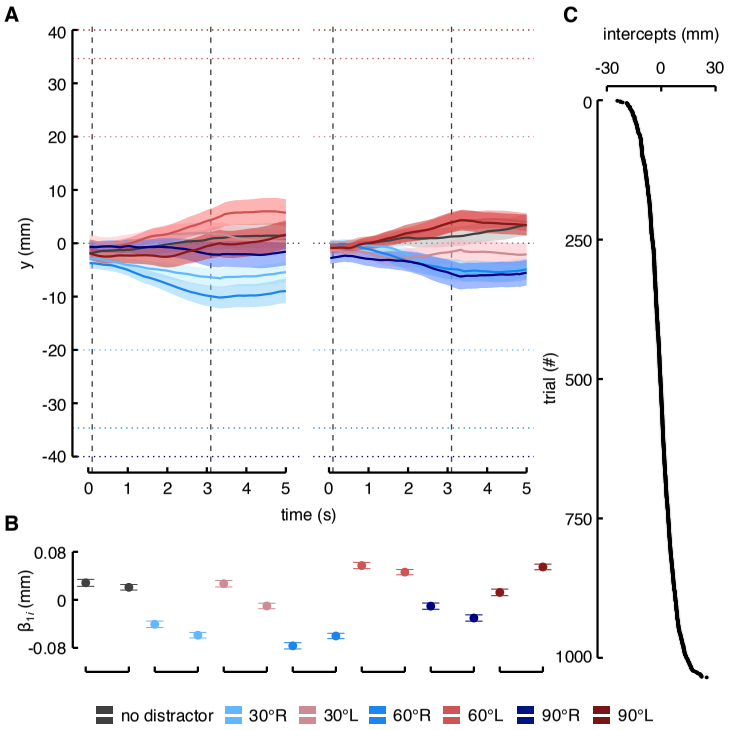

Fig. 2.14. Trajectories in optogenetically stimulated flies. *A*: average profile of the shift along y-axis per time and condition in the control group on the left and in E-PG>ChR2^{XXL} on the right. The shadow regions around the profiles, the horizontal dotted lines and the two vertical black dashed lines encode as in figure 2. *B*: estimated parameters of the fixed effect referred to the interaction between time, condition and group with corresponding confidence intervals (parametric bootstrap intervals of 10,000 simulations) at 97.5% level. On the left of each condition is represented the control group while on the right the E-PG>ChR2^{XXL}. *C*: plot of random effect. As in the previous figures, dots represent BLUPs while the horizontal lines crossing dots corresponds to the SD. Colour-coding is reported on the bottom of the panel.

Orientations

The flies' orientations in t0 – t3 time window substantially reflected the flies' trajectories whereby values were distributed around the zero with slight deviation to the left or to the right depending on the distractors (Fig. 2.15A). As for the trajectories, the model selection identified an effect associated to the group (Fig. 2.15B). This result confirmed a strange phenomenon: the flies ran towards the target changing much less the orientations in response to a distractor appearance than experiments not implying optogenetic stimulation. Following the distractor turn-off (i.e., t3 – t5 time window) flies showed a greater

variability among conditions in the orientations than the one during its presence. This behavior was still quite similar between the two groups as showed by the best model which did not consider the predictor referred to group.

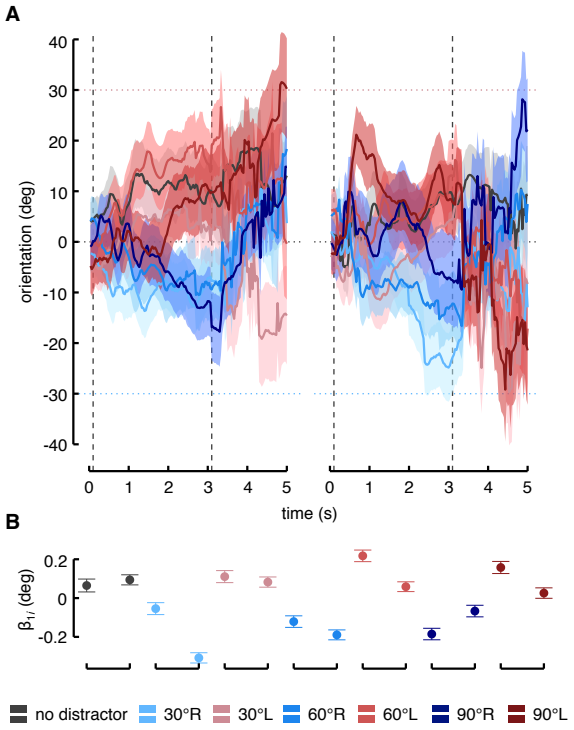

Fig. 2.15. Orientations in optogenetically stimulated flies. *A*: average profile of the orientation per time and condition in the control group on the left and in E-PG>ChR2^{XXL} on the right. The shadow regions around the profiles, the horizontal dotted lines and the two vertical black dashed lines encode as in figure 3. *B*: estimated fixed effect for the model confined to the time window t0 – t3. The parameters refer to the interaction between time, condition and group. The error bars correspond to confidence intervals (parametric bootstrap intervals of 10,000 simulations) at 97.5% level. Colour-coding, as previously described, is reported on the bottom right.

Forward velocity

To corroborate my suspicion, the average velocity profile showed in both groups a clear-cut negative peak of the forward velocity after the blue-light pulse (Fig. 2.16A). An abrupt reduction of the velocity appeared to be a drawback of the optogenetics. Likely, the blue-light frightened flies which dampened their running towards the target, after that they got back their initial goal represented by the target. Moreover, when the distractor was turned off, controls showed only sporadically changes in forward velocity. Remarkably, the E-PG>ChR2^{XXL} flies, similarly to what highlighted by the E-PG>Dop1R2^{RNAi} flies, showed a sharp peak of forward velocity about 200 ms after the distractor was turned off (Fig. 2.16B). This sharp peak was present in all distractor conditions but absent in the no distractor one, meaning that it was dependent from the distractor disappearance.

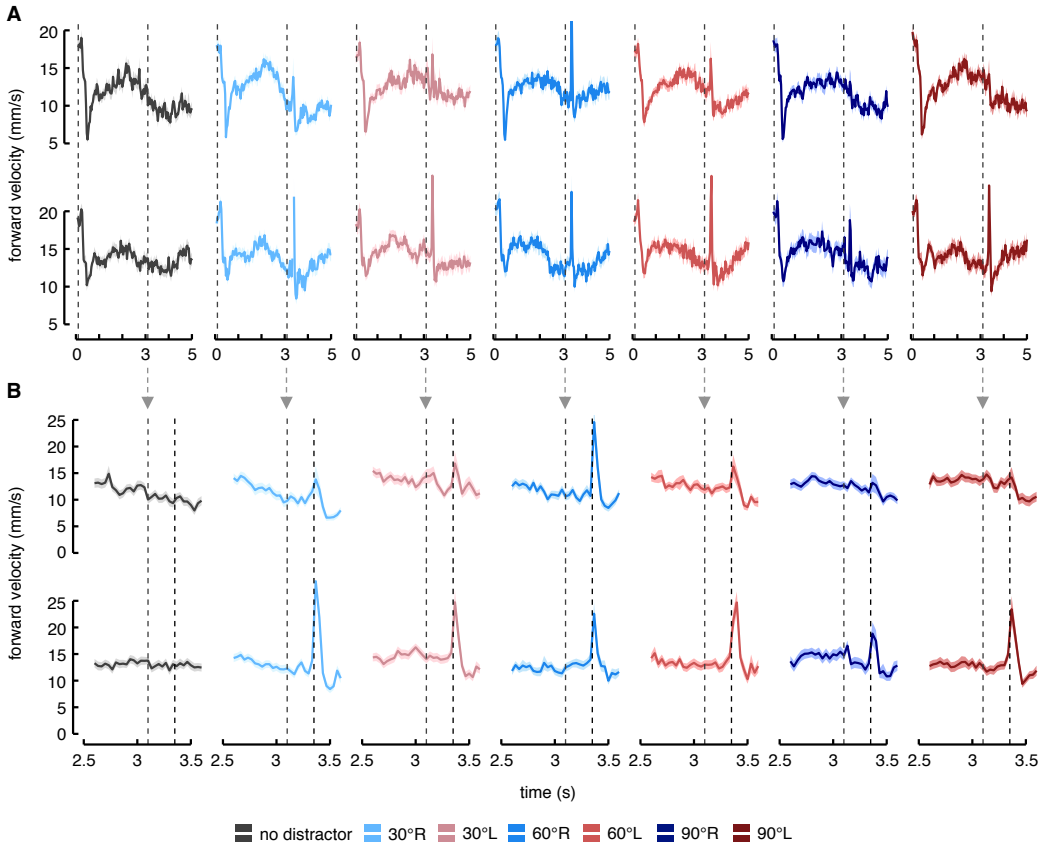

Fig. 2.16. Forward velocity in optogenetically stimulated flies. *A*: average profile of the flies' forwards velocity per condition along time. On the top the control group; on the bottom the E-PG>ChR2^{XXL}. The shadow regions around the profiles and the two vertical black dashed lines encode as in figure 4. *B*: enlargement of the time window between 2.5 and 3.5 s showing the forward velocity peak in the two groups. On the top the control group while on the bottom the E-PG>ChR2^{XXL}. The two vertical black dashed lines mark respectively the disappearance of the distractor at 3.1 s and the velocity peaks at 3.3 s ($F_{(1, 48)} = 12.61$, $p = .0009$). Colour-coding is reported on the bottom of the panel.

Angular velocity

Angular velocity showed an interesting profile. During the first second after the optogenetic stimulation and distractor appearance, the controls did not seem to widely change their angular velocity. On the contrary, the E-PG>ChR2^{XXL} seemed to response by changing their angular velocity much more regardless the condition (Fig. 2.17A). This resembles a "saccadic" activity widely increased which likely suggests an incapacity to maintain a correct heading to the goal.

Confirming the forward velocity peak, after 200 ms from the distractor turn off, also the angular velocity showed sharp peak (Fig. 2.17B).

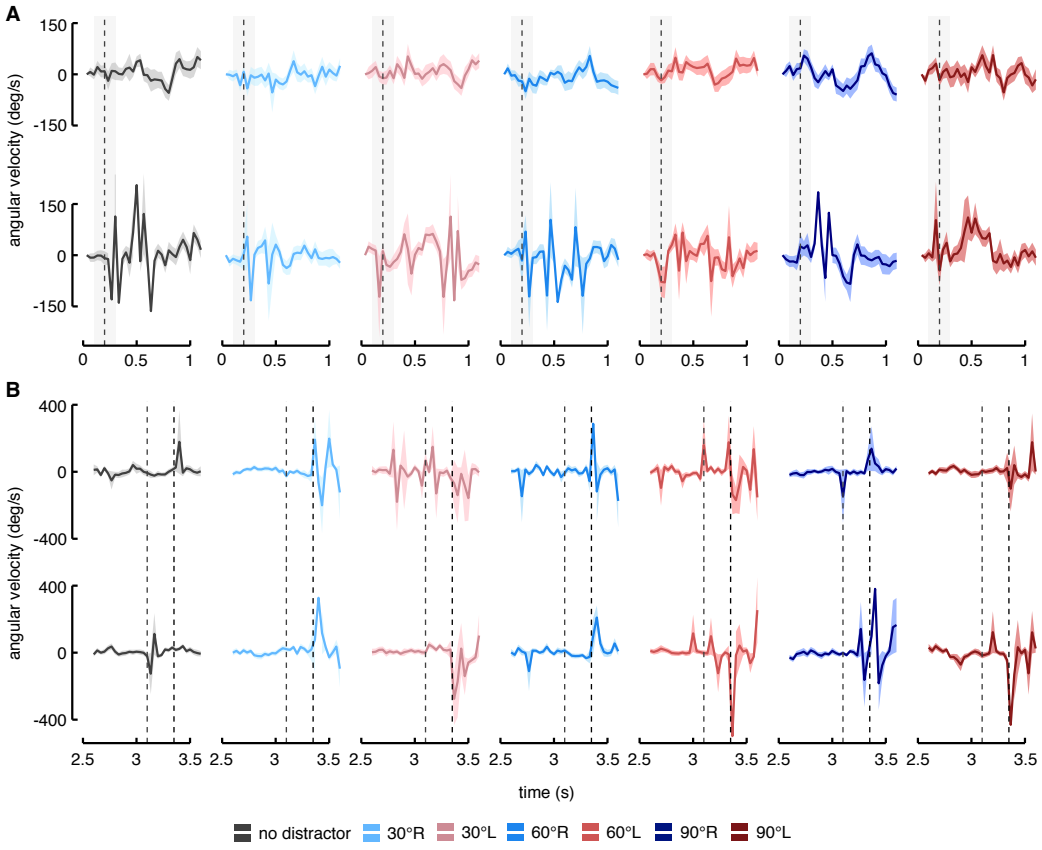

Fig. 2.17. Angular velocity in optogenetically stimulated flies. *A*: average profile of the angular velocity per condition within the first second after the crossing of the virtual window. On the top the control group; on the bottom the E-PG>ChR2^{XXL}. The shadow regions around the average profile represent SEM. The vertical black dashed line marks the distractor appearance, while the grey shadow rectangles represent the 200 ms optogenetic stimulations. *B*: average profile of the angular velocity per condition in the time window between 2.5 and 3.5 s. On the top the control group while on the bottom the E-PG>ChR2^{XXL}. The shadow regions around the average profile represent SEM. The two vertical black dashed lines mark respectively along time, the moment in which the distractor switch-off at 3.1 s and the peak of forward velocity at 3.3 s evident in figure 8 ($F_{(1, 48)} = 7.20$, $p = .01$). Colour-coding is reported on the bottom of the panel.

2.3.4 Discussion

In this study, I attempted to clarify the putative role of the E-PG neurons in an action-interference paradigm which involves selection of action (Frighetto et al., 2019). Specifically, I hypothesized different roles for two subtypes of the dopamine 1-like receptors within the E-PG neurons (Han et al., 1996; Kim et al., 2003): an activating role for the Dop1R1, which could favour the focus and the docking to a selected visual target, and an inhibiting role for Dop1R2, which could act reducing the background noise. For this purpose, I induced a knockdown of these DopR by means of the RNAi technique (Dietzl et al., 2007). Through this approach, the interference with one DopR subtype would result in an unbalance in favour of the other one. Thus, flies from the E-PG>Dop1R1^{RNAi} strain would express almost exclusively the Dop1R2 and vice versa for the E-PG>Dop1R2^{RNAi}.

My results should be interpreted taking into account such mechanism. The E-PG>Dop1R1^{RNAi} flies, having an unbalance towards the Dop1R2, would be more inclined to globally inhibit the wedges keeping the ring in a quite unstable dynamic in absence of a salient stimulus. In my experiments, though, the target represented a salient enough visual stimulus towards which the fly run, evident in the straight trajectory for the no distractor condition. Therefore, the presence of Dop1R1 might be relevant albeit not essential for engagement and maintaining of specific goals, in absence of which flies would be ready to anchor a new stimulus but without then pursuing it with high motivation. Our data seem to corroborate a congruent perspective showing that in E-PG>Dop1R1^{RNAi} flies: (i) the body saccade performed within the first 250 ms after the distractor turn-on, although in line with controls, tends to be greater in terms of amplitude as a sign of increased distractibility; (ii) their orientations remain aligned to the distractor even when it is turned off, meaning that no particular pressure aimed at returning towards the anchored original target is present. In this sense, the E-PG>Dop1R1^{RNAi} flies seem to be more interested in exploring the environment without maintaining the focus to a specific goal, either the original target or the distractor.

The E-PG>Dop1R2^{RNAi} flies instead, by relying on the Dop1R1 were less efficient in responding to novel visual stimuli remaining more focused to an engaged action than controls. This idea is supported by three main evidences: (i) the slow, small and delayed body saccade performed after the distractor turn-on seems to indicate a lower inclination to distractibility; (ii) for the distractor at 30 deg, which is likely the condition requiring the greater amount of inhibition to feed onto the target in order to shift towards the distractor, the E-PG>Dop1R2^{RNAi} have shown a smaller shift compared to controls; (iii) the forward velocity peak (also consistent with the angular velocity peak) after the distractor turn-off seems to indicate an abrupt need of the system to get back towards the original goal. This latter phenomenon may be conceptualized as if an enforced response during the distractor appearance were temporarily altering the flies' heading, which, just like a compressed spring then released, returns to its initial state upon the distractor disappearance.

The same phenomenon has been shown by the E-PG>ChR2^{XXL} flies which, after a brief overall activation of neurons, responded to the distractor turn-off with a sharp boost of forward velocity. Although our optogenetic experiments were affected by the side effect of the blue-light used, as evident in the abrupt dampening of velocity after the stimulation, we can clearly attribute the positive peak after the distractor turn-off to the E-PG activity. Likely, the global activation of the E-PG neurons resulted in an over engagement towards the target similarly to the dynamic generated by the knockdown of the Dop1R2, confirming they role in the inhibition of the system.

A data that does not fit my model, however, is referred to the forward velocity owned by flies at the distractor onset. Contrariwise to a reasonable implication associated with increased instability, the E-PG>Dop1R1^{RNAi} flies tended to a higher velocity than controls, while, counter-intuitively, the E-PG>Dop1R2^{RNAi} flies tended to a lower velocity. In this regard it has been recently proposed that the E-PG neurons may reflect a core interface between internal goals and motor actions, upon which, the others more complex abilities such as navigational, are built (Green et al., 2019). A synaptic transmission impairment of the E-PG neurons has shown to compromise the flies' ability to maintain the heading at

arbitrary angles and to reduce the forward walking velocity probably because of a poor matching between the E-PG phase and the internal goal (Green et al., 2019). Moreover, after the jumping in a new angular position of a visual stripe which the flies were fixating, a slow correction turning was evident. Therefore, a still unclear interacting mechanism between the action-interference task and the neural manipulation I performed might have determined my unexpected velocity results, whereby the alignment of more neuronal activities would allow to pursue a goal with high motivational state.

Recent results on turning behaviour by Kottler and coworkers (2019) have shown how the knockdown of Dop1R1 in the E-PG neurons (targeted with another driver line) accentuates the approach angle distribution towards ± 75 deg (i.e., the difference between the angle owned when the flies contact the arena edge and the angle owned when they enter a region delimited by 3 mm distance from the arena edge). This result has been interpreted as an exacerbation of decision-making process in which flies polarize the turning behaviour increasing the angle of incidence with respect to the arena edge (Kottler et al., 2019). According to our model this might be a consequence of the instability in the E-PG neurons due to the unbalance towards the Dop1R2 in a context without a prevalent goal which would take flies to easily focus and implement an action, such as the decision to turn right or left.

Nevertheless, the main difference of this study with mine is related to the driver line employed. I used a GAL4 line with a pattern consistent with the E-PG neurons whose a split version (i.e., SS00096) has been recently used in two studies (Giraldo et al., 2018; Kim et al., 2017b), while Kottler and collaborators have used the GAL4 line originally employed to identify the E-PG neurons (Seelig & Jayaraman, 2015; Wolff et al., 2015; Green et al., 2017). An extremely fascinating feature motivated the adoption of our driver line. Indeed, the promoter sequence under which its GAL4 is inserted corresponds to the putative enhancer fragment of the Dop1R2 (with 2943 residues). This means that the neurons targeted by the driver line I used have a high probability to express at least the Dop1R2.

In my study I did not manipulate the R-neurons but they could be involved in action selection process as well interacting with the E-PG neurons (Kottler et al.,

2019). It has been highlighted that the R-neurons affect the slow turning tendency in tethered flying flies depending on the visual experience; silencing these neurons, flies do not exhibit the innate behaviour for preferential orientation towards novel locations (i.e., previously uncued sides) any more (Shiozaki & Kazama, 2017). Thus, the maintenance of a memory or of a stable state until new sensory perturbations occur might be another important component of the action selection mechanism. The E-PG neurons show a persistent activity maintaining the "compass needle" over the standing in darkness (Seelig & Jayaraman, 2015). Their activity remains tethered to the position of one stripe even in the presence of another identical one and it does not always shifts instantaneously following an abrupt displacement of a visual stripe (Seelig & Jayaraman, 2015). Therefore, it would seem that the locking to one target is maintained across perturbations of the attractor ring or, at least, that a selected target is taken into account with a certain strength possibly to permit the accomplishment of a motor program. Our preferred idea is that this processes is achieved by an improvement of the signal-to-noise ratio through the dopamine modulation. Furthermore, similarly to what occurs in the mammalian brain (Grillner & Robertson, 2016), the signal involved in starting and halting an action sequence could be based on phasic dopamine release onto the EB in a manner similar to what is observed in the case of the nigrostriatal circuit of mice (Jin & Costa, 2010). The quantitative modulation of dopamine, via different receptors could engage and disengage the action programs, by respectively strengthening or weakening the signal-to-noise ratio. A high level of phasic release might enhance the specificity of action selection processes and movement initiation, while tonic release might inhibit the modules for action. This double mechanism would facilitate the emergence of motor responses from a repertoire of possible actions in order to readily cope with the sensory inputs determined by environmental variations. Fiore and collaborators (2015) have suggested that a phasic dopamine release would allow the system to change the strength of the connections between sensory inputs and the EB, thus affecting the probability that the related motor action would be selected again. Conversely, a tonic release would not alter the connections' strength but would make the global system

more stable (i.e., maintenance of selection) or unstable (i.e., sensitive to changes) depending on the receptor type involved (Fiore et al., 2015). My results suggest that two dopamine 1-like receptor subtypes would work in synergy with opposite roles: the Dop1R1 seems relevant for engagement of action while the Dop1R2 seems relevant for disengagement of action. I cannot definitely conclude that the E-PG neurons and the dopamine modulation of them are a fundamental core process of action selection but I can hint at it. Further experiments, by using improved behavioural paradigms and possibly combined with *in vivo* recording might ascertain this issue. A full comprehension of the mechanisms involved in action selection and the underlying neural bases represent a bullet point in neuroscience which has not been achieved yet.

2.4 NEUROCHEMICAL CHARACTERIZATION OF THE ACTION-SELECTION CIRCUITS

In the current work I imaged neuronal Ca^{2+}-activity in different circuits innervating the EB. Tangential and columnar neurons have been characterized with respect to their response to dopamine release. Through the knockdown of dopamine 1-like receptors in these different neuronal circuits I have highlighted interesting modulatory effects of dopamine depending on the type of receptor.

The results provide new insight concerning the pharmacological characterization of the neurons composing the EB and represent a further step in the understanding of the role played by the dopamine within a structure resembling the mammalian basal ganglia. To explain these findings a model of the basal ganglia-like network of the CX is advanced.

2.4.1 Introduction

In primates the action selection mechanism is played out in a group of subcortical nuclei called basal ganglia and their functions are critically dependent on dopamine (DeLong, 1990; Redgrave et al., 1999). Dysfunction of these nuclei may result in several pathological conditions related to motor control such as the Parkinson's disease (Redgrave et al., 2010a; Nelson & Kreitzer, 2014). Two main pathways, which consist of striatal projections to the basal ganglia output nuclei, control the selection process: the direct and the indirect pathway. These two pathways act together respectively to perform action selection by disinhibiting a selected motor program and inhibiting other competing ones (Grillner et al., 2005a). The same architecture has been also identified in the phylogenetically oldest group of vertebrates, such as the lamprey which diverged from the evolutionary line leading to primates some 560 million years ago (Ericsson et al., 2011; Stephenson-Jones et al., 2012). This suggests that the mammalian basal ganglia evolved through a functional replication of these circuits rather than a sequential adaptation of this ancestral architecture (Stephenson-Jones et al., 2011). Moreover, the striking conservation between so evolutionary distant

organisms has been demonstrated with respect to the dopamine modulation as well, providing further evidences in favour of an evolution's blueprint for the basal ganglia (Ericsson et al., 2013; Stephenson-Jones et al., 2013). Likewise mammals, the direct pathway is characterized by striatal projection neurons which express the dopamine D1 receptor acting as a brake for the GABAergic output neurons located in the internal segment of the *globus pallidus* and in the pars reticulata nucleus of the *substantia nigra* which are in turn tonically activate and keep the brainstem motor centres inhibited (Grillner & Robertson, 2016). On the contrary, the indirect pathway is characterized by striatal projection neurons which express the dopamine D2 receptor (Grillner & Robertson, 2016).

Recently, extensive correspondences in heritable ontogeny, neuroanatomical organization and function between the vertebrate basal ganglia and the insect CX have been put forward. Specifically, similarities have been found concerning the embryological derivation, orthologous genetic specification, neurochemicals and physiological properties (Strausfeld & Hirth, 2013b; Strausfeld & Hirth, 2013a). Furthermore, evolutionary corresponding computational mechanisms subtending the selection and maintenance of adaptive behaviours in vertebrates and insects have been also suggested in terms of dimensionality reduction and transition through attractor states (Fiore et al., 2015). These similarities have been considered parsimoniously as homology by common descendent. Despite such interesting evolution perspective, the speculative extension of this claim remains quite large and still under discussion (Farries, 2013). Indeed, someone can consider the similarities as due to convergent evolution. Furthermore, the main correspondence to the vertebrate basal ganglia, that is, the presence of two pathways modulated by dopamine remains elusive. In other words, whereas some behavioural effects of dopamine on the CX have been already shown (Lebestky et al., 2009; Kong et al., 2010; Kottler et al., 2019), no data concerning its neurophysiological modulation and even less with respect to distinct pathways are available so far.

Here, I tried to clarify the effects of dopamine on some circuits composing the CX, with particular reference to two tangential (i.e., R2 and R5) and one columnar neurons (i.e., E-PG) (Wolff et al., 2015; Omoto et al., 2018). By taking

advantage of the *in vivo* bioluminescence Ca^{2+} imaging technique (Martin et al., 2007), I recorded the activity in specific neural circuits in response to excitatory drugs with or without a previous application of dopamine. The aim of these experiments was to understand whether and how dopamine is able to modulate the response of the CX neural circuits likely involved in the action selection process and if so whether there were direct and indirect pathways. The neurofunctional model formalizing my hypotheses was focused on the attempt to show: (i) whether the E-PG neurons were modulated by the dopamine and whether the two subtypes of the dopamine 1-like receptors, Dop1R1 and Dop1R2, affected in the opposite way the state of excitability; (ii) if two sets of R-neurons, R2 and R5, likely expressing respectively dopamine 1-like and dopamine 2-like receptors (D2R) were modulated by dopamine in the opposite way, that is, activated the former ones and inhibited the second ones.

The results showed that the two subtypes of dopamine 1-like receptors modulate in opposite way the E-PG neurons while two distinct dopamine receptors, Dop1R1 and Dop2R, modulate in an opposite way two different sets of tangential neurons, R2 and R5. It means that two distinct pathways involving dopamine and based on different receptors as seen in vertebrate basal ganglia seem to be present in flies, exciting and inhibiting different tangential neurons which are probably GABAergic.

2.4.2 Methods

Fly stocks

Flies were maintained on standard medium at room temperature (i.e., 24°C). Newly eclosed males and females were kept 10/5 per vial for mating. A new version of the responder G5A line expressing 20 UAS repetitions, w^{1118};;P{$y^{+t7.7}$ w^{+mC}=20xUAS-G5A}attP2 (a courtesy of Barret D. Pfeiffer, Janelia Research Campus, Ashburn, VA, USA) was used for crossings with the driver lines targeting tangential and columnar neurons (Jenett et al., 2012; Pfeiffer et al., 2010). To target the R2 neurons I used the w^{1118};;P{$y^{+t7.7}$ w^{+mC}=GMR20D01-

GAL4}attP2 (BDSC #48889), while for the R5 neurons I used the w^{1118};;P{$y^{+t7.7}$ w^{+mC}=GMR72D06-GAL4}attP2 (BDSC #39769). The columnar E-PG neurons were targeted by using the w^{1118};;P{$y^{+t7.7}$ w^{+mC}=GMR70G12-GAL4}attP2 (BDSC #39552). Knockdown of dopamine 1-like receptors were performed by means of RNAi on Dop1R1 w^{1118};P{w^{+mC}=UAS-Dop1R1 RNAi}pKC43; (VDRC #107058/KK) and Dop1R2 w^{1118};P{w^{+mC}=UAS-Dop1R2 RNAi}pMF3; (VDRC #3392/GD) (Dietzl et al., 2007; Green et al., 2014). Therefore, *trans*-heterozygous lines bearing GAL4, 20xUAS-G5A and UAS-RNAi were also used (Fig. 2.18A). Imaging experiments were performed only on mated female of 4-5 days old.

Preparation of flies

Flies ready to be tested were prepared for *in vivo* brain imaging experiments as described by Martin and collaborators (2007). Briefly, an offspring collected from its food vials was ice-anesthetized and then, by gently grasping its wings with a forceps, positioned upside down on a plastic coverslip (22 x 22 x 0.157 mm) specifically designed to accommodate the upper half of its head inside a hole (BAH4469000001PK, Sigma-Aldrich, St. Louis, MO, USA). A drop of dental glue between the coverslip and the dorsal part of fly guaranteed the binding (Protemp 4®, 3M ESPE™, Seefeld, Germany, EU). The coverslip was previously prepared so as a hole of approximately 0.6 mm diameter at the centre by using a bodkin was performed and a thinner edge around it was made by using a cutting burr bit mounted on a rotary machine tool (Dremel 3000, Dremel®, Mount Prospect, IL, USA). This latter operation was necessary in order to make the workspace for dissecting of the upper half of the head as deeper as possible and at the same time to leave the fly's visual field in the lower half as wider as possible. Once the fly was glued to the coverslip and its head positioned through the hole in such a way that antennae were below the horizontal plane of the coverslip and the rest of the head capsule above it, the empty spaces around the fly's head were sealed using a special bio-compatible silicon (Kwik-Sil™, WPI, Sarasota, FL, USA). The entire preparation was fixed on an acrylic block with two small stripes of adhesive tape whereby the fly was tethered but free to move its legs for instance for

walking. A drop of Ringer's solution with pH = 7.3 containing 130 mM NaCl, 5 mM KCl, 2 mM $MgCl_2$, 2 mM $CaCl_2$, 36 mM sucrose and 5 mM HEPES-NaOH (Martin et al., 2007), was deposited over the upper half of the head and a tiny window between the eyes and just above the antennae was opened in the head capsule using a micro knives (#10315-12, Fine Science Tools GmbH, Heidelberg, Germany, EU) to expose the brain. The underlying neural sheath was also gently removed with forceps (Dumont #5SF, Fine Science Tools GmbH, Heidelberg, Germany, EU) in order to improve the exposition of the outer brain surfaces. Extremely care was taken to avoid any damage of the fly brain structures. Dissection procedure was performed under a fluorescent stereomicroscope (Leica MZ FLIII, Leica Microsystems GmbH, Wetzlar, DE, EU). The exposed fly brain was first incubated for 2 h in 100 µl of Ringer's solution containing 25 µM native water-soluble coelenterazine (NanoLight®, Prolume Ltd., Pinetop, AZ, USA). Subsequent to the incubation, 100 µl of fresh Ringer's solution was replaced to the preparation and the fly was ready to be imaged. In this condition, the fly was able to breathe via tracheal system and could be maintained alive for more than 24 h. However, before starting the recording an air puff was delivered with a mouth aspirator on the fly's legs to stimulate a locomotor reflex. If the fly did not show any response then it was not further considered for the experiment.

In vivo brain imaging

Bioluminescence signals (i.e., Ca^{2+}-response) in tangential and columnar neurons were recorded using an intensified CCD camera with a cooled (at -20°C) GaAsP photocathode (Turbo-Z™, Stanford Photonics Inc., Palo Alto, CA, USA) fitted onto a direct microscope (Axioplan 2, Carl Zeiss GmbH, Jena, Germany, EU) (Fig. 2.18B). The entire system was positioned on an anti-vibration table and housed inside a light-tight dark box (Science Wares Inc., Falmouth, MA, USA). Using a 20x water immersive objective lens (Zeiss N-Achroplan, N.A. 0.5) the spatial resolution was 480 x 360 µm (640 x 480 pixels), while using a 40x objective lens (Zeiss N-Achroplan, N.A. 0.75) it was 240 x 180 µm (1 pixels = 0.375 x 0.375 µm). To acquire and store data, each detected photon was assigned an x and y-

coordinate and a time point (i.e., x, y, t). Photon acquisition was carried out at 120 frames s^{-1}, providing 8.333 ms time resolution with extremely low background signal. The Photon Imager software (Science Wares Inc., Falmouth, MA, USA) written in LabView 2010 (National Instruments™, Austin, TX, USA) was used for this purpose. Image recordings were obtained from 10 to 20 flies per each genotype.

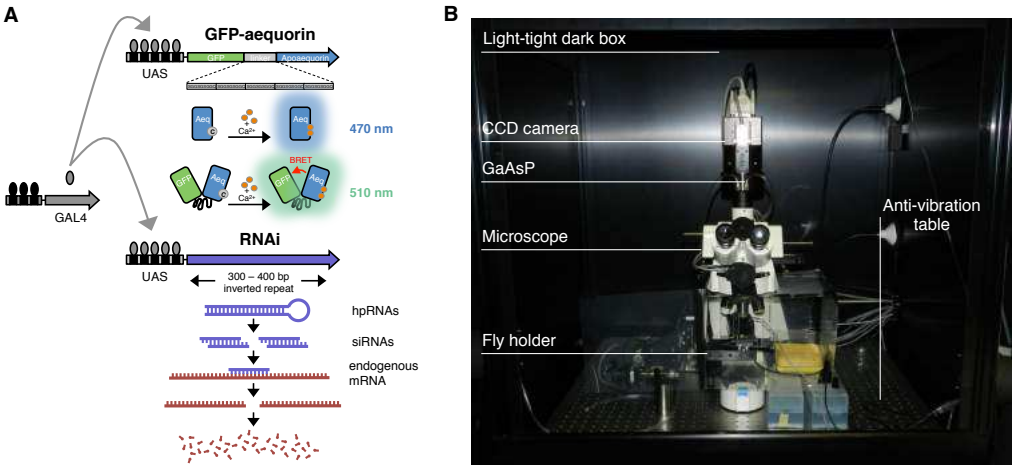

Fig. 2.18. Genetic techniques and Ca^{2+} imaging setup. *A*: responders activated by the driver GAL4 used in this study. On the top, schematic of GFP and aequorin fusion gene with upstream activation sequence (UAS). Model of blue light emission by aequorin (grey dot represents coelenterazine) and that one of green light emission by GFP-aequorin in response to high levels of Ca^{2+} (orange dots). On the bottom, schematic of the RNAi technique in which a double-stranded RNA (so called hairpin RNA, hsRNA) is expressed as a complementary sequence to a gene of interest under UAS. The dsRNA is then processed by Dicer-2 into siRNA which lead to sequence-specific degradation of the mRNA related to the gene of interest. *B*: image of the setup used for *in vivo* Ca^{2+} brain imaging based on the bioluminescence technique.

Pharmacology

To stimulate the targeted neurons in flies I used either nicotine or picrotoxin. Depending on the putative presynaptic neurons in input to the circuit under investigation I applied these two drugs as stimulants for eliciting a Ca^{2+}-response respectively activating the excitatory nicotinic acetylcholine receptors and blocking the $GABA_A$ receptors. Nicotine (N3876, Sigma-Aldrich, St. Louis, MO, USA) was prepared as a 10 mM stock solution in H_2O and diluted to 100 µM in

Ringer's solution as final concentration reached during the experiment (i.e., 1 µl application). Picrotoxin (P1675, Sigma-Aldrich, St. Louis, MO, USA) was prepared as a 25 mM stock solution in H_2O and then dissolved in Ringer's solution to 250 µM (i.e., 1 µl application). Dopamine (H8502, Sigma-Aldrich, St. Louis, MO, USA) was dissolved directly in Ringer's solution prepared without sucrose at 1 mM and diluted to 100 µM as result of a 10 µl application during the recording. Accordingly, I used Ringer's solution application instead of dopamine as control samples. KCl application was also used at the end of each trial to evoke a strong Ca^{2+}-response in order to check that the preparation were in good shape. KCl (P9333, Sigma-Aldrich, St. Louis, MO, USA) was prepared as a 3 M stock solution in H_2O and diluted to 100 mM in the bath during the experiment (i.e., 30 µl application). All drugs were applied using a micropipette directly positioned on the EB.

Data processing

Pre-processing of imaging data were analysed using the Photon Viewer (2.1) software (Science Wares Inc., Falmouth, MA, USA). Bioluminescence signals are presented as the total amount of emitted photons within a draw ROI. Using GFP images of individual expression patterns, collected before the beginning of the experiments, were identified the ROIs and confirmed by the visual verification of coverage of response region. ROI shape and size were held standard to each region among flies expressing in the same subset of neurons. To improve the signal-to-noise ratio, data were subjected to 1 s integration time (1 Hz) without applying any binning of pixels. The data frames were exported in .csv files and then imported in RStudio (RStudio Team, 2017) for data processing and subsequent statistical analyses. Duration, latency and total photons of the Ca^{2+}-response were automatically computed for each track within a routine in R. Basically, I considered as response onset the increase of 10% in number of photons s^{-1} with respect to a normalization performed on the basis of the maximum number of photons s^{-1} collected (i.e., the response peak). Moreover, to avoid false positive detections due to unrelated activity such as spotted increases

of photons s^{-1}, the response above the threshold of 10% had to be sustained for at least 2 s. Accordingly, the end of the response was defined as the decrease in the photons s^{-1} under the threshold of 10%. For the average profile the alignment was performed on the response peak that resulted at the centre and the time window set to 200 s (i.e., 100 s before and after the peak).

Statistical approach

The statistical approach was the same used in the previous sections of this chapter, that is, different LME models were computed with the R package *lme4* (Bates et al., 2014) and then compared by using the BIC (Schwarz, 1978) to select the most plausible model. An approximation of the BF was also computed to obtain a measure of the plausibility.

2.4.3 Results

Putative inputs to EB neurons and drug-evoked Ca^{2+}-activity

To test the drug-evoked response in different neurons of the CX, specifically targeting the EB, I used *in vivo* bioluminescence Ca^{2+} imaging as previously done (Pavot et al., 2015; Lark et al., 2016). By means of the GAL4-UAS binary system I expressed the bioluminescent molecule G5A in these EB neurons.

In order to focus the investigation on few driver lines expressing in selected EB neurons with a high probability to be also modulated by dopamine, I screened the expression patterns of a whole raft of GAL4 lines from the FlyLight database (Jenett et al., 2012). The prerequisites to include the lines were the innervation of EB and the concurrently expression of putative dopamine receptors. Three main GAL4 lines were finally selected for the experiments: two lines expressing in two different subsets of R-neurons and one line expressing in the E-PG neurons (Fig. 2.19A). The E-PG driver line, the R70G12, is the same used in the previous section of this thesis likely expressing Dop1R2. The first driver line targeting the tangential neurons, the R20D01, is selective for the R2 neurons as defined by

Omoto and colleagues (2018). Actually, this line has the GAL4 promoter sequence corresponding to the enhancer fragment of the nicotinic acetylcholine receptor (nAChR) α3 subunit (2684 residues). It is not directly a putative dopamine receptor-expressing line, however, it was selected because of the overlap in the expression pattern with another line targeting the R2 neurons but under the promoter of Dop1R1, the R72B07. This latter line was not selected because its pattern includes also the TuBu neurons (Fig. 2.19B). Therefore, I surmised that the R20D01 expressed the Dop1R1 besides the nAChR (likely heteromeric combination among nAChRα1, α3, α5 and β1). The second line targeting the tangential neurons, the R72D06, is selective for what they have been recently called R5 neurons and which correspond to the previously called R2 neurons (Omoto et al., 2018). This line is characterized for the GAL4 promoter sequence corresponding to the D2R (1694 residues), meaning that it likely expresses them.

Based on previous data which has shown that the great majority of the R-neurons are GABAergic (Kottler et al., 2017) and particularly the R2 neurons (EB1 driver targets what they have been previously called R2/$R4_m$) with estimate 94% of them, I hypothesized that the R20D01 only marginally had postsynaptic GABA receptors but rather nAChR. Thus, I thought to pharmacologically stimulate the R2 neurons (R2>G5A flies) using nicotine as excitatory drug. These neurons have also shown to respond retinotopically to visual inputs (Seelig & Jayaraman, 2013). Moreover, in previous data, the R2 neurons have shown an inter-layer connectivity with what I defined as R5 neurons (in Kottler et al., 2017 they were defined as R3 neurons) according to Omoto and colleagues (2018) because of their clear similarity with the neurons targeted by Liu and colleagues (2016) (Fig. 2.19C). Without knowing the direction of the information flow and the main presynaptic neurotransmitter employed by the R5 neurons but considering the connectivity between these two subsets of R-neurons, I hypothesized that the R5 neurons might be the postsynaptic input of the R2 neurons. Specifically, whether the R2 neurons are GABAergic, the R5 neurons should be inhibited via $GABA_A$ receptor.

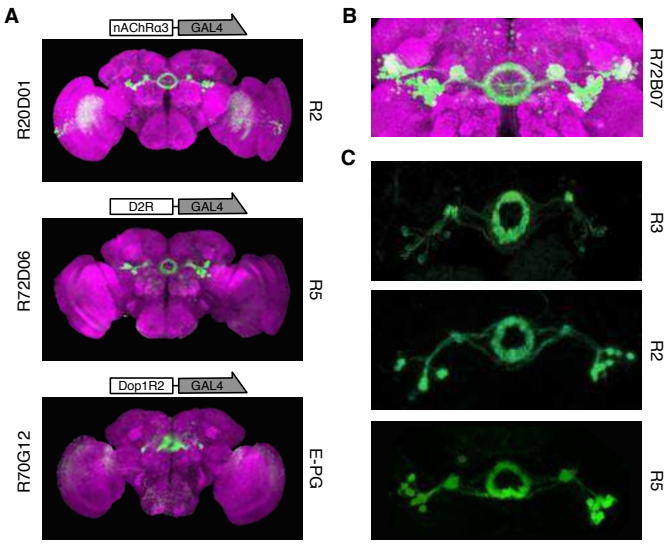

Fig. 2.19. Driver lines selected and neurons targeted. *A*: images taken from the FlyLight database (Jenett et al., 2012) of the pattern expressed by the lines selected. Starting from the top: the R20D01, with the promoter sequence corresponding to the putative enhancer sequence of the *nAChRα3* gene, targets the R2 neurons; the R72D06, with the promoter sequence of the *D2R* gene, targets the R5 neurons; and the R70G12, with the promoter associated to *Dop1R2* gene, targets the E-PG neurons. *B*: image from the FlyLight database of the expression pattern of R72B07 which has the promoter sequence associated to the *Dop1R1* gene. As we can clearly appreciated its pattern is widely superimposable with that one of R20D01 apart from the BU regions. *C*: expression patterns of three different driver lines. Starting from the top: confocal image from Kottler et al., 2017 of the nv45-LexA::VP16 driver line expressing GFP (LexAop-mCD8::GFP) which was considered to target R3 neurons; confocal image from Liu et al., 2016 of the split-GAL4 R58H05-DBD, R30G03-AD driver line expressing GFP (UAS-IVS-Syn21-GFP-p10) which was considered to target R2 neurons; and confocal image form FlyLight database (Jenett et al., 2012) of the R58H05 driver line expressing GFP (10xUAS-IVS-mCD8::GFP) which was considered by Omoto et al., 2018 to target the same neurons considered R2 by Liu et al., 2016 but which they newly defined as R5 neurons. I consider all these three driver lines, as well as the R72D06, targeting the same subset of R-neurons recently proposed as R5 neurons by Omoto et al., 2018.

A support to this idea comes from the expression pattern of the R70F01 line which expresses the GAL4 under a promoter inherited from the *resistant to dieldrin* (*Rdl*) gene which encodes for the $GABA_A$ receptor. This line is characterized for targeting a wide range of R-neurons which wrap almost all layers of the EB but only weakly, substantially saving, the R2. It resembles somehow the expression pattern of the c232 line regarding the outer region of the EB (i.e., $R4_d$). On the basis of this, I thought to pharmacologically disinhibit the R5 neurons (R5>G5A flies) using picrotoxin, a non-competitive blocker of $GABA_A$

receptor chloride channels. Then, since the columnar neurons have been recently proposed to be likely cholinergic (Franconville et al., 2018) and characterized by an extensive recurrent networking to update the fly's heading (Turner-Evans et al., 2017; Green et al., 2017), I thought to stimulate the E-PG neurons (E-PG>G5A flies) using nicotine. Actually, I did not have any confirmation concerning nAChR or metabotropic AChR expression in such neurons but I supposed a strong interaction with some other columnar neurons.

To test whether the predictions regarding the stimulant drugs were correct, I administered the drug applications in the open-brain preparations during the Ca^{2+} imaging recordings (Fig. 2.20A). A direct application of nicotine (1 µl) was delivered on the R2>G5A and on the E-PG>G5A flies, while application of picrotoxin (1 µl) was delivered on the R5>G5A flies. After 10 min of baseline recording, the drugs were applied over the preparation and the evoked response was recorded for a maximum period lasted 10 min. At the end of this period, 10 µl of KCl was applied as a stimulus control to verify the integrity of the brain preparation (Fig. 2.20B).

The results confirmed my expectations regarding the stimulation properties of the drugs used showing a strong increase in the Ca^{2+}-responses in all lines (Fig. 2.20C). Compared to the baseline activity, the drugs evoked responses that reached thousands of photons s^{-1} within the EB, meaning that very likely the tested neurons express the receptors hypothesized, despite that using a pharmacological approach as this makes almost impossible to exclude indirect responses caused by the activation of other neurons.

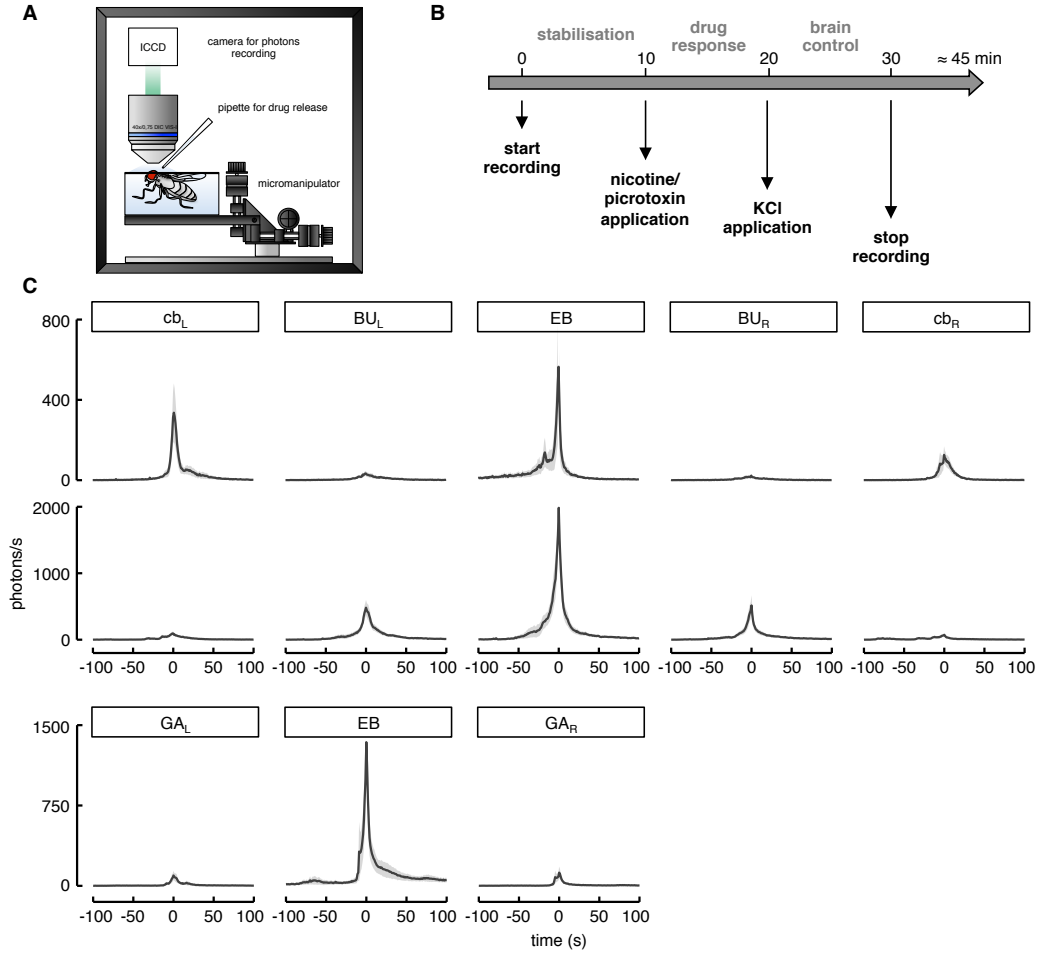

Fig. 2.20. Experimental procedure and Ca^{2+}-response to drugs application. *A*: cartoon of the fly preparation depicting the main components which are not drawn to scale. *B*: image of the protocol used to stimulate the neurons. *C*: Ca^{2+}-response profiles to drug application in the selected ROIs. Starting from the top: nicotine-evoked activity of the R2 neurons (R20D01 driver) in the five ROIs drawn around cell bodies (CB), BU and EB; picrotoxin-evoked activity of the R5 neurons (R72D06 driver) in the five ROIs drawn as in the previous neurons; and nicotine-evoked activity of the E-PG neurons (R70G12 driver) in the three ROIs drawn around the two GA regions and EB.

Dopamine modulation of Ca^{2+}-activity in EB neurons

To test the hypotheses related to the dopamine modulation of these neurons, I modified the previous protocol by adding a dopamine application 10 min before the stimulation in order to record whether and how it modulated the subsequent drug evoked-responses (Fig. 2.21A).

The R2 neurons showed enhanced Ca^{2+}-response to nicotine after the dopamine application compared to the condition without it as evident in the average response profile (Fig. 2.21B). However, to better understand the extent of the dopamine modulation, I fitted the data with different LME models considering several predictors such as the condition distinguishing the responses with or without dopamine application, the ROIs drawn and the time along which the responses were unfolded. For the R2 neurons I defined five ROIs encompassing all the EB, the two lateral BUs and the two lateral perikarya. I computed the BIC for the LME models comparison and the best one took into account the interaction between condition and ROIs as fixed effect (Table 13). This model was much more plausible than the one that considered only the ROIs as fixed effect (BF≈ 2073823) meaning that the increase of the response due to the dopamine application was not uniform among the five ROIs but some increased much more than others (Fig. 2.21C, D). Specifically, while the response in the BUs did not change too much, it increased in the perikarya and in the EB. The same best model was also found for the latency of the response showing a reduction particularly evident in the EB (Fig. 2.21E). These results corroborated the hypothesis that the R2 neurons were excited by the dopamine likely via Dop1R1 receptors.

Table 13. *Models selection*

Model	Df	BIC
$Y_{ij} = \beta_0 + \beta_1 D_{1i} D_{2i} + \lambda_i + \epsilon_{ij}$	12	312729.16
$Y_{ij} = \beta_0 + \beta_1 D_{1i} D_{2i} + \beta_2 X_{1i} + \lambda_i + \epsilon_{ij}$	13	312742.30
$Y_{ij} = \beta_0 + \beta_1 D_{1i} + \lambda_i + \epsilon_{ij}$	7	312754.79
$Y_{ij} = \beta_0 + \beta_1 D_{1i} + \beta_2 D_{2i} + \lambda_i + \epsilon_{ij}$	8	312756.75
$Y_{ij} = \beta_0 + \beta_1 D_{1i} D_{2i} X_{1i} + \lambda_i + \epsilon_{ij}$	22	312800.62
$Y_{ij} = \beta_0 + \beta_1 D_{2i} + \lambda_i + \epsilon_{ij}$	4	313287.87

Note. Y_{ij}: Ca^{2+}-response; D_1: ROI; D_2: condition; X_1: time; λ_i: random effects; ε_{ij}: error.

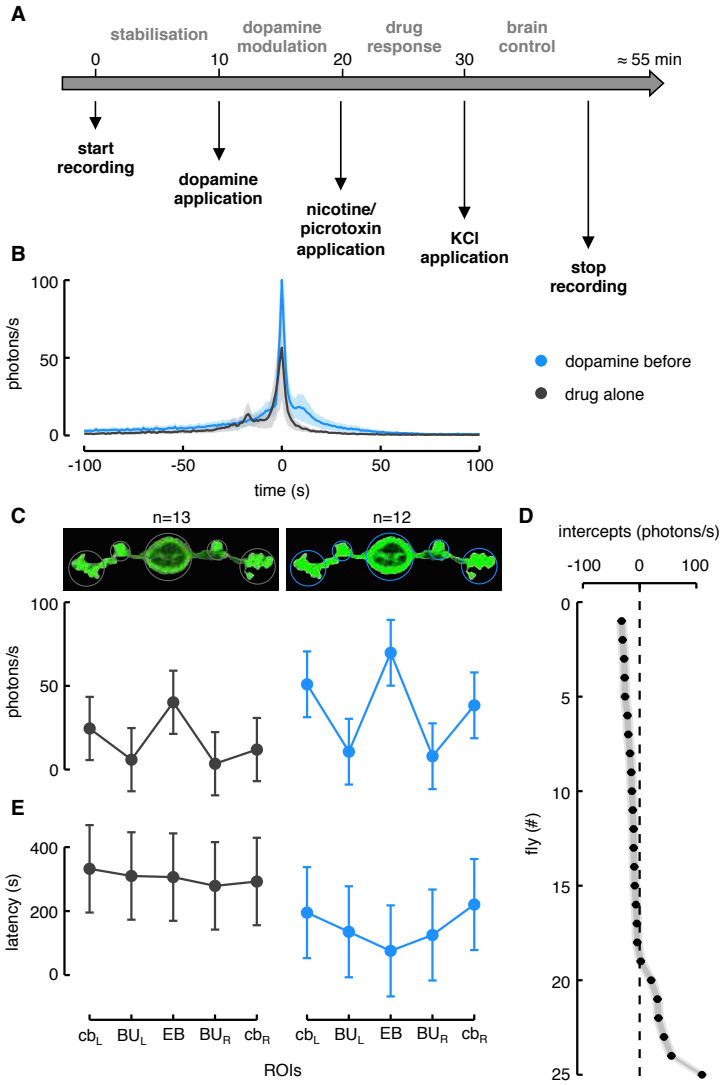

Fig. 2.21. Dopamine modulation in R2>G5A flies. *A*: image of the protocol used to modulate the neurons before the drug application. *B*: Ca^{2+}-response profiles of the R2 neurons in the EB ROI. In black is depicted the condition with the nicotine alone while in blue the condition with dopamine application before nicotine. *C*: estimated parameters of the Ca^{2+}-response referred to the interaction between condition and ROI (i.e., fixed effect) with corresponding confidence intervals (parametric bootstrap intervals of 10,000 simulations) at 97.5% level. On the left is represented the Ca^{2+}-response to nicotine alone in the five ROIs of the R2 neurons while on the right is represented their Ca^{2+}-response to nicotine after the dopamine application. *D*: plot of random effect referred to Ca^{2+}-response. Dots represent each fly (known as BLUPs, Best Linear Unbiased Predictions) while the horizontal lines crossing dots corresponds to the SD. *E*: estimated parameters of the response latency referred to the interaction between condition and ROI (i.e., fixed effect) with corresponding confidence intervals at 97.5% level. On the left is represented the latency response to nicotine alone in the five ROIs of the R2 neurons while on the right is represented their latency response to nicotine after the dopamine application.

On the contrary, the other class of R-neurons, the R5, showed a clear reduction of the Ca^{2+}-response after the dopamine release. As done for the R2 neurons, I tested and compared the same LME models to obtain a ranking of them. The ROIs for these neurons corresponded roughly to the ones of the R2 apart from the BUs which were encompassed by larger ROIs because of the particular ramifications projecting to the EB. Again, the best model was the one with the interaction between condition and ROI. It was much more probable than the one with only ROIs as fixed effect ($BF \approx 6.23 \times 10^{35}$) but in this case the responses decreased as consequence of dopamine specially in the BUs and EB (Fig. 2.22A, C). Still, the dopamine application increased the latency of the response as confirmed by the same best model (Fig. 2.22B). These results were stronger than the ones collected from the R2 neurons because the hypothesis upon which they relied on were already affected by a high probability concerning the D2R expression in the R5 neurons. I confirmed that the dopamine modulates these neurons via D2R, inhibiting the response and increasing the response latency.

The dopamine application on the E-PG neurons moderately increased the Ca^{2+}-response. Three ROIs were drawn, one encompassed the EB and two the laterally positioned GA regions. The deeper PB glomeruli innervated by these neurons and their perikarya were not considered because of the difficulties to image the PB from above and to standardize a common ROI dimension for the cell bodies. Among the LME models tested, the best one confirmed the interaction between condition and ROIs as fixed effect. This model was more probable than the simpler one which did not consider the condition ($BF \approx 436414$). Basically, the response did not change in the GA regions while it increased in the EB (Fig. 2.22D, F). Though, the response latency decreased quite uniformly for all the three ROIs (Fig. 2.22E). To sum up, the E-PG neurons were modulated by dopamine in terms of an increase of their activity.

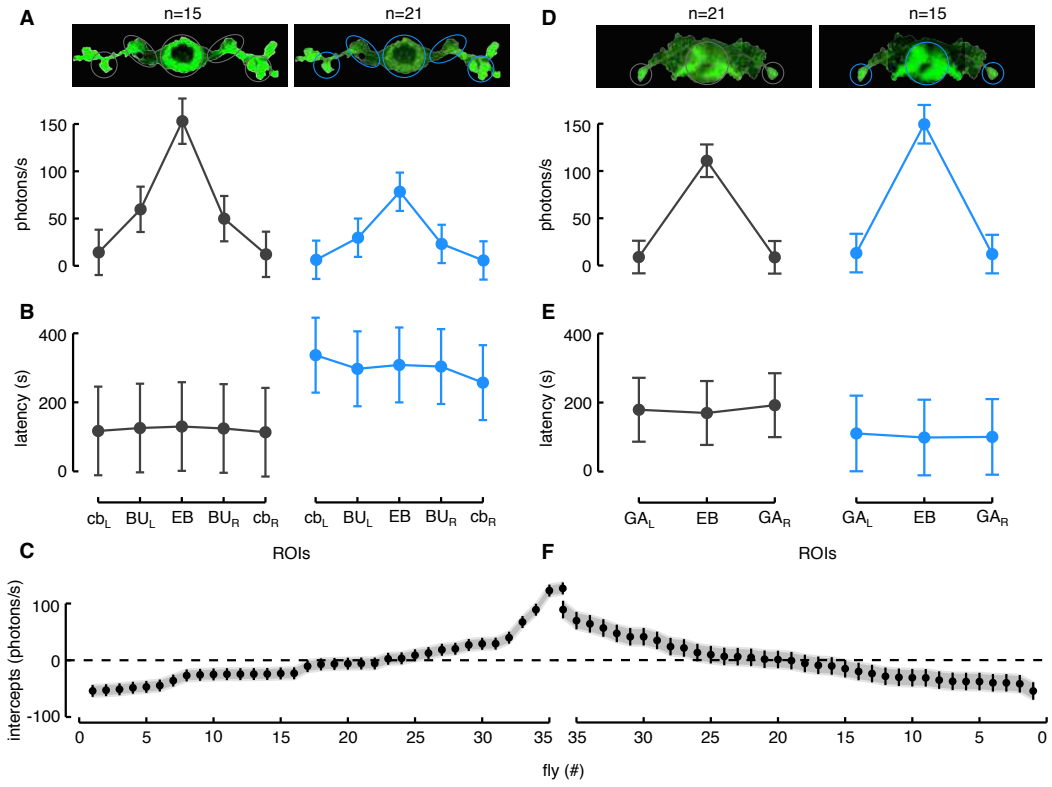

Fig. 2.22. Dopamine modulation of R5>G5A and E-PG>G5A flies. *A*: estimated parameters of the Ca^{2+}-response referred to the interaction between condition and ROI (i.e., fixed effect) with corresponding confidence intervals. On the left is represented the Ca^{2+}-response to picrotoxin alone in the five ROIs of the R5 neurons while on the right is represented their Ca^{2+}-response to picrotoxin after the dopamine application. *B*: estimated parameters of the response latency referred to the interaction between condition and ROI. On the left is represented the latency response to picrotoxin alone in the five ROIs of the R5 neurons while on the right is represented their latency response to picrotoxin after the dopamine application. *C*: plot of random effect referred to Ca^{2+}-response of R5 neurons. *D*: estimated parameters of the Ca^{2+}-response referred to the interaction between condition and ROI. On the left is represented the Ca^{2+}-response to nicotine alone in the three ROIs of the E-PG neurons while on the right is represented their Ca^{2+}-response to nicotine after the dopamine application. *E*: estimated parameters of the response latency referred to the interaction between condition and ROI. On the left is represented the latency response to nicotine alone in the three ROIs of the E-PG neurons while on the right is represented their latency response to picrotoxin after the dopamine application. *F*: plot of random effect referred to Ca^{2+}-response of E-PG neurons.

Knockdown of dopamine receptors in R2 neurons

Since the R2 neurons targeted by the line I used were not directly supported by a promoter sequence (under which the GAL4 was expressed) consistent with dopamine receptors, I directly tested if the Dop1R1 (likely expressed by these neurons) affected their nicotine-evoked response and if the dopamine increased their excitability via those specific receptors. For this purpose, I knocked down the Dop1R1 in the R2 by using the RNAi and *trans*-heterozygously expressing G5A for Ca^{2+} imaging (R2>G5A+Dop1R1^{RNAi}). Flies with downregulation of Dop1R1 in the R2 neurons showed a Ca^{2+}-response to nicotine similar to the one of normal flies. However, dopamine application prior to nicotine did not increase the excitability as seen in the normal flies (Fig. 2.23A, C). By comparing different LME models, the best model resulted to consider only the ROIs as fixed effect (BF $\approx$ 72715.77). It means that the Ca^{2+}-response to nicotine was not increased as a consequence of dopamine application in R2>G5A+Dop1R1^{RNAi} flies. In other words, the dopamine effect on the R2 neurons is due to the Dop1R1 and without them the increase in excitability is lost. On the contrary, a marginal effect due to dopamine was detected by the best model with respect to the response latency which remained only slightly more probable than the one with no condition as predictor (Fig. 2.23B). An interesting point in this regard is the fact that independently to dopamine the response latency was overall reduced in R2>G5A+Dop1R1^{RNAi} compared to R2>G5A flies.

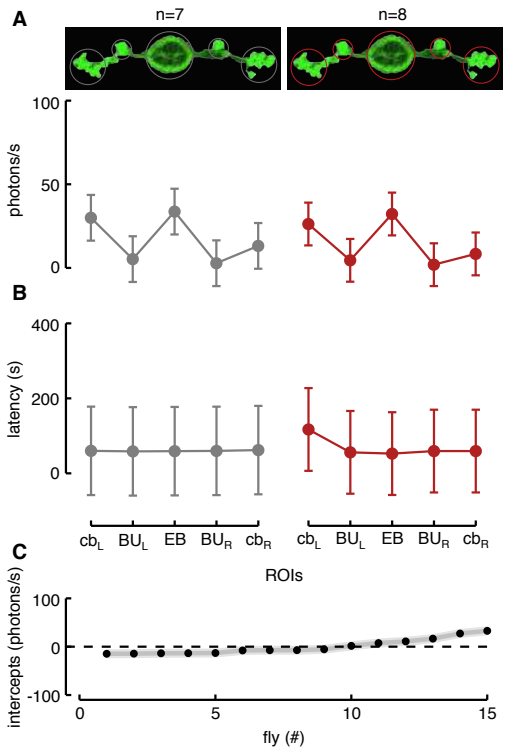

Fig. 2.23. Knockdown of Dop1R1 in R2>G5A flies. *A*: estimated parameters of the Ca^{2+}-response referred to the interaction between condition and ROI with corresponding confidence intervals. On the left is represented the Ca^{2+}-response to nicotine alone in the five ROIs of the R2 neurons with knockdown of Dop1R1 while on the right is represented their Ca^{2+}-response to nicotine after the dopamine application. *B*: estimated parameters of the response latency referred to the interaction between condition and ROI. On the left is represented the latency response to nicotine alone in the five ROIs of the R2 neurons with knockdown of Dop1R1 while on the right is represented their latency response to nicotine after the dopamine application. *C*: plot of random effect referred to Ca^{2+}-response.

Opposite modulation operated by Dop1R1 and Dop1R2 in E-PG neurons

The same approach was used to clarify the neural response of the E-PG neurons. As marked by the putative Dop1R2 expressed by the E-PG neurons and according to previous electrophysiological data recorded in other neurons of the CX, the most probable Ca^{2+}-response of E-PG neurons to the dopamine modulation should have been downward rather than upward (Pimentel et al., 2016). Surprisingly, my results showed an enhancement of the Ca^{2+}-response after the dopamine application. Thus, to better understand which were the dopamine receptors involved in it, I knocked down the Dop1R2 with RNAi (E-

PG>G5A+Dop1R2^{RNAi}). The downregulation of the Dop1R2 within the E-PG determined an increase of the Ca^{2+}-response to nicotine similar to the one provoked in normal flies by the dopamine modulation. The best model confirmed the interaction between condition and ROIs, meaning that the reduction of the Dop1R2 took the E-PG neurons to a higher level of excitability within the EB. This data seem to indicate that the Dop1R2 are inhibitory receptors acting to maintain the EB activity downward. Nevertheless, dopamine application before nicotine determined a reduction of the Ca^{2+}-response in E-PG>G5A+Dop1R2^{RNAi} flies compared to the nicotine application alone (BF $\approx 1.41 \times 10^{15}$) as shown by the best model (Fig. 2.24A, C). Moreover, the response latency to nicotine showed a reduction when dopamine was previously released (Fig. 2.24B). Noteworthy, this overall response reduction was fundamentally due to its brief duration which was actually characterized by a higher peak (Fig. 2.24D). Put simply, the dopamine application in E-PG>G5A+Dop1R2^{RNAi} flies appeared to make greater but very localized in time the nicotine-evoked response. These results are not easily interpretable but they seem to point out that other parallel actors were responsible for the complex response due to the dopamine modulation. The indirect dopamine increase in R2 neurons might be one of them. Specifically, by increasing GABAergic tone of the R2 neurons might result in overall inhibition of the E-PG neurons. Alternatively, another subtype of dopamine receptors such as the Dop1R1 might be expressed in the E-PG neurons. To test whether and how this receptor were involved in the dopamine modulation of the E-PG neurons, I performed the same experiments knocking down it (E-PG>G5A+Dop1R1^{RNAi}). The results showed that the dopamine application strongly decreases (BF $\approx 1.15 \times 10^{32}$) the Ca^{2+}-response to nicotine in E-PG>G5A+Dop1R1^{RNAi} (Fig. 2.24E, G). Importantly, an increase in the response latency was also evident with dopamine application (Fig. 2.24F). Overall these data converge towards a small, short and delayed nicotine-evoked response when dopamine was previously applied in E-PG>G5A+Dop1R1^{RNAi} flies (Fig. 2.24H). Hence, it is likely that in these flies an unbalance towards the Dop1R2 expressed by the E-PG neurons were the cause of their response to the dopamine application.

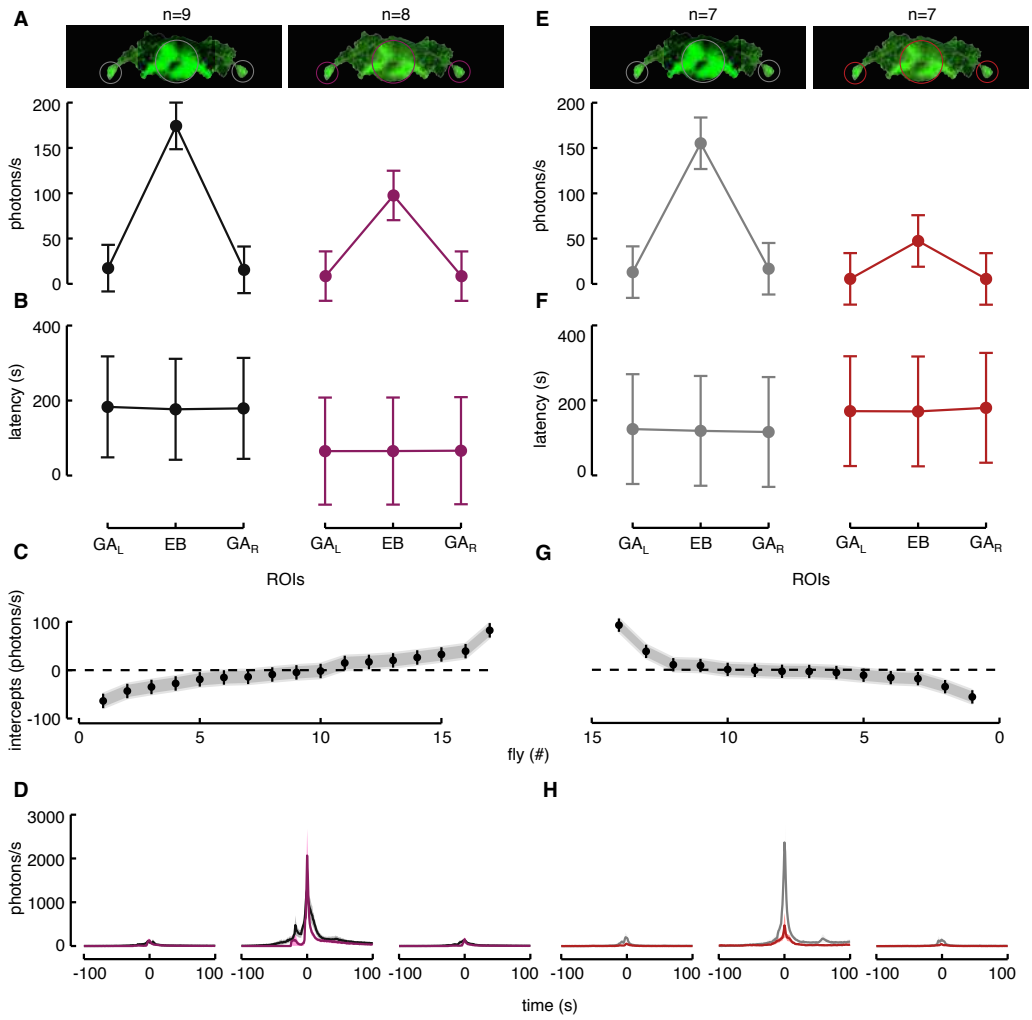

Fig. 2.24. Knockdown of Dop1R2 and Dop1R1 in E-PG>G5A flies. *A*: estimated parameters of the Ca^{2+}-response referred to the interaction between condition and ROI. On the left is represented the Ca^{2+}-response to nicotine alone in the three ROIs of the E-PG neurons with knockdown of Dop1R2 while on the right is represented their Ca^{2+}-response to nicotine after the dopamine application. *B*: estimated parameters of the response latency referred to the interaction between condition and ROI. On the left is represented the latency response to nicotine alone in the three ROIs of the E-PG neurons with knockdown of Dop1R2 while on the right is represented their latency response to nicotine after the dopamine application. *C*: plot of random effect referred to Ca^{2+}-response of E-PG neurons with Dop1R2 downregulation. *D*: Ca^{2+}-response profiles to nicotine of the E-PG neurons with Dop1R2 knockdown in the three ROIs: GA region on the left, EB and GA region on the right. *E*: estimated parameters of the Ca^{2+}-response in E-PG neurons with knockdown of Dop1R1 referred to the interaction between condition and ROI. On the left the condition with nicotine alone while on the right the condition with dopamine application before nicotine. *F*: estimated parameters of the response latency in E-PG neurons with knockdown of Dop1R1 referred to the interaction between condition and ROI. On the left the condition with nicotine alone while on the right the condition with dopamine application before nicotine. *G*: plot of random effect referred to Ca^{2+}-response of E-PG neurons with Dop1R2 downregulation. *H*: Ca^{2+}-response profiles to nicotine of the E-PG neurons with Dop1R1 knockdown in the three ROIs defined as in *G*.

2.4.4 Discussion

The dopaminergic PPM3 neurons innervate the EB and they have been compared to the mammalian pars compacta nucleus of the *substantia nigra* (Strausfeld & Hirth, 2013b). Kong and collaborators (2010) showed that the PPM3 stimulation increased locomotor activity levels and that the Dop1R1 receptors in the R2 neurons are essential for the ethanol-induced hyperactivity. Reduction of Dop1R1 in R2 resulted in reduced ethanol-induced hyperactivity. This resembles the vertebrate direct pathway where the D1 receptors work increasing the response of the striatal projection neurons. My data show for the first time a similar mechanism from a neurophysiological standpoint showing that the dopamine release on the R2 neurons modulates their response increasing the Ca^{2+}-activity via Dop1R1. On the contrary, a homolog indirect pathway in flies has never been suggested. Although Draper and collaborators (2007) showed that D2R plays a critical role in modulating locomotion and that reduction in this receptor decreased locomotor activity, no specific neuroanatomical structure was identified as the core of that behaviour. Administration of the synthetic agonist bromocriptine, a well-established human anti-Parkinson drug, was also able to restore the deficit determined by the D2R knockdown (Draper et al., 2007). Strikingly, I identified a similar D2-based modulatory pathway involving the R5 neurons. My data suggest that dopamine release on the R5 neurons would act by inhibiting their activity very likely via D2R.

I do not exclude that the flow of information between R2 and R5 can be bi-directional. Indeed, supposing that the R5 neurons are GABAergic as well (Kahsai & Winther, 2011; Kahsai et al., 2012; Zhang et al., 2013), a subset of the R2 neurons targeted by R20D01 might be the postsynaptic input of the R5 neurons. The expression pattern of the R76C05 line, which has the GAL4 promoter corresponding to the $GABA_B$ receptor subtype 3, is consistent with this idea. Probably, a subset of R5 neurons might release presynaptically a different neurotransmitter. For instance, Zhang and colleagues (2013) have found that approximately 2/3 of the neurons targeted by the c819 driver line, which has a pattern highly compatible with the R5 neurons, are GABAergic. By using the

same line, Kottler and coworkers (2017) have basically found the same result (i.e., 73% of them). However, other authors have demonstrated that this line would express the Choline acetyltransferase enzyme, meaning that these neurons are presumably cholinergic (Martín-Peña et al., 2014). In other words not all R5 neurons would be GABAergic (the majority anyway) but some of them might be cholinergic (likely a small group). Likewise the R2, I cannot rule out that the R5 neurons might be also excited by acetylcholine, in fact the R58E03 line shows an overlapped pattern with the R5 and its promoter sequence is compatible with that one of the *acetylcholinesterase* gene. In addition the VT004971 line with the promoter taken from nAChRα6 has an extremely akin pattern to the R5 neurons. Therefore, it is very likely that R2 and R5 neurons might share cholinergic excitatory inputs but diverge concerning the dopamine modulation. The multiple inputs to the R-neurons, such as dopamine, acetylcholine, GABA and other neurotransmitters, is in line with the fundamental function of the EB which is an integrative structure deployed to process information for the selection of action.

The E-PG neurons have shown to be modulated by dopamine which acts on two different subtype of dopamine 1-like receptors, the Dop1R1 and the Dop1R2. Although an indirect dopamine modulation of the E-PG neurons remains a possible confounding effect of my data, they suggest that the Dop1R1, which were likely expressed by E-PG>G5A+Dop1R2^{RNAi} flies, would work by increasing a brief and focused response in the E-PG neurons. While the Dop1R2, which were likely expressed by E-PG>G5A+Dop1R1^{RNAi} flies, would work by decreasing the overall response in the E-PG neurons. A dopamine modulation of E-PG neurons via Dop1R1 has been also demonstrated in behavioural experiments (Kottler et al., 2019). Interestingly, a structural connectivity between E-PG and R2 neurons has been recently shown with the GRASP and *trans*-Tango techniques (Kottler et al., 2019; Omoto et al., 2018). Nevertheless, a real functional connectivity has not been directly demonstrated yet. The R2 neurons might inhibit the E-PG neurons via $GABA_A$ receptor as highlighted by the R70F05 line which has the promoter corresponding to the enhancer of the *Rdl* and seems to target the E-PG neurons. In this sense, the R2 neurons after being activated by the visual system via nAChR would globally inhibit the E-PG neurons maybe to improve the signal-to-noise

ratio (Green & Maimon, 2018; Kim et al., 2017b). In parallel, the E-PG neurons would combine the visual information with the proprioceptive one arriving onto the PB and in turn sent to EB through the P-EN neurons which update the fly's heading. The most plausible candidates for providing proprioceptive information to the PB are the likely the cholinergic $PB_{G1/2\text{-}9}$.b-SPSi.s neurons which excite the P-EN1, the $PB_{G2\text{-}9}$.s-FB*l*3.b-NO_2D.b and $PB_{G2\text{-}9}$.s-FB*l*1.b-NO_3PM.b neurons (Franconville et al., 2018). Similarly, the P-EG neurons, which might receive motor efference copies or proprioceptive inputs in the PB from other neurons, inhibit the E-PG neurons by passing through a class of GABAergic interneurons defined GB-Eo which receive inputs in the GA region and send outputs in the EB (Franconville et al., 2018). In this regard, the VT004984 line which likely expresses the nAChRα6 subunit, seems to be a class of this interneurons innervating the GA region and a congruent pattern to that one of the P-EN within the EB. An important bottleneck of this complex circuit is represented by the PB18.s-Gx.Δ7Gy.b (briefly called Δ7) interneurons which receive inputs and relay them within the PB (Wolff et al., 2015). These neurons which are likely GABAergic or glutamatergic, receive activating inputs form the E-PG neurons and their activation leads to complex responses in many columnar neurons types: inhibiting the E-PG and the $PB_{G2\text{-}9}$.s-FB*l*3.b-NO_2V.b neurons, mildly activating the P-EN neurons and strongly provoking a rebound excitation of the $PB_{G2\text{-}9}$.s-FB*l*1.b-NO_3P.b neurons (Franconville et al., 2018). The Δ7 neurons have been proposed as the candidates to implement a lateral inhibition model at the basis of the single persistent bump of activity within the E-PG neurons because of their anatomical arrangement sending output in three glomeruli (each one offset by four glomeruli) and receiving inputs from all the others (Green & Maimon, 2018).

Although it is difficult to discretely localize the locus in which the action selection might be implemented, the structure in which converge the vast majority of different inputs including the ones from the MB (Zhang et al., 2013) and that recursively interact among them, is the EB. I argue that the putative localization of the decision-making process regarding, at least, the action direction should be the EB. Thus, within the EB would take place a recurrent networking at the basis of the integration between visual and proprioceptive

systems resulting in the by-product of attention which, straddling visuomotor information, allows for action selection (Krauzlis et al., 2014).

3 GENERAL DISCUSSION

The overarching question driving my thesis was whether mechanisms of selection for the control of action may be present in invertebrate animals such as *D. melanogaster*. Specifically, are flies able to inhibit unwanted visual information which might impact on the kinematic organization of the action? To answer this question and to clarify the underlying mechanisms I conducted a series of experimental studies which have been presented in the current thesis.

In the first study I revealed how *D. melanogaster* share with humans and non-human primates a behavioural response interpreted in terms of action-based attention (Frighetto et al., 2019). Specifically, flies were able to partially inhibit the reflex response towards the brief appearance of a distracting visual stimulus in order to finalize their action towards a target. As seen in mammals, this response is characterized by trajectory deviations towards a distractor presented closer to the target (Castiello, 1999). Such an effect would represent the consequence of an unconscious motor processing of the visual distractor which compete with the already engaged motor program for target reaching (Tipper et al., 1992). The resulting competition would favour the target through the implementation of an inhibitory mechanism which dampens the distractor from a motorically perspective, though affecting the trajectory. Similar behavioural strategies are evident in humans and non-human primates. This raises a more general question about the evolution of basic behavioural mechanisms, their similarities among evolutionarily distant organisms and how the nervous system evolved from the structural and functional point of view to solve such behavioral issues.

In the second study, I tried to better understand this behaviour by using a condition in which flies need to put in place a stronger inhibition (i.e., extended distractor's exposure time) for finalizing the action towards the target and by

increasing the number of distractor angulations. I showed how flies' responses were much more similar to a passively guided behaviour based on visual motion rather than to an active behaviour based on clear-cut selection between target and distractor. However, via simulation I identified two possibly distinct behaviours underlying the flies' responses. The first characterized by an internal selected heading that flies pursued considering both the visual stimuli displayed (i.e., target and distractor) as background stimuli to be reflexively compensated. While the second behaviour defined by an abrupt trajectory change from the target to the distractor. In this latter behaviour flies started to pursue the distractor on the basis of its motion along the retina. Therefore, I highlighted that the visual motion represents important information for controlling goal-directed actions but also that flies can actively select a specific goal on the basis of which the visual sensory system might be consequently modulated. The modulation of cells localized in primary stages of visual processing due to motorically actions of flies have been already demonstrated (Maimon et al., 2010; Kim et al., 2015; Kim et al., 2017a; Fujiwara et al., 2016; Chiappe et al., 2010), but the source of this kind of information remains unknown.

In the third study, I investigated the role played by a specific neural circuit, part of a suggested putative structure homologous to the mammalian basal ganglia. The recently shown features owned by the E-PG neurons (Turner-Evans & Jayaraman, 2016) prompted me to test whether and how they were involved in the action-interference task. In particular, I tested the idea of a specific dopamine modulation at the basis of the persistent peak of activity within the E-PG neurons serving the core mechanism of selection and maintaining of action. Albeit their marginal role in sketching out the flies' trajectories, I showed that the E-PG neurons seem to be inversely modulated by dopamine via two different subtypes of dopamine 1-like receptor. The Dop1R1 seems to maintain the heading towards a selected goal while the Dop1R2 seems to maintain the network ready to be engaged in a new goal. These results represent the first evidence in favour of different behavioural effects in pursuing a goal-directed action due to dopamine modulation of the CX via two different receptors.

In the fourth study, in order to directly test the dopamine modulation of CX neural circuits I recorded the drug-evoked response of tangential and columnar neurons by means of a Ca^{2+} imaging technique. I found that two different subsets of tangential neurons, the R2 and R5, are modulated by dopamine in the opposite way via two different receptors. The Dop1R1 increases the excitability of the R2 neurons, while the D2R decrease the excitability of the R5 neurons. Additionally, testing the dopamine modulation in E-PG neurons I demonstrated how the Dop1R1 allows a brief increase of the excitability while the Dop1R2 contributes to globally decrease the E-PG drug-evoked response. Together they synergically work for increasing the excitability of the E-PG neurons. These results suggest a common neural mechanism for action selection in vertebrate and invertebrate animals likely based on two dopamine pathways, the direct and the indirect one. To definitely claim that the action selection system in flies is based on two dopamine pathways as seen in mammals deserves further experiments. However, my data are the first experimental indication supporting this idea.

Overall, the experiments I conducted delineate an intriguing *fil rouge* concerning the selection for action process between distant organisms. This process would be subtended by an ancestral neural structure located in the fly central brain sharing the dopamine modulation similarly to what occurs in mammalian basal ganglia.

In the next sections I shall discuss my experiments proposing a new perspective concerning visual attention.

3.2 SELECTIVE VISUAL ATTENTION IN FLIES

Attention-like behaviour has been already studied in *D. melanogaster* (van Swinderen, 2011). By investigating this process treating flies as much as possible as “mini-humans”, a great deal of information has been gained (van Swinderen, 2011). Nevertheless one feature of this important and intriguing cognitive process remains elusive: to date how attention acts as a filter for the selection of motor output has never been properly tested in flies. For instance, flies showed to decrease their optomotor response frequency (of about 38%) to a moving stripe

when a second static stripe was present in the panorama compared to the condition with only one moving stripe (Wolf & Heisenberg, 1980). More recent data have shown that between the conditions with or without the static stripe the frequency and the dynamic of flies' responses were much the same but the spontaneous body saccades' dynamic differed indicating that other parameters besides visual motion influence them (Koenig et al., 2016b). This means that the flies are more attracted by a moving stripe than a static one according to the well-known salient visual feature represented by motion. Moreover, it indicates that flies can represent both visual stimuli with a consequent increased perceptual load and select one of them upon displacement. In accordance to this, the displacement of both stripes attracts flies to one of the two stripes randomly (Heisenberg & Wolf, 1984; Koenig et al., 2016b). Since we do not know whether flies were trying to fixate one of the two stripes before the displacement, little can be said regarding the possible inhibition processes.

The attention-like behaviour shown by flies is not only characterized by the ability to select a specific stimulus from others in space and time. Indeed, flies have shown cueing effect on optomotor competition which facilitates the flies' responses to the cued object (Sareen et al., 2011). This clearly means that flies can represent the visual space and maintain attention on a specific location previously activated. However, in these paradigms the fly does not face any need to inhibit distractions to remain focused on a selected goal.

Van Swinderen and colleagues (2007; 2009) showed that flies could inhibit the salient response to the wide-field optic flow to fixate a static stripe laterally placed in a eight-point choice maze. This likely suggests that flies can suppress a reflex if they are paying attention to a distant object. Notwithstanding, the flies' intentionality or fixation remained poorly determined as pre-condition to test the extent of suppression to distractors shown by flies.

Even though flies have shown to modulate simple reflexes on the basis of learning (Liu et al., 1999; Zhang et al., 2007a; Wolf & Heisenberg, 1991; Wolf & Heisenberg, 1997), the internal motivational states underlying goal-directed action have remained confused in experimentally controlled setting. The expectation that simple nervous system such the one owned by flies can only

respond reflexively to salient stimuli such as a visual stripe has been challenged in this thesis.

3.2.1 Methodological advance

Compared to the previously published data and literature, in this thesis I basically introduced two new fundamental factors which have never been taken into account before. The first factor is related to the abrupt appearance of a static "distractor" object which competed with a "target" for motor output. The second and interrelated factor is referred to the impermeability of an already engaged motor program towards a selected target object. Putting together these two new factors I have been able to address the question of whether a fly focused on an object could be influenced (interfered) by the appearance of a new object. The point was to understand whether selective visual attention was played a role in maintaining the action focused on target and resisting the interference when a visual distractor entered the visual system.

Other authors have already developed and employed paradigms similar to mine to study behavioural processes, such as visual working memory, fixation, mechanisms of orientation and attention (Neuser et al., 2008; Heisenberg & Wolf, 1984; Horn & Wehner, 1975). However, their approaches have been widely engrossed by sensorial perspective regardless the relationship with action. This is chiefly due to the cognitive psychology which has promoted systems separation (Cisek, 2007).

Studying attention-like processes from a purely perceptual point of view was not my aim. Rather, I revealed how selective mechanisms of attention inhibit unwanted information which has the potential to override an engaged motor program towards a selected target. It is within this framework, that I interpreted as an "inhibitory response" the slight detour in the trajectory which engages the fly towards the original target stimulus when the fly is "distracted" by another visual stimulus appearing at 60 deg flanking the original target stimulus. This effect has been consistently reported in both human and non-human primates (Castiello, 1999; Tipper et al., 1998; Sartori et al., 2014). Similarly I found a small

deviation (in favour of the distractor) from the trajectory directed towards the original target.

In a paradigm resembles mine (Neuser et al., 2008), when the fly crossed the centre of arena, the original stripe disappeared and the new stripe appeared laterally at 90 deg with respect to the fly. This new situation determined a re-orientation of the fly towards the new stripe which made a turn of angular distances between 75 and 105 deg. After 1 s the new stripe disappeared and, in a uniformly lit environment, the fly was left free to decide the subsequent path. In this paradigm, wild-type flies usually turn back towards the position of (the now invisible) original stripe, a behaviour consistent with a visual working memory mechanism, or possibly a reflection of the attentional focus being anchored to the original stripe. On the contrary, my paradigm was not designed to study visual working memory or visual attention tout court, but a selection-for-action mechanism (as seen in higher organisms) in which attention serving actions has the ability to inhibit alternative motor programs which may interfere with the one elicited by the original target.

In my paradigm the distractor was presented along with the target so as to elicit competition. This was crucial in order to understand how the system resolves the 'motor' conflict determined by the presence of the distractor.

Recently, Kirszenblat and colleagues (2018), in a study aimed at putting in relation sleep and visual selective attention, have employed a 'Buridan's paradigm' with flickering targets (7 Hz) to elicit fixation in walking flies and with two orthogonally positioned static stripes to distract them. In this paradigm they have shown how in normal, but much more in sleep deprived flies, the presence of the static stripes increases their distractibility (Kirszenblat et al., 2018).

However, this paradigm was different compared to mine. Specifically, neither engagement in the selected motor program for target reaching (i.e., a goal-directed action) nor distraction triggered on the basis of a specific spatial position of the fly, were employed by Kirszenblat and colleagues (2018). These two aspects make this paradigm completely different from the one I developed to test a specific experimental hypothesis. Pragmatically then, Kirszenblat and colleagues (2018) have: i) clipped the flies' wings and this manipulation is known

to have a strong impact on the flies' decision-making process (Gorostiza et al., 2016); ii) differentiated the intrinsic salience of targets and distractors whereas I did not manipulate the intrinsic salience of the stimuli in order to increase the competition between them; iii) presented persistent distractors without performing any kind of abrupt distraction or timing control but simply recorded the 'distractibility' of flies according to a single generic angular index of 'target deviation' throughout the entire video recording. Contrariwise, I abruptly presented flies with a distractor, while precisely recording the timing and position of the flies at the time the distraction occurred.

3.2.1 Innate preferences

Some considerations are in order concerning the use of the type of visual stimuli used in the present body of work. By using a tethered flight simulator, it has been demonstrated that flies are usually attracted towards long vertical bright or dark stripes, as an ethological reflex which guides flies towards elements resembling vegetative perches (Maimon et al., 2008). I described for the first time the free walking behaviour of flies consisting of recurrent orientation inversions (i.e., alternation between fixation and anti-fixation) between two diametrically opposed vertical bright stripes on a dark background. Pioneering studies had shown that recurrent inversion is maximized with vertical black stripes on a bright background (Bülthoff et al., 1982) and had considered the opposite contrast as a repellent configuration for flies (Heisenberg & Wolf, 1979). Notwithstanding these earlier observations, I observed a strong fixation response toward bright stripes in freely walking flies consistent with more recent studies using tethered flying flies (Reiser & Dickinson, 2008; Maimon et al., 2008). I am tempted to exclude that the recurrent direction inversions shown by the flies in our case was due to anti-fixation, because when presented with the distractor stripes flies were attracted to and maintained the distractor in front of them (suggesting fixation). Although the functional distinction between flying and walking paradigms, as well as differences in the experimental protocols, such as wing clipping (McEwen, 1918; Gorostiza et al., 2016), might be at the basis of these

contrasting findings, it is difficult to draw a coherent explanatory picture, and the exact reason for the discrepancies remains as yet unknown. Rather, it is possible that the intensity of the light used may have played a role in determining the discrepancies concerned with anti-fixation behaviour of the flies, since in the case of LED displays (such as those used in the present study) the maximum luminance reachable is 72 cd m^{-2} (cd m^{-2} = lux) (Reiser & Dickinson, 2008), while in the setups used in previous studies the luminance ranged between 300 and 1910 cd m^{-2} (Götz & Wenking, 1973; Bülthoff et al., 1982; Virsik & Reichardt, 1976), which is at least 4 times higher. This suggests that long vertical bars with high light intensities lead to avoidance, while long vertical bars of lower brightness (i.e., around 72 lx) would represent an attracting stimulus, possibly because under these conditions the bar appears similar to the reflectance of natural vegetation posts. This hypothesis seems to be corroborated by a report of Heisenberg and Wolf (1984), in which a grey background makes bright stripes as attractive as black stripes on a white background, while bright stripes on a black background produce anti-fixation behaviour.

3.2.2 Novelty effect

An interesting aspect of the present thesis suggests that the appearance of an abrupt visual stimulus produced a novelty effect in flies. In particular, this was manifested by the re-orienting behaviour of flies immediately following the appearance of the distractors. A similar effect has been reported for tethered flying flies which showed a preference for a previously uncued side of the arena when faced with bilateral stimuli (Shiozaki & Kazama, 2017). In neural terms, it has been suggested that the R-neurons, are involved in determining the slow turning tendency (i.e., body re-orientation) associated with this kind of visual experience. Silencing of those neurons abolishes the innate behaviour for preferential orientation towards novel stimuli (i.e., previously uncued sides) (Shiozaki & Kazama, 2017).

In another study using Ca^{2+} imaging, the authors found that visual responses in R-neurons are suppressed when competing stimuli are present in the

contralateral visual field (Sun et al., 2017). In this respect, contralateral suppression is hypothesized to act as a mechanism for location-based stimulus selection by reducing the responses of ipsilateral stimuli in the presence of a second stimulus. Furthermore, this suppressive effect appears to depend upon short-term stimulus history, specifically, R-neurons baseline activity showed a rebound after contralateral suppression, a phenomenon which could be involved in modulating the flies' subsequent visual responses to both ipsilateral and contralateral stimuli (Sun et al., 2017). Such evidence could partially explain our results, at least in terms of the novelty represented by the distractor.

3.2.3 Inhibitory mechanism

My data are consistent with the 'reactive turning tendency' described by Horn and Wehner (1975), who noted that flies preferred to orient towards a position midway between two vertical stripes placed at an angular distance less than 75 deg. The sudden appearance of the distractor added a 'turning tendency' of the body to the one already engaged. Though, differently from what reported by Horn and Wehner (1975), I observed that the trajectories did not lay exactly midway between the original stimulus and the distractor but they remained closer to the former. At a first glace it seemed to reveal that the original stimulus had acquired the status of a stronger landmark.

Subsequent data drew a slightly different picture in which the majority of flies engaged in a new motor program directed toward the distractors, while the minority of them remained closer to the target. The trajectories were not straight paths directly pointing towards one of the stimuli but they were delineated by an optomotor response based on one or both stimuli. Especially for distractors at 60 deg, these two types of trajectories were clearly linked with two types of early body saccades performed within the 250 ms after the distractor onset. In the first case flies responded to the abrupt distractor making a body saccade towards it and then increasingly reducing the angular error with respect of it. In the second case, they responded with the same body saccade but followed by one in the opposite direction and then maintaining the initial angular error with respect of

distractor. The maintaining of the error means that flies kept the same angulation referred to distractor throughout the path. Flies could decide to reach a new attracting object or to maintain an internal goal inhibiting the response towards that attracting object.

Therefore, the sign of inhibition was not only readable on the trajectories but also on the early saccadic responses. The trajectories were mostly the result of a visual motion based motor balance on which would act a decision-making process.

Such selection process would occur within the EB, and the manipulations of the E-PG neurons I have done corroborate this idea (Fiore et al., 2015; Fiore et al., 2017). The observation that the E-PG neurons show a persistent peak of activity maintaining the heading information even when the animal is in total darkness suggests the representation of an internal goal (Seelig & Jayaraman, 2015; Green et al., 2019). The activity of such neurons remains linked to the position of a single vertical stripe even in the presence of a second identical stripe and it does not always shift instantaneously following the abrupt displacement of a single visual target (Seelig & Jayaraman, 2015). It is remindful of an attentional focus but even more of an internal representation of a goal in space to select and accomplish an action directed to it. Thus, a well-established motor program towards a visual target might be more or less 'impermeable' to possible perturbations determined by appearance of other visual distractors depending on the strength of the activity peak and the inhibition of all the rest.

The fact that clearer effect of bimodal responses was evident with distractors at 60 deg might be due to the width of the peak of activity among the E-PG neurons ranging between 60 and 120 deg in tethered walking flies (Seelig & Jayaraman, 2015) and between 60 and 90 deg in tethered flying flies (Kim et al., 2017b). Maybe the no overlapping of the wedges possibly activated by angularly corresponding visual stimuli might generate the dichotomy in flies' heading choice. Two stripes spaced 60 deg might activate two different peaks of 120 deg width eliciting flies to select one of the two.

3.3 NEURAL BASES OF SELECTION FOR ACTION

The results of this thesis provide some insights regarding the modality used by attention to filter out stimuli and perform action selection. It has been proposed that selection mechanisms in vertebrates rely on the basal ganglia (Redgrave et al., 1999). In humans this neural structure plays an important role in the subconscious planning, execution and inhibition of motor programs (Castiello et al., 2000b). Interestingly, patients with Parkinson's disease show an increase of the interference effect when distracting objects evoke motor program that differ from the one elicited by the target (Castiello et al., 2000b; Castiello et al., 2000a). Instead, they do not show abnormal kinematics in visual perturbed movement suggesting a selective disruption of the open-loop (i.e., predictive motor control) but not of the closed-loop (i.e., visual feedback control) (Scarpa & Castiello, 1994). Thus, these patients are more reliant on visual feedback during movement control and they are unable to maintain a correct arm position when visual information is not provided (Cooke et al., 1978).

CX and basal ganglia, which appear to be linked from an evolutionary point of view (Strausfeld & Hirth, 2013b; Strausfeld & Hirth, 2013a), may also share common functional properties involved in the regulation of predictive motor control. The closed-loop behaviour for visuomotor control would rely on the optomotor balance circuits while the open-loop behaviour for goal-directed actions would rely on central circuits such as those of the EB.

Visuomotor process requires often the organism to act at very short notice for survival needs. Hence, an efficient computation and integration between visual and motor systems assure the organism to interact appropriately with its ecosystem. However, the idea behind the selection for action process as an unidirectional information flow requiring autonomous sensory encoding of the external environment performed before to implement an action does not seem so neat (Cisek, 2007). Knowing what is the object with which to interact before the specification of the motor program to act upon it, entails the separation of the concepts of perceptual, cognitive and motor systems. Nevertheless, this perspective is not appropriate for linking the neural level with the behavioural

one. The encoding of a visual environment might involve not only information about the identity of relevant objects but also information related to parameters of the possible actions that can be performed (Castiello, 1999; Castiello, 1996). The data I presented in this thesis agree with the idea that invertebrate animals such as *D. melanogaster* can select a target but distracting visual stimuli are taken into account from a motor point of view. It means that a target is not attained through a segregated visual sensory inhibition of unrelated stimuli but through an interface matching the motor system.

3.1.1 Spatial visual selection

In foveate animals the oculomotor system has evolved to allow the construction of an accurate visual representation through the selection of visual parameters characterizing objects concurrently with the specification of oculomotor commands necessary to fixate those objects (Awh et al., 2006). Abundant evidences have linked selective attention and oculomotor programming suggesting a common neural substrate (Moore & Zirnsak, 2017; Jonikaitis & Moore, 2019).

Spatial visual attention is a topic widely studied in humans and it is considered as a system that depends on a network of several anatomical areas (Petersen & Posner, 2012). On account that no verbal reports can be detected in non-human primates but only overt actions in response to stimuli, the studies regarding attention in these animals are by default involving the motor system. Nevertheless, built on clever experimental paradigms, cognitive processes for spatial visual selection and their underlying neural basis, analogous to those evidenced in humans, have also been shown in non-human primates (Desimone & Duncan, 1995; Reynolds & Chelazzi, 2004). Selective attention has been typically studied in terms of an orienting process mainly focused on spatial visual selection (Posner, 1980), less effort has been put in the comprehension of the kind of representations attention access to (Tipper, 1985).

Generally, the selection issue has been viewed as pure perceptual process whereby the visual information has to be progressively filtered out to convey the

appropriate parameterization to the motor system. Because attention can be either overtly or covertly oriented within the visual field, focusing on a specific location, it has been argued its independence from the motor system (Posner, 1980). Nevertheless, some authors have proposed a strict link between covert orienting attention and programming of saccadic eye movement, conceptualizing an hypothesis called "premotor theory of attention" (Rizzolatti et al., 1987). That is, attention would be shifted to a specific location when the saccadic eye movement program to fixate that location is ready to be executed (Awh et al., 2006). In other words, attention would be a by-product of oculomotor programming. Several electrophysiological data in monkeys have shown that the frontal eye field (FEF) and the superior colliculus (SC), two well-known regions involved in oculomotor programming, play a causal role in shifting spatial attention covertly, that is without an overt eye or body movement. For instance, microstimulation released onto a specific receptive field of FEF increases the sensitivity to changes in luminance of a spatially overlapping target (Moore & Fallah, 2004). Suprathreshold stimulations of FEF evoke overt saccades towards a specific spatial location, while subthreshold stimulations facilitate the covert selection of visual targets for subsequent saccades. Analogous results in enhancement of covert spatial attention have been found with subthreshold stimulation of the SC (Cavanaugh & Wurtz, 2004; Müller et al., 2005). Neuroimaging studies in humans have also corroborated such hypothesis founding strong overlap in the areas activated by covert spatial attention and saccadic eye movements such as FEF and intraparietal sulcus (Corbetta & Shulman, 2002). Thus, it may reasonably be supposed that the attentional mechanism relies on a unified circuit for retinotopic map and motor information, which are interrelated to carry out a goal-directed selection. Intriguingly, a subcortical neuronal circuit forms a loop involving intralaminar nuclei of thalamus and *substantia nigra* pars reticulata through caudate and putamen (Krauzlis et al., 2013). This circuit appears to play a specific role in processing salient events through the inputs to the intralaminar nuclei coming form the intermediate and deeper layers of the SC (Smith et al., 2004). Moreover, direct connections between these latter parts of the SC and the pars compacta of the

substantia nigra have been also demonstrated (McHaffie et al., 2005). A phylogenetically older subcortical closed-loop circuit than the cortico-basal ganglia, the SC-basal ganglia, might act independently, cooperatively or competitively to represent the location of relevant objects in space for subsequent selection and reinforcement learning within the basal ganglia (Redgrave et al., 2010b; Krauzlis et al., 2013). It is not surprising that, in order to sort out the affordances, attentional mechanism may coincide with the decision-making process (i.e., action selection) aimed at defining the parameterization of the action (i.e., action speciation) directed towards a specific item in the space (Cisek, 2007; Krauzlis et al., 2014).

3.1.2 Object visual selection

Compared to the spatial visual attention, the feature- or object-based attention, which is accomplished by relying on the features of an object, has been less studied (Noudoost et al., 2010). Classically, such attentional mechanism have been considered as a top-down process which highlights broadly across the visual field the components related to a specific feature (Maunsell & Treue, 2006). This mechanism favours the detection of a searched-for target matching the "attentional templates" retained in working memory in order to guide the visual selection (Desimone & Duncan, 1995). The extension of the contextual influences coming from the interaction activity between neurons responding to small portions of the visual field and those responding to larger regions, leads neurons of the visual cortex to a dependency from the global contours as well as from locally features' attributes (Gilbert & Li, 2013). For these reasons, the features of an object can be defined in the same way as configuration of non-spatial information or perceptions of an object as a whole (Olson, 2001). Through the use of training protocols combined with extracellular electrophysiological recordings, object-based attention has been foremost underpinned by a network of cortical areas not involving subcortical regions (Maunsell & Treue, 2006; Olson, 2001; Zhou & Desimone, 2011). However, the precise localisation of neural substrate for such attentional templates (i.e., representation of features), which enhance the

representation of stimuli resembling the target, is still ongoing. A compelling multi-unit recording study has provided evidence for the existence of a feature-based template for guiding visual search within the monkeys' ventral prearcuate (VPA) region of prefrontal cortex (Bichot et al., 2015). In this region, rather than visual cortical areas, might dwell the source of object-based attention necessary to generate priority maps in FEF. Strikingly, following deactivation of the VPA, by using muscimol (selective agonist for $GABA_A$ receptors) compound injections, the behavioural performance decreased drastically to find a contralateral target (i.e., increase in number of saccades) and the FEF units' activity for feature selection was completely abolished (Bichot et al., 2015). Thus, VPA region, which likely corresponds to 45A and 46v of cytoarchitectonic areas, would be fundamental for feature-based search behaviour (Moore & Zirnsak, 2017). Moreover, VPA would be homolog of the humans' inferior frontal junction which has been shown to direct the flow of visual processing during object-based attention synchronizing gamma oscillations with areas in the inferior temporal cortex (Baldauf & Desimone, 2014; Bichot et al., 2015). The emerging picture as regards visual selection of object with specific features appears extremely intriguing because the underlying neural mechanism seems to be independent from the engaging of pure visual areas. In particular, the FEF, known to be involved in eye movement, such as saccade and pursuit eye movements, has demonstrated to enhance and synchronize the V4 neurons in the extrastriate area, which are also positively modulated when covert spatial attention is retinotopically directed to the their receptive fields or when the latter are targets for saccades (Gregoriou et al., 2009; Moore & Armstrong, 2003). Similarly, in a visual search task the FEF showed an earlier onset of the object-based selection than V4 (Zhou & Desimone, 2011). Therefore, the flow of information in object-based attention seems to proceed from the prefrontal cortex, where the features are maintained during visual working memory, to the occipital and temporal areas via FEF. The same pathway is overlaid by the spatial visual attention. Indeed, FEF is one target of the ascending inputs to cortex from the SC passing through the mediodorsal thalamic nucleus (Krauzlis et al., 2013). What is the final aim of the selective attention other than to foveate target? It should not be

strange that different types of attentions share ultimately a common evolutive need: select an object to act upon it. The expansion of neocortex has allowed the number of features and meanings of stimuli to increase far beyond the capacity of retinotopically representation of visual space. However, these information, at the moment of action or perceptual selection, rely on the central components of an evolutionarily ancient selection mechanism based on SC-basal ganglia circuit (Krauzlis et al., 2013). This circuit is likely present in flies within the CX and it could tell us fundamental information about the mechanisms for guiding goal-directed behaviours.

3.1.2 Final remarks

Though the visual attention has lately begun to receive consideration in flies' neuroscience (Sareen et al., 2011; Koenig et al., 2016b; van Swinderen, 2011; de Bivort & van Swinderen, 2016), in the current thesis it has been studied with respect to a specific frame of reference. In other words, attention has been considered as a selection mechanism acting at the level of the integration between visual and motor systems.

Moreover, visual attention might be nothing more than an emerging result of the motor programming aimed at reaching a visual target (Rizzolatti et al., 1987). In so doing, visual attention can be affected by a newly attracting visual stimulus which compete for alternative motor program.

This theoretical framework is consistent with a recent idea proposed by Krauzlis and collaborators (2014), according to which the attention is an effect and not a cause of the value-based decision making carried out by the mammalian basal ganglia. Non-mammals such as birds, reptiles, amphibians and fish, which lack a neocortex, show evidence for selective attention (Krauzlis et al., 2018). This is why also invertebrate animals without the cortex such as *D. melanogaster* would exhibit behavioural and neurophysiological signs of attention (van Swinderen, 2011; de Bivort & van Swinderen, 2016).

Here, I put forward the idea of a common neural substrate in flies for attention and action selection which would correspond to an ensemble of neural circuits localized in the CX with a fundamental core represented by the E-PG neurons.

Future experiments employing the simultaneous combination of behavioural and physiological recordings in a unified setup might be extremely useful to elucidate the neural mechanism involved in the selection for action process (Seelig et al., 2010). Functional brain imaging in freely walking flies might be also a complementary tool for investigations in a much more ecological condition (Grover et al., 2016). Finally, the development of immersive virtual reality environment for the precise manipulation of sensorimotor feedback loops in unrestrained animals might be a promising setup for studying the relationship between attention and action selection (Stowers et al., 2017).

BIBLIOGRAPHY

Ache, J. M., Polsky, J., Alghailani, S., Parekh, R., Breads, P., Peek, M. Y., Bock, D. D., von Reyn, C. R. & Card, G. M. (2019). Neural Basis for Looming Size and Velocity Encoding in the Drosophila Giant Fiber Escape Pathway. *Curr. Biol.* **29**, 1073-1081.e4.

Agi, E., Langen, M., Altschuler, S. J., Wu, L. F., Zimmermann, T. & Hiesinger, P. R. (2014). The evolution and development of neural superposition. *J. Neurogenet.* **28**, 216–232.

Allport, D. A. (1987). Selection for Action: Some Behavioral and Neurophysiological Considerations of Attention and Action. In *Perspectives on Perception and Action* (ed. Heuer, H.) and Sanders, H. F.), pp. 395–419. Mahwah, NJ, USA: Lawerence Erlbaum.

Aptekar, J. W., Shoemaker, P. A. & Frye, M. A. (2012). Figure tracking by flies is supported by parallel visual streams. *Curr. Biol. CB* **22**, 482–487.

Aso, Y., Hattori, D., Yu, Y., Johnston, R. M., Iyer, N. A., Ngo, T.-T. B., Dionne, H., Abbott, L. F., Axel, R., Tanimoto, H., et al. (2014a). The neuronal architecture of the mushroom body provides a logic for associative learning. *eLife* **3**, e04577.

Aso, Y., Sitaraman, D., Ichinose, T., Kaun, K. R., Vogt, K., Belliart-Guérin, G., Plaçais, P.-Y., Robie, A. A., Yamagata, N., Schnaitmann, C., et al. (2014b). Mushroom body output neurons encode valence and guide memory-based action selection in Drosophila. *eLife* **3**, e04580.

Awh, E., Armstrong, K. M. & Moore, T. (2006). Visual and oculomotor selection: links, causes and implications for spatial attention. *Trends Cogn. Sci.* **10**, 124–130.

Azim, E. & Alstermark, B. (2015). Skilled forelimb movements and internal copy motor circuits. *Curr. Opin. Neurobiol.* **33**, 16–24.

Baek, M. & Mann, R. S. (2009). Lineage and birth date specify motor neuron targeting and dendritic architecture in adult Drosophila. *J. Neurosci. Off. J.*

Soc. Neurosci. **29**, 6904–6916.

Bahl, A., Ammer, G., Schilling, T. & Borst, A. (2013). Object tracking in motion-blind flies. *Nat. Neurosci.* **16**, 730–738.

Bahl, A., Serbe, E., Meier, M., Ammer, G. & Borst, A. (2015). Neural Mechanisms for Drosophila Contrast Vision. *Neuron* **88**, 1240–1252.

Bakdash, J. Z. & Marusich, L. R. (2017). Repeated Measures Correlation. *Front. Psychol.* **8**,.

Baldauf, D. & Desimone, R. (2014). Neural mechanisms of object-based attention. *Science* **344**, 424–427.

Bargiello, T. A., Jackson, F. R. & Young, M. W. (1984). Restoration of circadian behavioural rhythms by gene transfer in Drosophila. *Nature* **312**, 752–754.

Barton, K. (2019). *Mu-MIn: Multi-model inference*. R package version 1.43-6.

Bates, D., Mächler, M., Bolker, B. & Walker, S. (2014). Fitting Linear Mixed-Effects Models using lme4. *ArXiv14065823 Stat*.

Baubet, V., Le Mouellic, H., Campbell, A. K., Lucas-Meunier, E., Fossier, P. & Brúlet, P. (2000). Chimeric green fluorescent protein-aequorin as bioluminescent Ca2+ reporters at the single-cell level. *Proc. Natl. Acad. Sci. U. S. A.* **97**, 7260–7265.

Bausenwein, B., Dittrich, A. P. & Fischbach, K. F. (1992). The optic lobe of Drosophila melanogaster. II. Sorting of retinotopic pathways in the medulla. *Cell Tissue Res.* **267**, 17–28.

Behnia, R. & Desplan, C. (2015). Visual circuits in flies: beginning to see the whole picture. *Curr. Opin. Neurobiol.* **34**, 125–132.

Bellen, H. J., Tong, C. & Tsuda, H. (2010). 100 years of Drosophila research and its impact on vertebrate neuroscience: a history lesson for the future. *Nat. Rev. Neurosci.* **11**, 514–522.

Bender, J. A. & Dickinson, M. H. (2006). Visual stimulation of saccades in magnetically tethered Drosophila. *J. Exp. Biol.* **209**, 3170–3182.

Benzer, S. (1967). Behavioral mutants of drosophila isolated by countercurrent distribution. *Proc. Natl. Acad. Sci. U. S. A.* **58**, 1112–1119.

Bichot, N. P., Heard, M. T., DeGennaro, E. M. & Desimone, R. (2015). A Source for Feature-Based Attention in the Prefrontal Cortex. *Neuron* **88**, 832–

844.

Bidaye, S. S., Machacek, C., Wu, Y. & Dickson, B. J. (2014). Neuronal control of Drosophila walking direction. *Science* **344**, 97–101.

Bidaye, S. S., Bockemühl, T. & Büschges, A. (2018). Six-legged walking in insects: how CPGs, peripheral feedback, and descending signals generate coordinated and adaptive motor rhythms. *J. Neurophysiol.* **119**, 459–475.

Blondeau, J. & Heisenberg, M. (1982). The three-dimensional optomotor torque system of Drosophila melanogaster. *J. Comp. Physiol.* **145**, 321–329.

Boeddeker, N. & Egelhaaf, M. (2005). A single control system for smooth and saccade-like pursuit in blowflies. *J. Exp. Biol.* **208**, 1563–1572.

Bonfiglioli, C. & Castiello, U. (1998). Dissociation of covert and overt spatial attention during prehension movements: selective interference effects. *Percept. Psychophys.* **60**, 1426–1440.

Bonini, N. M. & Fortini, M. E. (2003). Human neurodegenerative disease modeling using Drosophila. *Annu. Rev. Neurosci.* **26**, 627–656.

Borst, A. (2009). Drosophila's view on insect vision. *Curr. Biol. CB* **19**, R36-47.

Borst, A. (2014). Fly visual course control: behaviour, algorithms and circuits. *Nat. Rev. Neurosci.* **15**, 590–599.

Borst, A., Haag, J. & Reiff, D. F. (2010). Fly motion vision. *Annu. Rev. Neurosci.* **33**, 49–70.

Boyden, E. S., Zhang, F., Bamberg, E., Nagel, G. & Deisseroth, K. (2005). Millisecond-timescale, genetically targeted optical control of neural activity. *Nat. Neurosci.* **8**, 1263–1268.

Brand, A. (1995). GFP in Drosophila. *Trends Genet. TIG* **11**, 324–325.

Brand, A. H. & Perrimon, N. (1993). Targeted gene expression as a means of altering cell fates and generating dominant phenotypes. *Dev. Camb. Engl.* **118**, 401–415.

Branson, K., Robie, A. A., Bender, J., Perona, P. & Dickinson, M. H. (2009). High-throughput ethomics in large groups of Drosophila. *Nat. Methods* **6**, 451–457.

Brooks, J. X. & Cullen, K. E. (2013). The primate cerebellum selectively encodes unexpected self-motion. *Curr. Biol. CB* **23**, 947–955.

Bulgheroni, M., Camperio-Ciani, A., Straulino, E., Sartori, L., D'Amico, E. & Castiello, U. (2017). Selective reaching in macaques: evidence for action-centred attention. *Anim. Cogn.* **20**, 359–366.

Bülthoff, H., Götz, K. G. & Herre, M. (1982). Recurrent inversion of visual orientation in the walking fly, Drosophila melanogaster. *J. Comp. Physiol.* **148**, 471–481.

Busch, C., Borst, A. & Mauss, A. S. (2018). Bi-directional Control of Walking Behavior by Horizontal Optic Flow Sensors. *Curr. Biol. CB* **28**, 4037-4045.e5.

Buschbeck, E. K. & Strausfeld, N. J. (1996). Visual motion-detection circuits in flies: small-field retinotopic elements responding to motion are evolutionarily conserved across taxa. *J. Neurosci. Off. J. Soc. Neurosci.* **16**, 4563–4578.

Büttner, U. & Kremmyda, O. (2007). Smooth pursuit eye movements and optokinetic nystagmus. *Dev. Ophthalmol.* **40**, 76–89.

Cande, J., Namiki, S., Qiu, J., Korff, W., Card, G. M., Shaevitz, J. W., Stern, D. L. & Berman, G. J. (2018). Optogenetic dissection of descending behavioral control in Drosophila. *eLife* **7**,.

Card, G. M. (2012). Escape behaviors in insects. *Curr. Opin. Neurobiol.* **22**, 180–186.

Card, G. & Dickinson, M. H. (2008). Visually mediated motor planning in the escape response of Drosophila. *Curr. Biol. CB* **18**, 1300–1307.

Carpenter, F. W. (1905). The Reactions of the Pomace Fly (Drosophila ampelophila Loew) to Light, Gravity, and Mechanical Stimulation. *Am. Nat.* **39**, 157–171.

Castiello, U. (1996). Grasping a fruit: selection for action. *J. Exp. Psychol. Hum. Percept. Perform.* **22**, 582–603.

Castiello, U. (1998). Attentional coding for three-dimensional objects and two-dimensional shapes. Differential interference effects. *Exp. Brain Res.* **123**, 289–297.

Castiello, U. (1999). Mechanisms of selection for the control of hand action. *Trends Cogn. Sci.* **3**, 264–271.

Castiello, U. (2001). The effects of abrupt onset of 2-D and 3-D distractors on prehension movements. *Percept. Psychophys.* **63**, 1014–1025.

Castiello, U. & Dadda, M. (2019). A review and consideration on the kinematics of reach-to-grasp movements in macaque monkeys. *J. Neurophysiol.* **121**, 188–204.

Castiello, U. & Umiltà, C. (1990). Size of the attentional focus and efficiency of processing. *Acta Psychol. (Amst.)* **73**, 195–209.

Castiello, U. & Umiltà, C. (1992). Splitting focal attention. *J. Exp. Psychol. Hum. Percept. Perform.* **18**, 837–848.

Castiello, U., Bennett, K. M., Bonfiglioli, C. & Peppard, R. F. (2000a). The reach-to-grasp movement in Parkinson's disease before and after dopaminergic medication. *Neuropsychologia* **38**, 46–59.

Castiello, U., Bonfiglioli, C. & Peppard, R. F. (2000b). Dopaminergic effects on the implicit processing of distractor objects in Parkinson's disease. *Exp. Brain Res.* **135**, 251–258.

Cavanaugh, J. & Wurtz, R. H. (2004). Subcortical modulation of attention counters change blindness. *J. Neurosci. Off. J. Soc. Neurosci.* **24**, 11236–11243.

Censi, A., Straw, A. D., Sayaman, R. W., Murray, R. M. & Dickinson, M. H. (2013). Discriminating external and internal causes for heading changes in freely flying Drosophila. *PLoS Comput. Biol.* **9**, e1002891.

Chalfie, M., Tu, Y., Euskirchen, G., Ward, W. W. & Prasher, D. C. (1994). Green fluorescent protein as a marker for gene expression. *Science* **263**, 802–805.

Chen, T.-W., Wardill, T. J., Sun, Y., Pulver, S. R., Renninger, S. L., Baohan, A., Schreiter, E. R., Kerr, R. A., Orger, M. B., Jayaraman, V., et al. (2013). Ultrasensitive fluorescent proteins for imaging neuronal activity. *Nature* **499**, 295–300.

Chiang, A.-S., Lin, C.-Y., Chuang, C.-C., Chang, H.-M., Hsieh, C.-H., Yeh, C.-W., Shih, C.-T., Wu, J.-J., Wang, G.-T., Chen, Y.-C., et al. (2011). Three-dimensional reconstruction of brain-wide wiring networks in Drosophila at single-cell resolution. *Curr. Biol. CB* **21**, 1–11.

Chiappe, M. E., Seelig, J. D., Reiser, M. B. & Jayaraman, V. (2010). Walking modulates speed sensitivity in Drosophila motion vision. *Curr. Biol. CB* **20**, 1470–1475.

Chieffi, S., Gentilucci, M., Allport, A., Sasso, E. & Rizzolatti, G. (1993). Study of selective reaching and grasping in a patient with unilateral parietal lesion. Dissociated effects of residual spatial neglect. *Brain J. Neurol.* **116 (Pt 5)**, 1119–1137.

Chow, B. Y., Han, X., Dobry, A. S., Qian, X., Chuong, A. S., Li, M., Henninger, M. A., Belfort, G. M., Lin, Y., Monahan, P. E., et al. (2010). High-performance genetically targetable optical neural silencing by light-driven proton pumps. *Nature* **463**, 98–102.

Chuong, A. S., Miri, M. L., Busskamp, V., Matthews, G. A. C., Acker, L. C., Sørensen, A. T., Young, A., Klapoetke, N. C., Henninger, M. A., Kodandaramaiah, S. B., et al. (2014). Noninvasive optical inhibition with a red-shifted microbial rhodopsin. *Nat. Neurosci.* **17**, 1123–1129.

Cisek, P. (2007). Cortical mechanisms of action selection: the affordance competition hypothesis. *Philos. Trans. R. Soc. Lond. B. Biol. Sci.* **362**, 1585–1599.

Clark, D. A., Bursztyn, L., Horowitz, M. A., Schnitzer, M. J. & Clandinin, T. R. (2011). Defining the computational structure of the motion detector in Drosophila. *Neuron* **70**, 1165–1177.

Coggshall, J. C., Boschek, C. B. & Buchner, S. M. (1973). Preliminary Investigations on a Pair of Giant Fibers in the Central Nervous System of Dipteran Flies. *Z. Für Naturforschung C* **28**, 783–784b.

Collett, T. S. & Collett, M. (2002). Memory use in insect visual navigation. *Nat. Rev. Neurosci.* **3**, 542–552.

Collett, T. S. & Land, M. F. (1975). Visual spatial memory in a hoverfly. *J. Comp. Physiol.* **100**, 59–84.

Colman, H. A., Remington, R. W. & Kritikos, A. (2017). Handedness and Graspability Modify Shifts of Visuospatial Attention to Near-Hand Objects. *PloS One* **12**, e0170542.

Cooke, J. D., Brown, J. D. & Brooks, V. B. (1978). Increased dependence on visual information for movement control in patients with Parkinson's disease. *Can. J. Neurol. Sci. J. Can. Sci. Neurol.* **5**, 413–415.

Corbetta, M. & Shulman, G. L. (2002). Control of goal-directed and stimulus-driven attention in the brain. *Nat. Rev. Neurosci.* **3**, 201–215.

Cosentino, C., Alberio, L., Gazzarrini, S., Aquila, M., Romano, E., Cermenati, S., Zuccolini, P., Petersen, J., Beltrame, M., Van Etten, J. L., et al. (2015). Optogenetics. Engineering of a light-gated potassium channel. *Science* **348**, 707–710.

Creamer, M. S., Mano, O. & Clark, D. A. (2018). Visual Control of Walking Speed in Drosophila. *Neuron* **100**, 1460-1473.e6.

Dana, H., Mohar, B., Sun, Y., Narayan, S., Gordus, A., Hasseman, J. P., Tsegaye, G., Holt, G. T., Hu, A., Walpita, D., et al. (2016). Sensitive red protein calcium indicators for imaging neural activity. *eLife* **5**,.

Dana, H., Sun, Y., Mohar, B., Hulse, B. K., Kerlin, A. M., Hasseman, J. P., Tsegaye, G., Tsang, A., Wong, A., Patel, R., et al. (2019). High-performance calcium sensors for imaging activity in neuronal populations and microcompartments. *Nat. Methods* **16**, 649–657.

Dawydow, A., Gueta, R., Ljaschenko, D., Ullrich, S., Hermann, M., Ehmann, N., Gao, S., Fiala, A., Langenhan, T., Nagel, G., et al. (2014). Channelrhodopsin-2-XXL, a powerful optogenetic tool for low-light applications. *Proc. Natl. Acad. Sci. U. S. A.* **111**, 13972–13977.

de Bivort, B. L. & van Swinderen, B. (2016). Evidence for selective attention in the insect brain. *Curr. Opin. Insect Sci.* **15**, 9–15.

de Vries, S. E. J. & Clandinin, T. R. (2012). Loom-sensitive neurons link computation to action in the Drosophila visual system. *Curr. Biol. CB* **22**, 353–362.

Deisseroth, K. (2011). Optogenetics. *Nat. Methods* **8**, 26–29.

Deisseroth, K. (2015). Optogenetics: 10 years of microbial opsins in neuroscience. *Nat. Neurosci.* **18**, 1213–1225.

Deisseroth, K. & Hegemann, P. (2017). The form and function of channelrhodopsin. *Science* **357**,.

DeLong, M. R. (1990). Primate models of movement disorders of basal ganglia origin. *Trends Neurosci.* **13**, 281–285.

Desimone, R. & Duncan, J. (1995). Neural mechanisms of selective visual attention. *Annu. Rev. Neurosci.* **18**, 193–222.

Dickinson, M. H. & Götz, K. G. (1996). The wake dynamics and flight forces of

the fruit fly Drosophila melanogaster. *J. Exp. Biol.* **199**, 2085–2104.

Dickinson, M. H. & Muijres, F. T. (2016). The aerodynamics and control of free flight manoeuvres in Drosophila. *Philos. Trans. R. Soc. Lond. B. Biol. Sci.* **371**,.

Dickinson, M. H., Farley, C. T., Full, R. J., Koehl, M. A., Kram, R. & Lehman, S. (2000). How animals move: an integrative view. *Science* **288**, 100–106.

Dietzl, G., Chen, D., Schnorrer, F., Su, K.-C., Barinova, Y., Fellner, M., Gasser, B., Kinsey, K., Oppel, S., Scheiblauer, S., et al. (2007). A genome-wide transgenic RNAi library for conditional gene inactivation in Drosophila. *Nature* **448**, 151–156.

Dionne, H., Hibbard, K. L., Cavallaro, A., Kao, J.-C. & Rubin, G. M. (2018). Genetic Reagents for Making Split-GAL4 Lines in Drosophila. *Genetics* **209**, 31–35.

Domenici, P., Schmitz, J. & Jamon, M. (1999). The relationship between leg stepping pattern and yaw torque oscillations in curve walking of two crayfish species. *J. Exp. Biol.* **202 Pt 22**, 3069–3080.

Donlea, J. M., Pimentel, D. & Miesenböck, G. (2014). Neuronal machinery of sleep homeostasis in Drosophila. *Neuron* **81**, 860–872.

Donlea, J. M., Pimentel, D., Talbot, C. B., Kempf, A., Omoto, J. J., Hartenstein, V. & Miesenböck, G. (2018). Recurrent Circuitry for Balancing Sleep Need and Sleep. *Neuron* **97**, 378-389.e4.

Donovan, E. R., Keeney, B. K., Kung, E., Makan, S., Wild, J. M. & Altshuler, D. L. (2013). Muscle activation patterns and motor anatomy of Anna's hummingbirds Calypte anna and zebra finches Taeniopygia guttata. *Physiol. Biochem. Zool. PBZ* **86**, 27–46.

Draper, I., Kurshan, P. T., McBride, E., Jackson, F. R. & Kopin, A. S. (2007). Locomotor activity is regulated by D2-like receptors in Drosophila: an anatomic and functional analysis. *Dev. Neurobiol.* **67**, 378–393.

Egelhaaf, M. (2006). The neural computation of visual motion information. In *Invertebrate vision*, p. Cambridge, UK: Cambridge University Press.

Ericsson, J., Silberberg, G., Robertson, B., Wikström, M. A. & Grillner, S. (2011). Striatal cellular properties conserved from lampreys to mammals. *J. Physiol.* **589**, 2979–2992.

Ericsson, J., Stephenson-Jones, M., Pérez-Fernández, J., Robertson, B., Silberberg, G. & Grillner, S. (2013). Dopamine differentially modulates the excitability of striatal neurons of the direct and indirect pathways in lamprey. *J. Neurosci. Off. J. Soc. Neurosci.* **33**, 8045–8054.

Farries, M. A. (2013). How "basal" are the basal ganglia? *Brain. Behav. Evol.* **82**, 211–214.

Fenk, L. M., Poehlmann, A. & Straw, A. D. (2014). Asymmetric processing of visual motion for simultaneous object and background responses. *Curr. Biol. CB* **24**, 2913–2919.

Fiala, A., Spall, T., Diegelmann, S., Eisermann, B., Sachse, S., Devaud, J.-M., Buchner, E. & Galizia, C. G. (2002). Genetically expressed cameleon in Drosophila melanogaster is used to visualize olfactory information in projection neurons. *Curr. Biol. CB* **12**, 1877–1884.

Fiore, V. G., Dolan, R. J., Strausfeld, N. J. & Hirth, F. (2015). Evolutionarily conserved mechanisms for the selection and maintenance of behavioural activity. *Philos. Trans. R. Soc. Lond. B. Biol. Sci.* **370**,.

Fiore, V. G., Kottler, B., Gu, X. & Hirth, F. (2017). In silico Interrogation of Insect Central Complex Suggests Computational Roles for the Ellipsoid Body in Spatial Navigation. *Front. Behav. Neurosci.* **11**, 142.

Fischbach, K.-F. & Dittrich, A. P. M. (1989). The optic lobe of Drosophila melanogaster. I. A Golgi analysis of wild-type structure. *Cell Tissue Res.* **258**, 441–475.

Fischer, J. A., Giniger, E., Maniatis, T. & Ptashne, M. (1988). GAL4 activates transcription in Drosophila. *Nature* **332**, 853–856.

Fortier, E. & Belote, J. M. (2000). Temperature-dependent gene silencing by an expressed inverted repeat in Drosophila. *Genes. N. Y. N 2000* **26**, 240–244.

Fosque, B. F., Sun, Y., Dana, H., Yang, C.-T., Ohyama, T., Tadross, M. R., Patel, R., Zlatic, M., Kim, D. S., Ahrens, M. B., et al. (2015). Neural circuits. Labeling of active neural circuits in vivo with designed calcium integrators. *Science* **347**, 755–760.

Fraenkel, G. S. & Gunn, D. L. (1961). *The Orientation of Animals: Kineses, Taxes and Compass Reactions*. New York, NY, USA: Dover Publications.

Franconville, R., Beron, C. & Jayaraman, V. (2018). Building a functional connectome of the Drosophila central complex. *eLife* **7**,.

Friggi-Grelin, F., Coulom, H., Meller, M., Gomez, D., Hirsh, J. & Birman, S. (2003). Targeted gene expression in Drosophila dopaminergic cells using regulatory sequences from tyrosine hydroxylase. *J. Neurobiol.* **54**, 618–627.

Frighetto, G., Zordan, M. A., Castiello, U. & Megighian, A. (2019). Action-based attention in Drosophila melanogaster. *J. Neurophysiol.*

Fry, S. N., Sayaman, R. & Dickinson, M. H. (2003). The aerodynamics of free-flight maneuvers in Drosophila. *Science* **300**, 495–498.

Fry, S. N., Rohrseitz, N., Straw, A. D. & Dickinson, M. H. (2009). Visual control of flight speed in Drosophila melanogaster. *J. Exp. Biol.* **212**, 1120–1130.

Frye, M. A. & Dickinson, M. H. (2004). Motor output reflects the linear superposition of visual and olfactory inputs in Drosophila. *J. Exp. Biol.* **207**, 123–131.

Fujiwara, T., Cruz, T. L., Bohnslav, J. P. & Chiappe, M. E. (2016). A faithful internal representation of walking movements in the Drosophila visual system. *Nat. Neurosci.*

Gal, R. & Libersat, F. (2006). New vistas on the initiation and maintenance of insect motor behaviors revealed by specific lesions of the head ganglia. *J. Comp. Physiol. A Neuroethol. Sens. Neural. Behav. Physiol.* **192**, 1003–1020.

Gao, S., Takemura, S.-Y., Ting, C.-Y., Huang, S., Lu, Z., Luan, H., Rister, J., Thum, A. S., Yang, M., Hong, S.-T., et al. (2008). The neural substrate of spectral preference in Drosophila. *Neuron* **60**, 328–342.

Gaveau, V., Pisella, L., Priot, A.-E., Fukui, T., Rossetti, Y., Pélisson, D. & Prablanc, C. (2014). Automatic online control of motor adjustments in reaching and grasping. *Neuropsychologia* **55**, 25–40.

Geurten, B. R. H., Jähde, P., Corthals, K. & Göpfert, M. C. (2014). Saccadic body turns in walking Drosophila. *Front. Behav. Neurosci.* **8**, 365.

Gibson, J. J. (1979). *The ecological approach to visual perception*. Boston, MA, USA: Houghton Mifflin.

Gilbert, C. D. & Li, W. (2013). Top-down influences on visual processing. *Nat. Rev. Neurosci.* **14**, 350–363.

Giraldo, Y. M., Leitch, K. J., Ros, I. G., Warren, T. L., Weir, P. T. & Dickinson, M. H. (2018). Sun Navigation Requires Compass Neurons in Drosophila. *Curr. Biol. CB* **28**, 2845-2852.e4.

Giurfa, M. (2013). Cognition with few neurons: higher-order learning in insects. *Trends Neurosci.* **36**, 285–294.

Gorostiza, E. A., Colomb, J. & Brembs, B. (2016). A decision underlies phototaxis in an insect. *Open Biol.* **6**,.

Götz, K. G. (1964). Optomoter studies of the visual system of several eye mutants of the fruit fly Drosophila. *Kybernetik* **2**, 77–92.

Götz, K. G. (1968). Flight control in Drosophila by visual perception of motion. *Kybernetik* **4**, 199–208.

Götz, K. G. (1975). The optomotor equilibrium of the Drosophila navigation system. *J. Comp. Physiol.* **99**, 187–210.

Götz, K. G. (1980). Visual Guidance in Drosophila. In *Development and Neurobiology of Drosophila*, pp. 391–407. Boston, MA, USA: Springer.

Götz, K. G. & Wenking, H. (1973). Visual control of locomotion in the walking fruitfly Drosophila. *J. Comp. Physiol.* **85**, 235–266.

Govorunova, E. G., Sineshchekov, O. A., Janz, R., Liu, X. & Spudich, J. L. (2015). Natural light-gated anion channels: A family of microbial rhodopsins for advanced optogenetics. *Science* **349**, 647–650.

Grabowska, M. J., Steeves, J., Alpay, J., van de Poll, M., Ertekin, D. & van Swinderen, B. (2018). Innate visual preferences and behavioral flexibility in Drosophila. *J. Exp. Biol.*

Gradinaru, V., Thompson, K. R. & Deisseroth, K. (2008). eNpHR: a Natronomonas halorhodopsin enhanced for optogenetic applications. *Brain Cell Biol.* **36**, 129–139.

Green, J. & Maimon, G. (2018). Building a heading signal from anatomically defined neuron types in the Drosophila central complex. *Curr. Opin. Neurobiol.* **52**, 156–164.

Green, E. W., Fedele, G., Giorgini, F. & Kyriacou, C. P. (2014). A Drosophila RNAi collection is subject to dominant phenotypic effects. *Nat. Methods* **11**, 222–223.

Green, J., Adachi, A., Shah, K. K., Hirokawa, J. D., Magani, P. S. & Maimon, G. (2017). A neural circuit architecture for angular integration in Drosophila. *Nature* **advance online publication**,.

Green, J., Vijayan, V., Mussells Pires, P., Adachi, A. & Maimon, G. (2019). A neural heading estimate is compared with an internal goal to guide oriented navigation. *Nat. Neurosci.*

Greenspan, R. J. (2008). The origins of behavioral genetics. *Curr. Biol. CB* **18**, R192-198.

Gregoriou, G. G., Gotts, S. J., Zhou, H. & Desimone, R. (2009). High-frequency, long-range coupling between prefrontal and visual cortex during attention. *Science* **324**, 1207–1210.

Grillner, S. & Robertson, B. (2016). The Basal Ganglia Over 500 Million Years. *Curr. Biol. CB* **26**, R1088–R1100.

Grillner, S., Hellgren, J., Ménard, A., Saitoh, K. & Wikström, M. A. (2005a). Mechanisms for selection of basic motor programs--roles for the striatum and pallidum. *Trends Neurosci.* **28**, 364–370.

Grillner, S., Kozlov, A. & Kotaleski, J. H. (2005b). Integrative neuroscience: linking levels of analyses. *Curr. Opin. Neurobiol.* **15**, 614–621.

Groth, A. C., Fish, M., Nusse, R. & Calos, M. P. (2004). Construction of transgenic Drosophila by using the site-specific integrase from phage phiC31. *Genetics* **166**, 1775–1782.

Grover, D., Katsuki, T. & Greenspan, R. J. (2016). Flyception: imaging brain activity in freely walking fruit flies. *Nat. Methods* **13**, 569–572.

Haag, J., Wertz, A. & Borst, A. (2010). Central gating of fly optomotor response. *Proc. Natl. Acad. Sci. U. S. A.* **107**, 20104–20109.

Haberkern, H. & Jayaraman, V. (2016). Studying small brains to understand the building blocks of cognition. *Curr. Opin. Neurobiol.* **37**, 59–65.

Haikala, V., Joesch, M., Borst, A. & Mauss, A. S. (2013). Optogenetic control of fly optomotor responses. *J. Neurosci. Off. J. Soc. Neurosci.* **33**, 13927–13934.

Hammond, S. M., Caudy, A. A. & Hannon, G. J. (2001). Post-transcriptional gene silencing by double-stranded RNA. *Nat. Rev. Genet.* **2**, 110–119.

Han, K. A., Millar, N. S., Grotewiel, M. S. & Davis, R. L. (1996). DAMB, a novel

dopamine receptor expressed specifically in Drosophila mushroom bodies. *Neuron* **16**, 1127–1135.

Hanesch, U., Fischbach, K.-F. & Heisenberg, M. (1989). Neuronal architecture of the central complex in Drosophila melanogaster. *Cell Tissue Res.* **257**, 343–366.

Harcombe, E. S. & Wyman, R. J. (1977). Output pattern generation by Drosophila flight motoneurons. *J. Neurophysiol.* **40**, 1066–1077.

Hardcastle, B. J. & Krapp, H. G. (2016). Evolution of Biological Image Stabilization. *Curr. Biol. CB* **26**, R1010–R1021.

Hardie, R. C. (1989). A histamine-activated chloride channel involved in neurotransmission at a photoreceptor synapse. *Nature* **339**, 704–706.

Hardie, R. C. & Juusola, M. (2015). Phototransduction in Drosophila. *Curr. Opin. Neurobiol.* **34**, 37–45.

Hardin, P. E., Hall, J. C. & Rosbash, M. (1990). Feedback of the Drosophila period gene product on circadian cycling of its messenger RNA levels. *Nature* **343**, 536–540.

Harris, R. M., Pfeiffer, B. D., Rubin, G. M. & Truman, J. W. (2015). Neuron hemilineages provide the functional ground plan for the Drosophila ventral nervous system. *eLife* **4**,.

Hassenstein, B. & Reichardt, W. (1956). Systemtheoretische Analyse der Zeit-, Reihenfolgen- und Vorzeichenauswertung bei der Bewegungsperzeption des Rüsselkäfers Chlorophanus. *Z. Für Naturforschung B* **11**, 513–524.

Heigwer, F., Port, F. & Boutros, M. (2018). RNA Interference (RNAi) Screening in Drosophila. *Genetics* **208**, 853–874.

Heinze, S. (2017). Unraveling the neural basis of insect navigation. *Curr. Opin. Insect Sci.* **24**, 58–67.

Heisenberg, M. (2003). Mushroom body memoir: from maps to models. *Nat. Rev. Neurosci.* **4**, 266–275.

Heisenberg, M. & Buchner, E. (1977). The role of retinula cell types in visual behavior of Drosophila melanogaster. *J. Comp. Physiol.* **117**, 127–162.

Heisenberg, M. & Wolf, R. (1979). On the fine structure of yaw torque in visual flight orientation of Drosophila melanogaster. *J. Comp. Physiol.* **130**, 113–130.

Heisenberg, M. & Wolf, R. (1984). *Vision in Drosophila: Genetics of Microbehavior (Studies of Brain Function)*. Berlin, Heidelberg, DE: Springer.

Heisenberg, M. & Wolf, R. (1988). Reafferent control of optomotor yaw torque in Drosophila melanogaster. *J. Comp. Physiol. A* **163**, 373–388.

Heisenberg, M., Wonneberger, R. & Wolf, R. (1978). Optomotor-blindH31—a Drosophila mutant of the lobula plate giant neurons. *J. Comp. Physiol.* **124**, 287–296.

Hendel, T., Mank, M., Schnell, B., Griesbeck, O., Borst, A. & Reiff, D. F. (2008). Fluorescence changes of genetic calcium indicators and OGB-1 correlated with neural activity and calcium in vivo and in vitro. *J. Neurosci. Off. J. Soc. Neurosci.* **28**, 7399–7411.

Henry, F. M. & Rogers, D. E. (1960). Increased response latency for complicated movements and a "memory drum" theory of neuromotor reaction. *Res. Q. Am. Assoc. Health Phys. Educ. Recreat.* **31**, 448–458.

Hesse, C. & Deubel, H. (2010). Advance planning in sequential pick-and-place tasks. *J. Neurophysiol.* **104**, 508–516.

Hesselberg, T. & Lehmann, F.-O. (2007). Turning behaviour depends on frictional damping in the fruit fly Drosophila. *J. Exp. Biol.* **210**, 4319–4334.

Hirsch, J. (1959). Studies in experimental behavior genetics. II. Individual differences in geotaxis as a function of chromosome variations in synthesized Drosophila populations. *J. Comp. Physiol. Psychol.* **52**, 304–308.

Homberg, U. (2008). Evolution of the central complex in the arthropod brain with respect to the visual system. *Arthropod Struct. Dev.* **37**, 347–362.

Horn, E. (1978). The mechanism of object fixation and its relation to spontaneous pattern preferences in Drosophila melanogaster. *Biol. Cybern.* **31**, 145–158.

Horn, E. & Wehner, R. (1975). The mechanism of visual pattern fixation in the walking fly, Drosophila melanogaster. *J. Comp. Physiol.* **101**, 39–56.

Houghton, G. & Tipper, S. P. (1994). A model of inhibitory mechanisms in selective attention. In *Inhibitory processes in attention, memory, and language*, pp. 53–112. San Diego, CA, USA: Academic Press.

Howard, L. A. & Tipper, S. P. (1997). Hand deviations away from visual cues:

indirect evidence for inhibition. *Exp. Brain Res.* **113**, 144–152.

Hsu, C. T. & Bhandawat, V. (2016). Organization of descending neurons in Drosophila melanogaster. *Sci. Rep.* **6**, 20259.

Ikeda, K. & Koenig, J. H. (1988). Morphological identification of the motor neurons innervating the dorsal longitudinal flight muscle of Drosophila melanogaster. *J. Comp. Neurol.* **273**, 436–444.

Inagaki, H. K., Jung, Y., Hoopfer, E. D., Wong, A. M., Mishra, N., Lin, J. Y., Tsien, R. Y. & Anderson, D. J. (2014). Optogenetic control of Drosophila using a red-shifted channelrhodopsin reveals experience-dependent influences on courtship. *Nat. Methods* **11**, 325–332.

Ito, K., Shinomiya, K., Ito, M., Armstrong, J. D., Boyan, G., Hartenstein, V., Harzsch, S., Heisenberg, M., Homberg, U., Jenett, A., et al. (2014). A systematic nomenclature for the insect brain. *Neuron* **81**, 755–765.

Iwasaki, S., Kobayashi, M., Yoda, M., Sakaguchi, Y., Katsuma, S., Suzuki, T. & Tomari, Y. (2010). Hsc70/Hsp90 chaperone machinery mediates ATP-dependent RISC loading of small RNA duplexes. *Mol. Cell* **39**, 292–299.

Jackson, S. R., Jackson, G. M. & Rosicky, J. (1995). Are non-relevant objects represented in working memory? The effect of non-target objects on reach and grasp kinematics. *Exp. Brain Res.* **102**, 519–530.

James, W. (1890). *The Principles of Psychology*. New York, NY, USA: H. Holt.

Jayaraman, V. & Laurent, G. (2007). Evaluating a genetically encoded optical sensor of neural activity using electrophysiology in intact adult fruit flies. *Front. Neural Circuits* **1**, 3.

Jenett, A., Rubin, G. M., Ngo, T.-T. B., Shepherd, D., Murphy, C., Dionne, H., Pfeiffer, B. D., Cavallaro, A., Hall, D., Jeter, J., et al. (2012). A GAL4-driver line resource for Drosophila neurobiology. *Cell Rep.* **2**, 991–1001.

Jin, X. & Costa, R. M. (2010). Start/stop signals emerge in nigrostriatal circuits during sequence learning. *Nature* **466**, 457–462.

Joesch, M., Plett, J., Borst, A. & Reiff, D. F. (2008). Response properties of motion-sensitive visual interneurons in the lobula plate of Drosophila melanogaster. *Curr. Biol. CB* **18**, 368–374.

Joesch, M., Schnell, B., Raghu, S. V., Reiff, D. F. & Borst, A. (2010). ON and

OFF pathways in Drosophila motion vision. *Nature* **468**, 300–304.

Johansson, R. S., Westling, G., Bäckström, A. & Flanagan, J. R. (2001). Eye-hand coordination in object manipulation. *J. Neurosci. Off. J. Soc. Neurosci.* **21**, 6917–6932.

Jonikaitis, D. & Moore, T. (2019). The Interdependence of Attention, Working Memory and Gaze Control: Behavior and Neural Circuitry. *Curr. Opin. Psychol.*

Kahsai, L. & Winther, A. M. E. (2011). Chemical neuroanatomy of the Drosophila central complex: distribution of multiple neuropeptides in relation to neurotransmitters. *J. Comp. Neurol.* **519**, 290–315.

Kahsai, L., Carlsson, M. A., Winther, A. M. E. & Nässel, D. R. (2012). Distribution of metabotropic receptors of serotonin, dopamine, GABA, glutamate, and short neuropeptide F in the central complex of Drosophila. *Neuroscience* **208**, 11–26.

Kain, J. S., Stokes, C. & de Bivort, B. L. (2012). Phototactic personality in fruit flies and its suppression by serotonin and white. *Proc. Natl. Acad. Sci. U. S. A.* **109**, 19834–19839.

Kaiser, M. & Libersat, F. (2015). The role of the cerebral ganglia in the venom-induced behavioral manipulation of cockroaches stung by the parasitoid jewel wasp. *J. Exp. Biol.* **218**, 1022–1027.

Kakaria, K. S. & de Bivort, B. L. (2017). Ring Attractor Dynamics Emerge from a Spiking Model of the Entire Protocerebral Bridge. *Front. Behav. Neurosci.* **11**, 8.

Kandel, E. R., Jessell, T. M., Schwartz, J. H., Siegelbaum, S. A. & Hudspeth, A. J. (2013). *Principles of Neural Science*. Fifth Edition. New York, NY, USA: McGraw Hill Professional.

Keleş, M. F. & Frye, M. A. (2017). Object-Detecting Neurons in Drosophila. *Curr. Biol. CB* **27**, 680–687.

Kennerdell, J. R. & Carthew, R. W. (1998). Use of dsRNA-mediated genetic interference to demonstrate that frizzled and frizzled 2 act in the wingless pathway. *Cell* **95**, 1017–1026.

Kennerdell, J. R. & Carthew, R. W. (2000). Heritable gene silencing in Drosophila using double-stranded RNA. *Nat. Biotechnol.* **18**, 896–898.

Kiehn, O. (2016). Decoding the organization of spinal circuits that control

locomotion. *Nat. Rev. Neurosci.* **17**, 224–238.

Kien, J. (1983). The initiation and maintenance of walking in the locust: an alternative to the command concept. *Proc. R. Soc. Lond. B Biol. Sci.* **219**, 137–174.

Kim, Y.-C., Lee, H.-G., Seong, C.-S. & Han, K.-A. (2003). Expression of a D1 dopamine receptor dDA1/DmDOP1 in the central nervous system of Drosophila melanogaster. *Gene Expr. Patterns GEP* **3**, 237–245.

Kim, A. J., Fitzgerald, J. K. & Maimon, G. (2015). Cellular evidence for efference copy in Drosophila visuomotor processing. *Nat. Neurosci.* **18**, 1247–1255.

Kim, A. J., Fenk, L. M., Lyu, C. & Maimon, G. (2017a). Quantitative Predictions Orchestrate Visual Signaling in Drosophila. *Cell* **168**, 280-294.e12.

Kim, S. S., Rouault, H., Druckmann, S. & Jayaraman, V. (2017b). Ring attractor dynamics in the Drosophila central brain. *Science*.

Kirszenblat, L., Ertekin, D., Goodsell, J., Zhou, Y., Shaw, P. J. & van Swinderen, B. (2018). Sleep regulates visual selective attention in Drosophila. *J. Exp. Biol.* **221**,.

Klapoetke, N. C., Murata, Y., Kim, S. S., Pulver, S. R., Birdsey-Benson, A., Cho, Y. K., Morimoto, T. K., Chuong, A. S., Carpenter, E. J., Tian, Z., et al. (2014). Independent optical excitation of distinct neural populations. *Nat. Methods* **11**, 338–346.

Koenig, S., Wolf, R. & Heisenberg, M. (2016a). Visual Attention in Flies-Dopamine in the Mushroom Bodies Mediates the After-Effect of Cueing. *PloS One* **11**, e0161412.

Koenig, S., Wolf, R. & Heisenberg, M. (2016b). Vision in Flies: Measuring the Attention Span. *PloS One* **11**, e0148208.

Kong, E. C., Woo, K., Li, H., Lebestky, T., Mayer, N., Sniffen, M. R., Heberlein, U., Bainton, R. J., Hirsh, J. & Wolf, F. W. (2010). A pair of dopamine neurons target the D1-like dopamine receptor DopR in the central complex to promote ethanol-stimulated locomotion in Drosophila. *PloS One* **5**, e9954.

Kottler, B., Fiore, V. G., Ludlow, Z. N., Buhl, E., Vinatier, G., Faville, R., Diaper, D. C., Stepto, A., Dearlove, J., Adachi, Y., et al. (2017). A lineage-

related reciprocal inhibition circuitry for sensory-motor action selection. *bioRxiv* 100420.

Kottler, B., Faville, R., Bridi, J. C. & Hirth, F. (2019). Inverse Control of Turning Behavior by Dopamine D1 Receptor Signaling in Columnar and Ring Neurons of the Central Complex in Drosophila. *Curr. Biol. CB*.

Krauzlis, R. J., Lovejoy, L. P. & Zénon, A. (2013). Superior colliculus and visual spatial attention. *Annu. Rev. Neurosci.* **36**, 165–182.

Krauzlis, R. J., Bollimunta, A., Arcizet, F. & Wang, L. (2014). Attention as an effect not a cause. *Trends Cogn. Sci.* **18**, 457–464.

Krauzlis, R. J., Bogadhi, A. R., Herman, J. P. & Bollimunta, A. (2018). Selective attention without a neocortex. *Cortex J. Devoted Study Nerv. Syst. Behav.* **102**, 161–175.

Kritikos, A., Bennett, K. M., Dunai, J. & Castiello, U. (2000). Interference from distractors in reach-to-grasp movements. *Q. J. Exp. Psychol. A* **53**, 131–151.

Lai, S.-L. & Lee, T. (2006). Genetic mosaic with dual binary transcriptional systems in Drosophila. *Nat. Neurosci.* **9**, 703–709.

Land, M. F. (1999). Motion and vision: why animals move their eyes. *J. Comp. Physiol. [A]* **185**, 341–352.

Land, M. F. & Collett, T. S. (1974). Chasing behaviour of houseflies (Fannia canicularis). *J. Comp. Physiol.* **89**, 331–357.

Lark, A. R., Kitamoto, T. & Martin, J.-R. (2016). In Vivo Functional Brain Imaging Approach Based on Bioluminescent Calcium Indicator GFP-aequorin. *J. Vis. Exp. JoVE*.

Lark, A., Kitamoto, T. & Martin, J.-R. (2017). Modulation of neuronal activity in the Drosophila mushroom body by DopEcR, a unique dual receptor for ecdysone and dopamine. *Biochim. Biophys. Acta* **1864**, 1578–1588.

Lebestky, T., Chang, J.-S. C., Dankert, H., Zelnik, L., Kim, Y.-C., Han, K.-A., Wolf, F. W., Perona, P. & Anderson, D. J. (2009). Two different forms of arousal in Drosophila are oppositely regulated by the dopamine D1 receptor ortholog DopR via distinct neural circuits. *Neuron* **64**, 522–536.

LeBlanc, K. A. & Westwood, D. A. (2016). Sequential actions: effects of upcoming perceptual and motor tasks on current actions. *Exp. Brain Res.* **234**,

955–962.

Lee, T. & Luo, L. (1999). Mosaic analysis with a repressible cell marker for studies of gene function in neuronal morphogenesis. *Neuron* **22**, 451–461.

Lehmann, F.-O. & Bartussek, J. (2017). Neural control and precision of flight muscle activation in Drosophila. *J. Comp. Physiol. A* **203**, 1–14.

Lenth, R. V. (2016). Least-Squares Means: The R Package lsmeans. *J. Stat. Softw.* **69**, 1–33.

Lima, S. Q. & Miesenböck, G. (2005). Remote control of behavior through genetically targeted photostimulation of neurons. *Cell* **121**, 141–152.

Lin, C.-Y., Chuang, C.-C., Hua, T.-E., Chen, C.-C., Dickson, B. J., Greenspan, R. J. & Chiang, A.-S. (2013a). A comprehensive wiring diagram of the protocerebral bridge for visual information processing in the Drosophila brain. *Cell Rep.* **3**, 1739–1753.

Lin, J. Y., Knutsen, P. M., Muller, A., Kleinfeld, D. & Tsien, R. Y. (2013b). ReaChR: a red-shifted variant of channelrhodopsin enables deep transcranial optogenetic excitation. *Nat. Neurosci.* **16**, 1499–1508.

Lindsay, T., Sustar, A. & Dickinson, M. (2017). The Function and Organization of the Motor System Controlling Flight Maneuvers in Flies. *Curr. Biol. CB* **27**, 345–358.

Liu, L., Wolf, R., Ernst, R. & Heisenberg, M. (1999). Context generalization in Drosophila visual learning requires the mushroom bodies. *Nature* **400**, 753–756.

Liu, G., Seiler, H., Wen, A., Zars, T., Ito, K., Wolf, R., Heisenberg, M. & Liu, L. (2006). Distinct memory traces for two visual features in the Drosophila brain. *Nature* **439**, 551–556.

Liu, Q., Liu, S., Kodama, L., Driscoll, M. R. & Wu, M. N. (2012). Two dopaminergic neurons signal to the dorsal fan-shaped body to promote wakefulness in Drosophila. *Curr. Biol. CB* **22**, 2114–2123.

Liu, S., Liu, Q., Tabuchi, M. & Wu, M. N. (2016). Sleep Drive Is Encoded by Neural Plastic Changes in a Dedicated Circuit. *Cell* **165**, 1347–1360.

Looger, L. L. & Griesbeck, O. (2012). Genetically encoded neural activity indicators. *Curr. Opin. Neurobiol.* **22**, 18–23.

Luan, H., Peabody, N. C., Vinson, C. R. & White, B. H. (2006). Refined spatial manipulation of neuronal function by combinatorial restriction of transgene expression. *Neuron* **52**, 425–436.

Maimon, G., Straw, A. D. & Dickinson, M. H. (2008). A simple vision-based algorithm for decision making in flying Drosophila. *Curr. Biol. CB* **18**, 464–470.

Maimon, G., Straw, A. D. & Dickinson, M. H. (2010). Active flight increases the gain of visual motion processing in Drosophila. *Nat. Neurosci.* **13**, 393–399.

Mamiya, A., Gurung, P. & Tuthill, J. C. (2018). Neural Coding of Leg Proprioception in Drosophila. *Neuron* **100**, 636-650.e6.

Mank, M., Santos, A. F., Direnberger, S., Mrsic-Flogel, T. D., Hofer, S. B., Stein, V., Hendel, T., Reiff, D. F., Levelt, C., Borst, A., et al. (2008). A genetically encoded calcium indicator for chronic in vivo two-photon imaging. *Nat. Methods* **5**, 805–811.

Mann, K., Gallen, C. L. & Clandinin, T. R. (2017). Whole-Brain Calcium Imaging Reveals an Intrinsic Functional Network in Drosophila. *Curr. Biol. CB* **27**, 2389-2396.e4.

Marr, D. (1982). *Vision: A Computational Investigation Into the Human Representation and Processing of Visual Information*. New York, NY, USA: W.H. Freeman.

Martin, J.-R. ed. (2012). *Genetically Encoded Functional Indicators*. New York, NY, USA: Humana Press.

Martin, J.-R. (2004). A portrait of locomotor behaviour in Drosophila determined by a video-tracking paradigm. *Behav. Processes* **67**, 207–219.

Martin, J.-R. (2008). In vivo brain imaging: fluorescence or bioluminescence, which to choose? *J. Neurogenet.* **22**, 285–307.

Martin, J. R., Raabe, T. & Heisenberg, M. (1999). Central complex substructures are required for the maintenance of locomotor activity in Drosophila melanogaster. *J. Comp. Physiol. [A]* **185**, 277–288.

Martin, J.-R., Rogers, K. L., Chagneau, C. & Brûlet, P. (2007). In vivo bioluminescence imaging of Ca signalling in the brain of Drosophila. *PloS One* **2**, e275.

Martinek, S. & Young, M. W. (2000). Specific genetic interference with

behavioral rhythms in Drosophila by expression of inverted repeats. *Genetics* **156**, 1717–1725.

Martín-Peña, A., Acebes, A., Rodríguez, J.-R., Chevalier, V., Casas-Tinto, S., Triphan, T., Strauss, R. & Ferrús, A. (2014). Cell types and coincident synapses in the ellipsoid body of Drosophila. *Eur. J. Neurosci.* **39**, 1586–1601.

Maunsell, J. H. R. & Treue, S. (2006). Feature-based attention in visual cortex. *Trends Neurosci.* **29**, 317–322.

Mauss, A. S., Vlasits, A., Borst, A. & Feller, M. (2017a). Visual Circuits for Direction Selectivity. *Annu. Rev. Neurosci.* **40**, 211–230.

Mauss, A. S., Busch, C. & Borst, A. (2017b). Optogenetic Neuronal Silencing in Drosophila during Visual Processing. *Sci. Rep.* **7**, 13823.

McElreath, R. (2016). *Statistical Rethinking: A Bayesian Course with Examples in R and Stan*. Boca Raton, FL, USA: Chapman and Hall/CRC Press.

McEwen, R. S. (1918). The reactions to light and to gravity in Drosophila and its mutants. *J. Exp. Zool.* **25**, 49–106.

McEwen, R. S. (1925). Concerning the Relative Phototropism of Vestigial and Wild Type Drosophila. *Biol. Bull.* **49**, 354–364.

McGuire, S. E., Le, P. T., Osborn, A. J., Matsumoto, K. & Davis, R. L. (2003). Spatiotemporal rescue of memory dysfunction in Drosophila. *Science* **302**, 1765–1768.

McHaffie, J. G., Stanford, T. R., Stein, B. E., Coizet, V. & Redgrave, P. (2005). Subcortical loops through the basal ganglia. *Trends Neurosci.* **28**, 401–407.

Meegan, D. V. & Tipper, S. P. (1998). Reaching into cluttered visual environments: spatial and temporal influences of distracting objects. *Q. J. Exp. Psychol. A* **51**, 225–249.

Meegan, D. V. & Tipper, S. P. (1999). Visual search and target-directed action. *J. Exp. Psychol. Hum. Percept. Perform.* **25**, 1347–1362.

Meier, M., Serbe, E., Maisak, M. S., Haag, J., Dickson, B. J. & Borst, A. (2014). Neural circuit components of the Drosophila OFF motion vision pathway. *Curr. Biol. CB* **24**, 385–392.

Melnattur, K. V., Pursley, R., Lin, T.-Y., Ting, C.-Y., Smith, P. D., Pohida, T. & Lee, C.-H. (2014). Multiple redundant medulla projection neurons mediate

color vision in Drosophila. *J. Neurogenet.* **28**, 374–388.

Mendes, C. S., Bartos, I., Akay, T., Márka, S. & Mann, R. S. (2013). Quantification of gait parameters in freely walking wild type and sensory deprived Drosophila melanogaster. *eLife* **2**, e00231.

Miesenböck, G. (2011). Optogenetic control of cells and circuits. *Annu. Rev. Cell Dev. Biol.* **27**, 731–758.

Minocci, D., Carbognin, E., Murmu, M. S. & Martin, J.-R. (2013). In vivo functional calcium imaging of induced or spontaneous activity in the fly brain using a GFP-apoaequorin-based bioluminescent approach. *Biochim. Biophys. Acta* **1833**, 1632–1640.

Mohammad, F., Stewart, J. C., Ott, S., Chlebikova, K., Chua, J. Y., Koh, T.-W., Ho, J. & Claridge-Chang, A. (2017). Optogenetic inhibition of behavior with anion channelrhodopsins. *Nat. Methods* **14**, 271–274.

Mondal, K., Dastidar, A. G., Singh, G., Madhusudhanan, S., Gande, S. L., VijayRaghavan, K. & Varadarajan, R. (2007). Design and isolation of temperature-sensitive mutants of Gal4 in yeast and Drosophila. *J. Mol. Biol.* **370**, 939–950.

Mongeau, J.-M. & Frye, M. A. (2017). Drosophila Spatiotemporally Integrates Visual Signals to Control Saccades. *Curr. Biol. CB* **27**, 2901-2914.e2.

Montell, C. (2009). A taste of the Drosophila gustatory receptors. *Curr. Opin. Neurobiol.* **19**, 345–353.

Mon-Williams, M., Tresilian, J. R., Coppard, V. L. & Carson, R. G. (2001). The effect of obstacle position on reach-to-grasp movements. *Exp. Brain Res.* **137**, 497–501.

Moore, T. & Armstrong, K. M. (2003). Selective gating of visual signals by microstimulation of frontal cortex. *Nature* **421**, 370–373.

Moore, T. & Fallah, M. (2004). Microstimulation of the frontal eye field and its effects on covert spatial attention. *J. Neurophysiol.* **91**, 152–162.

Moore, T. & Zirnsak, M. (2017). Neural Mechanisms of Selective Visual Attention. *Annu. Rev. Psychol.* **68**, 47–72.

Morgan, T. H. (1910). Sex limited inheritance in Drosophila. *Science* **32**, 120–122.

Mronz, M. & Lehmann, F.-O. (2008). The free-flight response of Drosophila to

motion of the visual environment. *J. Exp. Biol.* **211**, 2026–2045.

Muijres, F. T., Elzinga, M. J., Melis, J. M. & Dickinson, M. H. (2014). Flies evade looming targets by executing rapid visually directed banked turns. *Science* **344**, 172–177.

Muijres, F. T., Elzinga, M. J., Iwasaki, N. A. & Dickinson, M. H. (2015). Body saccades of Drosophila consist of stereotyped banked turns. *J. Exp. Biol.* **218**, 864–875.

Müller, J. R., Philiastides, M. G. & Newsome, W. T. (2005). Microstimulation of the superior colliculus focuses attention without moving the eyes. *Proc. Natl. Acad. Sci. U. S. A.* **102**, 524–529.

Murmu, M. S., Stinnakre, J. & Martin, J.-R. (2010). Presynaptic Ca2+ stores contribute to odor-induced responses in Drosophila olfactory receptor neurons. *J. Exp. Biol.* **213**, 4163–4173.

Nagel, G., Ollig, D., Fuhrmann, M., Kateriya, S., Musti, A. M., Bamberg, E. & Hegemann, P. (2002). Channelrhodopsin-1: a light-gated proton channel in green algae. *Science* **296**, 2395–2398.

Nagel, G., Szellas, T., Huhn, W., Kateriya, S., Adeishvili, N., Berthold, P., Ollig, D., Hegemann, P. & Bamberg, E. (2003). Channelrhodopsin-2, a directly light-gated cation-selective membrane channel. *Proc. Natl. Acad. Sci. U. S. A.* **100**, 13940–13945.

Nagel, G., Brauner, M., Liewald, J. F., Adeishvili, N., Bamberg, E. & Gottschalk, A. (2005). Light activation of channelrhodopsin-2 in excitable cells of Caenorhabditis elegans triggers rapid behavioral responses. *Curr. Biol. CB* **15**, 2279–2284.

Nakai, J., Ohkura, M. & Imoto, K. (2001). A high signal-to-noise Ca(2+) probe composed of a single green fluorescent protein. *Nat. Biotechnol.* **19**, 137–141.

Namiki, S. & Kanzaki, R. (2016). Comparative Neuroanatomy of the Lateral Accessory Lobe in the Insect Brain. *Front. Physiol.* **7**, 244.

Namiki, S., Dickinson, M. H., Wong, A. M., Korff, W. & Card, G. M. (2018). The functional organization of descending sensory-motor pathways in Drosophila. *eLife* **7**,.

Nelson, A. B. & Kreitzer, A. C. (2014). Reassessing models of basal ganglia

function and dysfunction. *Annu. Rev. Neurosci.* **37**, 117–135.

Nern, A., Pfeiffer, B. D. & Rubin, G. M. (2015). Optimized tools for multicolor stochastic labeling reveal diverse stereotyped cell arrangements in the fly visual system. *Proc. Natl. Acad. Sci. U. S. A.* **112**, E2967-2976.

Neuser, K., Triphan, T., Mronz, M., Poeck, B. & Strauss, R. (2008). Analysis of a spatial orientation memory in Drosophila. *Nature* **453**, 1244–1247.

Ni, J.-Q., Markstein, M., Binari, R., Pfeiffer, B., Liu, L.-P., Villalta, C., Booker, M., Perkins, L. & Perrimon, N. (2008). Vector and parameters for targeted transgenic RNA interference in Drosophila melanogaster. *Nat. Methods* **5**, 49–51.

Ni, J.-Q., Liu, L.-P., Binari, R., Hardy, R., Shim, H.-S., Cavallaro, A., Booker, M., Pfeiffer, B. D., Markstein, M., Wang, H., et al. (2009). A Drosophila resource of transgenic RNAi lines for neurogenetics. *Genetics* **182**, 1089–1100.

Ni, J.-Q., Zhou, R., Czech, B., Liu, L.-P., Holderbaum, L., Yang-Zhou, D., Shim, H.-S., Tao, R., Handler, D., Karpowicz, P., et al. (2011). A genome-scale shRNA resource for transgenic RNAi in Drosophila. *Nat. Methods* **8**, 405–407.

Nityananda, V. (2016). Attention-like processes in insects. *Proc. Biol. Sci.* **283**,.

Noudoost, B., Chang, M. H., Steinmetz, N. A. & Moore, T. (2010). Top-down control of visual attention. *Curr. Opin. Neurobiol.* **20**, 183–190.

Ofstad, T. A., Zuker, C. S. & Reiser, M. B. (2011). Visual place learning in Drosophila melanogaster. *Nature* **474**, 204–207.

Olsen, S. R. & Wilson, R. I. (2008). Cracking neural circuits in a tiny brain: new approaches for understanding the neural circuitry of Drosophila. *Trends Neurosci.* **31**, 512–520.

Olson, C. R. (2001). Object-based vision and attention in primates. *Curr. Opin. Neurobiol.* **11**, 171–179.

Omoto, J. J., Keleş, M. F., Nguyen, B.-C. M., Bolanos, C., Lovick, J. K., Frye, M. A. & Hartenstein, V. (2017). Visual Input to the Drosophila Central Complex by Developmentally and Functionally Distinct Neuronal Populations. *Curr. Biol. CB* **27**, 1098–1110.

Omoto, J. J., Nguyen, B.-C. M., Kandimalla, P., Lovick, J. K., Donlea, J. M. &

Hartenstein, V. (2018). Neuronal Constituents and Putative Interactions Within the Drosophila Ellipsoid Body Neuropil. *Front. Neural Circuits* **12**, 103.

Orban de Xivry, J.-J. & Lefèvre, P. (2007). Saccades and pursuit: two outcomes of a single sensorimotor process. *J. Physiol.* **584**, 11–23.

Osterwalder, T., Yoon, K. S., White, B. H. & Keshishian, H. (2001). A conditional tissue-specific transgene expression system using inducible GAL4. *Proc. Natl. Acad. Sci. U. S. A.* **98**, 12596–12601.

O'Sullivan, A., Lindsay, T., Prudnikova, A., Erdi, B., Dickinson, M. & von Philipsborn, A. C. (2018). Multifunctional Wing Motor Control of Song and Flight. *Curr. Biol. CB* **28**, 2705-2717.e4.

Panzeri, S., Harvey, C. D., Piasini, E., Latham, P. E. & Fellin, T. (2017). Cracking the Neural Code for Sensory Perception by Combining Statistics, Intervention, and Behavior. *Neuron* **93**, 491–507.

Patchay, S., Castiello, U. & Haggard, P. (2003). A cross-modal interference effect in grasping objects. *Psychon. Bull. Rev.* **10**, 924–931.

Patchay, S., Haggard, P. & Castiello, U. (2006). An object-centred reference frame for control of grasping: effects of grasping a distractor object on visuomotor control. *Exp. Brain Res.* **170**, 532–542.

Paulk, A. C., Stacey, J. A., Pearson, T. W. J., Taylor, G. J., Moore, R. J. D., Srinivasan, M. V. & van Swinderen, B. (2014). Selective attention in the honeybee optic lobes precedes behavioral choices. *Proc. Natl. Acad. Sci. U. S. A.* **111**, 5006–5011.

Pavot, P., Carbognin, E. & Martin, J.-R. (2015). PKA and cAMP/CNG Channels Independently Regulate the Cholinergic Ca(2+)-Response of Drosophila Mushroom Body Neurons. *eNeuro* **2**,.

Petersen, S. E. & Posner, M. I. (2012). The attention system of the human brain: 20 years after. *Annu. Rev. Neurosci.* **35**, 73–89.

Pfeiffer, K. & Homberg, U. (2014). Organization and functional roles of the central complex in the insect brain. *Annu. Rev. Entomol.* **59**, 165–184.

Pfeiffer, B. D., Jenett, A., Hammonds, A. S., Ngo, T.-T. B., Misra, S., Murphy, C., Scully, A., Carlson, J. W., Wan, K. H., Laverty, T. R., et al. (2008). Tools for neuroanatomy and neurogenetics in Drosophila. *Proc. Natl. Acad. Sci. U. S.*

A. **105**, 9715–9720.

Pfeiffer, B. D., Ngo, T.-T. B., Hibbard, K. L., Murphy, C., Jenett, A., Truman, J. W. & Rubin, G. M. (2010). Refinement of tools for targeted gene expression in Drosophila. *Genetics* **186**, 735–755.

Pfeiffer, B. D., Truman, J. W. & Rubin, G. M. (2012). Using translational enhancers to increase transgene expression in Drosophila. *Proc. Natl. Acad. Sci. U. S. A.* **109**, 6626–6631.

Pimentel, D., Donlea, J. M., Talbot, C. B., Song, S. M., Thurston, A. J. F. & Miesenböck, G. (2016). Operation of a homeostatic sleep switch. *Nature*.

Poehlmann, A., Soselisa, S., Fenk, L. M. & Straw, A. D. (2018). A unifying model to predict multiple object orienting behaviors in tethered flies. *bioRxiv* 379651.

Poggio, T. & Reichardt, W. (1973). A theory of the pattern induced flight orientation of the fly Musca domestica. *Kybernetik* **12**, 185–203.

Posner, M. I. (1980). Orienting of attention. *Q. J. Exp. Psychol.* **32**, 3–25.

Potter, C. J., Tasic, B., Russler, E. V., Liang, L. & Luo, L. (2010). The Q system: a repressible binary system for transgene expression, lineage tracing, and mosaic analysis. *Cell* **141**, 536–548.

R Development Core Team (2017). *R: A Language and Environment for Statistical Computing*. R Foundation for Statistical Computing. Vienna, Austria.

Redgrave, P., Prescott, T. J. & Gurney, K. (1999). The basal ganglia: a vertebrate solution to the selection problem? *Neuroscience* **89**, 1009–1023.

Redgrave, P., Rodriguez, M., Smith, Y., Rodriguez-Oroz, M. C., Lehericy, S., Bergman, H., Agid, Y., DeLong, M. R. & Obeso, J. A. (2010a). Goal-directed and habitual control in the basal ganglia: implications for Parkinson's disease. *Nat. Rev. Neurosci.* **11**, 760–772.

Redgrave, P., Coizet, V., Comoli, E., McHaffie, J. G., Leriche, M., Vautrelle, N., Hayes, L. M. & Overton, P. (2010b). Interactions between the Midbrain Superior Colliculus and the Basal Ganglia. *Front. Neuroanat.* **4**,.

Reichardt, W. & Poggio, T. (1975). A theory of the pattern induced flight orientation of the fly Musca domestica II. *Biol. Cybern.* **18**, 69–80.

Reichardt, W. & Wenking, H. (1969). Optical detection and fixation of objects by fixed flying flies. *Naturwissenschaften* **56**, 424–425.

Reiser, M. B. & Dickinson, M. H. (2008). A modular display system for insect behavioral neuroscience. *J. Neurosci. Methods* **167**, 127–139.

Reynolds, J. H. & Chelazzi, L. (2004). Attentional modulation of visual processing. *Annu. Rev. Neurosci.* **27**, 611–647.

Ribeiro, I. M. A., Drews, M., Bahl, A., Machacek, C., Borst, A. & Dickson, B. J. (2018). Visual Projection Neurons Mediating Directed Courtship in Drosophila. *Cell* **174**, 607-621.e18.

Riddoch, M. J., Humphreys, G. W. & Edwards, M. G. (2000). Visual affordances and object selection. *CONTROL Cogn. Process. Atten. Perform. XVIII* **18**,.

Rieche, F., Carmine-Simmen, K., Poeck, B., Kretzschmar, D. & Strauss, R. (2018). Drosophila Full-Length Amyloid Precursor Protein Is Required for Visual Working Memory and Prevents Age-Related Memory Impairment. *Curr. Biol. CB* **28**, 817-823.e3.

Rister, J. & Desplan, C. (2011). The retinal mosaics of opsin expression in invertebrates and vertebrates. *Dev. Neurobiol.* **71**, 1212–1226.

Rister, J., Pauls, D., Schnell, B., Ting, C.-Y., Lee, C.-H., Sinakevitch, I., Morante, J., Strausfeld, N. J., Ito, K. & Heisenberg, M. (2007). Dissection of the peripheral motion channel in the visual system of Drosophila melanogaster. *Neuron* **56**, 155–170.

Rizzolatti, G., Riggio, L., Dascola, I. & Umiltá, C. (1987). Reorienting attention across the horizontal and vertical meridians: evidence in favor of a premotor theory of attention. *Neuropsychologia* **25**, 31–40.

Rogers, K. L., Stinnakre, J., Agulhon, C., Jublot, D., Shorte, S. L., Kremer, E. J. & Brûlet, P. (2005). Visualization of local Ca2+ dynamics with genetically encoded bioluminescent reporters. *Eur. J. Neurosci.* **21**, 597–610.

Rogers, K. L., Martin, J.-R., Renaud, O., Karplus, E., Nicola, M.-A., Nguyen, M., Picaud, S., Shorte, S. L. & Brûlet, P. (2008). Electron-multiplying charge-coupled detector-based bioluminescence recording of single-cell Ca2+. *J. Biomed. Opt.* **13**, 031211.

Roman, G., Endo, K., Zong, L. & Davis, R. L. (2001). P[Switch], a system for spatial and temporal control of gene expression in Drosophila melanogaster. *Proc. Natl. Acad. Sci. U. S. A.* **98**, 12602–12607.

Rosten, E. & Drummond, T. (2006). Machine Learning for High-Speed Corner Detection. In *Computer Vision – ECCV 2006*, pp. 430–443. Berlin, Heidelberg: Springer.

RStudio Team (2017). *RStudio: Integrated Development for R*. RStudio, Inc. Boston, MA, USA.

Rubin, G. M. & Lewis, E. B. (2000). A brief history of Drosophila's contributions to genome research. *Science* **287**, 2216–2218.

Rubin, G. M. & Spradling, A. C. (1982). Genetic transformation of Drosophila with transposable element vectors. *Science* **218**, 348–353.

Saling, M., Alberts, J., Stelmach, G. E. & Bloedel, J. R. (1998). Reach-to-grasp movements during obstacle avoidance. *Exp. Brain Res.* **118**, 251–258.

Sandoval Similä, S. & McIntosh, R. D. (2015). Look where you're going! Perceptual attention constrains the online guidance of action. *Vision Res.* **110**, 179–189.

Sareen, P., Wolf, R. & Heisenberg, M. (2011). Attracting the attention of a fly. *Proc. Natl. Acad. Sci. U. S. A.* **108**, 7230–7235.

Sartori, L., Camperio-Ciani, A., Bulgheroni, M. & Castiello, U. (2014). Monkey see, monkey reach: action selection of reaching movements in the macaque monkey. *Sci. Rep.* **4**, 4019.

Scarpa, M. & Castiello, U. (1994). Perturbation of a prehension movement in Parkinson's disease. *Mov. Disord. Off. J. Mov. Disord. Soc.* **9**, 415–425.

Schnell, B., Joesch, M., Forstner, F., Raghu, S. V., Otsuna, H., Ito, K., Borst, A. & Reiff, D. F. (2010). Processing of horizontal optic flow in three visual interneurons of the Drosophila brain. *J. Neurophysiol.* **103**, 1646–1657.

Schnell, B., Raghu, S. V., Nern, A. & Borst, A. (2012). Columnar cells necessary for motion responses of wide-field visual interneurons in Drosophila. *J. Comp. Physiol. A Neuroethol. Sens. Neural. Behav. Physiol.* **198**, 389–395.

Schwarz, G. (1978). Estimating the Dimension of a Model. *Ann. Stat.* **6**, 461–464.

Seelig, J. D. & Jayaraman, V. (2013). Feature detection and orientation tuning in

the Drosophila central complex. *Nature* **503**, 262–266.

Seelig, J. D. & Jayaraman, V. (2015). Neural dynamics for landmark orientation and angular path integration. *Nature* **521**, 186–191.

Seelig, J. D., Chiappe, M. E., Lott, G. K., Dutta, A., Osborne, J. E., Reiser, M. B. & Jayaraman, V. (2010). Two-photon calcium imaging from head-fixed Drosophila during optomotor walking behavior. *Nat. Methods* **7**, 535–540.

Sherrington, C. (1906). *The Integrative Action of the Nervous System*. New Haven, CT, USA: Yale University Press.

Shih, C.-T., Sporns, O., Yuan, S.-L., Su, T.-S., Lin, Y.-J., Chuang, C.-C., Wang, T.-Y., Lo, C.-C., Greenspan, R. J. & Chiang, A.-S. (2015). Connectomics-based analysis of information flow in the Drosophila brain. *Curr. Biol. CB* **25**, 1249–1258.

Shimomura, O. (1997). Membrane permeability of coelenterazine analogues measured with fish eggs. *Biochem. J.* **326 (Pt 2)**, 297–298.

Shimomura, O., Inouye, S., Musicki, B. & Kishi, Y. (1990). Recombinant aequorin and recombinant semi-synthetic aequorins. Cellular Ca2+ ion indicators. *Biochem. J.* **270**, 309–312.

Shinomiya, K., Karuppudurai, T., Lin, T.-Y., Lu, Z., Lee, C.-H. & Meinertzhagen, I. A. (2014). Candidate neural substrates for off-edge motion detection in Drosophila. *Curr. Biol. CB* **24**, 1062–1070.

Shiozaki, H. M. & Kazama, H. (2017). Parallel encoding of recent visual experience and self-motion during navigation in Drosophila. *Nat. Neurosci.*

Silies, M., Gohl, D. M., Fisher, Y. E., Freifeld, L., Clark, D. A. & Clandinin, T. R. (2013). Modular use of peripheral input channels tunes motion-detecting circuitry. *Neuron* **79**, 111–127.

Simon, J. C. & Dickinson, M. H. (2010). A new chamber for studying the behavior of Drosophila. *PloS One* **5**, e8793.

Simpson, J. H. & Looger, L. L. (2018). Functional Imaging and Optogenetics in Drosophila. *Genetics* **208**, 1291–1309.

Singmann, H., Bolker, B., Westfall, J. & Aust, F. (2018). *afex: Analysis of Factorial Experiments*. R package version 0.19-1.

Smith, Y., Raju, D. V., Pare, J.-F. & Sidibe, M. (2004). The thalamostriatal

system: a highly specific network of the basal ganglia circuitry. *Trends Neurosci.* **27**, 520–527.

Soechting, J. F. & Flanders, M. (1989). Errors in pointing are due to approximations in sensorimotor transformations. *J. Neurophysiol.* **62**, 595–608.

Sperry, R. W. (1952). Neurology and the mind-brain problem. *Am. Sci.* **40**, 291–312.

Spradling, A. C. & Rubin, G. M. (1982). Transposition of cloned P elements into Drosophila germ line chromosomes. *Science* **218**, 341–347.

Srinivasan, M. V. & Zhang, S. (2004). Visual motor computations in insects. *Annu. Rev. Neurosci.* **27**, 679–696.

Stephenson-Jones, M., Samuelsson, E., Ericsson, J., Robertson, B. & Grillner, S. (2011). Evolutionary conservation of the basal ganglia as a common vertebrate mechanism for action selection. *Curr. Biol. CB* **21**, 1081–1091.

Stephenson-Jones, M., Ericsson, J., Robertson, B. & Grillner, S. (2012). Evolution of the basal ganglia: dual-output pathways conserved throughout vertebrate phylogeny. *J. Comp. Neurol.* **520**, 2957–2973.

Stephenson-Jones, M., Kardamakis, A. A., Robertson, B. & Grillner, S. (2013). Independent circuits in the basal ganglia for the evaluation and selection of actions. *Proc. Natl. Acad. Sci. U. S. A.* **110**, E3670-3679.

Stone, T., Webb, B., Adden, A., Weddig, N. B., Honkanen, A., Templin, R., Wcislo, W., Scimeca, L., Warrant, E. & Heinze, S. (2017). An Anatomically Constrained Model for Path Integration in the Bee Brain. *Curr. Biol. CB* **27**, 3069-3085.e11.

Stowers, J. R., Hofbauer, M., Bastien, R., Griessner, J., Higgins, P., Farooqui, S., Fischer, R. M., Nowikovsky, K., Haubensak, W., Couzin, I. D., et al. (2017). Virtual reality for freely moving animals. *Nat. Methods*.

Strausfeld, N. J. (1999). A brain region in insects that supervises walking. *Prog. Brain Res.* **123**, 273–284.

Strausfeld, N. J. (2012). *Arthropod Brains: Evolution, Functional Elegance, and Historical Significance*. Cambridge, MA, USA: Harvard University Press.

Strausfeld, N. J. & Bassemir, U. K. (1985). Lobula plate and ocellar interneurons converge onto a cluster of descending neurons leading to neck and leg motor

neuropil in Calliphora erythrocephala. *Cell Tissue Res.* **240**, 617–640.

Strausfeld, N. J. & Hirth, F. (2013a). Homology versus convergence in resolving transphyletic correspondences of brain organization. *Brain. Behav. Evol.* **82**, 215–219.

Strausfeld, N. J. & Hirth, F. (2013b). Deep homology of arthropod central complex and vertebrate basal ganglia. *Science* **340**, 157–161.

Strauss, R. (2002). The central complex and the genetic dissection of locomotor behaviour. *Curr. Opin. Neurobiol.* **12**, 633–638.

Strauss, R. & Heisenberg, M. (1993). A higher control center of locomotor behavior in the Drosophila brain. *J. Neurosci. Off. J. Soc. Neurosci.* **13**, 1852–1861.

Strauss, R. & Pichler, J. (1998). Persistence of orientation toward a temporarily invisible landmark in Drosophila melanogaster. *J. Comp. Physiol. [A]* **182**, 411–423.

Straw, A. D., Lee, S. & Dickinson, M. H. (2010). Visual control of altitude in flying Drosophila. *Curr. Biol. CB* **20**, 1550–1556.

Strother, J. A., Nern, A. & Reiser, M. B. (2014). Direct observation of ON and OFF pathways in the Drosophila visual system. *Curr. Biol. CB* **24**, 976–983.

Strother, J. A., Wu, S.-T., Rogers, E. M., Eliason, J. L. M., Wong, A. M., Nern, A. & Reiser, M. B. (2018). Behavioral state modulates the ON visual motion pathway of Drosophila. *Proc. Natl. Acad. Sci. U. S. A.* **115**, E102–E111.

Struhl, G. & Basler, K. (1993). Organizing activity of wingless protein in Drosophila. *Cell* **72**, 527–540.

Sturtevant, A. H. (1915). Experiments on sex recognition and the problem of sexual selection in Drosoophilia. *J. Anim. Behav.* **5**, 351–366.

Sun, Y., Nern, A., Franconville, R., Dana, H., Schreiter, E. R., Looger, L. L., Svoboda, K., Kim, D. S., Hermundstad, A. M. & Jayaraman, V. (2017). Neural signatures of dynamic stimulus selection in Drosophila. *Nat. Neurosci.*

Suver, M. P., Mamiya, A. & Dickinson, M. H. (2012). Octopamine neurons mediate flight-induced modulation of visual processing in Drosophila. *Curr. Biol. CB* **22**, 2294–2302.

Suver, M. P., Huda, A., Iwasaki, N., Safarik, S. & Dickinson, M. H. (2016). An

Array of Descending Visual Interneurons Encoding Self-Motion in Drosophila. *J. Neurosci. Off. J. Soc. Neurosci.* **36**, 11768–11780.

Szüts, D. & Bienz, M. (2000). LexA chimeras reveal the function of Drosophila Fos as a context-dependent transcriptional activator. *Proc. Natl. Acad. Sci. U. S. A.* **97**, 5351–5356.

Takemura, S.-Y., Lu, Z. & Meinertzhagen, I. A. (2008). Synaptic circuits of the Drosophila optic lobe: the input terminals to the medulla. *J. Comp. Neurol.* **509**, 493–513.

Takemura, S., Karuppudurai, T., Ting, C.-Y., Lu, Z., Lee, C.-H. & Meinertzhagen, I. A. (2011). Cholinergic circuits integrate neighboring visual signals in a Drosophila motion detection pathway. *Curr. Biol. CB* **21**, 2077–2084.

Takemura, S., Bharioke, A., Lu, Z., Nern, A., Vitaladevuni, S., Rivlin, P. K., Katz, W. T., Olbris, D. J., Plaza, S. M., Winston, P., et al. (2013). A visual motion detection circuit suggested by Drosophila connectomics. *Nature* **500**, 175–181.

Takemura, S.-Y., Nern, A., Chklovskii, D. B., Scheffer, L. K., Rubin, G. M. & Meinertzhagen, I. A. (2017). The comprehensive connectome of a neural substrate for "ON" motion detection in Drosophila. *eLife* **6**,.

Talay, M., Richman, E. B., Snell, N. J., Hartmann, G. G., Fisher, J. D., Sorkaç, A., Santoyo, J. F., Chou-Freed, C., Nair, N., Johnson, M., et al. (2017). Transsynaptic Mapping of Second-Order Taste Neurons in Flies by trans-Tango. *Neuron* **96**, 783-795.e4.

Tammero, L. F. & Dickinson, M. H. (2002). The influence of visual landscape on the free flight behavior of the fruit fly Drosophila melanogaster. *J. Exp. Biol.* **205**, 327–343.

Tammero, L. F., Frye, M. A. & Dickinson, M. H. (2004). Spatial organization of visuomotor reflexes in Drosophila. *J. Exp. Biol.* **207**, 113–122.

Tipper, S. P. (1985). The negative priming effect: inhibitory priming by ignored objects. *Q. J. Exp. Psychol. A* **37**, 571–590.

Tipper, S. P., Lortie, C. & Baylis, G. C. (1992). Selective reaching: evidence for action-centered attention. *J. Exp. Psychol. Hum. Percept. Perform.* **18**, 891–905.

Tipper, S. P., Howard, L. A. & Jackson, S. R. (1997). Selective Reaching to Grasp: Evidence for Distractor Interference Effects. *Vis. Cogn.* **4**, 1–38.

Tipper, S. P., Howard, L. A. & Houghton, G. (1998). Action-based mechanisms of attention. *Philos. Trans. R. Soc. Lond. B. Biol. Sci.* **353**, 1385–1393.

Tresilian, J. R. (1998). Attention in action or obstruction of movement? A kinematic analysis of avoidance behavior in prehension. *Exp. Brain Res.* **120**, 352–368.

Triphan, T., Poeck, B., Neuser, K. & Strauss, R. (2010). Visual targeting of motor actions in climbing Drosophila. *Curr. Biol. CB* **20**, 663–668.

Tsubouchi, A., Yano, T., Yokoyama, T. K., Murtin, C., Otsuna, H. & Ito, K. (2017). Topological and modality-specific representation of somatosensory information in the fly brain. *Science* **358**, 615–623.

Turner-Evans, D. B. & Jayaraman, V. (2016). The insect central complex. *Curr. Biol. CB* **26**, R453-457.

Turner-Evans, D., Wegener, S., Rouault, H., Franconville, R., Wolff, T., Seelig, J. D., Druckmann, S. & Jayaraman, V. (2017). Angular velocity integration in a fly heading circuit. *eLife* **6**,.

Tuthill, J. C. & Wilson, R. I. (2016). Parallel Transformation of Tactile Signals in Central Circuits of Drosophila. *Cell* **164**, 1046–1059.

Tuthill, J. C., Nern, A., Holtz, S. L., Rubin, G. M. & Reiser, M. B. (2013). Contributions of the 12 neuron classes in the fly lamina to motion vision. *Neuron* **79**, 128–140.

Tuthill, J. C., Nern, A., Rubin, G. M. & Reiser, M. B. (2014). Wide-field feedback neurons dynamically tune early visual processing. *Neuron* **82**, 887–895.

Ueno, T., Tomita, J., Tanimoto, H., Endo, K., Ito, K., Kume, S. & Kume, K. (2012). Identification of a dopamine pathway that regulates sleep and arousal in Drosophila. *Nat. Neurosci.* **15**, 1516–1523.

van Alphen, B. & van Swinderen, B. (2013). Drosophila strategies to study psychiatric disorders. *Brain Res. Bull.* **92**, 1–11.

van Breugel, F. & Dickinson, M. H. (2012). The visual control of landing and obstacle avoidance in the fruit fly Drosophila melanogaster. *J. Exp. Biol.* **215**,

1783–1798.

van Swinderen, B. (2007). Attention-like processes in Drosophila require short-term memory genes. *Science* **315**, 1590–1593.

van Swinderen, B. (2011). Attention in Drosophila. *Int. Rev. Neurobiol.* **99**, 51–85.

van Swinderen, B., McCartney, A., Kauffman, S., Flores, K., Agrawal, K., Wagner, J. & Paulk, A. (2009). Shared visual attention and memory systems in the Drosophila brain. *PloS One* **4**, e5989.

Venkatasubramanian, L. & Mann, R. S. (2019). The development and assembly of the Drosophila adult ventral nerve cord. *Curr. Opin. Neurobiol.* **56**, 135–143.

Venken, K. J. T., Simpson, J. H. & Bellen, H. J. (2011). Genetic manipulation of genes and cells in the nervous system of the fruit fly. *Neuron* **72**, 202–230.

Virsik, R. P. & Reichardt, W. (1976). Detection and tracking of moving objects by the fly Musca domestica. *Biol. Cybern.* **23**, 83–98.

von Holst, E. & Mittelstaedt, H. (1950). Das Reafferenzprinzip. *Naturwissenschaften* **37**, 464–476.

von Philipsborn, A. C., Liu, T., Yu, J. Y., Masser, C., Bidaye, S. S. & Dickson, B. J. (2011). Neuronal control of Drosophila courtship song. *Neuron* **69**, 509–522.

von Reyn, C. R., Breads, P., Peek, M. Y., Zheng, G. Z., Williamson, W. R., Yee, A. L., Leonardo, A. & Card, G. M. (2014). A spike-timing mechanism for action selection. *Nat. Neurosci.* **17**, 962–970.

von Reyn, C. R., Nern, A., Williamson, W. R., Breads, P., Wu, M., Namiki, S. & Card, G. M. (2017). Feature Integration Drives Probabilistic Behavior in the Drosophila Escape Response. *Neuron* **94**, 1190-1204.e6.

Waddell, S. & Quinn, W. G. (2001). What can we teach Drosophila? What can they teach us? *Trends Genet. TIG* **17**, 719–726.

Wang, J. W., Wong, A. M., Flores, J., Vosshall, L. B. & Axel, R. (2003). Two-photon calcium imaging reveals an odor-evoked map of activity in the fly brain. *Cell* **112**, 271–282.

Warren, T. L., Weir, P. T. & Dickinson, M. H. (2018). Flying Drosophilamelanogaster maintain arbitrary but stable headings relative to the angle of polarized light. *J. Exp. Biol.* **221**,.

Webb, B. (2004). Neural mechanisms for prediction: do insects have forward models? *Trends Neurosci.* **27**, 278–282.

Weir, P. T. & Dickinson, M. H. (2012). Flying Drosophila orient to sky polarization. *Curr. Biol. CB* **22**, 21–27.

Weir, P. T. & Dickinson, M. H. (2015). Functional divisions for visual processing in the central brain of flying Drosophila. *Proc. Natl. Acad. Sci. U. S. A.* **112**, E5523-5532.

Welsh, T. & Elliott, D. (2004). Movement trajectories in the presence of a distracting stimulus: evidence for a response activation model of selective reaching. *Q. J. Exp. Psychol. A* **57**, 1031–1057.

Welsh, T. N., Elliott, D. & Weeks, D. J. (1999). Hand deviations toward distractors. Evidence for response competition. *Exp. Brain Res.* **127**, 207–212.

Wernet, M. F., Labhart, T., Baumann, F., Mazzoni, E. O., Pichaud, F. & Desplan, C. (2003). Homothorax switches function of Drosophila photoreceptors from color to polarized light sensors. *Cell* **115**, 267–279.

Wernet, M. F., Velez, M. M., Clark, D. A., Baumann-Klausener, F., Brown, J. R., Klovstad, M., Labhart, T. & Clandinin, T. R. (2012). Genetic dissection reveals two separate retinal substrates for polarization vision in Drosophila. *Curr. Biol. CB* **22**, 12–20.

Wertz, A., Haag, J. & Borst, A. (2012). Integration of binocular optic flow in cervical neck motor neurons of the fly. *J. Comp. Physiol. A Neuroethol. Sens. Neural. Behav. Physiol.* **198**, 655–668.

Wietek, J., Wiegert, J. S., Adeishvili, N., Schneider, F., Watanabe, H., Tsunoda, S. P., Vogt, A., Elstner, M., Oertner, T. G. & Hegemann, P. (2014). Conversion of channelrhodopsin into a light-gated chloride channel. *Science* **344**, 409–412.

Wolf, R. & Heisenberg, M. (1980). On the fine structure of yaw torque in visual flight orientation of Drosophila melanogaster. *J. Comp. Physiol.* **140**, 69–80.

Wolf, R. & Heisenberg, M. (1991). Basic organization of operant behavior as revealed in Drosophila flight orientation. *J. Comp. Physiol. [A]* **169**, 699–705.

Wolf, R. & Heisenberg, M. (1997). Visual space from visual motion: turn integration in tethered flying Drosophila. *Learn. Mem. Cold Spring Harb. N* **4**,

318–327.

Wolff, T. & Rubin, G. M. (2018). Neuroarchitecture of the Drosophila central complex: A catalog of nodulus and asymmetrical body neurons and a revision of the protocerebral bridge catalog. *J. Comp. Neurol.*

Wolff, T., Iyer, N. A. & Rubin, G. M. (2015). Neuroarchitecture and neuroanatomy of the Drosophila central complex: A GAL4-based dissection of protocerebral bridge neurons and circuits. *J. Comp. Neurol.* **523**, 997–1037.

Wosnitza, A., Bockemühl, T., Dübbert, M., Scholz, H. & Büschges, A. (2013). Inter-leg coordination in the control of walking speed in Drosophila. *J. Exp. Biol.* **216**, 480–491.

Yamaguchi, S., Wolf, R., Desplan, C. & Heisenberg, M. (2008). Motion vision is independent of color in Drosophila. *Proc. Natl. Acad. Sci. U. S. A.* **105**, 4910–4915.

Yamaguchi, S., Desplan, C. & Heisenberg, M. (2010). Contribution of photoreceptor subtypes to spectral wavelength preference in Drosophila. *Proc. Natl. Acad. Sci. U. S. A.* **107**, 5634–5639.

Yizhar, O., Fenno, L. E., Davidson, T. J., Mogri, M. & Deisseroth, K. (2011). Optogenetics in neural systems. *Neuron* **71**, 9–34.

Young, J. M. & Armstrong, J. D. (2010a). Building the central complex in Drosophila: the generation and development of distinct neural subsets. *J. Comp. Neurol.* **518**, 1525–1541.

Young, J. M. & Armstrong, J. D. (2010b). Structure of the adult central complex in Drosophila: organization of distinct neuronal subsets. *J. Comp. Neurol.* **518**, 1500–1524.

Yu, D., Baird, G. S., Tsien, R. Y. & Davis, R. L. (2003). Detection of calcium transients in Drosophila mushroom body neurons with camgaroo reporters. *J. Neurosci. Off. J. Soc. Neurosci.* **23**, 64–72.

Zanker, J. M. (1990). The wing beat of Drosophila Melanogaster. I. Kinematics. *Philos. Trans. R. Soc. Lond. B Biol. Sci.* **327**, 1–18.

Zehring, W. A., Wheeler, D. A., Reddy, P., Konopka, R. J., Kyriacou, C. P., Rosbash, M. & Hall, J. C. (1984). P-element transformation with period locus DNA restores rhythmicity to mutant, arrhythmic Drosophila melanogaster.

Cell **39**, 369–376.

Zemelman, B. V., Nesnas, N., Lee, G. A. & Miesenbock, G. (2003). Photochemical gating of heterologous ion channels: remote control over genetically designated populations of neurons. *Proc. Natl. Acad. Sci. U. S. A.* **100**, 1352–1357.

Zhang, K., Guo, J. Z., Peng, Y., Xi, W. & Guo, A. (2007a). Dopamine-mushroom body circuit regulates saliency-based decision-making in Drosophila. *Science* **316**, 1901–1904.

Zhang, W., Ge, W. & Wang, Z. (2007b). A toolbox for light control of Drosophila behaviors through Channelrhodopsin 2-mediated photoactivation of targeted neurons. *Eur. J. Neurosci.* **26**, 2405–2416.

Zhang, F., Prigge, M., Beyrière, F., Tsunoda, S. P., Mattis, J., Yizhar, O., Hegemann, P. & Deisseroth, K. (2008). Red-shifted optogenetic excitation: a tool for fast neural control derived from Volvox carteri. *Nat. Neurosci.* **11**, 631–633.

Zhang, Z., Li, X., Guo, J., Li, Y. & Guo, A. (2013). Two clusters of GABAergic ellipsoid body neurons modulate olfactory labile memory in Drosophila. *J. Neurosci. Off. J. Soc. Neurosci.* **33**, 5175–5181.

Zheng, L., Nikolaev, A., Wardill, T. J., O'Kane, C. J., de Polavieja, G. G. & Juusola, M. (2009). Network adaptation improves temporal representation of naturalistic stimuli in Drosophila eye: I dynamics. *PloS One* **4**, e4307.

Zheng, Z., Lauritzen, J. S., Perlman, E., Robinson, C. G., Nichols, M., Milkie, D., Torrens, O., Price, J., Fisher, C. B., Sharifi, N., et al. (2018). A Complete Electron Microscopy Volume of the Brain of Adult Drosophila melanogaster. *Cell* **174**, 730-743.e22.

Zhou, H. & Desimone, R. (2011). Feature-based attention in the frontal eye field and area V4 during visual search. *Neuron* **70**, 1205–1217.

Zhu, Y., Nern, A., Zipursky, S. L. & Frye, M. A. (2009). Peripheral visual circuits functionally segregate motion and phototaxis behaviors in the fly. *Curr. Biol. CB* **19**, 613–619.

Zordan, M. A. & Sandrelli, F. (2015). Circadian Clock Dysfunction and Psychiatric Disease: Could Fruit Flies have a Say? *Front. Neurol.* **6**, 80.

Zuker, C. S. (1996). The biology of vision of Drosophila. *Proc. Natl. Acad. Sci. U. S. A.* **93**, 571–576.

ACKNOLEDGMENTS

Fist of all, I have to thank my supervisors Prof. Umberto Castiello and Prof. Aram Megighian for giving me the great opportunity to carry out the work included in this thesis. They were a fundamental support and point of reference during the three years of the PhD. In particular they gave me the freedom at the basis of creativity and to pioneer this research.

I really thank Prof. Mauro A. Zordan for his aid in designing the experiments, for helping with the writing and for the helpful discussions. I am grateful to Dr. Paola Cisotto for her precious help in genetic crossings.

I thank Prof. Jean-René Martin for teaching me how to perform brain imaging experiments. The last experiment of this thesis would not have been possible without his kind collaboration.

A big thank you goes to the master students who helped me in collecting the data: Dr. Giulio M. Menti and Dr. Salvi Ferraj. I extended my gratitude to all students who have attended the lab to fulfil their undergraduate thesis throughout these years: Nicola, Giorgia, Matteo P., Matteo S., Camilla, Giovanni and Riccardo.

I am indebted to my parents, Antonio and Maria Angela, for the immeasurable support they have given me and that I can only pay back with a huge hug. Thank you to my brother Andrea, his wife Michela and my lovely nieces Micol and Agnese for their closeness.

The research is a boundless job which permeates all aspects of your life because ideas and troubles come up without respecting working hours. For this reason the greatest thank you goes to Maria Elena who has always supported me despite my mistakes and bad moods in tough times. In the last year, painful moments have tested her but she never missed her amazing strength. She is the person to which I dedicate this work.

PUBBLICATIONS AND PRESENTATIONS ASSOCIATED TO THIS THESIS

Full peer review journal articles

Frighetto, G., Zordan, M. A., Castiello, U. & Megighian, A. (2019). Action-based attention in Drosophila melanogaster. *Journal of Neurophysiology*. https://doi.org/10.1152/jn.00164.2019.

In preparation

Frighetto, G., Zordan, M. A., Castiello, U. & Megighian, A. Response to visual perturbation in freely walking Drosophila.

Frighetto, G., Zordan, M. A., Castiello, U. & Megighian, A. A putative neural circuit for selection and control of action in Drosophila.

Frighetto, G., Zordan, M. A., Castiello, U., Megighian, A. & Martin, J. R. Dopamine modulation of Drosophila ellipsoid body neurons.

International academic conference presentations

Frighetto, G., Zordan, M. A., Castiello, U. & Megighian, A. Selection for action in fruit fly. Joint International Meeting of the Federation of European Physiological Society (FEPS) and the Italian Physiological Society (SIF), Bologna (IT), September 10th - 13th, 2019. Poster.

Frighetto, G., Zordan, M. A., Castiello, U. & Megighian, A. Action-based attention in Drosophila melanogaster. 6th European Student Conference on Behaviour & Cognition, Padova (IT), September 4th - 7th, 2019. Oral presentation.